Control and Protection in Low Voltage Grid with Large Scale Renewable Electricity Generation

Mustafa, Ghullam

Publication date:
2014

Document Version
Publisher's PDF, also known as Version of record

Control and Protection in Low Voltage Grid with large scale renewable electricity generation

By

Ghullam Mustafa Bhutto

Department of Energy Technology

DEPARTMENT OF ENERGY TECHNOLOGY
AALBORG UNIVERSITY

A Dissertation Submitted to
The Faculty of Engineeringand Science, Aalborg University
in Partial Fulfillment for the Degree of Doctor of Philosophy

May 2014
Alborg, Denmark

Control and Protection in Low Voltage Grid with large scale renewable electricity generation

gmu@et.aau.dk/gmustafabhutto@yahoo.com

Department of Energy Technology

Pontoppidanstraede 101, room 120 | 9220 Aalborg East | Denmark
Phone: (+45) 9940 3320 | Email: cgr@et.aau.dk

Employee No. 118265 | EAN: 5798 000 42 08 16 | VAT No.: 29 10 23 84

Printed in Denmark by UniPrint, 2014

ISBN: 978-87-92846-36-5

Read about the department and the research activities at www.et.aau.dk

Statement

1. Thesis Title

Control and Protection in Low Voltage Grid with large scale renewable electricity generation

2. Name of the PhD student

Ghullam Mustafa Bhutto

3. Name of the Supervisor

Birgitte Bak-Jensen and Jayakrishnan Pillai

4. List of Publications

Paper 1: Ghullam Mustafa, Birgitte Bak-Jensen, Pukar Mahat, "Modeling of the CIGRE Low Voltage Test Distribution Network and the Development of Appropriate Controllers", International Journal of Smart Grids and Clean Energy (SGCE), Vol. 2 No. 2, pp. 184-192, 2013.

Paper 2: Ghullam Mustafa, Birgitte Bak-Jensen, Pukar Mahat, and Ribeiro P. F,"Mitigation of voltage sags in CIGRE Low Voltage Distribution Network" Proceedings of the 5th IEEE PES Asia-Pacific Power and Energy Engineering Conference, APPEEC 2013. IEEE Press, 2013.

Paper 3: Ghullam Mustafa, Birgitte Bak-Jensen, Pukar Mahat, Cecati Carlo, "Mitigation of Unbalanced Voltage Sags and Voltage Unbalance in CIGRE Low Voltage Distribution Network", Journal of Energy and Power Engineering (EPE), Vol. 5, pp. 551-559, 2013.

Paper 4: Ghullam Mustafa, Birgitte Bak-Jensen, Bak Claus Leth, Pillai, Jayakrishnan Radhakrishna, "Protection of Low Voltage CIGRE Distribution Network", Journal of Smart Grid and Renewable Energy, (SGRE)Vol. 4, No. 9, pp. 489-500,2013.

5. This present report combined with the above listed scientific papers has been submitted for assessment in partial fulfilment of the PhD degree. The scientific papers are not included in this version due to copyright issues. Detailed publication information is provided above and the interested reader is referred to the original published papers. As part of the assessment, co-author statements have been made available to the assessment committee and are also available at the Faculty of Engineering and Science, Aalborg University

Acknowledgment

I am very thankful to the Department of Energy Technology, Aalborg University (ET, AAU) and Quaid-E-Awam University of Engineering Sciences & Technology Nawabshah, Pakistan for the financial support.

I express my utmost gratitude to my PhD supervisor, Associate Professor, Birgitte Bak-Jensen for supervision and valuable guidance during the entire period of my PhD studies. I am also thankful to my co-supervisor, Assistant Professors, Pukar Mahat and Jayakrishnan Pillai for his supervision, his suggestion and encouragement throughout the period of this work.

I would also like to thank DTU wind energy for providing real wind speed data. Special thanks to Kai Strunz for providing the CIGRE test network set up and data for LV distribution network.

I would like to express my sincere gratitude to all my colleagues of the Department of Energy Technology, especially Zakir Hussain Rather for his nice cooperation and discussions.

Most especially, my parents, wife, children and my brother Ghullam Hussain deserve special mention for their patience and constant support.

Last but not the least I thank my God who gave strength and support to carry out my work successfully.

Ghullam Mustafa Bhutto

Aalborg, Denmark, 2014

Abstract

Distributed Generation (DG) technology especially renewable energy sources such as Wind Turbine Generations (WTGs), photovoltaic (PV) generations, energy storages etc. has played a vital role in the modern power industry due to some environmental and some cost benefits. The important benefits of renewable energy based DGs are reduced CO_2 emission, reduced operational cost as almost no fuel is used for their operation and less transmission and distribution losses as these units are normally built near to the load centers. This has also resulted in some operational challenges due to the unpredictable nature of such power generation sources. Some of the operational challenges include voltage variations due to power fluctuations coming from the DG units. On the other hand, it has also opened up some opportunities. One of the opportunities is islanding operation of the distribution system with DG unit(s). Islanding is a situation where electrical system becomes electrically isolated from the rest of the power network and yet continues to be energized by the DG units connected to it.With the increased penetration of DG units, islanded operation of the distribution network is used to improve the reliability of power supply if various issues regarding islanding are properly tackled. Some of the serious issues with islanding are the Island Detection (ID), voltage and the frequency control, load control and protection.

In this dissertation, some of the major technical issues such as voltage control in case of the wind speed and solar irradiation fluctuations are tackled. The CIGRE Low Voltage (LV) network comprising two solar PV generating units of 3 kW and 4 kW, one 5.5 kW fixed-pitch fix speed WTG and two battery units each producing energy of 30kwh and 21kwh has been chosen for the study. The study of this network in the case of transients such as short circuit faults has been made. The mitigation of symmetrical and unsymmetrical voltage sags has also been addressed here. The components of the CIGRE network are modelled in DIgSILENT power factory software 15.0 and the control system for PV and battery inverters have been developed. Two Static Compensator (STATCOM) controllers have been developed for the PV units and two Battery Energy Storage System (BESS) based STATCOM controllers have been developed for battery units. The controllers are developed in such a way that they inject/absorb desired amount of the reactive power in order to maintain the constancy of the voltage in the network.

Some of the protection related issues have also been addressed in this dissertation. The short circuit power of a distribution system changes when it changes its states. Short circuit power also changes when some DG units are disconnected. This may result in elongation of the fault clearing time of the protective devices and might cause unnecessary operation of the protective devices. Therefore, the protection of the distribution system has been developed which is accurate and satisfy the economic criteria as well. The protection of the different components of the CIGRE distribution network has been presented in case of bi-directional flow of the current. It is proposed that the protection of the entire CIGRE network is mainly developed by using fuses due to economic reasons. The voltage based protection is also proposed somewhere in this network for

thecases when fuses are not enough to protect, such as in the case of islanding where the flow of the current has the reverse direction. Over speed protection of the WTG in case of loss of grid due to symmetric and asymmetric faults is also developed in this thesis. This is done by using a mechanical braking system in order to stop the generator. The protection of PV and battery inverters is also presented in this study. The protection of the inverters is made by using ultra-fast fuses. The issues of the protection of the solar PV structure against over voltages in case of islanding from the main power grid are also described here. This is achieved by using switch disconnection devices.

The issues of the voltage and the frequency control in case of islanding are addressed in this study and these issues of voltage and frequency in islanded Micro Grid (MG) has been successfully tackled in this dissertation. This is done by developing appropriate controllers. Initially islanding is detected by using an Island Detection (ID) detection technique which is based on voltage phase angle difference between grid side and DG side of the network. This is a more recent ID technique and has some advantages over other ID detection techniques such as false detection in case of transient or over load conditions.

The development of controllers for all the DG units in the islanded MG is different as compared to the grid connected mode. The controllers are developed in such a way that they ensure the constancy of the voltage and the frequency of the entire islanded MG. In case of the grid connected mode, all of the inverter controllers can either be developed in Power/Voltage (PV) mode or Active power/Reactive power (PQ) mode. In case of islanding with several parallel inverters available in the network; one of the inverter controllers must be developed to Voltage-Frequency(VF)mode; and the others in either PV or PQ modes. The operation of the MG with several PV inverters and single VF inverter is similar to the operation of MG with a synchronous machine as slack bus. The VF inverter establishes the voltage and the frequency references for the operation of all other PV/PQ inverters in the case when the MG islanded from the main power grid. Acting as the voltage source, VF inverter is responsible for controlling the voltage and frequency of the island MG. It injects or absorbs active and reactive powers if frequency or voltage in MG decreases or increases respectively. It requires the significant amount of energy available in the power source with very fast response. A VF control cannot be used for wind and solar power generations because they are unpredictable and depend on the weather conditions (i.e. wind speed and solar irradiance). The VF controller can be used for the inverters of the BESS system, especially the inverter of the bigger energy storage capability. Therefore, when the operating mode of the CIGRE network changes from the grid connected to the islanded mode, the control system should switch from the PV/PQ mode to VF mode for this unit. The switching of the control system is based on the Island Detection (ID) technique.

Issues related to grid reconnection have also been described in this thesis. The DG control strategy needs to be changed again when the islanded network is reconnected back to the transmission grid. Hence, grid reconnection detection has been proposed to detect when the islanded distribution system is reconnected back to the transmission grid. One of the grid reconnection detection techniques based on the

synchronization of the voltage, the frequency and phase angle between the distribution system and the transmission grid has been proposed here.

The algorithms, models and methodologies developed during this research study have been tested in a CIGRE low voltage distribution network. The simulation results show that they are able to correctly identify the states of the distribution system in different operating conditions of the network, maintain the voltage during stochastic generation changes, mitigate voltage dips in the different fault conditions, control voltage and frequency during island mode. The simulation results show that the distribution system can survive for long time (i.e. up to 45 minutes) in the islanded condition. The results also show the islanded distribution system can successfully reconnect back to the transmission grid.

The research study shows that integration of renewable energy based DGs is a viable, cost effective and environment friendly solution for the modern power network. The distribution network such as CIGRE network and systems like that comprising wide variety of DGs can operate in stable, controlled, reliable and secure manners.

Abstrakt

Distribueret Generations teknologi (DG) især i form af vedvarende energikilder såsom vindmøller (WTGs), solceller (PV), energilagre osv. spiller en afgørende rolle i det moderne el-system på grund af deres miljø og omkostningsmæssige fordele. De vigtige fordele ved vedvarende energikilder er reduceret CO_2 emission, reducerede driftsomkostninger da der næsten ingen brændstof bruges til deres drift, samt mindre transmissions-og distributionstab, da disse enheder normalt er bygget tæt på belastningscentrene. Dette har resulteret i nogle driftsmæssige udfordringer på grund af den uforudsigelige produktion fra sådanne energikilder. Nogle af de driftsmæssige udfordringer omfatter spændingsvariationer på grund af effektudsving fra DG enhederne. På den anden side har det også åbnet nogle muligheder. En af de muligheder, er ø- drift af distributionssystemet via de decentrale enheder. Ø-drift er en situation, hvor det elektriske system bliver isoleret fra resten af el-nettet, og alligevel fortsætter med at være forsynet via DG - enheder tilsluttet til det. Med den øgede tilslutning af DG-enheder, kan ø-drift af distributionsnettet anvendes til at forbedre pålideligheden i nettet, hvis forskellige problemer i forhold til ø-driften takles korrekt. Nogle af de alvorligste problemer med ø-drift detektering af overgang til ø-drift (ID), spændings og frekvens kontrol, last kontrol og beskyttelse.

I denne afhandling, er nogle af de væsentlige tekniske spørgsmål såsom spændings kontrol ved vind- og solindfalds fluktuationer. Et CIGRE lavspændings (LV) test netværksmodel bestående af to solcelleanlæg på 3 kW og 4 kW, en 5,5 kW fast pitch og fast hastigheds vindmølle og to batterilagre på 30kWh og 21kWh er valgt til undersøgelsen. Der er også foretaget analyser af dette netværk i tilfælde af transienter såsom kortslutning fejl. Reducering af symmetriske og usymmetriske spændingsdyk er også behandlet her. Komponenterne i CIGRE nettet er modelleret i DIgSILENT Power Factory software 15.0 og kontrolsystemet til PV og batteri konvertere er blevet udviklet. To statiske kompensatorer (Statcom) er blevet udviklet til PV –enhederne og der er også udviklet STATCOM styringer til de to energilagre (BESS). Regulatorerne er udviklet på en sådan måde, at de injicerer / absorberer den ønskede mængde reaktive effekt med henblik på at opretholde konstant spænding i nettet.

Der er også set på forskellige beskyttelsesrelaterede problemer i afhandlingen. Kortslutningseffekten ændrer sig i distributionssystemet, når dets status ændres til ø-drift. Kortslutningseffekten ændres også når nogle af DG-enhederne afbrydes. Dette kan resultere i forlængelse af frakoblingstiden for beskyttelsesudstyret eller kan forårsage unødig aktivering afbeskyttelsesudstyret. Derfor er der udviklet en beskyttelse til distributionssystemet, som er nøjagtig og opfylder de økonomiske kriterier. Beskyttelsen af de forskellige komponenter i CIGRE distributionsnet er blevet præsenteret i tilfælde af bi-direktional strøm. Det foreslås, at beskyttelsen af hele CIGRE netværket primært bliver udviklet ved hjælp af sikringer på grund af økonomiske årsager. Det foreslås dog også spænding baseret beskyttelse i de tilfælde, hvor sikringer er ikke nok til at

sikre beskyttelsen, såsom i tilfælde med ø-drift hvor strømmen løber mod transmissionsnettet. Overhastighedsbeskyttelse af WTG i tilfælde af frakobling fra nettet på grund af symmetriske og asymmetriske fejl er også udviklet i denne afhandling. Dette gøres ved hjælp af et mekanisk bremsesystem for at stoppe generatoren. Beskyttelse af PV og batterikonverterne præsenteres også i denne afhandling. Beskyttelsen af konverterne er lavet ved hjælp af ultra- hurtige sikringer. Beskyttelsen af solcelleanlæggene mod overspænding i tilfælde af ø-drift er også beskrevet her. Dette opnås ved hjælp af relæenheder. Spændings og frekvens kontrol i tilfælde af ø-drift behandles også med succes i denne afhandling. Dette gøres ved at udvikle egnede styringer. Ø-driften detekteres ved hjælp af en ø-detekteringsenhed (ID), der er baseret på fasevinkelforskellen for spædingen mellem netsiden og den isolerede side af nettet. Dette er en nyere ID teknik der har nogle fordele frem for andre ID teknikker i forhold til falsk detektion i tilfælde af forbigående eller overbelastningsforhold.

Udviklingen af styringerne for alle DG enhederne i ø-drift nettet (mikronettet (MG)) er anderledes i forhold til net-tilsluttet tilstand. Regulatorerne er udviklet på en sådan måde, at de sikrer konstant spænding og frekvens i ø-drift nettet. I tilfælde af net-tilsluttede forhold, kan alle de konverterne enten udvikles til Strøm / Spænding (PV) drift eller Aktiv effekt / Reaktiv effekt (PQ) drift. I tilfælde af ø-ddrift med flere parallelle konvertere til rådighed i nettet, skal en af de konverterstyringerne udvikles til spænding - frekvens (VF) drift, og de andre til enten PV eller PQ drift. Driften af MG med flere PV konvertere og en enkelt VF inverter svarer til driften af et MG med en synkron maskine. VF- konverteren fastlægger spændings- og frekvensreferencer til drift af alle andre PV / PQ invertere i det tilfælde, hvor MG er isoleret fra hovednettet. Fungerende som spændingskilden, er VF konverteren ansvarlig for at styre spændingen og frekvensen i mikro-nettet. Det forsyner eller absorberer aktiv og reaktiv effekt hvis henholdsvis frekvensen eller spændingen i mikro-nettet falder eller stiger. Det kræver en betydelig mængde energi til rådighed i strømkilden og med meget hurtig respons. En VF styring kan ikke anvendes ved vind-og solenergi kilderne fordi deres produktion er uforudsigelige og afhænger af vejrforholdene (dvs. vindhastighed og solindstråling). VF-styringerne kan bruges til konverterne i BESS systemet, især konverteren for den største lagerkapacitet. Når driftsformen af for CIGRE-net-modellen ændres fra net-tilsluttet til ø-drift skal styresystemet derfor skifte fra PV / PQ tilstand til VF tilstand for denne enhed. Dette skift i styresystemet er Baseret på ø-driftsdetekteringen.

Forhold omkring net-gentilslutning er også beskrevet i denne afhandling. DG styringsstrategien skal igen ændres når mikro-nettet igen tilsluttes transmissionsnettet. Derfor er der lavet en genindkoblings procedure til at registrere, når ø-drifts distributionssystemer kan genindkobles til transmissionsnettet. Denne genindkoblingsprocedure er baseret på synkronisering af spænding, frekvens og fasevinkel mellem distributionssystemet og transmissionsnettet.

De algoritmer, modeller og metoder, der er udviklet i løbet af dette studie er blevet testet i et CIGRE lavspændings distributionsnet. Simuleringen viser, at de er i stand til korrekt at identificere status for distributionssystemet i forskellige driftsbetingelser, kan vedligeholde spændingen under stokastiske produktionsforhold, kan minimere spændingsfald under forskellige fejltilstande, og kan styre spænding og frekvens under ø -drift. Simuleringsresultaterne viser, at distributionssystemet kan overleve i lang tid (dvs. op til 45 minutter) i ø-drift situation. Resultaterne viser også at ø-drift distributionssystemet med held kan genindkoble til transmissionsnettet.

Forskningen viser at integration af vedvarende energi baseret kilder er en levedygtig, omkostningseffektiv og miljøvenlig løsning for den moderne el-nettet. Distributionsnet såsom CIGRE netværket og systemer som det, bestående af en bred vifte af distribuerede energikilder, kan operere i stabile, kontrollerede, pålidelige og på sikre måder.

Table of Contents

Chapter 1

Introduction

Central Generation (CG) is the electric power production by central power plants that provide bulk power. Most of these generating plants use fossil, hydro and nuclear fuels etc. to produce power. The generation of power using CG technologies requires huge investment and running cost and large infrastructure. These generating units have many environmental impacts as well. These generating units require large transmission lines to deliver power to the customers which are one of the drawbacks because of heavy line losses [1].

Due to environment concerns and world wise increase in oil prices, the new trend in the modern power industry is towards renewable energy based Distributed Generation (DG). DG is small generating power plants which are built near the load center. DG sources include small-scale, environment friendly technologies (i.e. Photovoltaic, Wind power, Energy storage etc.). As an example, Edison's Pearl Steam Power Plant supplied 500 customers with electricity in downtown New York in 1882 [2]. DG technology especially renewable energy sources have played a vital role in the modern power industry due to some environmental and cost benefits. The important benefits of renewable DG are reduced CO_2 emission, reduced operational cost as almost no fuel is used for their operation and less transmission and distribution losses as these units are normally built near to the load centers [3], [4]. Distributed Generation can be also used as standby/back up power to improve availability and reliability of the power system in case of islanding [5].

1.1Background and Motivation

The widespread need for an increasing power demand has increased the need for better economies of scale [6]. The best way to promote the economies of the scale is to use localized DGs. The amount of the power lost is less because electricity is produced nearby the load centers. In 2009, renewable energy holds one-fourth of the total global installed power capacity and it has supplied 18% of the global electricity supply [7]. Many countries have set there ambitious targets to promote renewable electricity. In the European Union (EU), goals are set for 35% of electricity generation from the renewable sources in 2020 and one-third of the electricity are estimated to be produced from the wind energy [8]. The wind power is one of the fastest growing renewable energy technologies, especially in the offshore sector. Apart from large scale hydro and offshore wind farms, most of the renewable energy sources are DG. Hence, the increase in share of renewable generation can be treated as an increase in the penetration of distributed generation [9]. Recent studies have shown that the difference in the cost of electricity production between large and small scale generation has been reduced to 30% in 2000 from 60% in 1960 [9]. This is mainly due to the advancement in technologies like wind turbines, micro hydro, gas turbines, fuel cells and photovoltaic together with new innovation in power electronics. Fig. 1.1shows the share of the renewable power producing units in the total

electricity generation in Europe and Denmark [10] in the recent years. The share of electricity generated from renewable sources in the total electricity consumption in Europe has increased from 13.4% in 1998 to 16.7% in 2008. In Denmark, this share of renewable sources has increased significantly from 11.7% in 1998 to 28.7% in 2008.

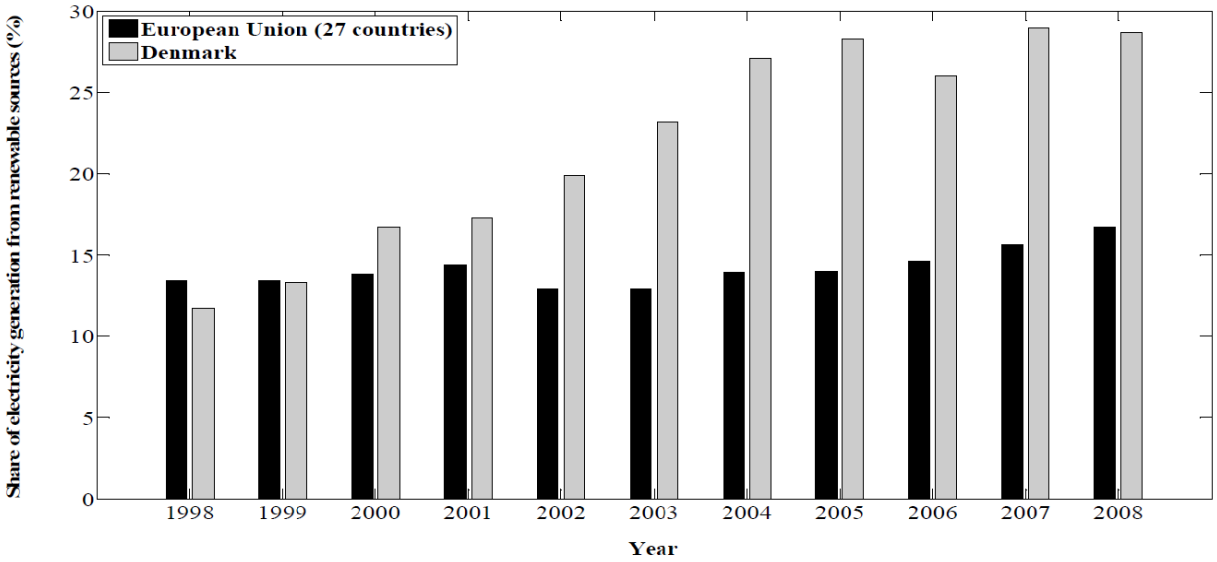

Fig. 1.1 The share of renewable sources in total electricity generation [10]

In fact, many distribution systems around the world have a significant penetration of DG. In United States, the capacity of DG resources has increased from 9579MW in 2004 to 22636MW in 2008 [11]. In the U.K, installed capacity of DG has grown from 1.2 GW in 1993/4 to over 12 GW in 2008 [12]. Denmark has experienced a vast growth in distributed generation since the late 1980s. Two kinds of DG technology mainly wind turbines and small gas turbines based combined heat and power plants are used in Denmark. About one half of the electricity production capacity in west Denmark is equally dominated by these two types of DG units [13]. Denmark has always promoted renewable energy and decentralized generation as a part of its liberal energy policy and has also set targets for integrating more renewable energy in the years ahead. A 30% share of renewable energy is targeted in the Danish energy supply by 2020 [14], [15].

The European Union has set a target of 20% energy from the renewable sources by 2020. The electricity generation from the renewable source based DG isexpected to rise to about 1,280 TWh/yr in 2030 from 490 TWh/yr in 2005 and the share ofthe electricity generation in the gross total electricity generation to increase from about 15% to approximately 26% during the same timeframe[16]. A considerable portion of these renewable source based generating units will be smallgenerating units connected to distribution systems. However, the increase in the popularity of DG isnot only due to environmental concerns but also due to various other benefits.

The overall cost of power production by using DG units is low as compared to the conventional power plants. According to the International Energy Agency (IEA), such kind of the production could result in cost savings in the transmission and the distribution of about 30% of the electricity costs [17]. A significant penetration of DGs has opened the doors for the operation of the distribution system in islanding in order to improve the reliability. DG units can be used to deliver the active and the reactive power in case of islanding in order to control the voltage and the frequency of the islanded distribution network.DGs can also be used to deliver the power at the time of peak loads when the electricity prices are high which might be helpful to reduce the electricity cost of the customers [18].

The major focus is on the DG units such as small WTG, photovoltaics and energy storages in this research study. The basics of each type of DG units are described below:

1.1.1 Basics of the Wind Energy Generations

Wind energy is clean and sustainable. It is one of the fastest growing renewable energy resources. The term wind power describes the process by which the wind energy is converted into the electricity. The conversion of kinetic energy of the wind energy involves aerodynamics, mechanical system, electrical systems and power system. A wind turbine is an electromechanical device which converts kinetic energy from wind into electrical energy [19], [20]. The turbine power P_T is given by the following equation:

$$P_T = 1/2 * \rho * C_p * \pi * R^2 * V^3 \quad \ldots\ldots\ldots\ldots\ldots\ldots\ldots\ldots\ldots\ldots\ldots\ldots\ldots\ldots\ldots\ldots\ldots\ldots\ldots\ldots\ldots\ldots \quad (1.1)$$

Where, ρ is the air density, R is the turbine rotor radius; V is the wind velocity and C_p is the power coefficient. According to equation 1 the turbine power is directly proportional to the cube root of wind velocity.

Installed wind power capacity has been progressively growing over the last two decades. Fig. 1.2 shows the growth the installed wind power capacity world wise as of 2012 [21]. Installed global wind power capacity has been increased from approximately 6.1 GW in 1996 to 283 GW by 2012 as shown in fig. 1.2. Fig. 1.3 shows the cumulative installed wind capacity of the wind power in top ten countries of the world as of and 2012 [21].

Wind turbines are available in a variety of sizes and power ratings. Small wind turbines from few kilowatts are used for residential or commercial purposes and large turbine are used for the industrial purposes. The evolution in the wind turbine size can be clearly depicted in fig. 1.4. It can been seen in fig. 1.4 that the wind turbine available in early 1980 was that with 50 kW power rating and 15 m rotor diameter. The wind turbines can be found today up to 7.5 MW with a rotor diameter of 126 m.

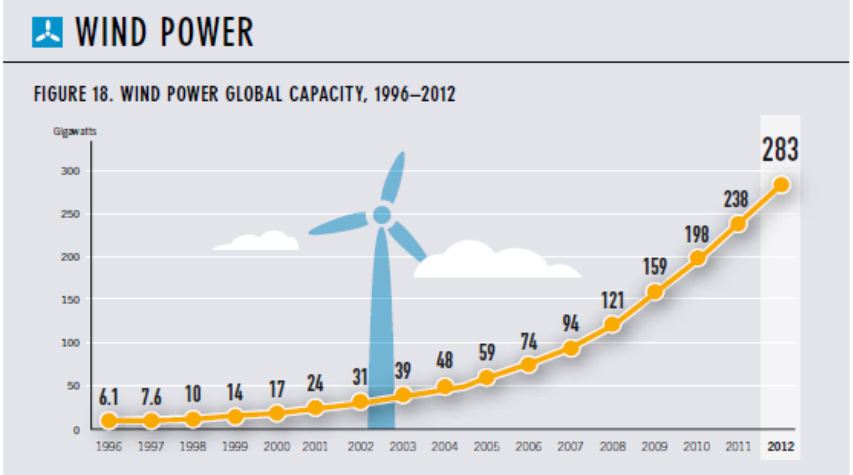

Fig. 1.2 Global annual and cumulative installed wind power capacity [21]

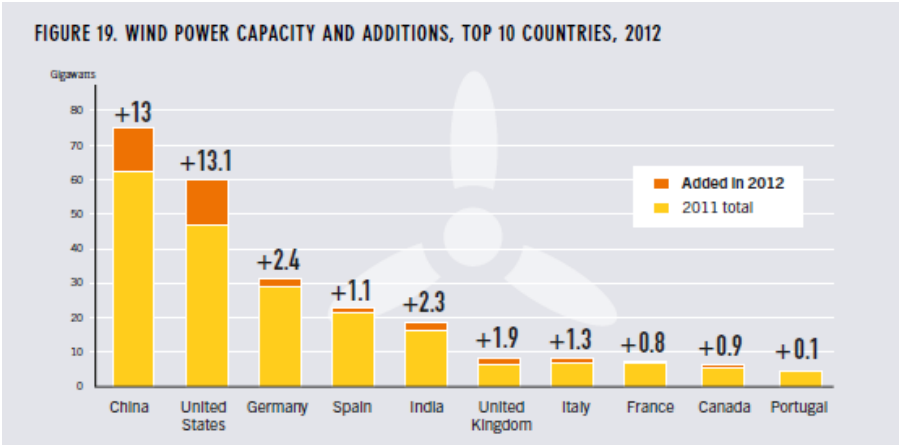

Fig. 1.3 Installed wind power capacity of top ten countries as of 2012 [21].

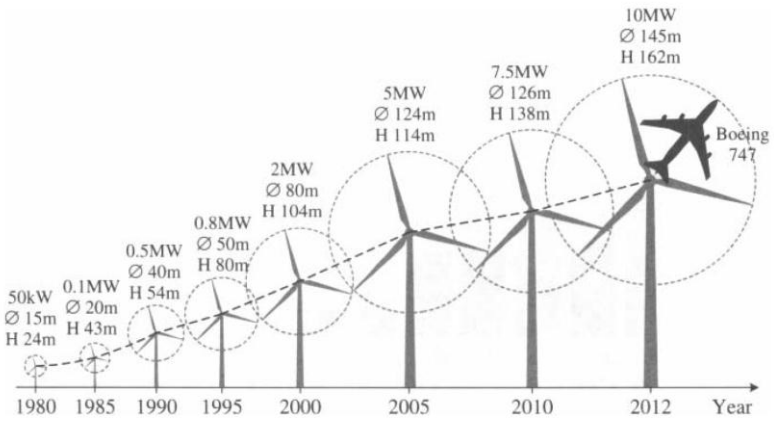

Fig. 1.4 The evaluation of the wind turbine size (Ø: Rotor diameter, H: Tower height [20]

Wind turbines can be classified into fixed-speed and variable speed turbines [22]. The fixed speed wind turbines operate at almost constant speed of the rotor whereas variable speed wind turbines rotate at a wide range of the speeds. The squirrel cage induction generator can be used for the fixed-speed wind turbines whereas Doubly Fed Induction Generator (DFIG) or Permanent Magnates Synchronous Generators (PMSG) can be used for variable speed wind turbines. The main advantages of variable speed wind turbines over the fixed-speed wind turbines are the good controllability of power as pitch angle controller is used to regulate the power output in case of wind variations, improved power quality and reduced mechanical stresses [23]. The main disadvantages are the increased cost and more power losses because of inclusion of a power converter. As this study is about large scale integration of small sized DG units; the fixed-speed wind turbine is used for this study.

1.1.2 Basics of Photovoltaic Generation

Photovoltaic (PV) generation system is becoming quite famous among sustainable generations due to many advantages such as no fuel cost, no pollution, no noise and less maintenance requirement. PV cells are composed of semi-conductor devices which converts solar energy directly into electrical energy. In simple words, a PV cell can be explained as a two terminal device that conducts like a diode in dark and produce photo voltage when illuminated by light. This voltage drives the current through an external circuit and thereby produces power [24].

The installed PV power in 2009 was 6.4 GW which is equivalent to approximately one-sixth of the installed wind power. The forecast for 2014 is 30 GW for PV, close to the 28.7 GW for Wind Power (WP) forecast 6 years ago (for 2008) [25]. The worldwide PV power has reached to 100 GW by the end of year 2011 as shown in fig. 1.5 [21].

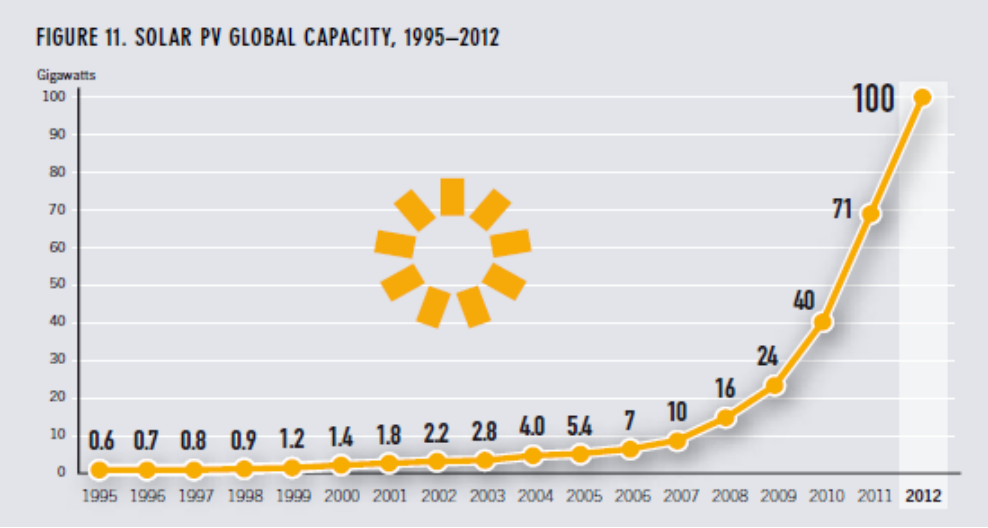

Fig. 1.5 PV power installed worldwide by 2011 [21].

Today, there are several PV parks installed in Spain, Germany and Portugal. The Penetration of PV power is quite low but it is estimated by European Photovoltaic Industry Association (EPIA) that it could be as high as of 20% in 2020.

An ideal PV cell represented as an ideal dc-current source connected in parallel with a diode is shown in fig. 1.6. The current source represents the current generated by PV cell as a result of photons falling on its surface. This current is dependent on the amount of solar irradiation. In the absence of light, the PV cell behaves like a diode.

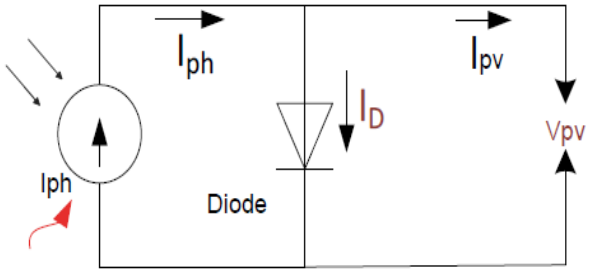

Fig. 1.6 Equivalent circuit of an ideal PV cell [24]

As the power output of PV cell is DC, a Voltage Source Converter (VSC) is used to converter DC power into AC power. PV inverters operate in a certain range of voltages. If voltage goes beyond limits, it will stop its operation [26].The inverter is used to regulate the AC and DC-link voltages of the network and this is done by developing a suitable control system for the specified PV inverter. The development of the control system for PV inverters will be described later in the text. Most inverters of PV systems include isolation transformer wheregalvanic separates the AC and DC circuits [27]. The current trend in the modern power system is towards the use of the transformer-less PV inverters. The advantages of the transformer-less inverter over the inverters using transformers include improved efficiency (i.e. 2% more efficient than with the inverters using transformers), low weight and low cost [28]. The transformer-less PV inverters are used for the PV generating units in this research.

1.1.3 Basics of Energy Storage System

The power output of Renewable Energy Source (RES) based DGs is difficult to predict due to their intermittent nature. These fluctuations in the power might result in variations of the network voltage and the frequency because of the imbalances between the power generations and the load consumption. It is very important for any power system, including stand-alone systems to maintain power quality at the specified levels. The restoration of the voltage and the frequency in the network are the most important in this regard.

In order to maintain the voltage and the frequency within the prescribed limits, a popular technique is the utilization of the Energy Storage System (ESS). The storage devices are used for the regulation of the power

networks and enable the penetration of DG units both in the grid connected or stand-alone systems and ensure the increased penetration of DGs. The ESS can store surplus power produced in the grid and can release the energy into the electricity grid in the case of generation deficit. This property of ES systems can smoothen the short term as well as long-term variations in the power caused by DG units and could also provide PQ control functions and behaves like power system balancing and reserve units. Fig. 1.7 presents comparison of various electricity storage technologies based their power ratings and storage duration [29].

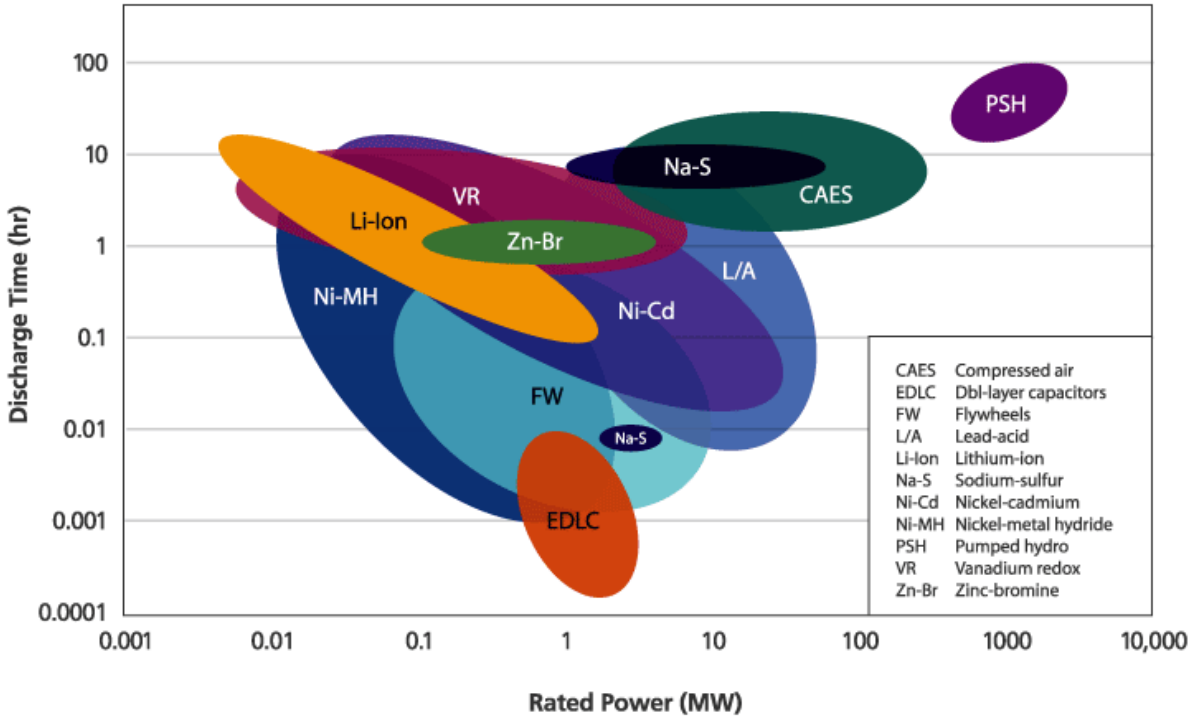

Fig. 1.7 Comparison of electricity storage technologies based on rated power and storage duration [29]

The Pumped Hydro Storage (PHS) and Compressed Air Energy Storage (CAES) are large-scale storage technologies in terms of power and energy capacity. The flow batteries like vanadium redox and zinc-bromide have the characteristics of longer storage duration compared to the typical electro-chemical batteries. However, this technology has some disadvantages such as high capital and the running cost [30].

The storage technology based on the battery principles are used in this research. The lead acid batteries are the most mature technology among the electrochemical batteries. Some of the largest battery storage plants installed include 20 MW, 14MWh (lead acid) at Puerto Rico, and a 27 MW, 6.75MWh (nickel cadmium) at Alaska are used for the spinning reserve, voltage and frequency control applications [30], [31]. Compared to these batteries, the Lithium-ion batteries have dominating characteristics because of higher storage efficiency and high storage capacity [32].

1.2 Problem Statement

Power Quality (PQ) is one of the main objectives of the power system. It is the aim of the utilities to continuously deliver the power to the customers at the constant voltage and constant frequency. The intermittent and uncontrolled nature of the renewable energy sources cause problems with the quality of the power. This quality related problems include disturbances in the voltage, oscillations in power flow through the lines etc. The disturbance in the voltage can cause the disconnection of the sensitive equipment and may lead to huge economical loss due to the damaged products. Most of DGs such as Wind power, Photovoltaic etc. employ VSCs for their operation. The inverters are very sensitive to voltage disturbances. A disturbance in the voltage can cause disconnection of the inverters from the grid that leads to the loss of energy. Due to this reason the role of Custom Power Controllers (i.e. the power electronics based controllers used in distribution network) is increasing day by day. Some of the issues concerning DG have been discussed in [33-35].

The DGs can have a transient effect on the voltage level. Let's take the example of the WTG working as DG unit. The WTG produces power when the turbine is rotating at nominal wind speed. The WTG stops producing the power in the case when wind speed exceeds the cut out speed. The grid sees this sudden loss of power as a transient effect on the voltage which might leads to voltage sag. Voltage Sag (VS) defined by IEEE standards 1159-1995 is the reduction in the value of RMS voltage between 0.1 to 0.9 p.u at the power frequency with the duration from 0.5 cycles to 1 min; this represents one of the most important causes of poor power quality [36]. The modern power industry comprises Voltage Source Converter (VSC) based equipments which are very sensitive to voltage sags/swells. Sag or swells in the voltage may cause tripping of such sensitive equipments which can cause damage to the production of plants. This may lead to huge economical loss.

Voltage unbalance is also one of PQ related problem. Voltage in power system; can be unbalanced due to the several reasons. One of the major reasons of the voltage unbalance is an uneven distribution of single phase loads that draw unbalanced currents from the system [37], [38]. These unbalance currents will create unequal heating in each of the phases which creates unbalance heating in cables and other parts of the network, which might reduce the life time of the cables and other components [39], [40]. Another reason for voltage unbalance is due to unbalanced faults. The unbalance in the voltage due to this reason is severe. A recent survey about PQ problems based on interviews and web based submission, conducted over a two-year period in 8 European countries has been presented in [41]. The cost of wastage due to poor PQ has been presented in this survey report.

The significant penetration of DG units presents complexity in the protection of the power network due to bi-directional flow of the current and different short circuit power. The protection of the network with DGs in modern power network is challenge for the protection engineers. The study about the protection of the network in the case of DGs is presented in literature [42-45].

The availability of DGs is a favorable condition to operate the distribution network in islanding.Apart from the improved reliability, islanding operation can be helpful to improve the overall security in the distribution network. As for the customers, the main benefit of islanding is the reduction of voltage sags and interruptions from the outages which appears in the distribution and the transmission systems. It was common practice in power network to shut down all DG units once the distribution system is islanded. IEEE-1547-2003 standards requires islanding to be detected and DG be disconnected within 2 seconds [46]. Similarly, IEC 61727 also require islanding detection and DG disconnection at most within 2 seconds [47].With the sufficient availability of the DG penetration in many distribution networks, the practice of disconnecting DG units after islanding is no longer anobvious solution.

The overall object of this study is to model and analyze the CIGRE LV distribution network with the large scale integration of DG units including small WTG, PV units, batteries etc. This is done in order to operate the distribution grid in the stable and the controlled manners meeting the load requirements both in grid connected and islanded mode. The hypothesis of this research study is given below:

- It is necessary to control the voltage of the distribution network by injecting or absorbing the reactive power in stationary, transient and islanded conditions.
- The control of the reactive power is needed to achieve the maximum power transfer capabilities of the power generating units, reduce line losses and to improve the power factor of the DG units in the CIGRE network.
- It is also desirable to mitigate the voltage sags (i.e. balanced and unbalanced) and the problems of voltage unbalance in the CIGRE network.
- The control of active power is achieved by matching load-generation balance in CIGRE network by using DG units in the grid connected and islanded conditions. It is needed for the control of the network frequency.
- The protection of the different components and the equipments in any network is the prime requirement of the modern power industry. The issues concerning with the protection of different components of the CIGRE network including inverters, the power generating units, cables, bus bars etc. needs to be investigated in order to operate the network in the secured manners.
- Islanding is used to improve the reliability of the power networks. The main problems concerning islanding such as island detection, the voltage and frequency control needs to be tackled.
- Although islanding improves the reliability of the power networks, however the reliability in case of the grid connected conditions is more than islanding. Due to this reason, it is essential to reconnect the islanded distribution system with the transmission grid.

The problems of the PQ due to the integration of DG units such as voltage/power fluctuations, voltage unbalance, voltage sags (i.e. balanced and unbalanced), issues related to the protection of the distribution

network has been addressed in this dissertation. The solution for such kind of PQ related problems have been presented and some of the controllers have been developed in order to tackle such kinds of the problem. The issues related to islanded operation of the distribution system in case of DGs penetration have also been presented in this study.

1.3 Research Objectives

As described in the previous section that PQ of the distribution network is affected with large scale integration of DG units and also by some of the transient conditions. Apart from the PQ problems DG creates problems with protection of the network. Therefore, the overall objective of this research is to monitor and control such kinds of the issues. The whole research is divided into different case studies and simulations are performed using DIgSILENT power factory software version 15.0. The main objectives of this research study are as follows:

1. To develop control techniques which can be helpful to tackle problems of voltage fluctuations due to the stochastic nature of DGs in the grid connected mode.
2. To develop control strategies which can be helpful to mitigate the problems of voltage sags (i.e. balanced and unbalanced) and voltage unbalance.
3. To solve problems with over current protection of the distribution system and to develop the protection in different parts of the network by ensuring the correct operation of the protection devices in both the directions (i.e. grid side and DG side).
4. To develop an effective state detection technique which should correctly identify when the distribution system is islanding (i.e. Islanding detection) and when distribution system is reconnected (i.e. Grid reconnection detection).
5. To develop a control strategy which ensure the correct transition between different modes of the operation and to ensure the constancy of the voltage and the frequency within the PQ limits in an islanded distribution system.

1.4 Project limitations

The limitations of this research study are as follows:

1. This study is only limited to investigate the behavior of the CIGRE network with a significant penetration of the DG units and other protection issues in the same network. The similar research study and the methodologies can be implemented in many other distribution networks comprising large share of renewable energy based DG units.
2. This study is only performed at 400 V systems, the issues related to the DGs at the MV are not considered.

3. The models have been developed in DIgSILENT power factory software version 15.0 and many of the standard models available in DIgSILENT have been used.
4. A DC-current source model available in DIgSILENT power factory software is used to represent the solar PV generating unit. The detailed model of PV units showing temperature effects and solar tracking effects has not been developed.
5. An infinite DC-voltage source model available in DIgSILENT power factory software is used to represent battery energy storage system. The characteristics of battery charger ratings are not accounted in the battery storage model in this study.
6. The grid is considered to be strong in this study.
7. The financial issues related to the network protection and island detection have not been covered in this research.

1.5Main contributions of the thesis

The main contributions of the thesis are summarized below:

1. Modeling of the CIGRE low voltage network together with the control system for PV solar generating units based on the STATCOM principles.The purpose of the PV-STATCOM controller is to regulate AC and DC-link voltages in distribution network.
2. A methodology to compensate the voltage and the power disturbances in the distribution network due to uncontrolled and intermittent nature of DGs.
3. Astudy about mitigation of symmetric voltage sags.
4. A study about mitigation of asymmetric voltage sags and voltage unbalances.
5. Development of protection system for the distribution network against symmetric and asymmetric faults.
6. Amethodology to control the voltage of the CIGRE low voltage test network for the grid connected and islanded system.
7. A methodology to control the frequency of the CIGRE low voltage test network for the islanded system.
8. The methodology to control the voltage and the frequency of the islanded MG in case of load step changes and the sudden loss of the generating units.
9. A methodology to study about the reconnection detection
10. A study about the grid reconnection and synchronization of the two systems (i.e. Transmission and the distribution system)

1.6 Outline of the thesis

The PhD contains seven chapters and two appendixes. It is organized as follows:

Chapter 1: Introduction

This chapter presents the evaluation of the DG markets. The basics of some renewable energy based DG units used in the CIGRE network (i.e. WTG, PVs, energy storages etc.) together with the grid integration issues have been described in this chapter. The objectives, scopes, limitations and main contribution of the study are also presented in this chapter.

Chapter 2:Modeling of CIGRE Low Voltage Distribution Network and the development of appropriate controllers for grid connected applications

The CIGRE LV distribution network comprising DG units has been used as a test network for this study. The different components of the CIGRE network are introduced in this chapter. The modeling of the all components of the CIGRE network has been performed in this chapter. This chapter also describes the development of appropriate controllers concerning the DG units in the CIGRE network.

Chapter 3:The behavior of Distribution grid with DG integration under stationary, dynamic and transient conditions and voltage control

The uncontrolled nature of the DG units causes the problems with the network voltages and creates the oscillations in the power output of the DGs. This chapter presents the methodology to control the voltage and the oscillations in the power output of the DG units due to stochastic changes in weather. The faults in power system networks create problems of voltage sags. The study about the CIGRE network in the transient conditions and mitigation of voltages sags (i.e. balanced and unbalanced) and voltage unbalances have been also performed in this chapter.

Chapter 4:Short circuit protection of CIGRE Low Voltage Distribution Network

When a distribution system changes states from a grid connected condition to an islanded condition or vice versa, there is a significant difference in the fault power. This chapter presents the protection of the CIGRE network against three phase and single phase to ground fault. This study includes the protection of cables, bus bars, loads, inverters, DG units etc. The study about the over speed protection of the WTG in case of loss

of grid due to the faults is also presented in this chapter. This chapter presents some of the problems concerning the protection of the network by using current based protection devices such as fuses and proposes the voltage based protection is this network in some conditions when current based protection devices fail to operate and causes large delay in their operation.

Chapter 5:Island operation of distribution grid with Distributed Generations

The problems concerning islanding such as islanding detection, voltage and the frequency control has been solved in this chapter. The development of the controller which works in island mode is described here. The control of the voltage and the frequency in the islanded MG in case of the step load changes and the sudden loss of DG unit(s) have been also presented in this chapter.

Chapter 6: Grid Reconnection

This chapter presents some criteriato reconnect energized islanded distribution system back to the transmission grid. Agrid reconnection detection based on the synchronization of the voltage, frequency and phase angles of the two systems has been also presented in this chapter.

Chapter 7: Conclusions and future work

Some conclusions have been presented in this chapter. The contributions of this research study have been also presented here. This chapter proposes some of the works which can be done in the future with reference to the work presented in this research.

Appendix A

It presents data for the different components of the CIGRE test distribution system such as cables, inverters, WTG, etc. and it's concerning models. Some of the data concerning protection devices which are used to protect the different components of the CIGRE network are also presented.

Appendix B

The inverse time current characteristics of some fuses uses in the CIGRE network are presented with the help of figure in this appendix.

Chapter 2

Modeling of CIGRE Low Voltage Distribution Network and the development of appropriate controllers for grid connected applications

2.1. Introduction to the CIGRE low voltage distribution network

A test distribution network set up by CIGRE comprising Wind Turbine Generator (WTG), PV solar generation units and energy storages devices has been chosen for this study. The single line diagram of this distribution system is shown in fig. 2.1.

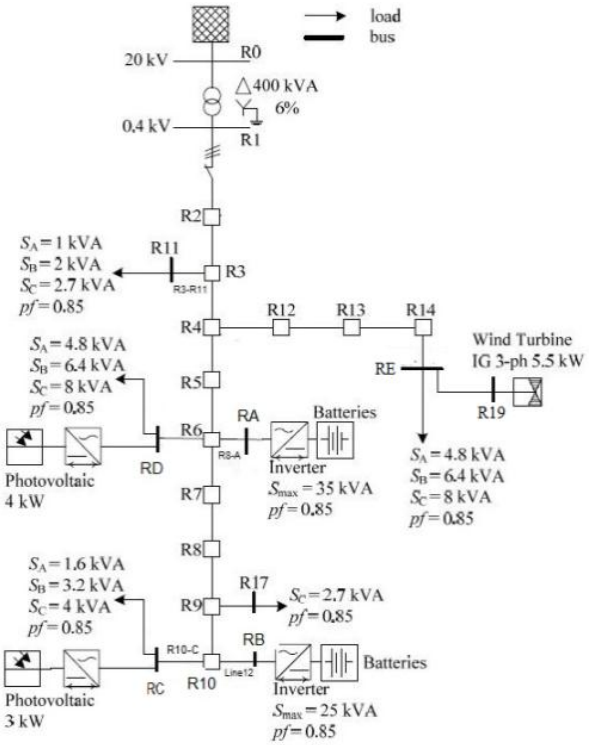

Fig.2.1 CIGRE distribution system test network [48]

In this network, there are two PV solar generation units of 3kW and 4kW connected at bus RC and RD, respectively. There is one fixed-pitch fixed speed wind turbine generator of 5.5 kW connected at bus R19. The power factor of the WTG is 0.91 and a capacitor bank is used to operate this machine at unity power factor.There are two batteries 30 kWh and 21 kWh, employing VSCs of 35 kVA and 25 kVA, both operating at the power factor of 0.85 and connected at bus RA and at bus RB respectively. All these DG units are integrated into the main power grid through a 0.4MVA, 20/0.4kV delta-star-grounded three-phase distribution transformer. Unbalanced loads are aggregated at the 0.4 kV voltage levels and are connected at bus RC, RD, RE, R11 and bus R17. The power is delivered to the loads by distribution cables. The detailed data concerning cables is given in table A1 in appendix A. The short circuit power of the main power grid is

considered 500 MVA and is assumed to be strong grid in this study. The CIGRE report has also provided daily load profile pattern of the distribution network [48] as shown in fig. 2.2. The profile shown in fig. 2.2 is for the residential, industrial and the commercial loads but the network under this research as shown in fig. 2.1 only uses the residential load profile.

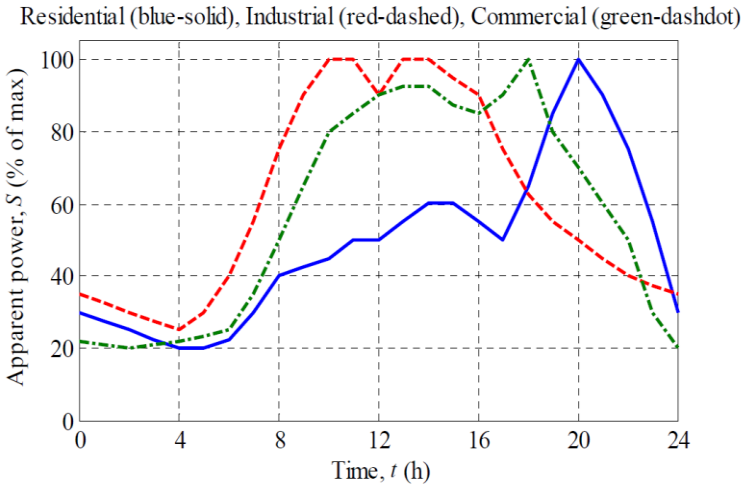

Fig.2.2 The daily load profile pattern of the distribution network [48]

Two inverters named VSC1 and VSC2 are used for the battery applications whereas other two VSC3 and VSC4 are used for PV applications. The power and voltage ratings of the inverters used in the network are shown in table. A2 in appendix A. The inverters mentioned in table A2 are used to provide the active and the reactive powers in order to control the voltage and the frequency at the same time. The power ratings of VSC3 and VSC4 used for the PV applications are chosen bit higher than the PV power because they have to counteract problems of the voltage at their AC terminals during fluctuations of the solar irradiance and are also responsible to provide compensation against voltage sags.

2.2 Modeling of the CIGRE network grid and its components

The CIGRE network is modeled in DIgSILENT power factory software package version 15.0 by using built-in and DIgSILENT Simulation Language (DSL) models. The built-in models are available in the DIgSILENT library and the DSL models are developed based on mathematical equations. The modeling of some of the electrical components of the CIGRE network such as transformer, grid, cables, bus bars, loads etc. is simple and further details can be found in the literature [49]. The standard built-in models available in DIgSILENT library are used to model the above mentioned components and are therefore not described here. Adetailed description about modeling of the DG units such as the WTG, PV units, Battery Energy Storage System (BESS) together with the development of appropriate control system is presented in this chapter. The modeling of the stochastic nature of DG units as well as the modeling of load fluctuations is also described here.

2.3 Modeling of Wind Turbine

The primary components of the WTG for modelling purpose are the turbine rotor (prime mover), a shaft and gearbox unit and an electric generator. During implementation of the wind turbine generator model in DIgSILENT, different built-in models are used for the WTG components, e.g. generator and capacitor. The procedures of modeling the WTG are available in various literatures [49-51]. The WTG is modeled according to [52] as a fixed pitch and fixed speed wind turbine in this case. The simplified block diagram of the fixed-speed fixed pitch WT model is shown in fig. 2.3.

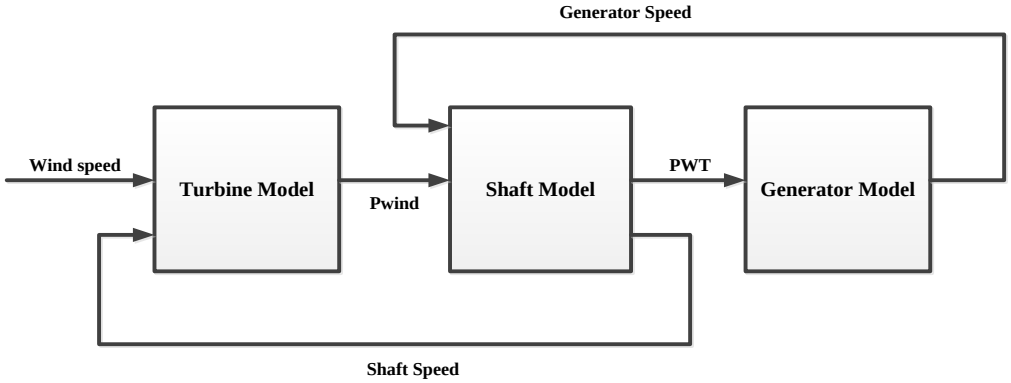

Fig. 2.3 The simplified block diagram of WT model

The wind speed is the input to the turbine model as shown in fig. 2.3. It uses wind speed and produces the output signal Pwind (i.e. the power available in the wind) and is given by the equation 1.1. It is input to the shaft model which generates the aerodynamic torque in the shaft and thereby produces P_{WT} (i.e. power from wind turbine to the generator or the mechanical power). The aerodynamic torque T_{rot} generated by wind and the mechanical power P_{WT} obtained at the output of the shaft are given by equation 2.1 and 2.2 respectively.

$$T_{rot}=\frac{1}{\omega_{rot}} C_p[\frac{\rho\pi R^2 V^3}{2}] \quad (2.1)$$

$$P_{WT}=\frac{\omega_{gen}}{n} T_s \quad (2.2)$$

Where, ω_{rot} is rotor speed, ω_{gen} is the generator speed and T_s is the mechanical torque on the low speed shaft of the machine.

The generator is used to convert the mechanical power into electrical power. The built-in model of the squirrel cage induction machine is used to represent the model of the generator in this study. The data concerning the electrical model of the squirrel cage induction generator is presented in table A3 in appendix A.

The stochastic wind speed can be modelled by using a measurement file, and use it as input for fig. 2.3. In DIgSILENT, a measurement file 'ElmFile' is used for the modeling of stochastic wind speed. A measurement file takes the data from the given 'text file' and delivers its value as a stochastic wind speed to the turbine model.

The variations in the wind speed modelled for 12 hours are shown in fig. 2.4. The wind speed data of 1st January 2009 for East Denmark given by DTU wind energy has been used here.

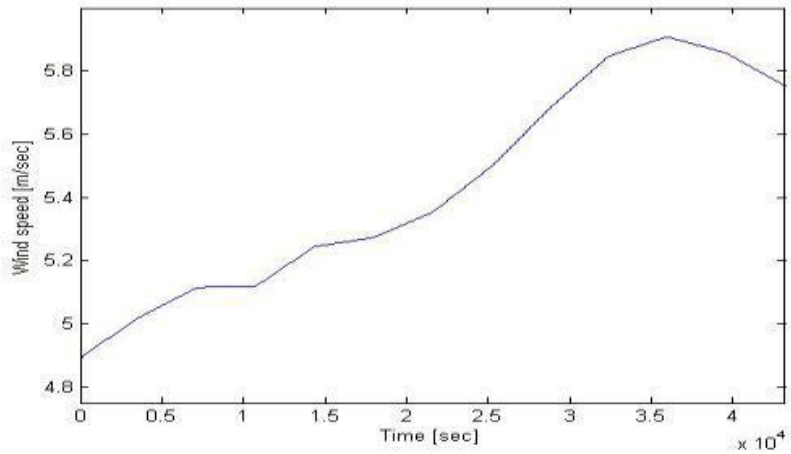

Fig. 2.4 Wind variations during 1st of January 2009 for East Denmark for 12 hours [53]

2.4 Modeling of PV Generator System

As the power output of the PV is current dependent, the solar cell can be modelled as a dc-current source [54]. Since the power output of the PV cell is DC, a VSC is used to convert DC power into AC power. The built-in model of a PWM AC/DC converter is used for the VSC in this study. Fig. 2.5 shows the equivalent circuit of the PWM inverter model representing the self- commutated voltage source converter. The circuit is built with valves with turn-off capability (Two dashes), which are usually realized by Gate Turn-Off thyristors (GTOs) or Insulated Gate Bipolar Transistors (IGBTs) [55].

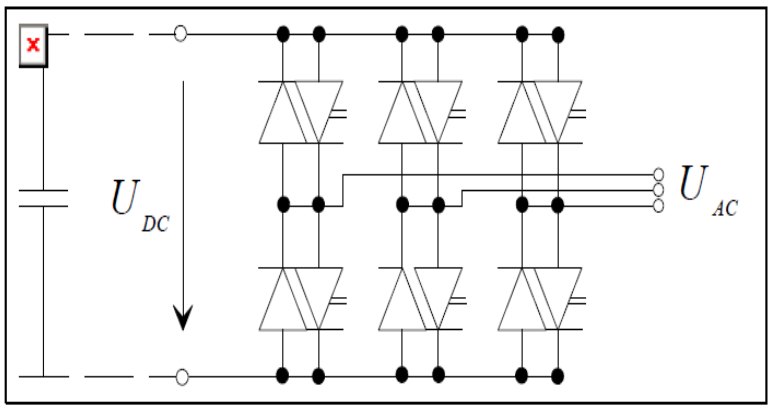

Fig. 2.5 Equivalent circuit of PWM inverter model [55]

The advantage of GTO thyristors is that it can handle more power than IGBTs. The disadvantages of a GTO inverter is that the inverter requires very complicated circuits to control its valves and that it has lower efficiency [56]. As this study is carried out for low power applications, IGBT is used here.

The DC-link capacitor is shown with a redsymbolwith the red color in the PWM inverter model in fig. 2.5 which means that this component is not part of this model [55]. The built-in model for the DC capacitor available in DIgSILENT library is used in this regard. The purpose of DC-link capacitor is to provide temporary injection or absorption of the active power in order to control the DC-link voltage of the inverter and thereby the power output of PV units.

2.4.1 Development of the control system for PV-STATCOM

The PV solar units used in this network are operated as STATCOMs and thereby named PV-STATCOM. The controller of the PV-STATCOM is used to regulate the AC and DC-link voltages of the distribution network. Such kind of controller is being developed in the university lab of Sarnia, Canada for a 10 kW PV system [57]. A cascade controller is used for the control of the VSC. It is comprised of an outer controller and an inner controller [58]. The selection of the outer controllers depends on the application. Here, STATCOM controllers for the PV applications are used for the voltage regulation. The block diagram of the cascade controller comprising outer controller and an inner controller for this application is shown in fig. 2.6.

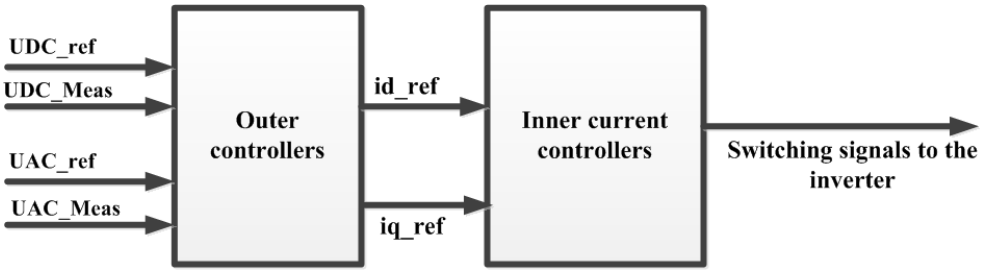

Fig. 2.6 Cascade controller for PV-STATCOM system

The cascade controllershown in fig. 2.6comprises outer controllers (i.e. one for AC and the other for DC voltage) and the inner current controllers (i.e. one for the d component and other for the q component of the current).The purpose of the outer controllers is to the regulate AC and the DC-link voltages of the VSC. The block diagram of the voltage controller which works as an outer controller is shown in fig. 2.7. This controller compares measured and reference values of the DC-link voltage and sends the error signal ‘dUDC’ to the PI controller which makes the error signal equal to zero [59] and thereby generates active current reference ‘id_ref’ as shown in fig. 2.7.

It also compares measured and reference voltages at the AC side of the VSC and sends error signal ‘dUAC’ to the PI controller responsible for the AC voltage control. This PI controller generates the reactive current reference (iq_ref) and decides the injection or the absorption of the reactive power.

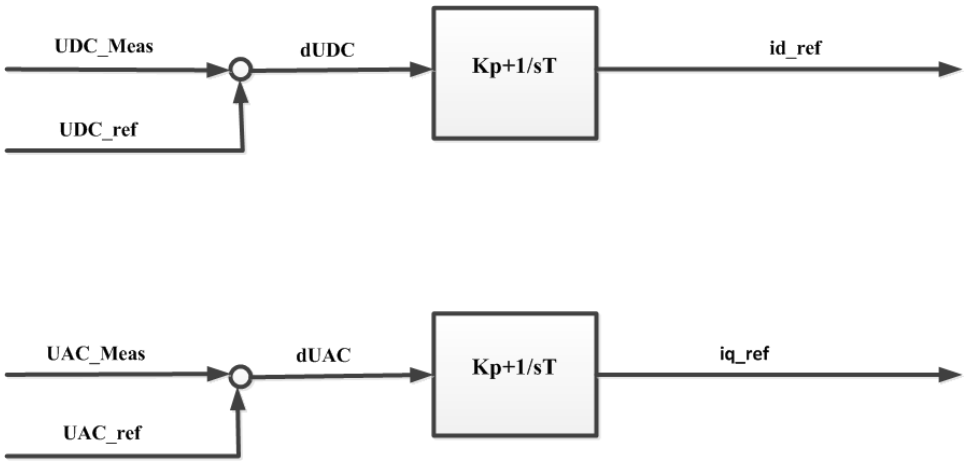

Fig. 2.7 The AC and DC-link voltage controllers of STATCOM

The inner current controller in general is faster than the outer controller and uses two PI controllers responsible for controlling the respective active and reactive currents. The block diagram of current controller is displayed in fig. 2.8. The working principle of this controller is follows:

- Three phase grid currents are measured at a certain point
- The three phase currents are transformed from the three-phase coordinate system to the fixed αβ-coordinate system and then to the rotating dq-coordinate system. The transformation angle is required to transform the quantities from the fixed αβ-coordinate to the dq coordinate system. This transformation angle is obtained by using a Phase Lock Loop (PLL) [58]. With the chosen PLL [58], the d-component of the current vector becomes the active current component (d-current) and q-component becomes reactive current component (q-current).
- The d and q components of the currents are compared with the reference value of the currents obtained from the outer controllers
- Two PI controllers one for the d component and other for the q component of the current are used. The difference of the d component and q components of the currents are sent to the respective PI controllers. The PI controllers calculate the voltage references for d and component of the voltage (i.e. ud_ref and uq_ref in fig. 2.8).
- The dq components of the voltage are then transformed into αβ-coordinate and then into the three-phase coordinate system.
- The three phase voltages are sent to the PWM block which calculates the duty-cycle [56] in the PWM block and sends the switching pulses the VSC valves.

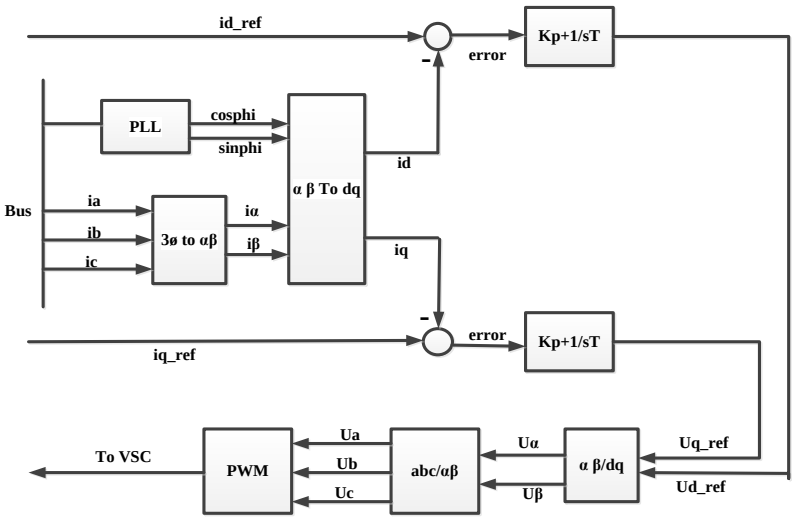

Fig. 2.8 The block diagram of the current controller [58]

2.5 Modeling of Battery Energy Storage System

The storage battery is a group of one or more electrochemical cells connected in series or parallel in order to stabilize the electrical distribution system. The Battery Energy Storage System (BESS) is incorporated with STATCOM named as BESS-STATCOM or E-STATCOM, which has both active and reactive power controllability. Most of the methods used for battery modelling are complex and time consuming [60-64]. The need for an accurate and complete battery model is dependent on the field of its application. A wide range of battery models are used for simulation studies in various literatures like mathematical, electrical or electrochemical models [65].

Electrochemical models are the most accurate and mainly used to optimize the physical design aspects of batteries and characterize the fundamental mechanisms of power generation. However, they are complex and time consuming [60]. Mathematical models use stochastic approaches or empirical equations which can predict efficiency and capacity. However, these models are often inaccurate (5-20% error) and have no direct relation between model parameters and the voltage-current characteristics of the batteries [61], [62].The most commonly used method for representing batteries in circuit simulations are the electrical models. The Thevenin-based model is the most generally used electric-circuit based representation of a battery in published research works [63], [64]. This model consists of an ideal voltage source in series with an internal resistance and a parallel RC network. The drawback of this model is an inaccurate estimation of the battery State Of Charge (SOC). The model in [66] discusses a typical thevenin model which can provide accurate battery SOC.

The BESS-STATCOM in this work is modeled using a thevenin equivalent representation of the Lithium ion battery and is shown in Fig. 2.9 [67], [32]. The thevenin-based model is the most generally used electric circuit based representation of a battery in the published research works [67], [32]. This model consists of an ideal voltage source in series with an internal resistance and a parallel RC network.The specification of a

single cell of lithium ion battery shown in table A4 in appendix A is taken from [68]. The built-in model of an infinite DC voltage source is used for the modeling of the BESS in DIgSILENT power factory software version 15.0 [69].

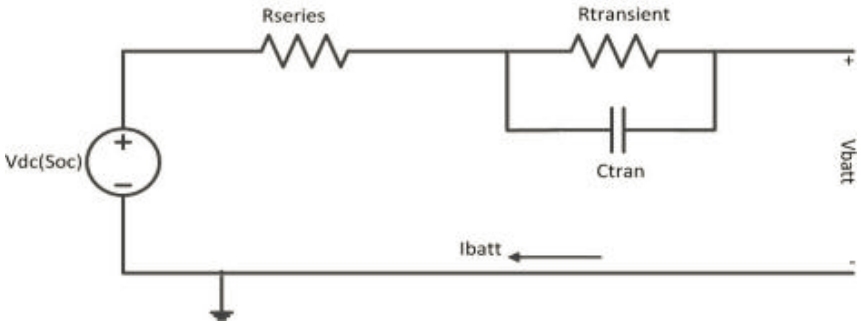

Fig. 2.9. Electrical model of the Lithium ion battery [67], [32]

In order to obtain desired amount of power output from the battery1, 170 cells have been connected in series and 6 cells in parallel. The total capacity of battery1 in this study is 42 Ah (i.e. 7 Ah* number of parallel connected cells). The maximum and minimum voltage of the battery is 714 V (i.e. 4.2* number of series connected cells) and 425 V (i.e. 2.5* number of series connected cells) respectively.

As the power output of the battery is DC, an inverter is used to convert DC power into AC power. The same model of PWM inverter which is shown in fig. 2.5is used in this case as well.

2.5.1Development of the control system for BESS-STATCOM

In order to control the voltage at the Point of Common Coupling (PCC), reactive power and charge/discharge rate of the battery, it is necessary to develop its controller. The block diagram of the control system of battery storage is shown in Fig. 2.10.

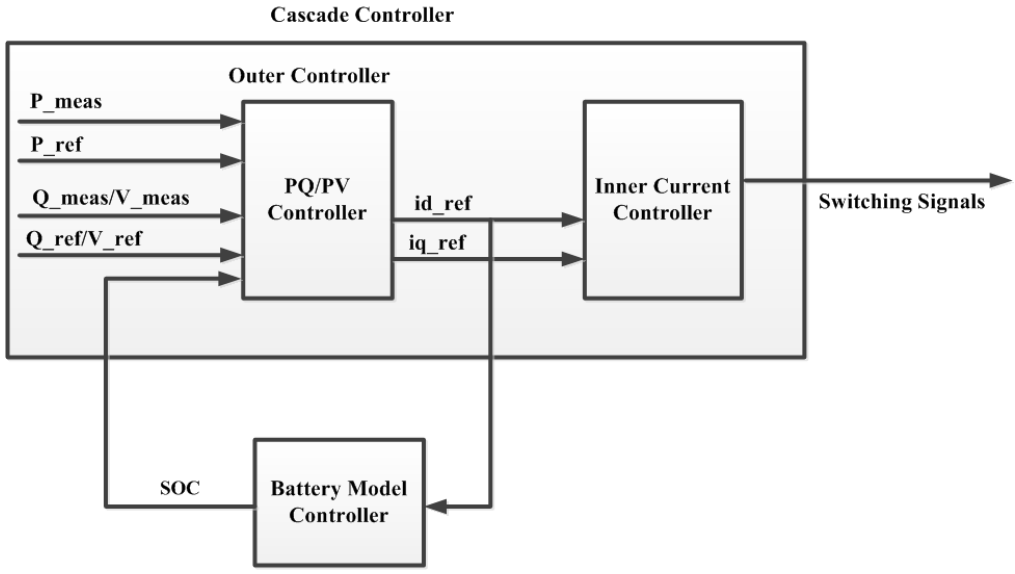

Fig. 2.10 The block diagram of control system for BES system

The control system of the BES system shown in fig. 2.10 is a cascade controller employing outer and inner current controllers. The outer controller can either be a PQ or PV depending upon the application. If it is desirable to control the active and reactive power of the network, BES can use a PQ controller as the outer controller. On the other hand, if the requirement is to control the active power and voltage at the PCC then a PV controller is used instead of PQ. The PQ/PV controller which works as the outer controller is shown in fig. 2.11. This controller compares measured and reference values of the active power and sends the error signal 'dP' to the PI controller.The PI controller receiving 'dP' and 'SOC' as its inputs is designed in such a way that if there is mismatch between measured and reference active powers, the PI controller should generate the missing signal 'D' in order to make the error signal equal to zero [59] and if the state of charge of battery is outside of the limits of 20% or 95%, the output signal 'D' of the controller should be zero. This is in order to avoid damage of the battery and to preserve battery life and thus, the SOC is limited within 20-95% [32]. The limits (i.e. B_max and B_min) have been set in this PI controller in order to model the battery for obtaining the desired amount of the power. The output 'D' of the PI controller is sent to the charge controller block as shown in fig. 2.11 which controls the current in and out of the battery and decides it's charging and discharging rate.

It also compares measured and reference values of the reactive power or the voltage at the point of connection and sends error signal 'dQ/dU' to another PI controller. This PI controller generates the reactive current reference 'iq_ref'in order to control the flow of the reactive power through the lines or decides the injection or the absorption of the reactive power for the voltage restoration.

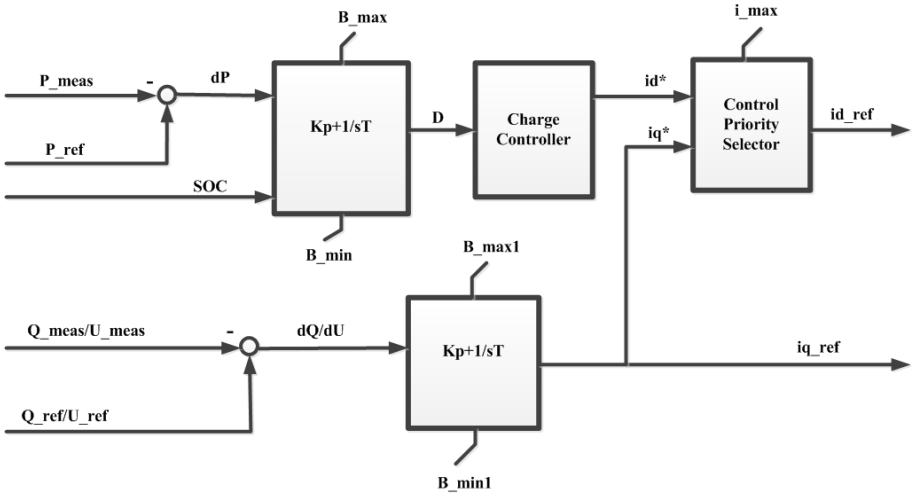

Fig. 2.11 PQ/PV controller of BES system

The share of the active and the reactive power from the PQ/PV controller is according to the equation 2.3 and equation 2.4 and depends on if the control system has been given the voltage control or the reactive control priority and is decided by the control priority selector block as shown in fig. 2.11.

$$id\_ref=\sqrt{i\_max^2-iq\_ref^2} \quad \text{(Voltage control priority)} \quad (2.3)$$

$$iq\_ref=\sqrt{i\_max^2-id\_ref^2} \quad \text{(Reactive power control priority)} \quad (2.4)$$

Where i_max lies between +-1 p.u. The control system of the battery inverter producing id_ref according to equation 2.3 is said to have the voltage control priority. If the inverter delivers 1 p.u of the reactive power then according to equation 2.3, the inverter has no more active power to inject (i.e. id_ref=0). A battery is said to be charged at its maximum rate if the control system follows equation 2.4. According to equation 2.4 if the inverter delivers 1 p.u of the active power, the inverter has no more reactive power. The inverter in this case operates in the reactive power control mode.

These currents references (i.e. id_ref and iq_ref) are the inputs to the current controller which decides the duty cycle for the switches used in the converter. The details of the current controller are described in section 2.4.1.

The battery controller block is also added in fig. 2.10. This block receives the active current reference (i.e. id_ref) from the current controller at its input and integrates it in order to get the State of Charge (SOC). The signal SOC is sent to the control block employing PI controller as shown in fig. 2.11 which in turn decides the amount of id_ref according to the value of SOC. This block makes the id_ref equal to zero if the SOC of the battery is either 20% or 95% [32]. The battery control block is shown in fig. 2.12 and the values of the parameters used in this control block are shown in table A5 in appendix A.

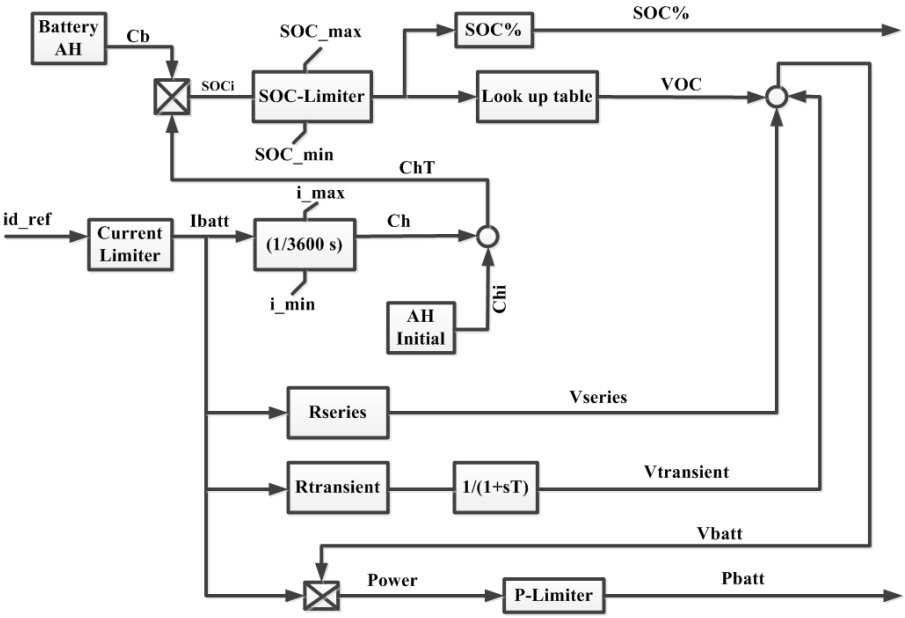

Fig. 2.12 The block diagram of the battery control model

The current in or out of the PQ/PV controller (i.e. id_ref) is integrated in order to give a relative charge 'Ch' which when added or subtracted (based on charging or discharging mode) to the initial charge ' Ch_i ' in ampere-hours, and gives the total charge 'ChT' of a battery as shown in equation2.5.

$$ChT=Ch_i+\int_{imin}^{imax}(I_{batt}).dt \qquad (2.5)$$

This quantity is further normalized to the battery capacity so that the state of charge lies between 20 and 95%. A lookup table is used for finding battery state of charge from open circuit voltage. The resultant battery voltage (V_{batt}) is obtained by combining series resistance voltage drop (V_{series}) and equivalent transient voltage response ($V_{transient}$) with the open circuit voltage (V_{OC}) as seen in equation 2.6.

$$V_{batt}=V_{OC}+V_{series}+V_{transient} \quad (2.6)$$

To get the power output (P_{batt}) of battery, the battery current (I_{batt}) and the battery resultant voltage (V_{batt}) is multiplied as seen in equation 2.7.

$$P_{batt}=I_{batt}*V_{batt} \qquad (2.7)$$

2.6 Modeling of load fluctuations according to CIGRE network data

The different unbalanced loads are used at the different busses in the CIGRE network as shown in fig. 2.1. The built-in model of three-phase loads available in DIgSILENT library as shown in fig. 2.13 is used to represent the load model in DIgSILENT.

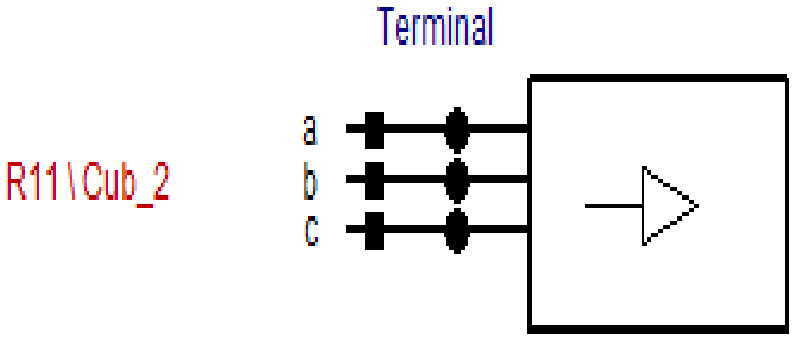

Fig. 2.13 The built-in model of three-phase constant impedance load connected at bus R11

To model three-phase unbalanced loads according to the CIGRE network data, it is necessary to develop a DSL model. The dynamic model with input definitions for General load is shown in fig. 2.15 [70]. As shown in fig. 2.14, the load model has Pext (Active power) and Qext (Reactive power) as its inputs.

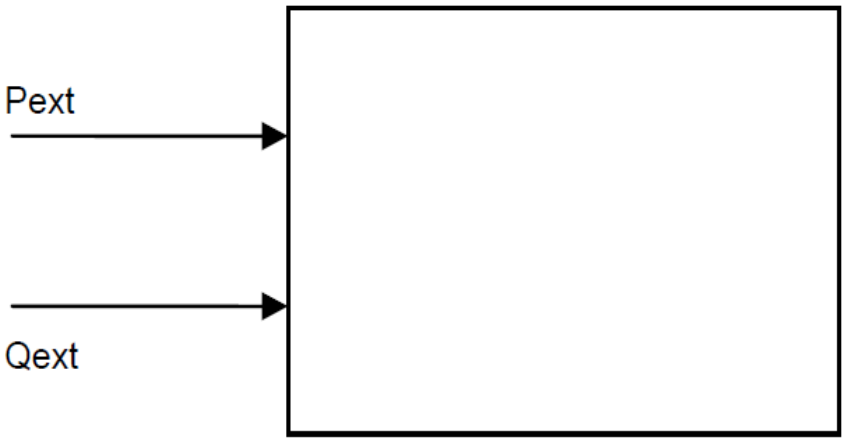

Fig. 2.14 Input definitions of General Load model [70]

The Pext and Qext only work for single-phase loads. Therefore, to model three-phase unbalanced load, 3 monophasic loads are used and each load is controlled through Pext and Qext separately. Fig. 2.15 shows 3 monophasic loads representing phase_a, phase_b and phase_c connected at the bus. The technology of the load is defined as 1-phase at the Basic Bata tab for the load type in DIgSILENT software.

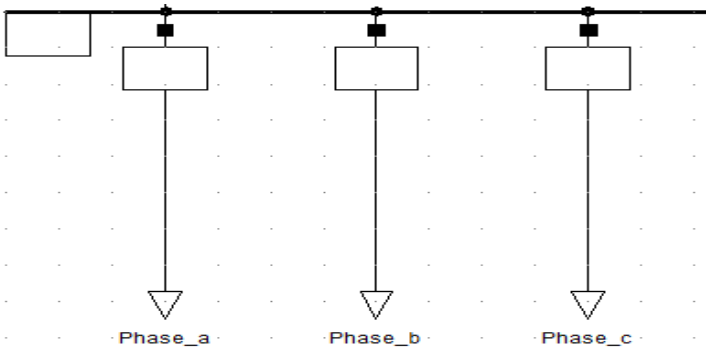

Fig. 2.15 Three monophasic load representation in DIgSILENT

The measurement file (ElmFile) is used for modeling of the three-phase unbalanced loads according to the CIGRE load profile as shown in fig. 2.2. The measurement file is used to measure active and reactive power data from the file [71] and sends the corresponding signals to load model. The composite frame model for the modeling of load fluctuations is shown in fig. 2.16. It can be seen in fig. 2.16 that the active and the reactive power of the load are defined by the measurement file.

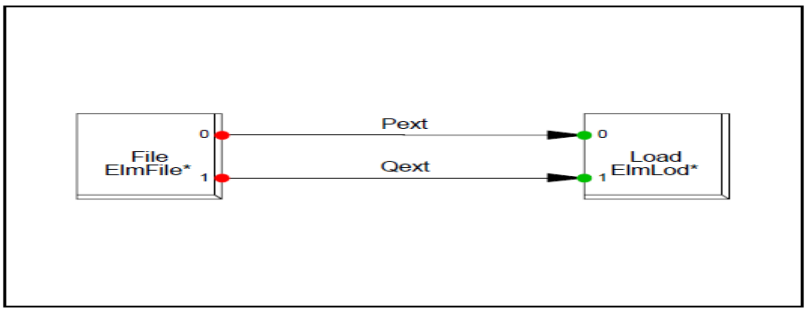

Fig. 2.16 The composite frame for modeling the general load [71]

Hence, all components of the CIGRE network have been modeled in DIgSILENT. The whole test distribution network modeled in DIgSILENT is shown in fig. 2.17.

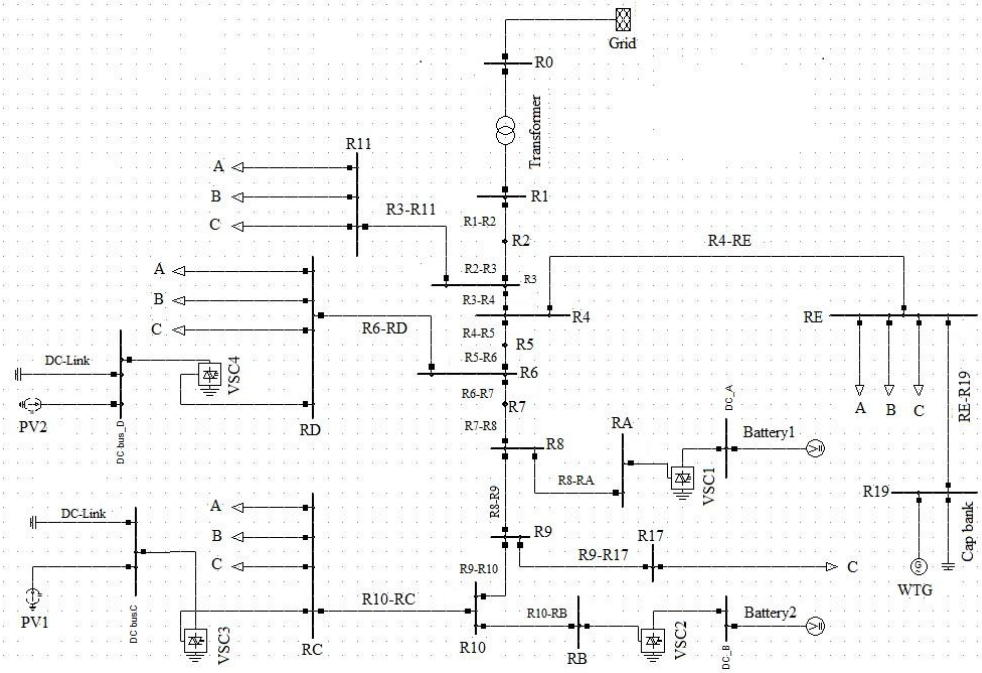

Fig. 2.17 The whole model of the CIGRE model developed in DIgSILENT power factory software

2.7 Summary

The different components are the CIGRE low voltage distribution network have been introduced and modeled in this chapter. The modeling of the CIGRE network is done in DIgSILENT power factory software version 15.0. The modeling of the WTG and wind fluctuations has been investigated in detail. The development of STATCOM controllers for PV applications hasalso been presented here. Finally, the control system of BESS-STATCOM together with SOC representation has also been developed in this chapter.

Chapter 3

The behavior of Distribution grid with DG integration under stationary, dynamic and transient conditions and the voltage control

3.1 Introduction

The integration of Distribution Generation (DG) units into today's distribution grid is increasing rapidly. The main promotion in their familiarity is because of favorable environment effects and some cost benefits [3], [4] etc. Since, the generation of these units is not constant due to their intermittent and uncontrolled nature; they present problems with the quality of the power. The quality related problems include the disturbances in the network voltage, oscillations in the power flow through the line, voltage sags/swells etc. The disturbance in the voltage might cause disconnection of sensitive equipments available in the power network which leads to huge economical loss. The bad quality of the voltage also results in damaged products inthe specific industries.

An increase or decrease in the voltage requires a desired amount of the reactive power to be absorbed or injected to counteract the disturbances. The flow of the reactive power through the lines/cables reduces the power transfer capability of the lines/cables and increases the flow of the current which leads to losses. It is therefore, necessary to control the voltage and reactive power of the distribution network in order to ensure stable operation of the system and operate the lines near to their safe thermal loadings. Custom power devices can be used in this regard [72]. Customs power devices are the power electronics based devices such as Dynamic Voltage Restorer (DVR), the Distribution Static Compensator (D-STATCOM) etc. The VSC is a main component in these kinds of devices. Benefits of using VSCs are sinusoidal currents, controllable reactive power to regulate power factor or bus-voltage level and independent control of active and reactive power [58]. This study is done by using D-STATCOMs and BESS-STATCOMs. The control system for these devices is described in chapter 2.

This chapter presents the introduction about the integration effects of DG units on power and the network voltage. It should be noted that the integration of DG unit(s) into the grid is done by using a 0.4 MVA, 20kV/0.4 kV DyN transformer. The neutral of the transformer is grounded with low impedance, (i.e. $Z=(0.0032+j0.0128)\Omega$ in this research study.Section 3.2 presents the validation of the developed controller in order to control the network voltage and damp the oscillations in the active power due to the variations in the weather conditions. The brief discussion about the importance of reactive power is given in section 3.3. The control strategy which is used to control the flow of the reactive power in the CIGRE network is described here and the simulation results are presented in this section. The study about the behavior of CIGRE network

in case of transient conditions is presented in section 3.4. The mitigation of voltage sags (balanced and unbalanced) together with the mitigation of the voltage unbalance in the network is described in this section.

3.2 The control of the voltage and the power output of DG units in case of stochastic changes in wind speed and the solar irradiance

The variations in the wind speed or fluctuations in solar irradiations have adverse effect on the voltage and thereby power out of DG units. In order to verify the performance of the controllers used in the network, simulation results are presented in the case of some events applied on the network.

At 30 s, the output power of the PV2 is reduced in order to simulate a reduction in the solar irradiation. The power output of PV2 in this case is shown in Fig. 3.1. Initially, PV2 is producing full power (i.e. 4 kW). Due to clouds the power of the PV2 is reduced to 0.4 kW at 30 s. As the power output of PV2 decreases, the AC and the DC voltagesat the terminals of PV2 inverter (i.e. VSC4) also decreases as shown in fig. 3.2.

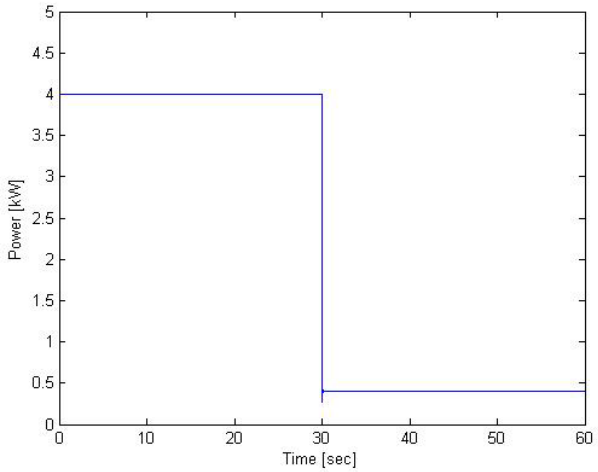

Fig. 3.1 Power delivered by PV2

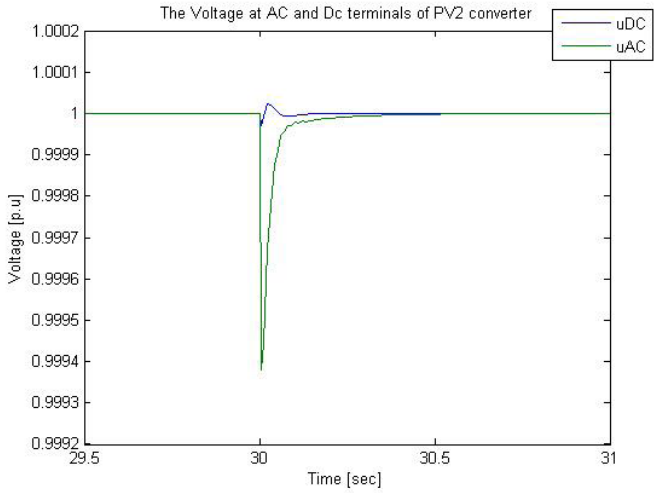

Fig. 3.2 Voltages at the AC and DC terminals of PV2 inverter

The AC and DC voltage controllers of the STATCOM controller developed as shown in fig. 2.7 are used to control the voltages at the terminals of VSC2. The voltage at the AC terminals of VSC2 is controlled if the desired amount of the reactive power is to be injected by the inverter. The reactive power produced by VSC2 is shown in fig. 3.3. It can be seen in fig. 3.3 that VSC2 deliver 14.6 kvar in the normal operating condition. This reactive power in the normal operation is used to meet the reactive power load demands and other minor disturbances due to load unbalances. When the voltage at its AC terminals decreases, it injects 18.13 kvar of reactive power in order to maintain the voltage to its pre-fault value.

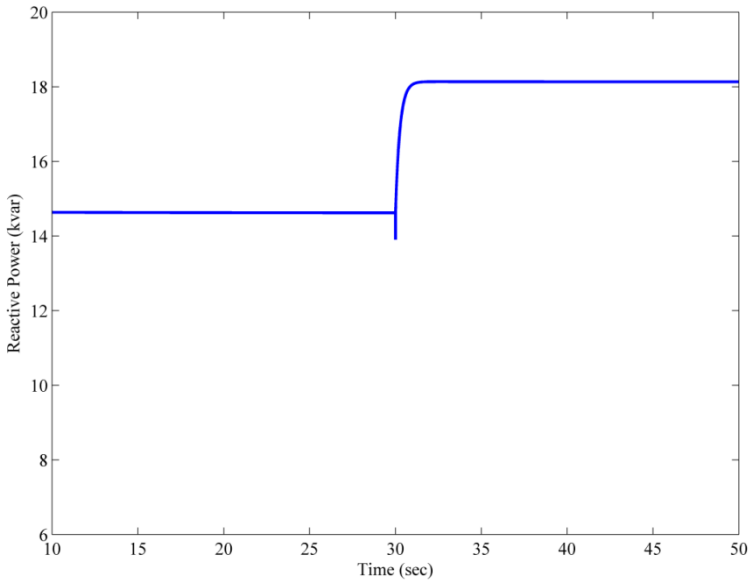

Fig. 3.3 The reactive power produced by VSC2

The DC link capacitors connected at the DC side bus C and bus D as shown in fig. 2.17 are used to provide temporary injection or absorption of the active power. The DC voltage controller responsible to control the DC-link voltage of VSC2 compares the measured and reference values of voltage and sends error signal to the PI controller. The PI controller makes a decision and sends a signal to the DC capacitor in order to charge/discharge according to DC-link voltage variation. A DC-link capacitor provides temporary injection of the active power when the DC-link voltage decreases and vice versa. It can be seen in fig. 3.2 that the voltage controllers of the PV-STATCOM system have restored the voltages to their pre-fault values in very short duration.

Next the controllers are to be verified with the wind power fluctuations, fluctuations in the power output of a PV system and also load changes for the unbalanced loads. The 12 hours wind speed data of 1st January 2009 for East Denmark given by DTU wind energy is used, as shown in fig. 2.4 and the power output of a PV system is assumed for a sunny day. The fluctuations in the power output of the WTG and PV2 for 12 hours is shown in Fig. 3.4.

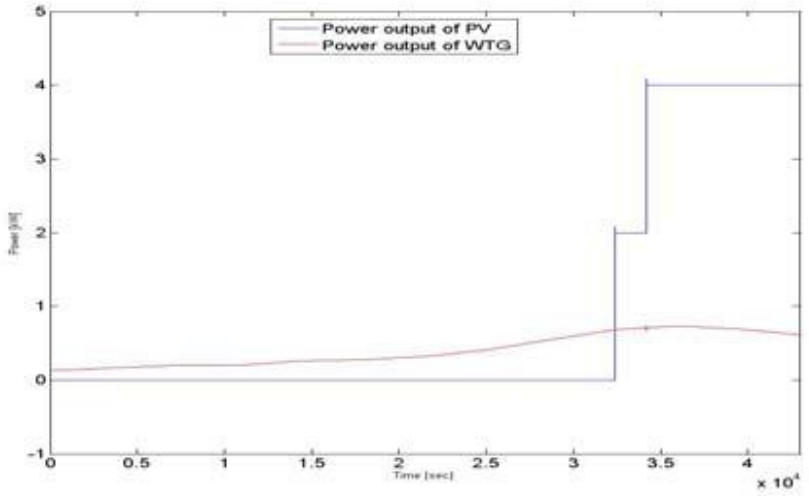

Fig. 3.4. The power output of PV2 and the WTG

The load variations for all three phases for 12 hours at bus D is shown in Fig. 3.5.The load demand is met by the WTG, PV system and the grid. The power delivered by the grid to meet the load demand and to charge the batteries is shown in Fig. 3.6. Initially the grid is delivering more power in order to charge the batteries together with the load demand and when both the batteries are fully charged it delivers less power as shown in Fig. 3.6.The fluctuations in the power delivered by the WTG, PV2 and the grid cause the problems with the network voltage. The fluctuations in the voltage are shown in Fig. 3.7. The first peak in the voltage is due to the power delivered by the grid to charge the batteries in minimized by the control system; the second and third peak is due to the fluctuations in the power output of PV2. In all the cases, the control system is able to maintain the voltage in the desired range within very short duration. The control of the voltage in other parts of the network is done by using the other relative controllers available there in the same way. The further details about the voltage control in other parts of the network are not described in this section and are presented in section 3.4.

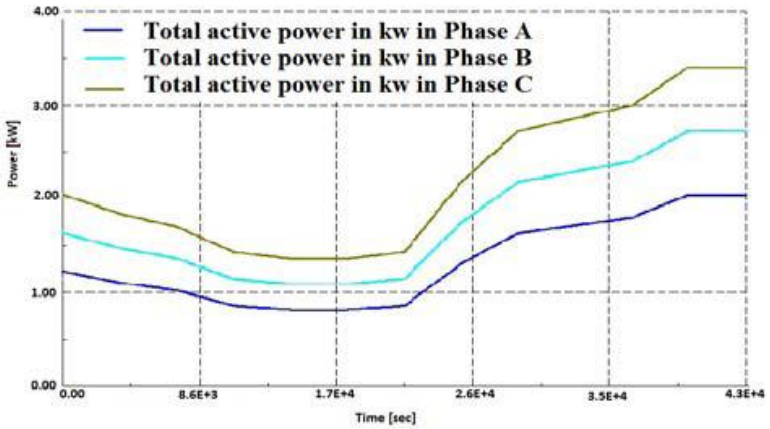

Fig. 3.5. The 12 hours fluctuations in the three phases load at Bus D

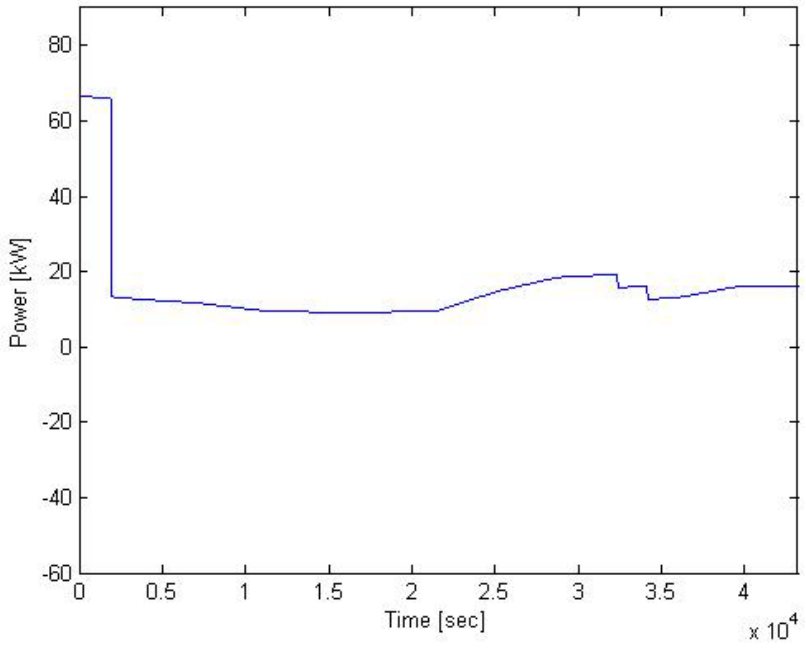

Fig.3.6. Power delivered by the grid

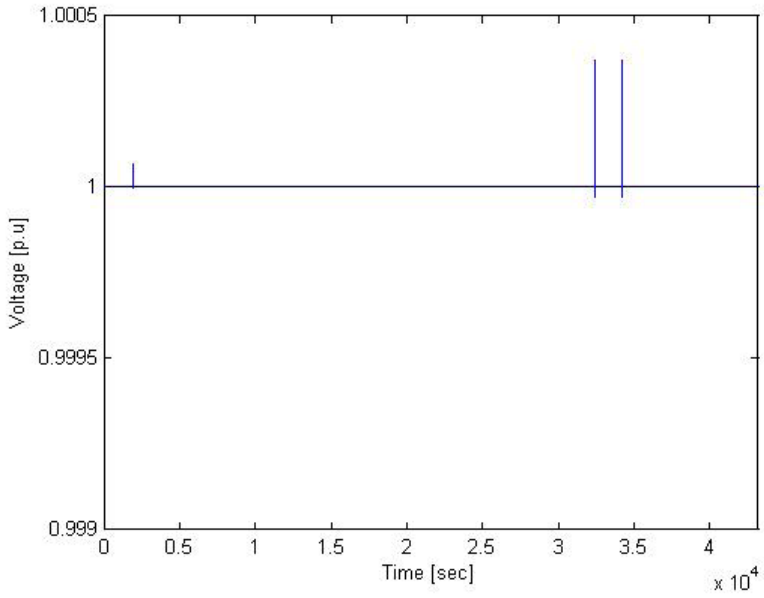

Fig.3.7. Voltage at bus D

The charging of the batteries can be done slower or faster by using different Charging rates (C rates). The PQ/PV controller developed as shown in fig. 2.11 uses the charge controlling block. This block controls the flow of the current and charges batteries at different C rates. The plot of currents flowing from the grid through cable R8-RA to charge the battery1 at 1 C and ½ C rates is shown in Fig. 3.8. The flow of current from the grid reduces to zero when battery is charged up to the specified limits as shown in Fig. 3.8.

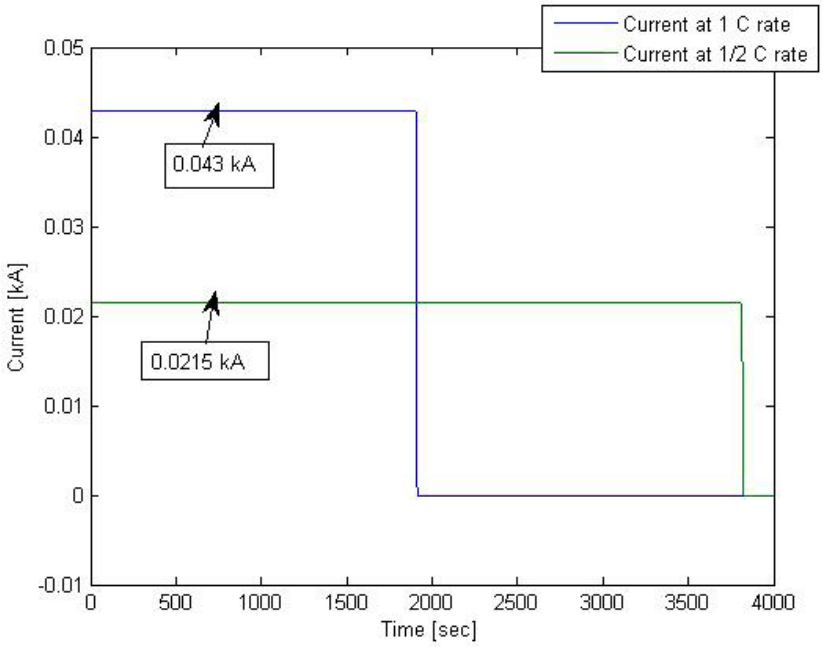

Fig.3.8. Currents to charge battery1 at two different C rates

The plots for the battery SOC at two different rates (i.e. 1 C and ½ C rates) are shown in Fig. 3.9. The grid is delivering 43 A to charge the battery1 which is connected at bus RA at 1 C rate. In this condition battery is charging faster. The battery is drawing half of the rated current at ½ C rate and is charging slowly. The battery takes longer time to charge it up to the desired limit in this case as shown in Fig. 3.9.

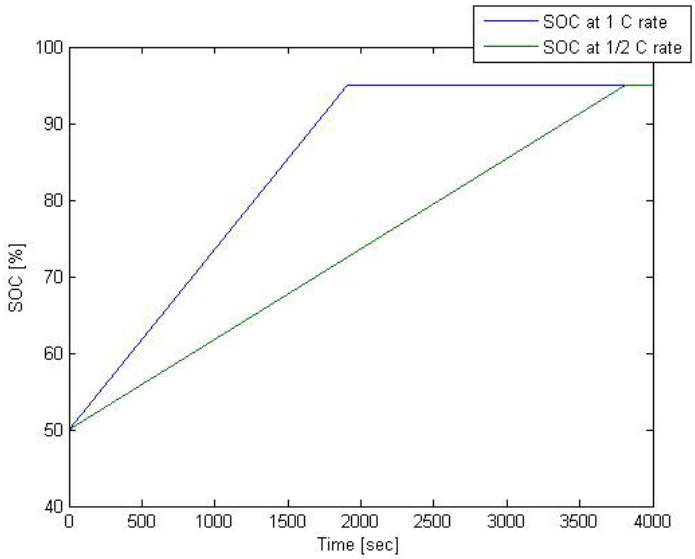

Fig.3.9 Sate of charge (SOC) of the battery at the two different rates

3.3 Reactive power control in the CIGRE network

The consumption of the reactive power in the distribution network together with DG units is stochastic in nature. The uncertain variation in the flow of the reactive power causes variations in the voltage at PCC. It

also reduces the power factor and the efficiency and affects the real power production capability of the generating unit(s). It is therefore desirable to control reactive power in order to ensure the proper operation of the distribution system to prevent damages such as overheating of generating units and cables, to reduce the power losses, improve power factor and increase the active power transfer capability of the system.
The PQ controller shown in fig. 2.11 is used in this regard. The purpose of this controller is to maximize the active power by controlling the reactive power of the network equal to zero. This is done by setting the parameter Q_ref=0 in the control block shown in fig. 2.11.The reactive power flowing through the cable R8-RA in this case is shown in fig. 3.10.

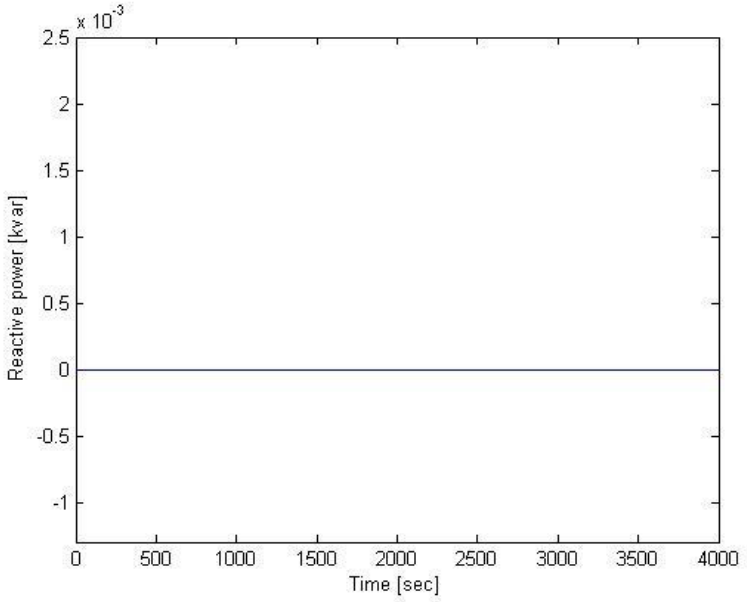

Fig. 3.10 The Reactive power through line R8-RA

This figure shows the developed controller has successfully controlled the reactive power through the line/cable equal to zero. The flow of the reactive in other parts of the network can be controlled in the same way.

3.4 Study of the CIGRE network in case of the transient conditions

The transient study of the network is performed by applying a short circuit faults (i.e. 3-phase or single-phase to ground faults) in the different parts of the network.A huge amount of the current normally flows towards the faulted point wherethe voltage is reduced or zero due to the fault. This reduction of the voltage on the faulted point causes the voltage sags in different parts of the network. Voltage sags are undesirable in the power system and presents adverse effects the power system equipments. The study about the effects of voltage sags on different components of the CIGRE network together with the study about the mitigation of the symmetrical and the asymmetrical voltage sags ispresented in this section.

3.4.1 Study of the network in case of 3-phase short circuit faults

This study is performed by using a 3-phase fault at bus R0 (i.e. Medium Voltage 'MV' bus) of the CIGRE Network with different values of fault impedances in order to see the effectiveness of the developed controller with respect to the depth of the voltage sags. The effect of the voltage sags on different components of the CIGRE network (i.e. the WTG and the loads) is studied in this section.

For the first case a three phase fault with fault impedance of 1 Ω (Z_f =1 Ω) is applied at time t=5 s on bus R0 and is cleared after 150 ms. The voltage on the faulted phases decreases as shown in fig. 3.11. It can be seen in fig. 3.11 that voltage on this bus decreases to 0.72 p.u (i.e. it is voltage sag of 28%). This kind of fault also causes voltage sag in different parts of the CIGRE network. The voltage on bus RA, RB, RC, RD, RE, R11 and bus R17 without compensation is shown in fig. 3.12. The depth of the voltage sag on different buses depends on the amount of current delivered by the grid and DG units and the network impedances between the fault and the current sources. The behavior of different components of CIGRE network during voltage sag is different and is described below.

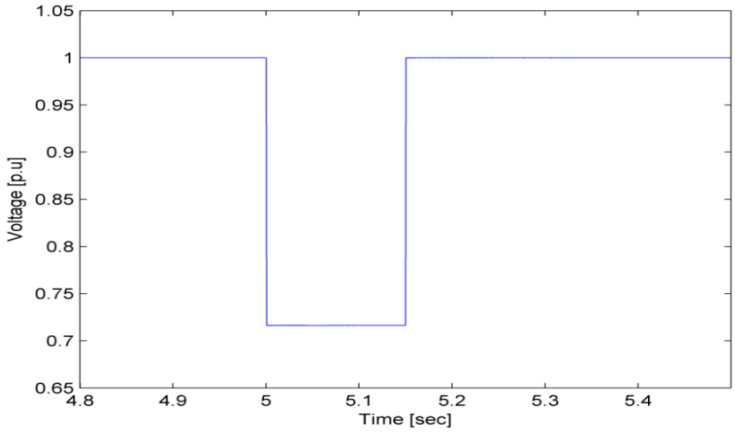

Fig. 3.11 Voltage on bus R0 in case of a three phase fault with a fault impedance of 1 Ω

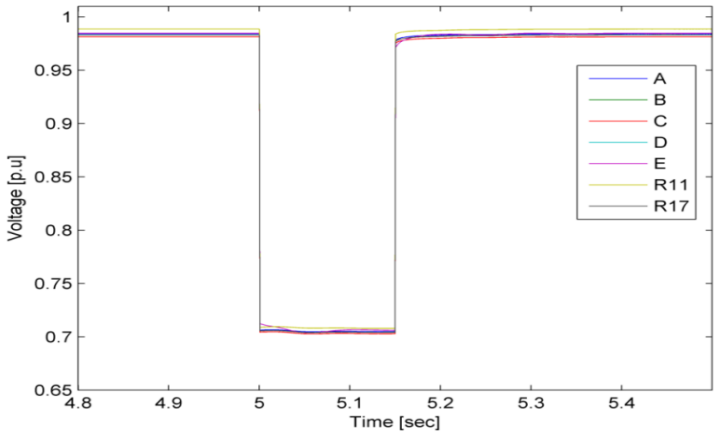

Fig. 3.12 Voltage sags on the different parts of the network in case of a three phase fault with fault impedance of 1 Ω. The labels refer to voltages at the actual bus numbers

3.4.1.1 The effect of voltage sags on the WTG

The behavior of the wind turbine generator in case of voltage sag depends on its technology. The 5.5 kW squirrel cage induction generator used for this study is a fixed pitch and fixed speed WTG and is connected at bus RE where a voltage sag has appeared. In the case of a squirrel cage induction generator, there is a decrease in active power supplied to the grid due to the voltage sag. Similarly, the reactive power consumed by the machine is reduced due tothe demagnetization of the generator. The severity of demagnetization depends of the depth of sag. When the faultis cleared the induction generator absorbs reactive power from the grid for its magnetization [73], [74]. The active and the reactive power of the WTG are shown in fig. 3.13. A minus sign shows the magnetization of the induction generator and plus sign for the demagnetization in the simulation result of fig. 3.13.

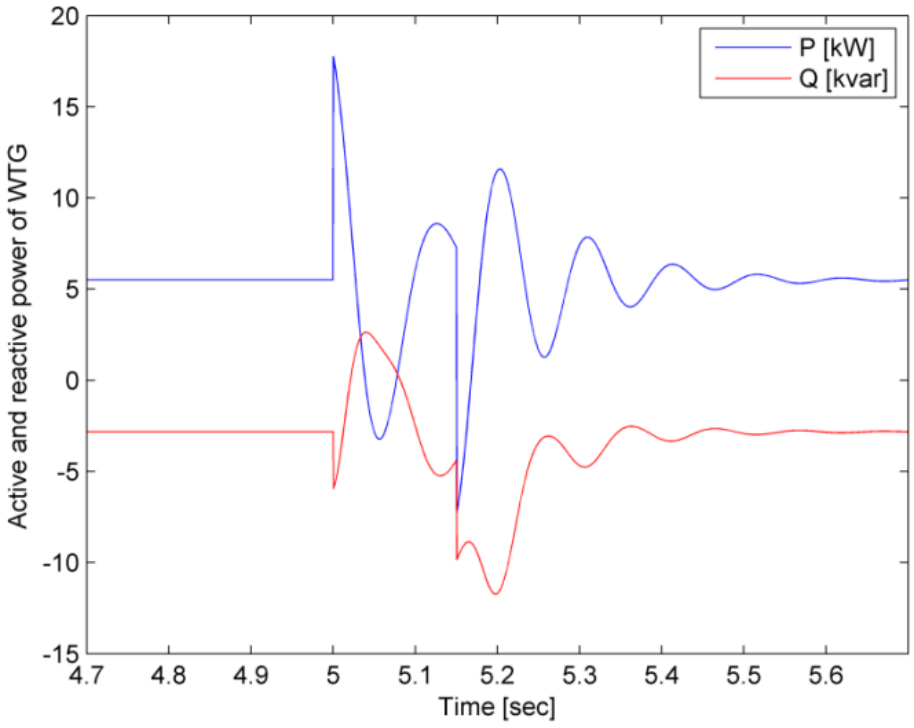

Fig. 3.13 The active and the reactive power of the WTG in case of a three phase fault with fault impedance of 1 Ω.

Further, themechanical torque of the machine is considered to be constant at the constant wind speed and the voltage sag causes a reduction in the electrical torque which increases the speed of the generator [74]. Fig. 3.14 shows the mechanical and the electrical torques of the wind turbine generator.

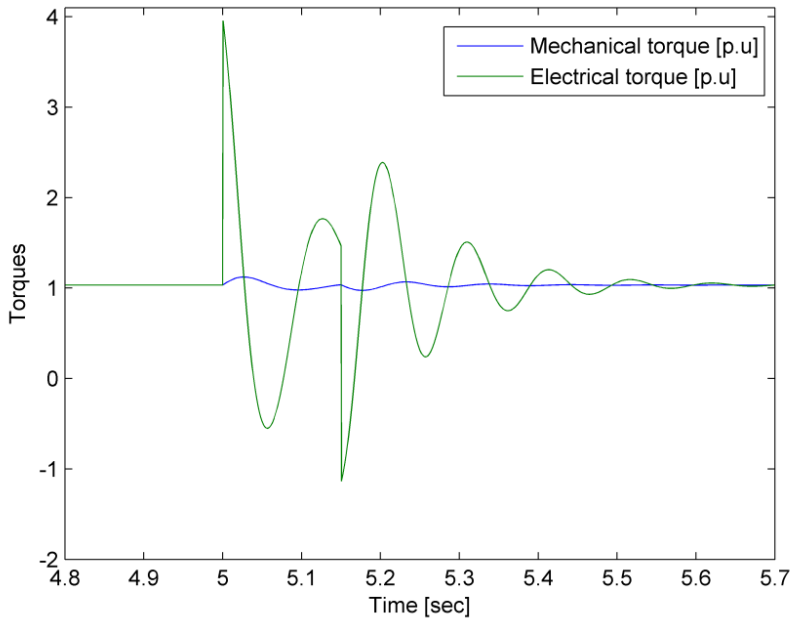

Fig. 3.14 The mechanical and the electrical torques of the WTG in case of a three phases fault with fault impedance of 1 Ω.

The current of the WTG increase up to 3.7 times the nominal value during the initial start of voltage sag for a short duration and then it becomes less than its nominal current as shown in fig. 3.15 [75]. The short duration peak in the current gives the short duration peak in the electrical torque and the active power output of the WTG as shown in fig.3.14 and fig. 3.13 respectively. This initial peak in the electrical torque of the machine reduces the speed of generator at the initial instant as shown in fig. 3.16.

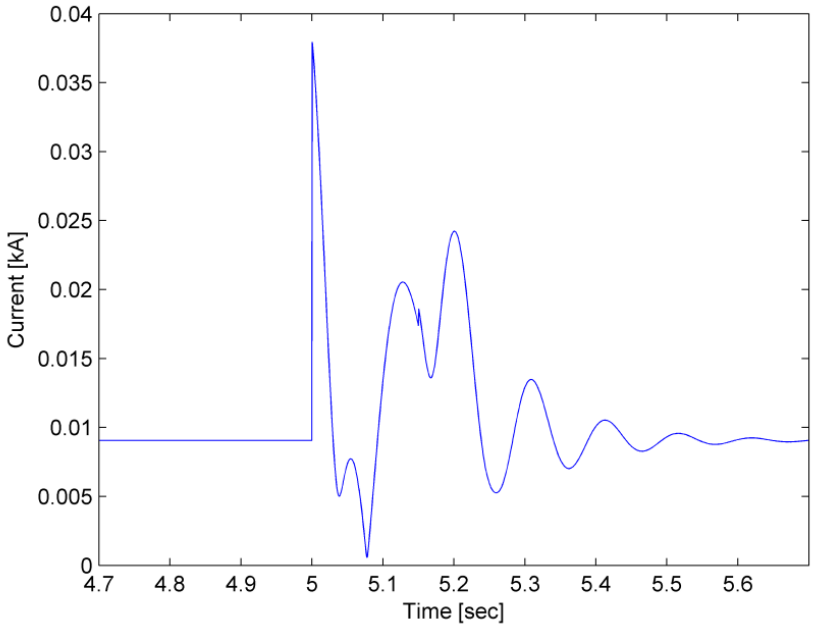

Fig. 3.15 The current of the WTGin case of a three phase fault with fault impedance of 1 Ω.

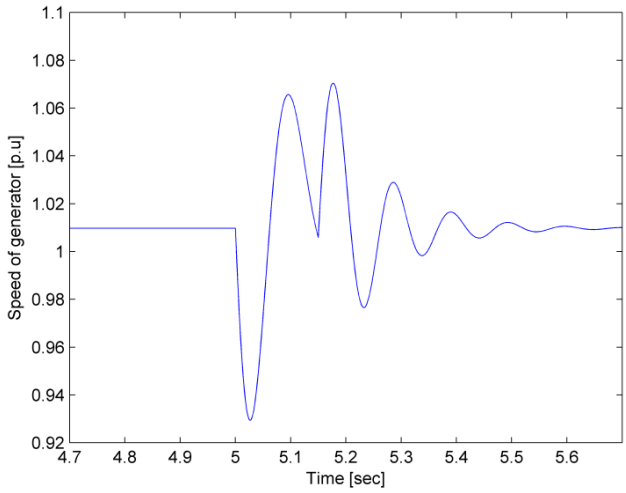

Fig. 3.16 The speed of the WTGin case of a three phase fault with fault impedance of 1 Ω.

If the over speed protection of the wind turbine limit is reached, the WTG has to be disconnected from the grid and stopped. This situation leads to an interruption of the production.

3.4.1.2 The effect of voltage sags on the loads

Unbalanced loads are connected at bus RC, RD, R11and bus R17 of the CIGRE network as shown in fig. 2.18. Any deviation in the voltage adversely affects them. A sag in the voltage reduces the illuminating intensity of lighting loads. The effects of voltage sag are different for the different loads. The adverse effects of the voltage sag on the sensitive house hold loads have been described in [76].

The currents in each phase of loads on bus RC and bus RD are shown in fig. 3.17 and fig. 3.18 respectively. In normal operating conditions different phases of the load carry different currents as they are unbalanced. The current in all phases decreases due to a voltage sag on the connected bus as shown in these figures.

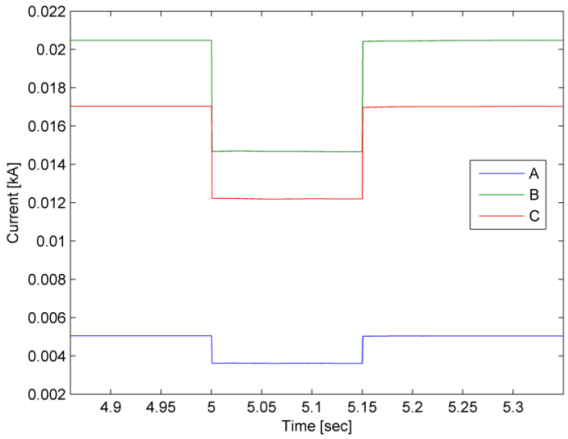

Fig. 3.17 The currents in three phases of the load on bus RC in case of a three phase fault with fault impedance of 1 Ω.

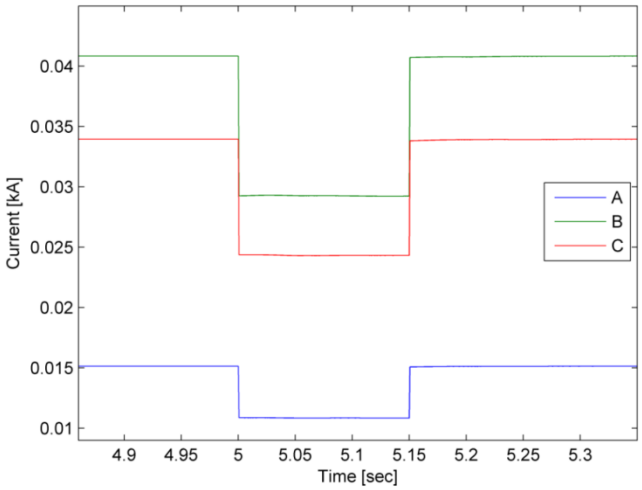

Fig. 3.18 The currents in three phases of the load on bus RD in case of a three phase fault with fault impedance of 1 Ω.

3.4.1.3 The effects of the voltage sagson the power output of PV units

The voltage sag on the AC terminals of the PV inverters causes a reduction in its DC-link voltage which in turn decreases the power output of the PV units. Hence, voltage sag is undesirable and it must be compensated as soon as possible.The simulations results are not presented in this section. Further details above this can be read in section 3.4.1.3.

3.4.1.4 Mitigation of symmetric voltage sags by using STATCOM Controllers

When STATCOM is used in distribution systems it can protect the distribution networks against voltage sags by injecting the required amount of reactive power. According to EN 50160 standards the voltage tolerance limit in the low voltage Danish distribution networks is +-10% [77].

Four D-STATCOMs, with proper controllers are employed at bus RA, RB, RC and bus RD. Two of them are used for PV applications and are only injecting/absorbing reactive power and injecting active power. The other two are equipped with batteries in order to inject/absorb both active and reactive powers. These controllers are responsible for the voltage stabilization of the whole CIGRE network together with the external grid. Each D-STATCOM controller comprises two outer and two inner PI controllers and are detailed described in chapter 2 of this thesis. The outer controllers of the PV inverters are responsible for maintaining the AC and DC-link voltages. The inverters of the two BESS-STATCOMs are named VSC1 and VSC2 and are connected at bus RA and RB respectively. The inverters of the two PV STATCOMs are named VSC3 and VSC4 and are connected at bus RC and RD respectively.

The voltage in the network is restored back to the permissible limits by the injection/absorption of the reactive power by the controllers during a fault. All four controllers participate in the compensation of the

voltage sag.If the voltage of the bus is greater than the voltage of an inverter connected on that bus, the reactive power is absorbed by the inverter and vice versa [78].The contribution of the reactive power from the different converters (i.e. VSC1, VSC2, VSC3 and VSC4) is according to their rated power. The power and voltage ratings of the inverters used in the network are shown in table A2 in appendix A.

The voltages on the AC and DC sides of bus RC and bus RD are shown in fig. 3.19. It can be seen in this figure that the DC-link voltages of VSC3 and VSC4 decrease because of voltage sag which has appeared at the time equal to t=5 s. A decrease in these voltages cause the power outputs of PV1 and PV2 delivered to the DC terminals of the respective inverters to decrease as shown in fig. 3.20. It can be seen in fig. 3.20 that PV1 and PV2 are producing the rated powers (i.e. 3 kW and 4 kW) respectively in the normal operating conditions (i.e. full sunny day) which decrease when voltage sag appears at t= 5 s.

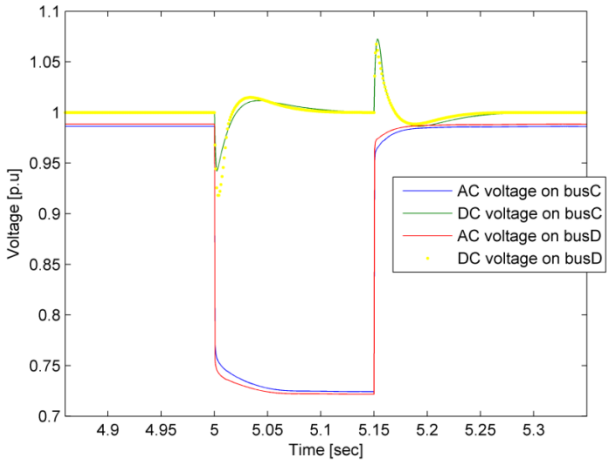

Fig.3.19 The AC and DC-link voltages of VSC3 and VSC4 in case of a three phase fault with fault impedance of 1 Ω.

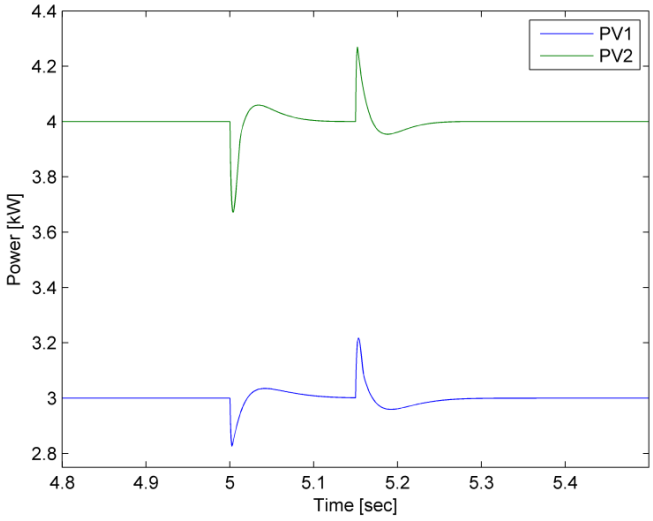

Fig. 3.20The Power output of PV1 and PV2 on DC sides of the respective inverters in case of a three phase fault with fault impedance of 1 Ω.

The DC voltage controller of the respective D-STATCOM as shown in fig. 2.7is used to control the DC-link voltage and thereby the power output of the PV units. It can be seen in fig. 3.19 and fig. 3.20 that the DC voltage controllers have controlled the DC-link voltages and maintained the power outputs of PV1 and PV2 at its pre-fault value in a short duration.

When the fault is cleared after 150 ms, the DC-link voltages as shown in fig. 3.19 increase at that time. The increase in the DC-link voltages at the time of short circuit clear is because of the short time availability of active power injection by the DC-link capacitors until they fully return to charging mode. This peak in DC-link voltage causes the active power output of these units to increase as shown in fig. 3.20. When the DC-link voltages are brought back to nominal values, the productions of these units come to the nominal value again.

The AC voltages in different parts of the network are controlled by the continuous monitoring of the reactive power. The voltage controllers of PV-STATCOMs have been developed in this regard. The control system of the batteries should operate in PV mode. The control systems of all the inverters measure the voltages at its PCC, compare it with the reference values of the voltage and inject/absorb the desired amount of the reactive power. The reactive powers injected by the battery inverters (i.e. VSC1 and VSC2) when their respective controllers charge them at full charging rates and the reactive power delivered by the PV inverters (i.e. VSC3 and VSC4) are shown in fig. 3.21 and fig. 3.22 respectively.

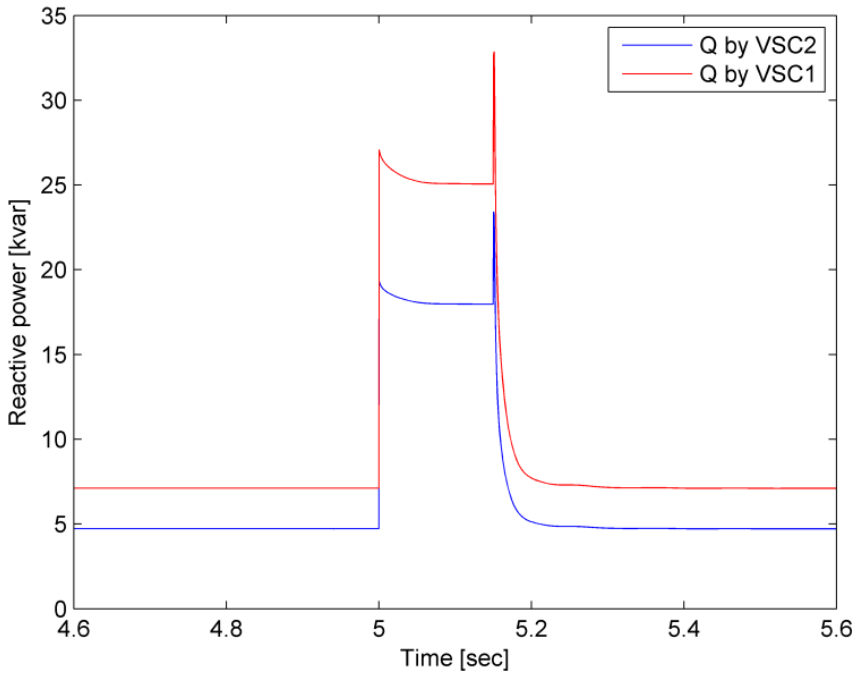

Fig. 3.21 The reactive power injected by VSC1 and VSC2 in case of a three phase fault with fault impedance of 1 Ω.

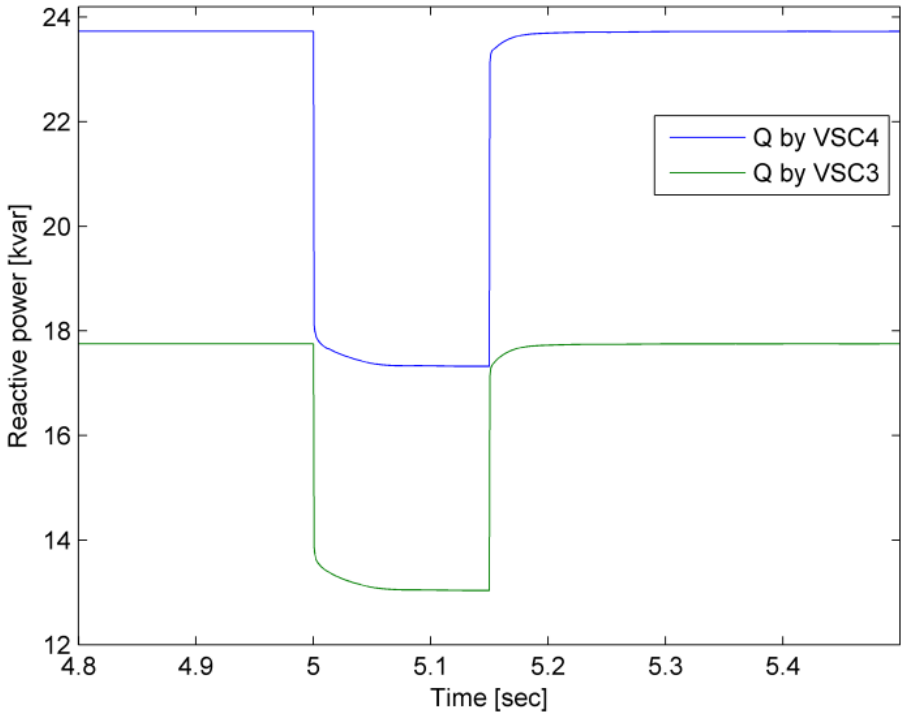

Fig. 3.22 The reactive power injected by VSC3 and VSC4 in case of a three phase fault with fault impedance of 1 Ω.

As shown in fig. 3.21, VSC1 and VSC2 deliver small amounts of reactive power during the steady state conditions but injectmaximum amount of the reactive power during voltage sag. It can be seen in fig. 3.22 that VSC3 and VSC4 are injecting nearly full amount of the reactive power in the normal operating conditions. The injection of the reactive power in the normal operating conditions is because of the line voltage drops and the other load unbalances in the network. The reactive power deliveredby these controllers is even not enough to restore the voltage onthese buses up to 1 p.u during steady state operation because inverters do not have availability of the reactive to return it to 1 p.u.When the voltage sag appears at t=5 s, the controllers do nothave enough reactive power to compensate for it and hencethe distribution system operates in under voltage condition. Since reactive power is a function of the voltage; therefore, the decrease in the voltage reduces the amount of the reactive power ($Q=VI\sin\phi$) produced by the inverters as shown in fig. 3.22.

The voltage on bus RA, RB, RC, RD, RE, R11 and bus R17 in this case is shown in fig. 3.23. It can be seen in this figure thatall the controllers in the CIGRE test network are not able tocompensate the voltage sag up to a desirable operating limits.

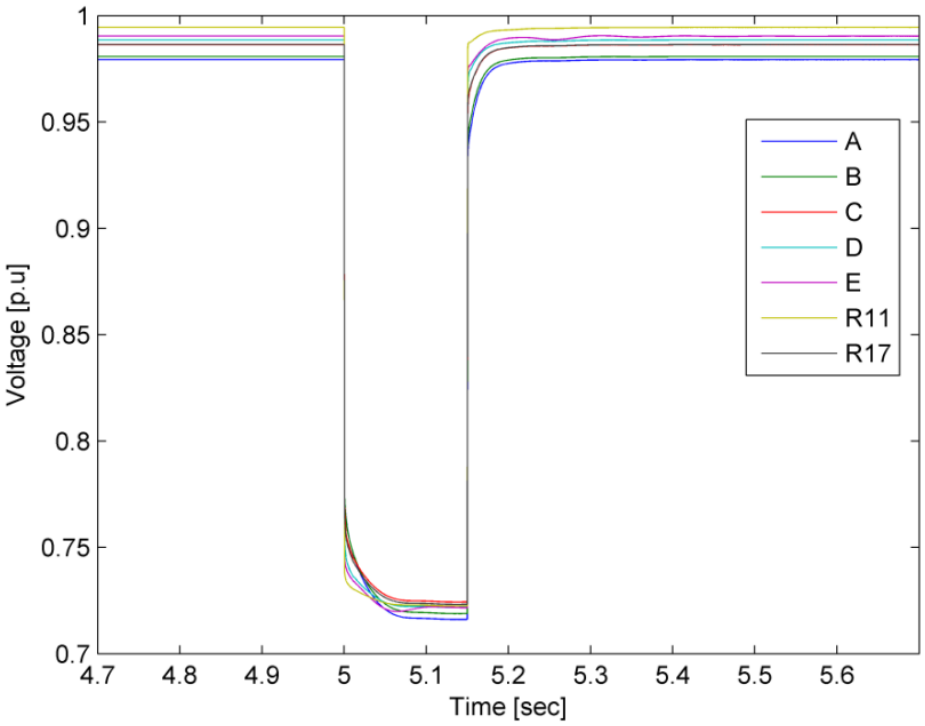

Fig. 3.23 The Voltage on different parts of network with compensationin case of a three phase fault with fault impedance of 1 Ω.

The voltage profile in the entire parts of the CIGRE can be improved if batteries are charged at slow rates rather than full charging rates. The batteries when charged at full rates draw more currents than the case when they are charging slowly. The slow charging rates gives less voltage drops across the lines. The plots of the current drawn by both the batteries from the grid for two different charging rates (i.e. 1 C rate and 1/10 C rate) flowing through line R8-RA and R10-RB is shown in fig. 3.24 and fig. 3.25 respectively.

It can be seen in fig. 3.24 and fig. 3.25 that both batteries carry different amount the currents at the different charging rates during normal operating conditions. The batteries are charged slowly when current flows according to 1/10th rate. The current flowing through these lines increases when the short circuit fault occurs at t=5 s in the network. The increase in the current through these lines during a fault at a slower charging rate is less as compared to a faster one and gives less voltage drop across the lines. The voltages on bus RA, RB, RC, RD, RE, R11 and bus R17 in this case is shown in fig. 3.26. It can be seen in fig. 3.26 that the voltage in the different parts of low voltage CIGRE network have been improved a little but the existing controllers are still unable to compensate the voltage sags of this depth up to the desired level.

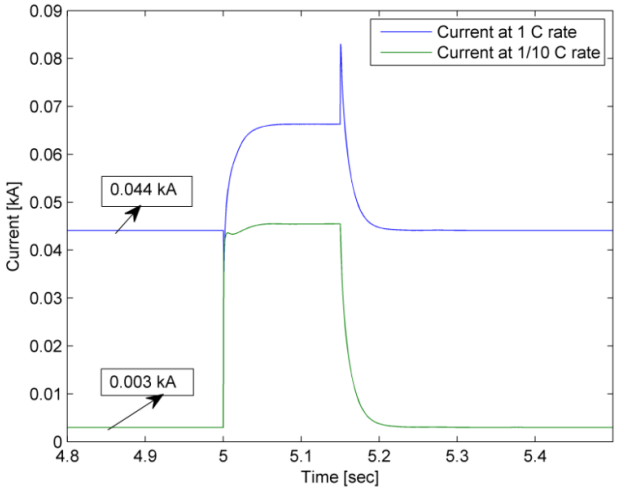

Fig. 3.24 The current through line R8-RA for two different charging rates of the batteries

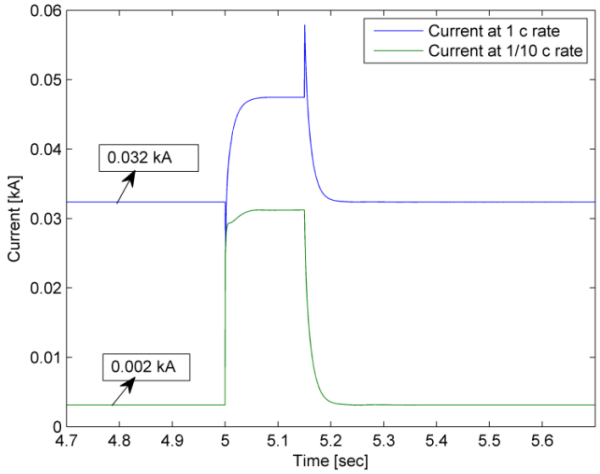

Fig. 3.25 The current through line R10-RB for two different charging rates of the batteries

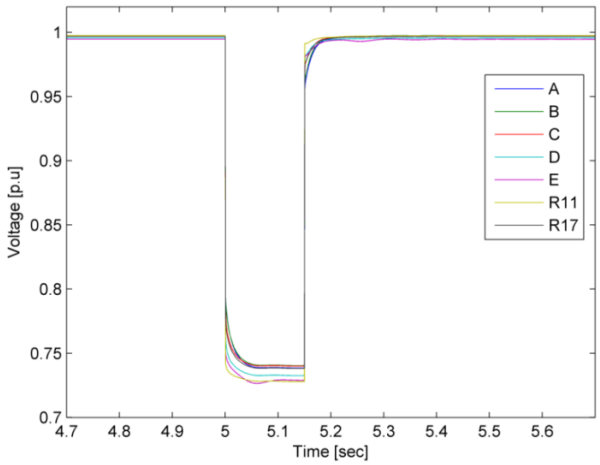

Fig. 3.26 The voltage on the different parts of network with compensation when batteries are charged at 1/10th charging rate

Alternately, a three phase fault with a fault impedance of 2 Ω (i.e. $Z_f = 2\Omega$) is applied at time equal t=5 s on the bus R0 instead. This is done in order to test the effectiveness of the controllers for less deep voltage sags as compared to the previous case. The voltage on the bus R0 and the voltage sag in the other parts of network without using controllers are shown on fig. 3.27 and fig. 3.28 respectively.

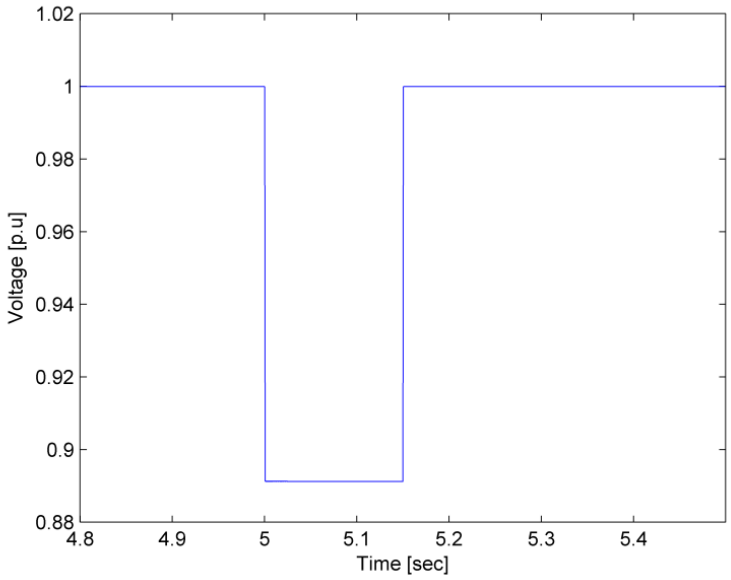

Fig. 3.27 The voltage on bus R0 when the fault appears with 2Ω fault impedance

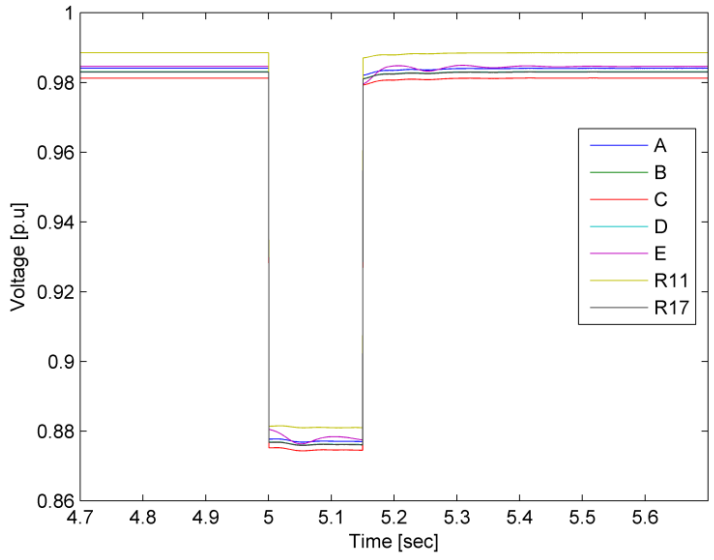

Fig. 3.28 The voltage on different parts of network when fault appears with 2Ω fault impedance

The voltage on bus R0 decreases to 0.88 p.u (i.e. voltage sag of 12%) inthis case as shown in fig. 3.27. The sag depth in this case is shallow because of bigger fault impedance as compared to theprevious one. The compensation in this case is made by the existing controllers in the same way as explained before. The

voltage in the different parts of the network when the batteries are charged at full charging rates is shown in fig. 3.29. It can be seen in this figure that the voltage in the network is improved but it is still less than the power quality limits for Danish low voltage grids [77].

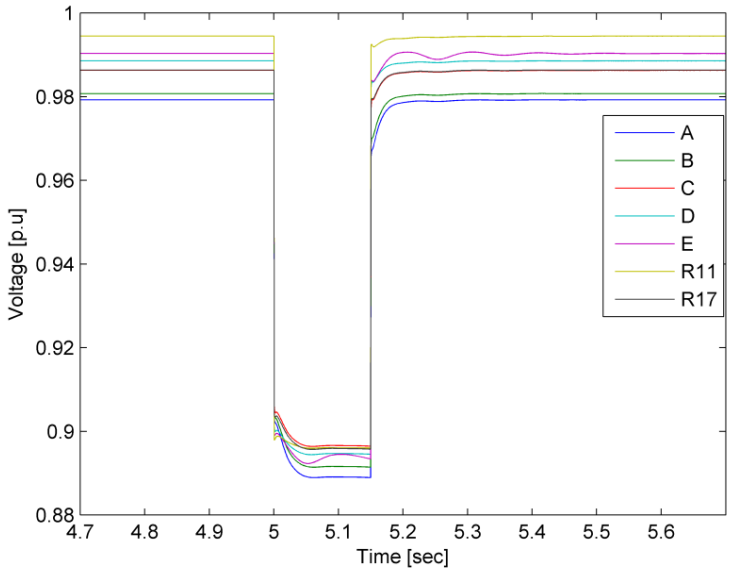

Fig. 3.29 The voltage inthe different parts of network when batteries charged at full charging rate in case a 2 Ω fault impedance

By using the method of slow charging of the batteries, the voltage in the network has been restored to the permissible limits according to Danish standards as shown in fig. 3.30.

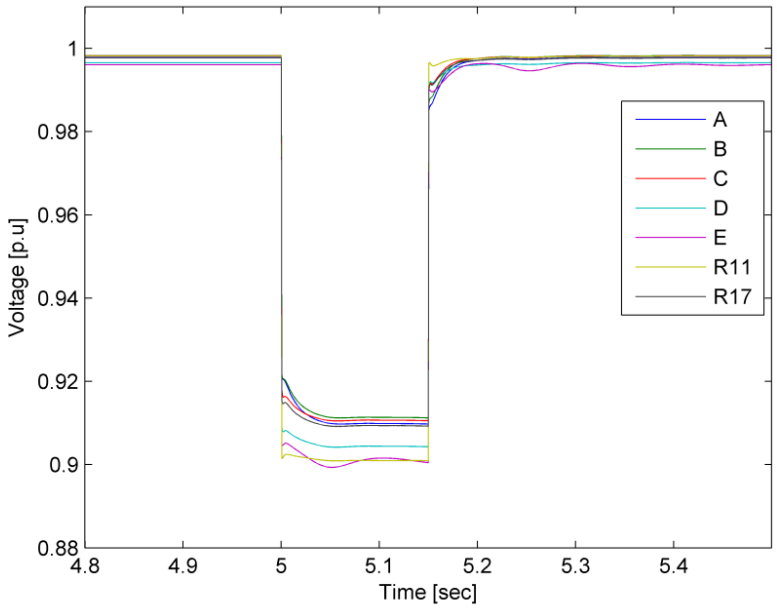

Fig. 3.30 The voltage in the different parts of network when batteries charge at slow rate in case a 2 Ω fault impedance

The D-STATCOM controller of battery2 and STATCOM controller of PV1 are delivering the reactive power which is summed up at the same connection point (i.e. R10 as shown in fig. 2.18). This is the reason why the voltage on the buses of these controllers (i.e. bus RB and Bus RC) is improved more than the other buses as shown in fig. 3.30. The voltage on Bus RB during voltage sag is improved slightly better than the voltage on bus RC because of the higher rating of the inverter (i.e. VSC2) used on this bus as compared to the inverter on bus RC.

3.4.2 Study of the network in case of single phase to ground faults

The majority of faults in power system are single phase to ground faults [79], which leads to unbalanced voltage sags in the network. Unbalanced or asymmetric fault involves all kinds of sequence quantities: positive, negative and zero sequence, whereas voltage sags due to symmetric fault contains only positive sequence quantities.

According to European standards, the percent Voltage Unbalance Factor (VUF) is defined by the ratio of the negative sequence voltage to the positive sequence voltage [80-82]. According to IEEE Std. 1547.2-2008 the voltage unbalance factor should be below "2% to 3%" in stationary conditions.

This study is performed by using single phase to ground fault at bus R0 (i.e. Medium Voltage 'MV' bus) of the CIGRE network with different values of fault impedances in order to see the effectiveness of the developed controller with respect to the depth of the voltage sags. The study about the occurrence of both unbalanced voltage sags and voltage unbalancesand its mitigation in the CIGRE network is presented in this section. The discussion about the propagation of the unbalanced voltage sags from the primary of the transformer to its secondary is also presented in this section.

3.4.2.1 Study of the network without using controllers in case of single phase to ground fault

To have a base study case, all the controllers have been disabled in order to study the impacts of unbalanced loads and unbalanced faults on the voltage in different parts of the low voltage CIGRE network. The voltage unbalance exists from the beginning of the simulation results due to the availability of unbalanced loads which are connected to the network. Next, a single line to ground fault on phase A with a 0 Ω fault impedance is applied at time equal to t=2 s on the 20 kV Medium Voltage (i.e. R0) bus in order to simulate a case of severe unbalance. The fault is cleared at 2.15 s. The magnitude and phase angles of the voltage in the three phases at bus R0 are shown in fig. 3.31 and fig. 3.32respectively.

It can be seen in fig. 3.31 that voltage in all three phases of bus R0 are not exactly equal in magnitude but are nearly the same during the normal operating conditions. This minor difference in the three phase voltages in the normal operation is because of the minor load unbalances. At time equal to t=2 s, the voltage in the affected phase becomes zero and the voltage in the other two phases remain nearly the same as shown in fig.

3.31 The results shown in fig. 3.31 are matching with the references [83], [84]. With respect to the phase angles, fig. 3.32 shows no changes in the voltage phase angles in the healthy phases whereas there is a reasonable change in the voltage phase angle in the affected phase.

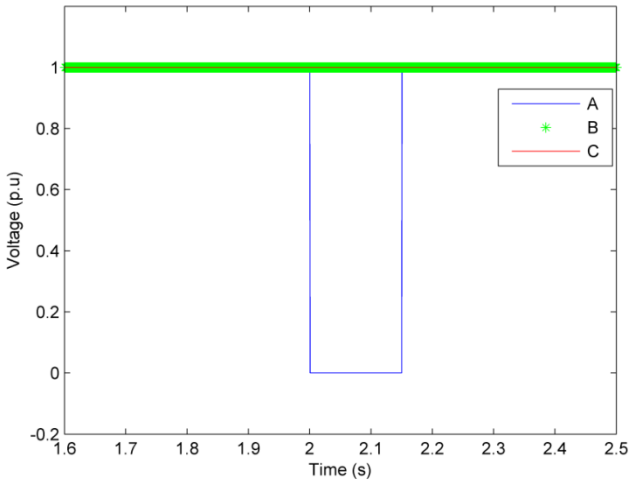

Fig. 3.31 The voltage in three phases of bus R0 for single phase to ground fault on phase A with $Z_f = 0\,\Omega$

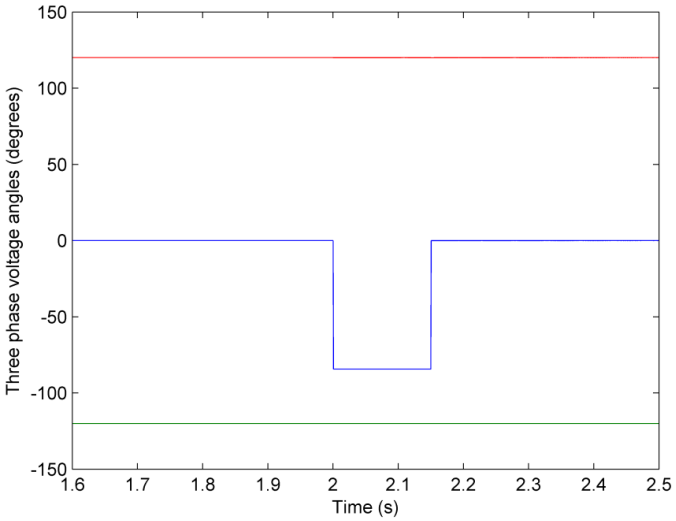

Fig. 3.32 The angles of three phase voltages on bus R0 in case L-G fault on phase A with $Z_f = 0\,\Omega$

This kind of voltage sag on the primary side of the transformer creates unbalanced voltage sags in the other parts of the network. Depending on the type of the faults on the primary of the transformer and the transformer winding connections between the medium voltage and low voltage network, different types of the voltage sags appears in DG side of the network. A detailed discussion about the influence of the transformer winding connection on the propagation of voltage sags is presented in [83], [85]. The

transformation of voltages from primary (i.e. delta) of the transformer to its secondary (i.e. star) in this study is described with the help of fig. 3.33 [86].

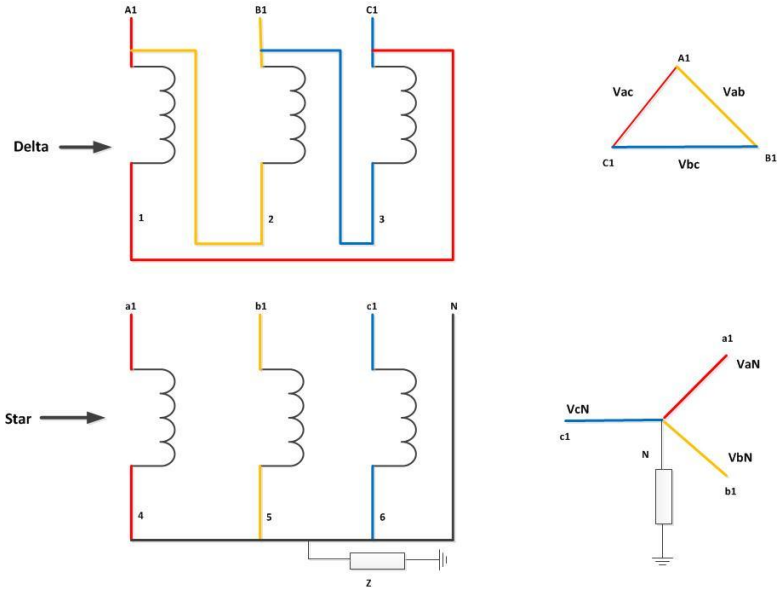

Fig. 3.33 The transformation of voltages from primary of DYN1 transformer to secondary [86].

In delta wye configuration of the transformer, the value of phase to neutral voltage on secondary (i.e. shown with colored lines R, Y and B) is equal to that of the line voltage at the primary divided by $\sqrt{3}$ [87]. The line to line primary voltages are given in equation 3.1.

$$\begin{aligned} V_{ba} &= V_b - V_a \\ V_{cb} &= V_c - V_b \\ V_{ac} &= V_a - V_c \end{aligned} \tag{3.1}$$

Putting the values of phase voltages with respect to their phase angles obtained from fig. 3.32 in equation 3.1, the line to line voltages on the primary of the transformer can be calculated.

$$V_{ba} = 1 < -120^0 - 0 < -84^0$$
$$V_{ba} = 1 < -120^0$$

The voltage V_{ba} on the primary corresponds to the voltage in phase B on the secondary of the transformer as shown in fig. 3.33 and is given by $V_{bN} = V_{ba}/\sqrt{3}$ which is equal to $0.578 < -120^0$ p.u.

$$V_{cb} = 0.999 < 120^0 - 1 < -120^0$$
$$V_{cb} = 1.723 < 90^0$$

The voltage V_{cb} on the primary corresponds to the voltage in phase C on secondary of the transformer as shown in fig. 3.33 and is given by $V_{cN} = V_{cb} / \sqrt{3}$ which is equal to 0.999<90 ^{0} p.u.

$V_{ac} = 0 - 0.999 < 120^0$

$V_{ac} = 0.999 < -60^0$

The voltage V_{ac} on the primary corresponds to the voltage in phase A on the secondary of the transformer as shown in fig. 3.33 and is given by $V_{aN} = V_{ac} / \sqrt{3}$ which is equal to 0.578<-60° p.u.

Therefore, the voltage in the three phases of bus R1 is shown in fig. 3.34. At t=2 s, the voltage profile on this bus changes as shown in Fig. 3.34. It can be seen that voltage in the three phases is nearly the same in the normal conditions. This voltage profile of this bus changes at t= 2 s when the fault appears on bus R0 and is shown in fig. 3.34.

Fig. 3.34 depicts that there is voltage sag of 42.3 % in phase A and 42.4% in phase B on the bus R1. Phase C on this bus is unaffected. A slight difference in voltage sag on phase A and B is due to the slight difference in their loadings. The load on phase A is slightly less than the load on phase B on this bus, so the voltage sag on phase B is slightly deeper than on phase A. When the fault is cleared after 150 ms, the voltage in all the phases return to pre-fault values. The results shown in fig. 3.34 also match with [83], [85], [88].

The voltage in the different parts of the network in its three phases such as on bus RA, RB, and bus RC is shown in fig. 3.35, 3.36 and fig. 3.37 respectively. Similar to fig. 3.34, there is mild unbalance in the voltages in the normal operating conditions due to the unbalanced loads and severe unbalance due to the unbalanced fault.

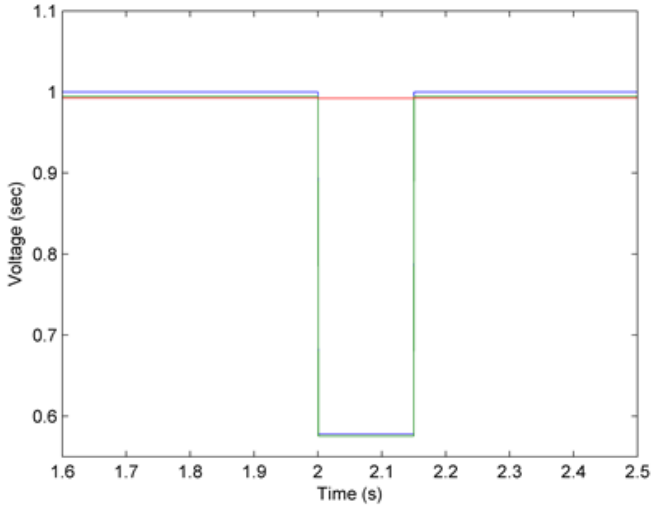

Fig. 3.34 The voltage on bus R1 in case of single phase to ground fault with fault impedance of 0 Ω (blue line: phase A, green line: phase B, red line: phase C).

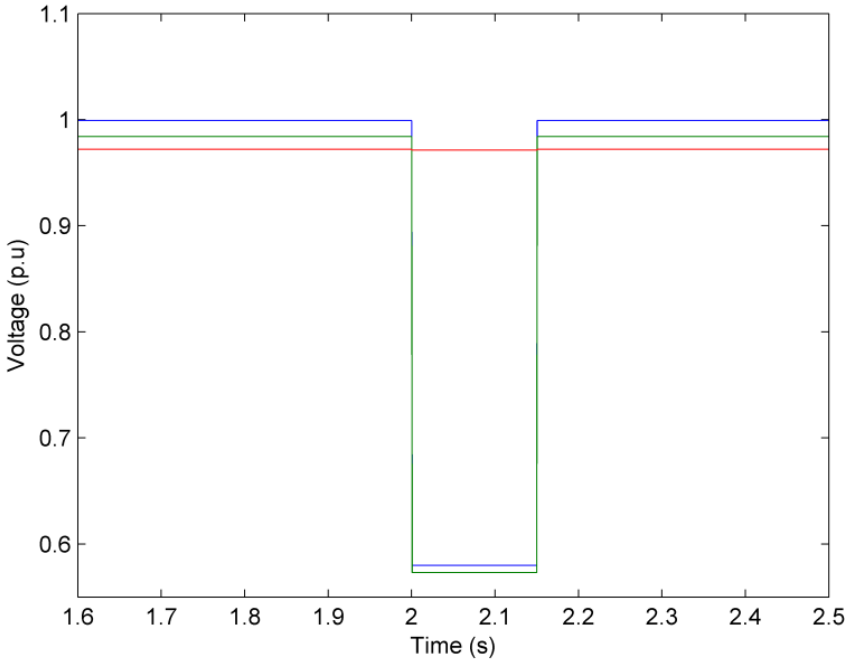

Fig. 3.35 The voltage in three phases of bus RAin case of single phase to ground fault with fault impedance of 0 Ω (blue line: phase A, green line: phase B, red line: phase C).

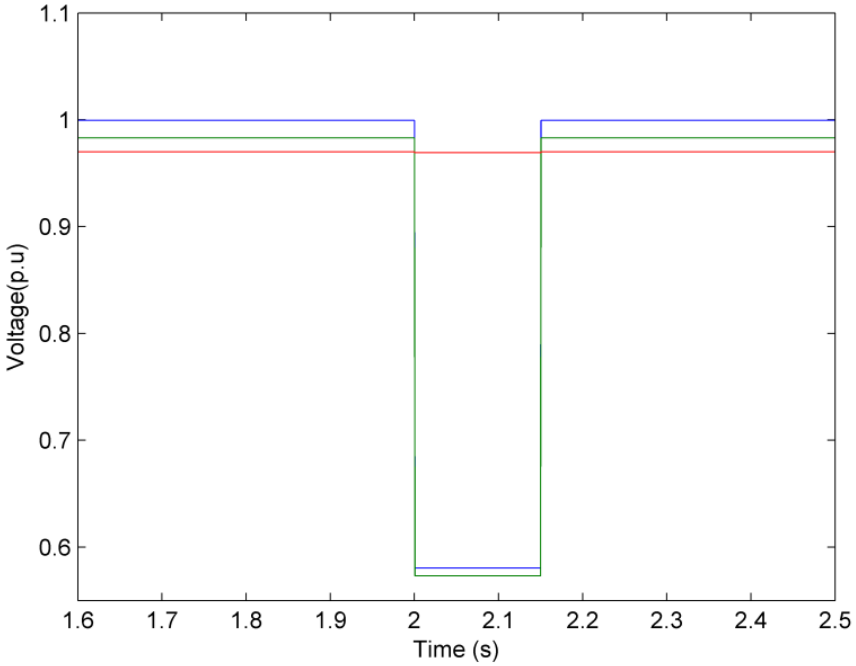

Fig. 3.36 The voltage in three phases of bus RB in case of single phase to ground fault with fault impedance of 0 Ω (blue line: phase A, green line: phase B, red line: phase C).

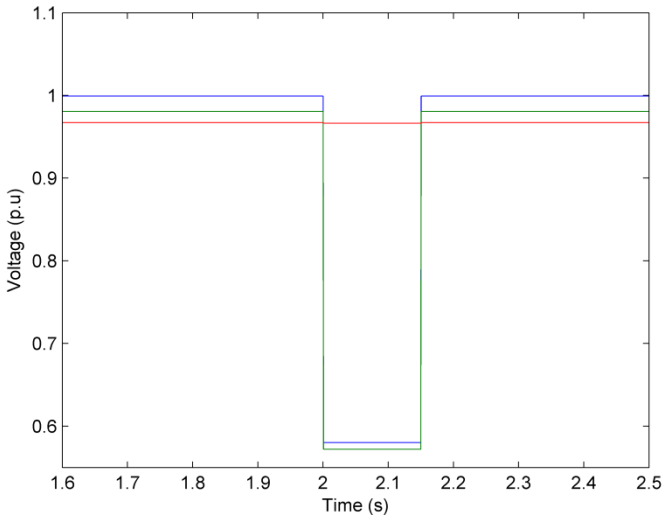

Fig. 3.37 The voltage in three phases of bus RC in case of single phase to ground fault with fault impedance of 0 Ω (blue line: phase A, green line: phase B, red line: phase C).

Table 3.1 shows the unbalance factor in different parts of CIGRE distribution network under mild and severe unbalance. This table depicts that there are minor voltage unbalances in the different parts of the network in the normal operating conditions due to the availability of unbalanced loads in the network and the severe unbalances due to L-G fault.

Table 3.1. The voltage unbalance factors in the different parts of the network for normal and the faulted conditions without compensation

Bus No	%(VUF) in normal operating conditions	%(VUF) during fault
RA	0.45	49.64
RB	0.48	49.6
RC	0.5	49.59
RD	0.43	49.638
R11	0.31	49.66
R15	0.395	49.74
R17	0.55	49.55

3.4.2.2 Mitigation of unbalanced voltage sags and the voltage unbalances

Four STATCOM controllers are used in order to inject/absorb the desired amount of reactive power in each of the phases in order to restore the voltage of different phases to permissible limits and mitigate the problems of voltage unbalances. The reactive power injected/absorbed by all of the four VSCs in the three phases of bus RA, RB, RC and bus RD are shown in fig. 3.38, 3.39, 3.40 and fig. 3.41 respectively.

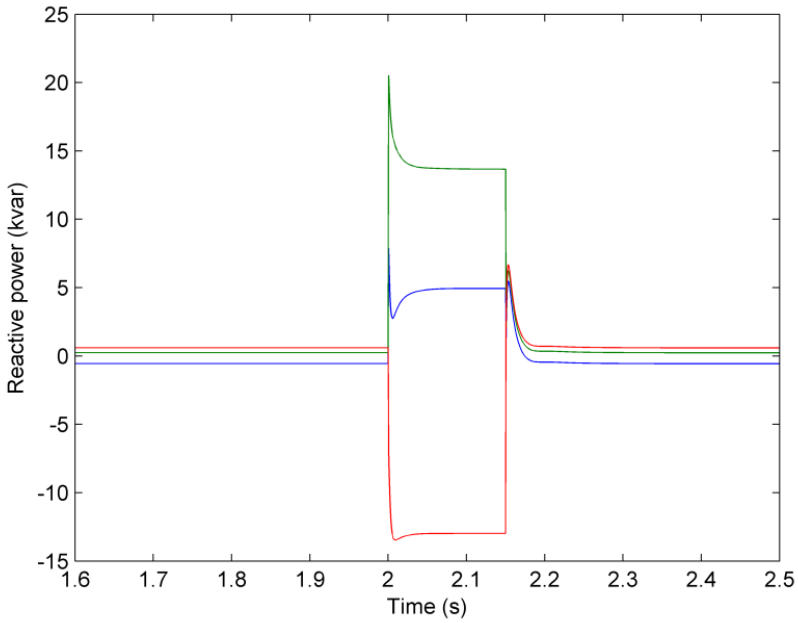

Fig. 3.38 The reactive power of VSC1 in its three phasesin case of single phase to ground fault with fault impedance of 0 Ω (blue line: phase A, green line: phase B, red line: phase C).

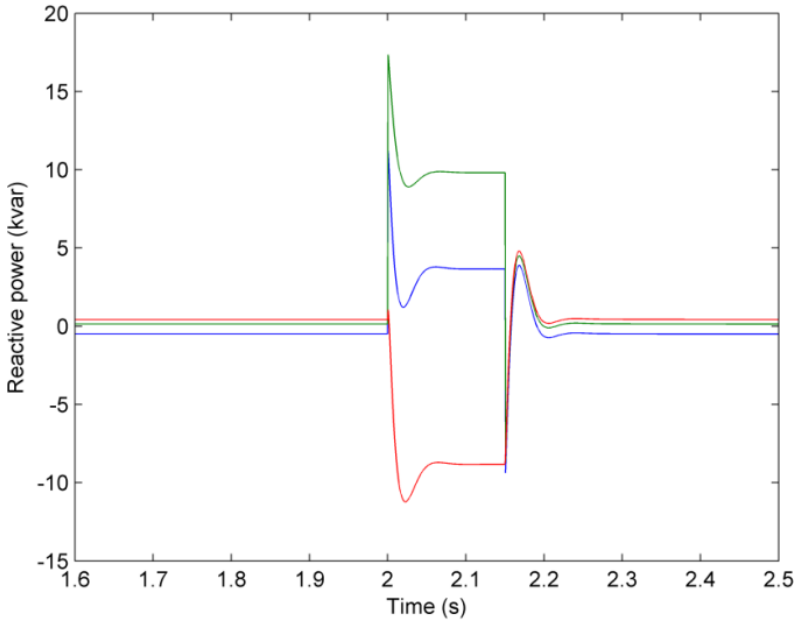

Fig. 3.39 The reactive power of VSC2 in its three phasesin case of single phase to ground fault with fault impedance of 0 Ω (blue line: phase A, green line: phase B, red line: phase C).

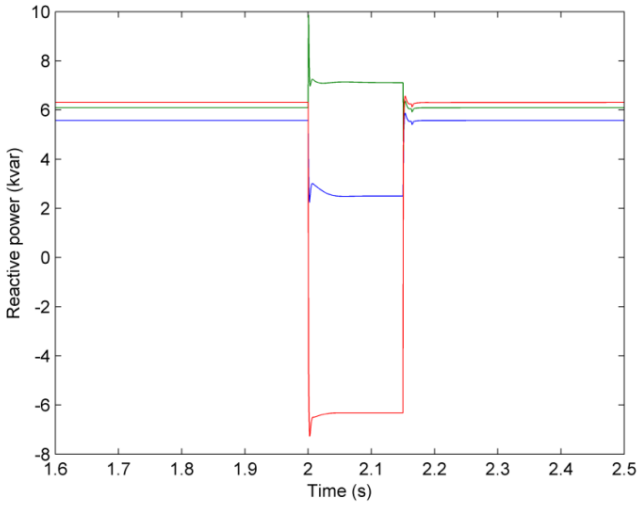

Fig. 3.40 The reactive power of VSC3 in its three phasesin case of single phase to ground fault with fault impedance of 0 Ω (blue line: phase A, green line: phase B, red line: phase C).

The reactive power is injected in the different phases of bus RA, RB, RC and bus RD in the normal operating conditions in order to reduce the unbalance factor as shown in fig. 3.38, 3.39, 3.40 and fig. 3.41 respectively. It can be seen in fig. 3.38 and fig. 3.39 that VSC1 and VSC2 deliver small amounts of reactive power during steady state condition but inject/absorb maximum amount of reactive power during the unbalanced voltage sag. Since two phases (i.e. phase A and phase B) have voltage sags in the network buses therefore all of the inverters are injecting reactive power in these two phases at t=2 s as shown in fig. 3.38, 3.39, 3.40 and fig. 3.41.

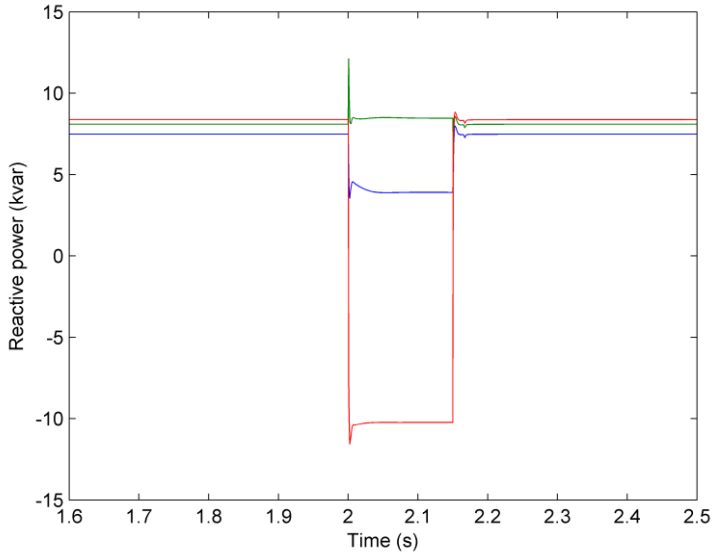

Fig. 3.41 The reactive power of VSC4 in its three phasesin case of single phase to ground fault with fault impedance of 0 Ω(blue line: phase A, green line: phase B, red line: phase C).

The reactive power injected by all of the inverters in phase B is a little bit higher than phase A because voltage sag in phase B is a little deeper than in phase A in all of the branches. Phase C in all branches of the network has not voltage sag so in general there should be no injection of the reactive power by the inverters in this phase. But the purpose of the controllers developed for this study is not only to mitigate voltage sag but also to compensate against voltage unbalances in the network. Due to this reason reactive power is absorbed in phase C in order to reduce the unbalance factor.

There is an increase in the flow of the currents delivered by the inverters of the DG units used in the network at the time of the short circuit. This rise of the current is controlled by using current limiters in the control system of the respective inverter so the IGBTs may not damage against over currents. The peaks in the reactive powers of VSC1 and VSC2 in each of the phase as shown in fig. 3.38 and fig. 3.39 are due to this phenomenon.

The injection of the reactive by VSC3 and VSC4 as shown in fig. 3.40 and fig. 3.41 is done in the same way as described in section 3.4.1.4. The inverters inject/absorb reactive according to the value of the voltage measured at their points of connection. The reason for the decrease of the reactive in some of the phases of these inverters is the same as explained in section 3.4.1.4. The peaks in the reactive power in fig. 3.40 and fig. 3.41 at the beginning and at the end of voltage sag are due to the charging and discharging of DC-link capacitors in order to maintain the constancy of DC-link voltages of the PV inverters.

The new value of voltage in each of the phases in per unit in the different parts on the network after using compensation and the voltage unbalance factors in the normal and the fault periods are shown in table 3.2. This result shows that the controllers to some extent have mitigated the voltage sags in the different phases and have improved the unbalance factors.The unbalance factors in the fault conditions are still not within an acceptable range.The voltages in phase A and phase B are also not improved up to the acceptable limits [77] because the converters do not have enough reactive power capacity to mitigate voltage sags and the voltage unbalances of such big depth.

Table3.2. The voltage in three phases in different parts of the network and voltage unbalanced factors for the normal and the single phase fault conditions with compensation

Bus No.	VOLTAGE IN NORMAL CONDITIONS			%UF IN NORMAL OPERATION	VOLTAGE DURING FAULTS			%UF DURING FAULT
	A	B	C		A	B	C	
RA	1.007	0.9986	0.9949	0.299	0.69	0.54	0.912	33.2
RB	1.0066	0.9991	0.9956	0.32	0.691	0.545	0.9087	32.4
RC	1.0078	0.9982	0.994	0.34	0.68	0.55	0.91	32.55
RD	1.0061	0.9977	0.9936	0.299	0.654	0.56	0.926	35.5
R11	1.0045	0.9976	0.9945	0.22	0.61	0.579	0.95	40.2
R15	1.0052	0.996	0.9904	0.295	0.626	0.57	0.939	38.3
R17	1.0077	0.9992	0.992	0.39	0.67	0.56	0.914	33.33

To figure out the limit of the converters in relation to the voltage sag depth for the mitigation of voltage sag, a single phase to ground fault on phase A at the bus R0 with a fault impedance of 3 Ω is applied at the time equal to t=2 s. The fault is cleared at 2.15 s. The voltages in the three phases of the R0 bus in this case are shown in fig. 3.42. It can be seen in fig. 3.42 that the voltage in the effected phase during the fault is reduced but not equal to zero as in the last case.

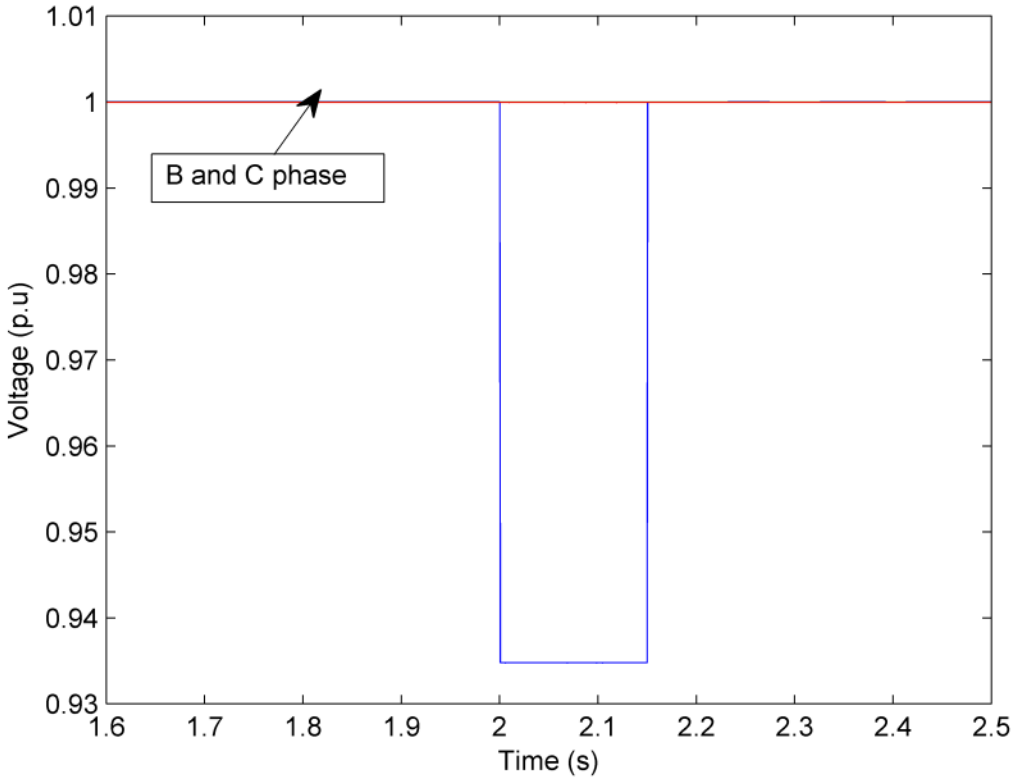

Fig. 3.42 The voltage in three phases of bus R0for L-G fault on phase A with Z_f =3 Ω. (blue line: phase A, green line: phase B, red line: phase C).

The fault on bus R0 creates unbalanced voltage sags in different parts of the network gird. The transformation of voltage sag from the delta side of the transformer to its wye side is according to fig. 3.33. The voltages in three phases of bus R1 when all of the controllers are disabled and obtained by using above transformation method in this new case is shown in fig. 3.43. The values of the voltage during fault in each of the phases have been verified by using equation 3.1. The resultsobtained by analytical method using equation 3.1 are matching with the simulation results and are shown in fig. 3.43.

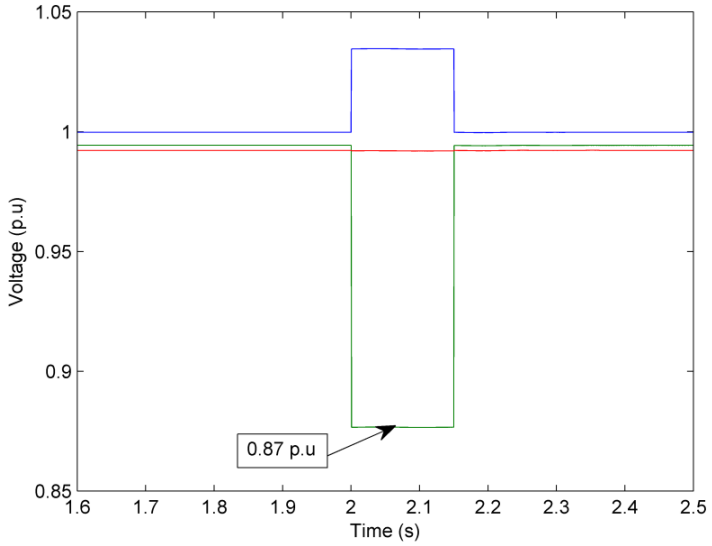

Fig. 3.43 The voltage on bus R1 for L-G fault on phase A with Z_f =3 Ω when all of the controllers are disabled (blue line: phase A, green line: phase B, red line: phase C).

The mitigation of voltage sag of this magnitude can be made by using the developed controllers. To illustratea simple case the voltage on one of the buses (i.e. bus RA) without and with controllers in this case is shown in fig. 3.44 and fig. 3.45 respectively. It can be seen in fig. 3.44 that without using controllers, phase B of bus RA of the network is less than 90% which is not within a tolerable limit according to IEEE standard 1159-1995 and Danish standards [77]. By using the existing controllers the voltages in all of the phases are restored within the permissible limits of +-10% [77] according to IEEE standard 1159-1995 and Danish standards.

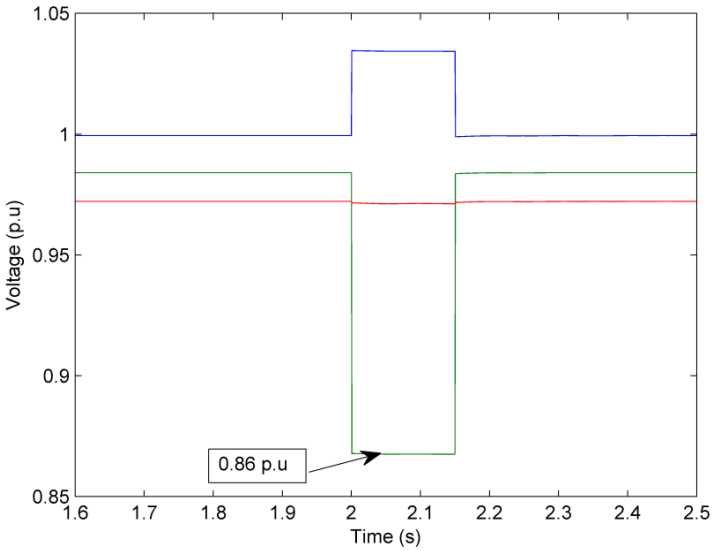

Fig. 3.44 The voltage in three phases of bus RA for L-G fault on phase A with Z_f =3 Ω when controllers are disabled (blue line: phase A, green line: phase B, red line: phase C).

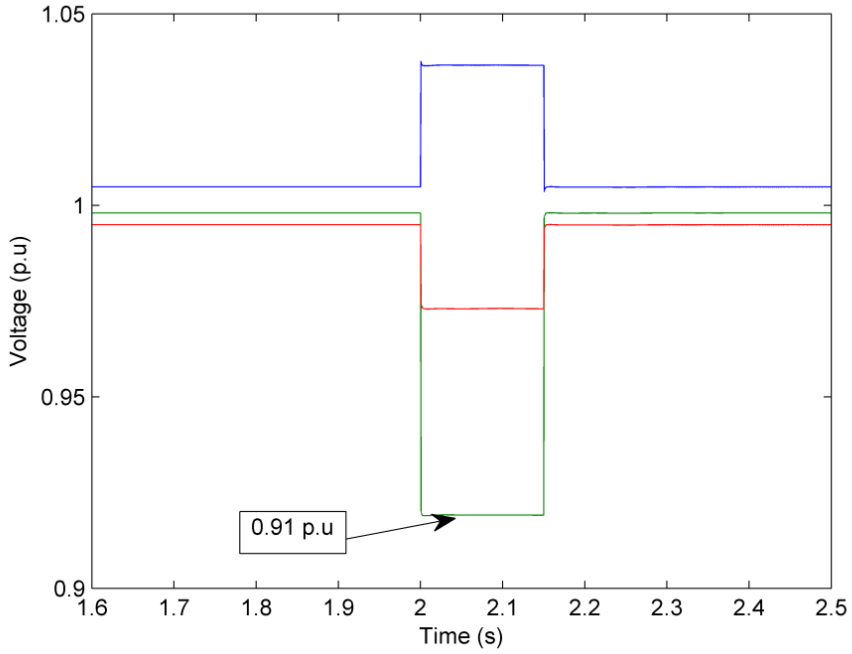

Fig. 3.45 The voltage in three phases of bus RA for L-G fault on phase A with Z_f =3 Ω by using existing controllers (blue line: phase A, green line: phase B, red line: phase C).

The voltages in each phase of the buses in the different parts of the network and unbalance factors in the faulted conditions with and without using compensation are presented in table 3.3. This table shows that the voltages in all parts of network in each of the phases are restored within permissible limits and the voltage unbalances during the fault are also reduced to a smaller value by using the developed controllers. The controllers have successfully mitigated the unbalanced voltage sags in all parts of the network grid but they are unable to maintain the unbalance factor limit according to IEEE standards 1547.2-2008 during the fault. The only way to restore the unbalance factor according to the standards is to use bigger size of the battery units rather than the existing ones.

Table 3.3. The voltage in three phases in different parts the network and voltage unbalance factors during fault with and without compensation for L-G fault on phase A with Z_f =3 Ω

Bus No	VOLTAGE DURING FAULT WITH NO COMPENSATION			%UF WITH NO COMPENSATION	VOLTAGE DURING FAULT WITH COMPENSATION			%UF WITH COMPENSATION
	A	B	C		A	B	C	
RA	1.034	0.867	0.97	9.22	1.0366	0.919	0.97	6.46
RB	1.034	0.866	0.969	9.2	1.0367	0.92	0.97	6.3
RC	1.034	0.864	0.966	9.26	1.037	0.918	0.97	6.38
RD	1.033	0.866	0.97	9.4	1.0356	0.91	0.979	6.9
R11	1.034	0.87	0.98	9.27	1.033	0.90	0.988	7.69
R15	1.0336	0.879	0.974	9.45	1.034	0.90	0.98	7.38
R17	1.035	0.867	0.967	9.24	1.036	0.916	0.975	6.5

3.5 Summary

The study about the behavior of the stochastic changes in the wind speed and solar irradiance on the power output of DG units and the network voltages has been presented in this section. The validation of the developed controllers described in chapter 2 in order to control the voltages with respect to the changes in wind speed and solar irradiance has been given in this chapter. The simple case about the control of the reactive power in the CIGRE network has also been performed here. The study about the behavior of the CIGRE network in transient conditions has been described. This is done by applying symmetric and asymmetric faults in the different parts of the network. The effects of the voltage sags on the different components of the tested network have been described with the help of simulation results. The mitigation of the balanced and unbalanced voltage sags and the voltage unbalances has also been presented in this chapter. The mitigation of the voltage sags in case of short circuit fault (i.e. balanced and unbalanced) with different values of the fault impedances has been tested and conclusion has been made that controllers can only compensate against voltage sags up to specific range.

Chapter 4

Short circuit protection of the CIGRE low voltage distribution network

4.1 Introduction

The main objective of the protective schemes in the power network is to keep the system stable and secure by isolating the faulted section in the shortest possible time, leaving as much of its portion as possible unaffected. The security of the power network is threatened due to the occurrences of the faults.A short circuit fault is the most common fault in power systems. A short circuit fault carries enormous amount of current which generates tremendous heat and poses risks of fire, damage to the other equipments and potential electrical shocks to the people. If a short circuit is not removed or a faulty portion is not quickly isolated from the healthy system, it will spread into healthy part of the network and may cause over loads and possibly cause damage to the transmission lines/cables, bus bars and other equipments. It is therefore, necessaryto protect the equipments of the power network against the short circuits by using short circuit protection devices and ensuring their proper coordination in order to avoid false tripping.The protection of the power network together with the increased penetration of DG units is a complex process and is a challenge for the protection engineers. In case of DG unit(s), power is fed from the different sources, and it is difficult to fix the fault level of the location and time of the operation of protection devices at the particular point in the network.

This chapter presents a detailed study about protection of the low voltage CIGRE network against short circuit faults. This study is performed by applying symmetrical (i.e. 3-phase fault) and asymmetrical faults (i.e. single phase to ground fault) with and without fault impedance at different locations of the network. The different components of the CIGRE network (i.e. transformer, WTG, lines, bus bars, battery inverters and PV inverters) can be protected either by circuit breakers or by fuses. Typically, transformers below 1000 kVA are protected by using fuses [89]. According to Schneider electric [90] and Danfoss, low voltage inverters for PV applications and battery storages are protected against short circuit currents by using fuses. Therefore, this study about the protection of LV CIGRE distribution network against short circuit current is mainly performed by using fuses as protection devices. The under voltage relays are used to clear a fault if fuses are unable to clear faults in some conditions. These relays can also be used in the case when fuses take longer time to clear fault such as fault with some fault impedance etc.

A fuse is a protection device, which is used to provide over current protection of either the load or source circuit. It comprises of fusible element (i.e. metal wire) which melts when too much current flows across it. It is used to interrupt the excessive flow of the current through electrical circuit which may cause the severe damage to it due to overheating or fire. Fuses are selected to allow passage of normal current plus a marginal percentage (i.e. 25%) to allow excessive current only for short duration [91], [92]. When the current in any

of the branches of the network exceeds 125% of the normal value, the fusible element of the fuse connected to that branch blows out and disconnect that branch from the rest of network. The melting of fuse follows an inverse time-overcurrent characteristic i.e. higher the current, the less will be the time for the fuse to melt and vice versa. The following criteria must be followed to ensure proper selection of the fuse:

1. **Selection of the voltage rating of the fuse**

The voltage of the fuse should be equal to or more than the voltage of circuit to be protected [93]. Usually three-phase fusing will require a fuse of phase-to-phase voltage capability, whereas single-phase fusing will require a fuse with only phase-to-ground voltage rating.

2. **Selection of the nominal current of the fuse**

The nominal current of the fuse which is also called as amperage value of the fuse should be greater than the maximum continuous load current at which fuse operates. The nominal value of current for the fuse is equal to 125% of the maximum continuous current in the line.

3. **Time current characteristics (TCC) coordination**

Fuses normally have inverse time current characteristics. These characteristics ensure that fuses are able to isolate the faulty section of the power system in short duration if current seen by the fuses increases beyond the rated values.

The rated current of the transformer, WTG, loads and VSCs have been calculated by using simple mathematical relations. Considering the two winding 0.4 MVA, 20 kV/0.4 kV, DyN1 transformer shown in fig. 2.1,the line rated current on the 20 kV side of the transformer is given by equation 4.1.

$$I_{rated} = \frac{S}{V_{L-L} * \sqrt{3}} \quad \text{..... (4.1)}$$

Where S is apparent power rating of the transformer and V_{L-L} is the line to line voltage on delta side of the transformer.

$$I_{rated} = \frac{0.4 * 10^3}{20 * \sqrt{3}}$$

$$I_{rated} = 11.547 \text{ A}$$

Similarly, the rated current of the VSCs used in the network is calculated by using equation 4.1. The rated currents of the cables/lines are chosen according to their parameters provided by CIGREas shown in table A1 in appendix A. The unbalanced loads are aggregated at the 0.4 kV voltage levels and are connected at bus RC, RD, RE, R11and bus R17. The rated current in each of the single phase loads are calculated by using their apparent power ratings mentioned in fig. 2.1 and their voltage levels (i.e. $I_{rated}=S/V_{phase}$). The power factor of the 5.5 kW Wind Turbine Generator (WTG) used in the CIGRE network is 0.91.The capacitor bank

used on bus R19 is used to operate this machine at the unity power factor. The rated current of the WTG is calculated by using equation 4.2.

$$I_{rated} = \frac{P}{\sqrt{3} * V_{L\_L} * \cos\theta} \quad \text{(4.2)}$$

$$I_{rated} = 8.69\,\text{A}$$

The rating of the fuses selected to protect the different components of the CIGRE network which are labeled as shown in fig.4.1 and are presented in table 4.1.

Some of fuses selected in table4.1are even little less than 125% of the rated current because the next available fuse is of much bigger rating. For example, the fuse selected for load-RE is 40 A; whereas 125% of the rated current in the phase C of this load is 43.4A which is higher than the fuse rating.A40A fuse is selected because next available fuse is 50A, therefore, if the 50A fuse is selected for this load then it might cause delay in the protection.

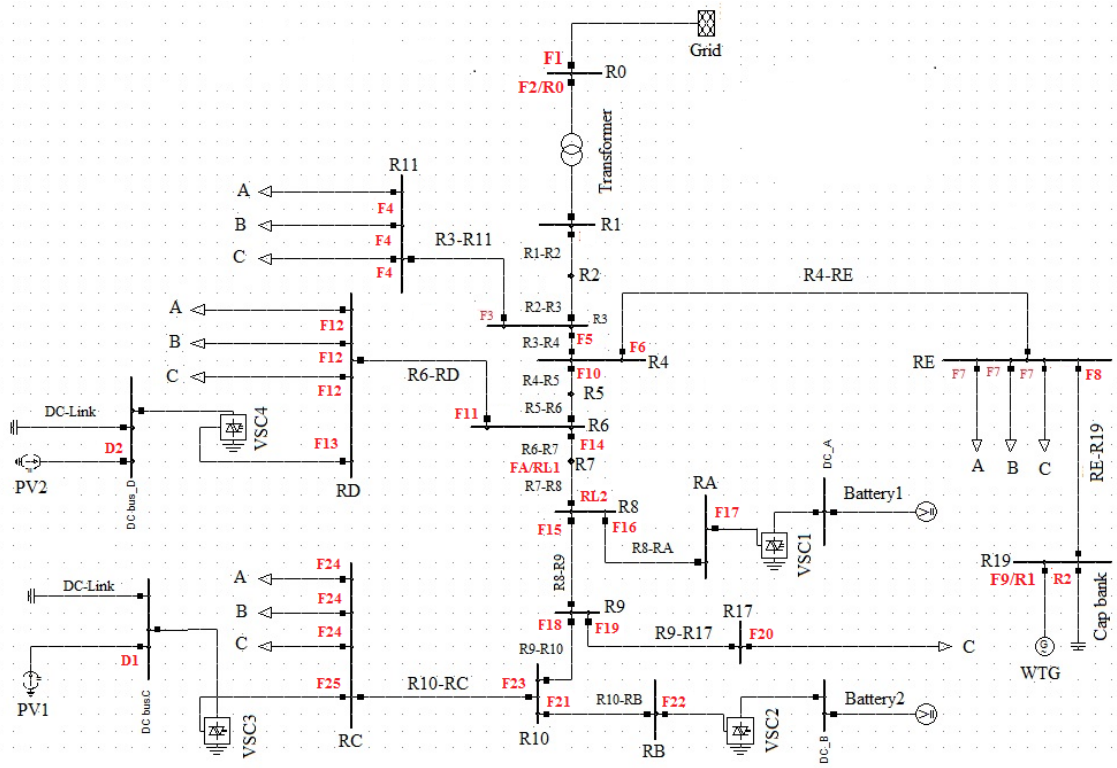

Fig.4.1 The single line diagram of the CIGRE network modeled in DIgSILENT together with protection devices

Table4.1. The rating of different fuses used at different locations of the CIGRE network

Lines/DGS/VSCS/Loads		Rated current [A]	Fuse current [A] i.e. 125% of Inom	Fuse selected	Name of the fuse in network
Grid		11.5	14.45	20	F1
T/f. Prim		11.55	14.45	16	F2
R3-R11		162	202.5	200	F3
R3-R4		401	501.25	500 1000*	F5
R4-RE		304	380	400 500*	F6
RE-R19		304	380	400	F8
R4-R5		401	501.25	500 800*	F10
R6-RD		199	248.75	250	F11
VSC4		34.68	43.35	40	F13
R6-R7		401	501.25	500 630*	F14
R7-R8		401	501.25	500 630*	FA
R8-R9		401	501.25	500 630*	F15
R8-A		162	202.5	200	F16
VSC1		50.58	63.32	63	F17
R9-R10		401	501.25	500	F18
R9-R17		162	202.5	200	F19
R10-RB		162	202.5	200	F21
VSC2		36.13	45.16	50	F22
R10-C		162	202.5	200	F23
VSC3		26	32.5	32	F25
WTG		8.69	10.86	10	F9
Load_RC	Phase A	6.9	8.7	20	F24
	Phase B	13.9	17.4		
	Phase C	17.4	21.7		
Load_RD	Phase A	20.86	26	40	F12
	Phase B	27.8	34.8		
	Phase C	34.8	43.4		
Load_RE	Phase A	20.86	26	40	F7
	Phase B	27.8	34.8		
	Phase C	34.8	43.4		
Load_R11	Phase A	4.35	5.44	16	F4
	Phase B	8.7	10.87		
	Phase C	11.74	14.67		
Load_R17	Phase C	11.74	14.67	16	F20

The selected rating of fuses denoted by '*****' shown in table 4.1 is different because of coordination purposes. Concerning the protection of the CIGRE network in its central parts, fuse selected for cable R9-R10 is of 500 A. There are many other cables in this part of the network which transfer the power to and from the grid. In order to ensure the protection coordination and to save as much portion of the network as possible during the fault, fuses in this section are used sequentially higher than the fuse for cable R9-R10. It can be seen in table 4.1 that a 500 A fuse (i.e. F18) is used to protect cable R9-R10. The fuses in the upstream section of the network in its central parts are 630 A, 800 A and 1000 A. The rating of fuse F5 (i.e. 1000 A) which is used to protect cable R3-R4 is higher as compared to the rating of fuse F18 (i.e. 500 A). This is because there is no other fuse available in between 800 A to 1000 A. This is a main drawback of the current based protection by using fuses in this part. Other details and most suitable method to protect this network in central parts are described in section 4.5.

The contents of this chapter are organized as follows: Section 4.2 presents the study of the network in the case when protection is made against 3-phase faults with and without fault impedance. The over speed protection of the WTG in the case of loss of grid due to 3-phase fault is also described in this section. The study about the protection of the CIGRE inverters is presented in section 4.3. The disconnection of the solar PV cell structure in the case when in island is also described in this section. Section 4.4 presents the results about the protection against single-phase to ground fault and the disconnection of the WTG in that case. The study about the protection of the CIGRE network in its central part is given in section 4.5. Finally, the summaryof this chapter is presented in section 4.6.

4.2 Protection of the CIGRE network against 3-phase faults

The study about the protection of the network in this case is carried out by introducing a 3-phase fault with and without fault impedance at different locations of the CIGRE network. Fuses and under voltage relays available at the different locations are used to clear this kind of fault.

4.2.1 Protection of the network in case of 3-phase faults without fault impedance

To study protection of the CIGRE network grid, a three phase fault with fault impedance of zero ohm (Z_f =0) is applied at time equal to t=5 s at the terminals of the WTG (i.e. bus R19). In order to ensure the reliability and security of the network, this kind of fault must be removed from the grid side and from the WTG side quickly. The procedure of clearing the fault from both the sides of the fault is described below:

The voltage at the WTG bus (i.e. bus R19) due to this kind of fault becomes zero and hence, the active power output of generator becomes zero. According to the technical regulations 3.2.1 for electricity generation facilities with a rated current of 16 A per phase or lower, the WTG must be disconnected if its terminal voltage falls below 0.9 p.u [94].

The current produced by the WTG at the instant of the short circuit fault starts to increase to a very high value before decaying completely to zero as shown in fig. 4.2. The rise in this current at t=5 s is because of inrush current flowing to the faulted point. The induction machines deliver about six times rated current during this time [95-97]. This fault characteristic of the WTG is due to the inertia in the presence of field flux produced by the induction from the stator. This flux decays on the loss of the voltage because of the fault at the terminals of the machine. This current decays to zero as shown in fig. 4.2 and is because of the loss of field excitation (i.e. loss of stator flux).

The current shown in fig. 4.2 decreases to zero before reaching to the activation time of fuse F9 (i.e. 273 ms at this value of current as seen from the inverse time characteristic of fuses in fig. B1 in appendix B). The observed current is not within the range of the selected fuse operating characteristics; therefore, the disconnection of the WTG from the faulted point is not possible by using the fuse in this case. An under

voltage relay is used instead of fuse in this case. The voltage is sensed by the relay R1 as shown in fig. 4.1 and sends trip signals to the circuit breaker which disconnects the WTG from the faulted point. The time of operation of this relay depends on how low the voltage is at the terminal of the WTG. According to ANSI CS84.1-1995 if the voltage is below 0.5 p.u then the time to clear the fault should be maximum 0.16 s and if the voltage is in between 0.5p.u and 0.88 p.u the time to clear fault should be less than 2 s. Since the voltage on the terminals of the WTG due to the fault is zero (i.e. voltage is below 0.5 p.u); therefore, the fault should be cleared within 0.16 s. The operation of the circuit breaker receiving the trip signal by relay R1 is shown in fig. 4.3. The Breaker status is assumed closed when it shows 1 on the plot and is opened when it displays 0 on the plot as shown in fig. 4.3.

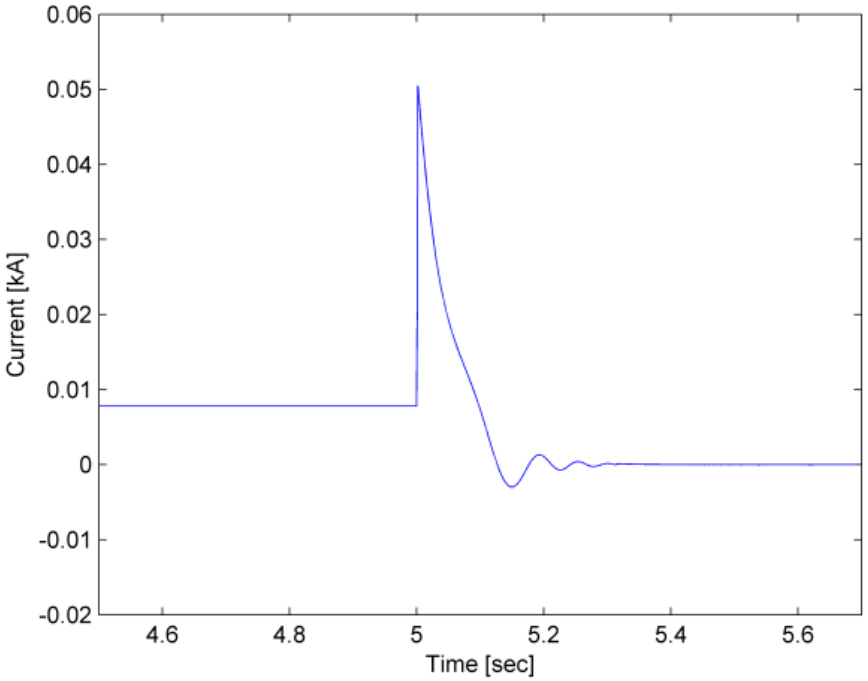

Figur 4.2 Current of the WTG when a 3-phase fault with fault impedance of 0 **Ω** is on its terminals

The capacitor bank is used at bus R19 as shown in fig. 2.1 in order to improve the power factor of the WTG; this capacitor also needs protection against the fault at bus R19. The voltage at the point of connection of this capacitor decreases to zero due to the short circuit fault as shown in fig. 4.4. The production of reactive current by the capacitor bank required for the magnetizationof the WTG stator winding decreases to zero because of its zero voltage at this time t= 5 s. This current is shown in fig. 4.5. It can be seen in fig. 4.5 that the capacitor bank delivers some amount of the reactive current (i.e. minus sign shows the current is injected) in order to excite the stator of the WTG in the normal operating conditions. The injection of the current by the capacitor bank decreases to zero at the time when the voltage at its terminals becomes zero as shown in fig. 4.4. Therefore, the current based protection is not valid in this regard. The under voltage relay R2 shown

in fig. 4.1 is used in this case. The operation of the circuit breaker used to disconnect the capacitor bank is the same as shown in fig. 4.3 because both the relays are sensing the same voltage and are connected at the same bus.

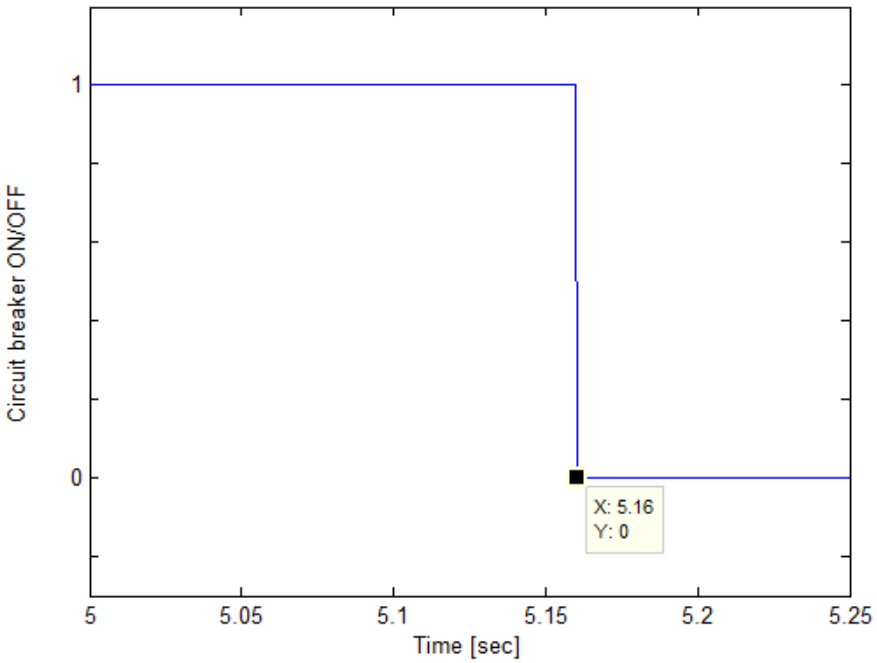

Fig. 4.3 The operation of the circuit breaker in case of a three phase fault with fault impedance of 0 Ω on bus R19.

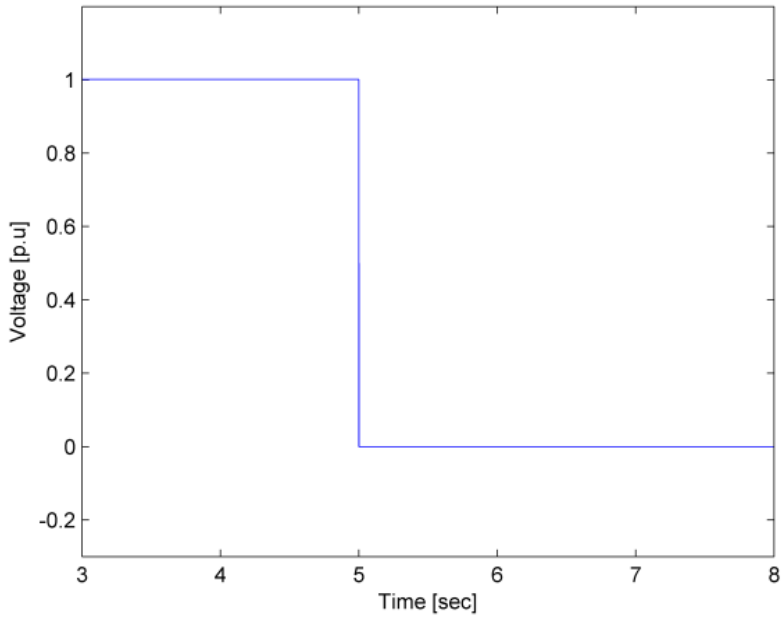

Fig. 4.4 The voltage of the capacitor bank in case of a three phase fault with fault impedance of 0 Ω on bus R19.

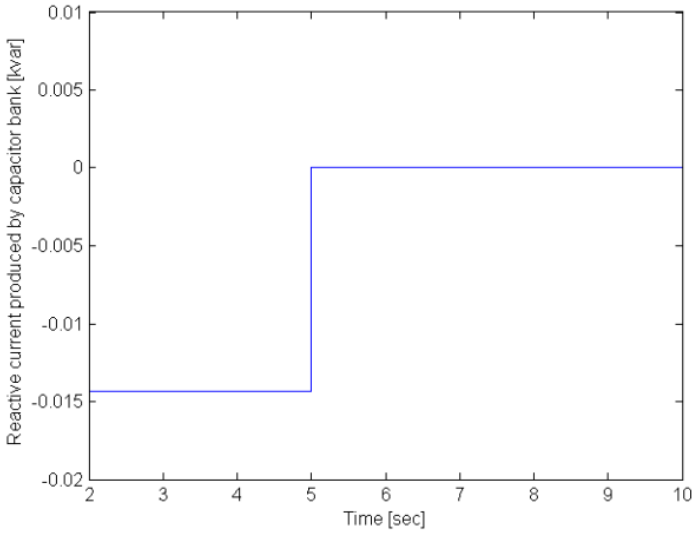

Fig. 4.5 The reactive current delivered by the capacitor bank connected at bus R19 in case of a three phase fault with fault impedance of 0 Ω on bus R19.

The voltage on bus RE is unbalanced because of the three single phase loads connected on this bus. Due to this reason, the short circuit current flowing through the upstream cable RE-R19, which is connected on bus R19 (i.e. faulted bus) will also be unbalanced. The current flowing through the three phases of cable RE-R19 is shown in fig. 4.6. In the normal operating condition, a current with magnitude of 16.5 A is flowing in the three phases of the cable RE-R19. This current increases to 2.56 kA at the instant of the fault at t= 5 s as shown in this figure. The short circuit currents in the three phases during the fault are a little bit different because of the voltage unbalance.

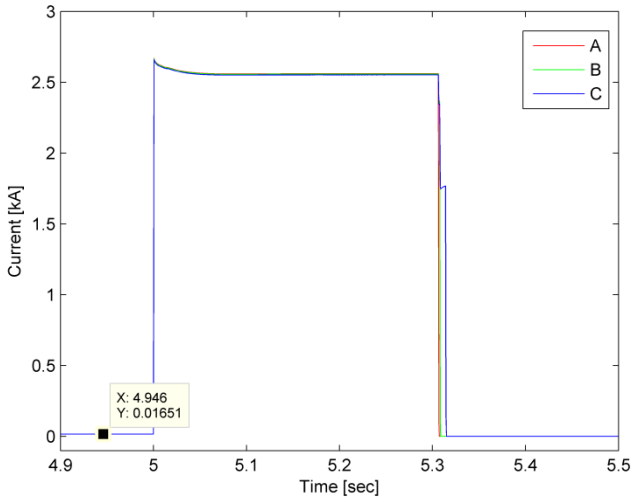

Fig. 4.6 The current flowing through cable RE-R19 in case of a three phase fault with fault impedance of 0 Ωon bus R19 and with the operation of protection devices.

Fuse F8 used to disconnect this faulty section of the network from the grid side blows in 313 ms according to the inverse time current characteristics of this fuse as shown in fig. B1 in appendix B. It can be seen in fig. 4.6 that the disconnection in the different phases is made at different times since the current is bit differentin the three phases. Hence, the fault has been isolated from both the sides of network (i.e. grid side and WTG side).

The electrical power output of the WTG becomes zero because of zero voltage at its terminals (i.e. bus R19). A WT receiving a constant wind speed, with no transfer of electrical power, rapidly increases the speed of the generator. Therefore, it is essential that the wind turbine stops automatically if the generator is disconnected from the electrical grid [98]. The Danish wind turbines are required to be protected either by aerodynamic brakes or mechanical brakes [98]. Aerodynamic braking uses pitch angle mechanism and it is used for pitch controlled wind turbines or active stall controlled turbines and is expensive for small wind turbines like the ones considered under this study. Mechanical braking is the most common method used for the small wind turbines [99], [100] and this mechanism is used to stop the 5.5 kW wind turbine used in the CIGRE network in the case of the loss of the grid supply in this study.

The block diagram of the mechanical brake model developed in DIgSILENT power factory software version 15.0 is shown in fig. 4.7.

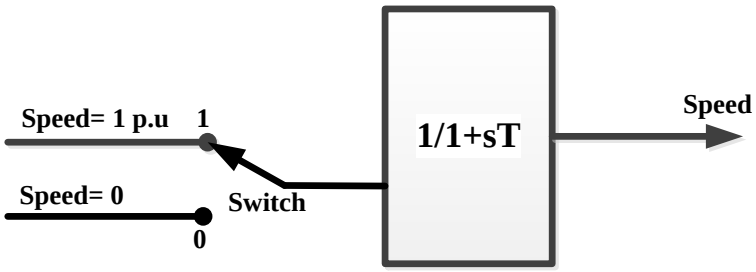

Fig. 4.3 The model of mechanical brake

The brake model comprises a switch together with a first order time lag function which is represented by the transfer function 1/1+sT, where T is the time constant that ensures the actuation time of the brake. The position of the switch remains at 1 when the generator operates at the speed of 1 p.u. in the normal operating condition. However, if the speed of the rotor increases beyond 1.2 p.u. [100], the switch changes its position from 1 to 0 and makes the shaft reference speed equal to zero which in turn reduces the mechanical torque of the machine in order to stop the generator. The actuation time (i.e. 10 s) of the brake [101], [102] is ensured by setting the time constant (T) of the time lag function.

The electrical and the mechanical torques of the squirrel cage induction generator working as WTG is shown in fig. 4.8. It can be seen in fig. 4.8 that both the torques are equal in the normal operating conditions whereas the electrical torque of the WTG becomes zero at the instant of three phase fault. The peak in the electrical torque at the instant of the short circuit fault is due to the short circuit current produced by the WTG. The braking mechanism is activated at the time equal to t=5.6 s as the generator speed observed is

more than 1.2 p.u and the brakes are applied on the turbine shaft. The mechanical torque decreases to zero as shown in fig. 4.8 due to the applied brake on the shaft. The speed of the WTG with braking mechanism is shown in fig. 4.9 It can be seen in fig. 4.9 that the WTG has been stopped in the case of loss of grid due to a 3-phase fault within the actuation time of t=10 s.

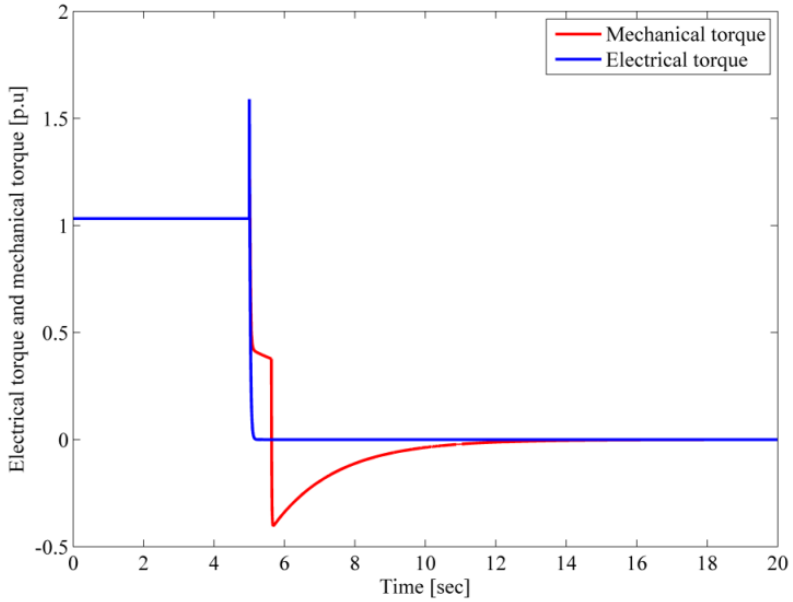

Fig. 4.8 The electrical and the mechanical torques of the WTG in case of loss of grid

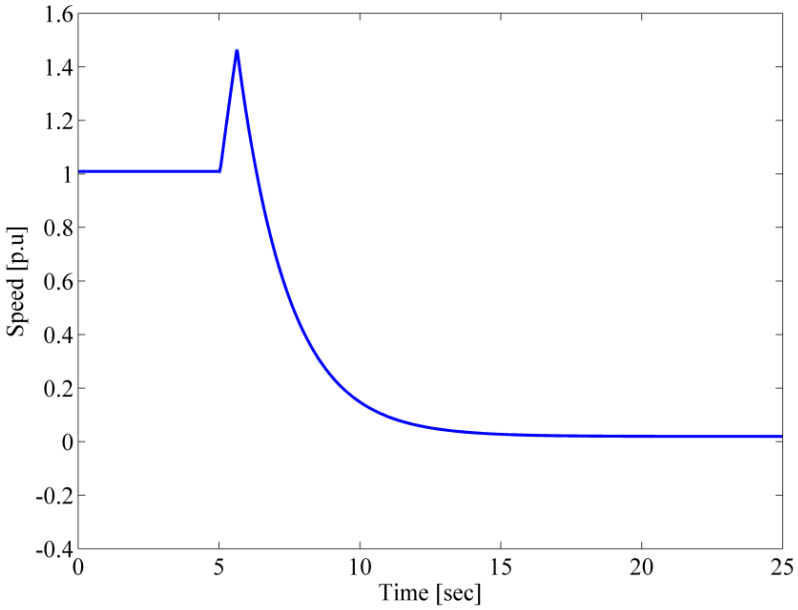

Fig. 4.9 The speed of WTG with braking mechanism in case of loss of grid

To study the protection in the other parts of the network, a three phase fault with a fault impedance of zero ohm (Z_f =0) is applied at time t=5 s on the MV bus (i.e. bus R0). There is a bi-directional flow of the current to the fault point in this condition. The fuse F1 shown in fig. 4.1 is used to disconnect the faulty section from the grid side which enters the distribution system into island. Fuse F1 is selected to the next higher rated available fuse than that of fuse F2 to ensure protection coordination. Fuse F2 do not clear the fault because it was originally selected for the protection in the forward direction (i.e. in grid connected mode). The distribution network has now only a small amount of short circuit power when it is isolated from the grid, that's why fuse F2 does not clear the fault from the backward direction. The details about why fuse F2 do not clear the fault is described below with the help of simulation results. A fault still exist in the islanded portion of the network as it was only cleared from the grid side, therefore; to clear the fault in the islanded portion of the network; a new approach using under voltage relays is introduced here. The under voltage relay R0 is used to isolate the fault from the DGs side of the network in this regard.

The current delivered by the external grid and passing through fuse F1 is shown in fig. 4.10. It can be seen in fig. 4.10 that the grid delivers a huge amount of the current at the instant of the fault. When the fuse of 20 A (i.e. F1) sees this value of the current it blows within a very short duration as shown in fig. 4.10. Hence, the fault has been cleared from the grid side and it should also be cleared from the DGs side very quickly.

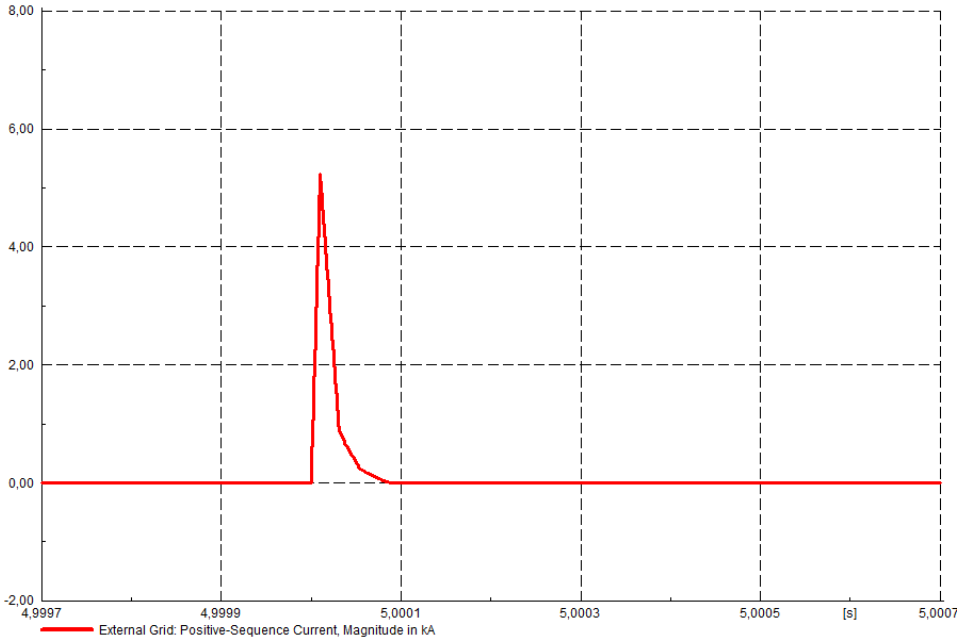

Fig. 4.10 Grid current in case of a three phase fault with fault impedance of 0 Ω at MV bus.

The operating characteristics of a fuse are shown in fig. 4.11. It can be seen in fig. 4.10 that time for pre-arcing starts when the fault appears on bus R0. At the peak value of the current arcing time starts and it takes some time to blow the fusing element of the fuse. The plot shown in fig. 4.10 follows the characteristics shown in fig. 4.11.

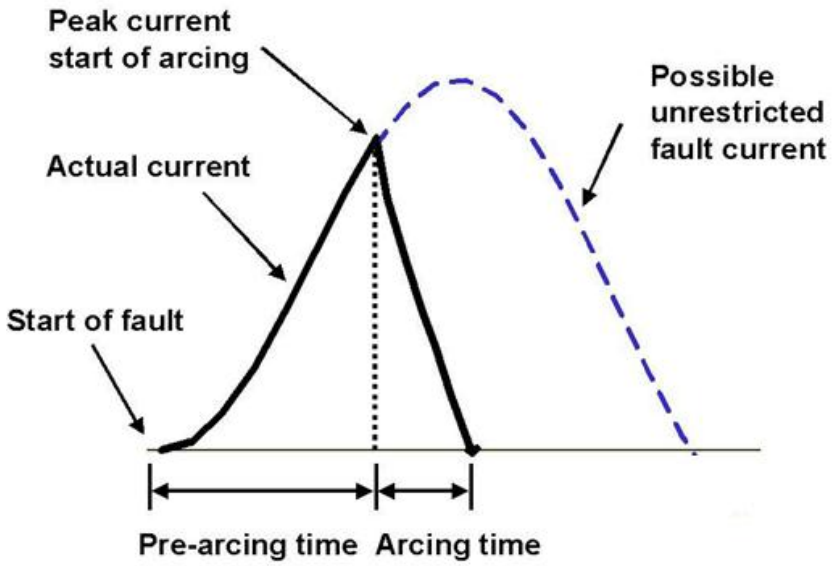

Fig. 4.11 The operating characteristics of fuse [103]

The current seen by fuse F2 is shown in fig. 4.12. It can be seen in fig. 4.12 that the current which passes through fuse F2 increases at the instant of a fault and soon it decays. The peak in the current at the initiation of the fault is due to the current surge produced by the DG units and it decays because of the current limiters used for these units. This current is coming from the DG side of the Micro Grid (MG) and passes through the 400 kVA transformer used between LV and MV buses. This current flowing through LV to the HV winding of the transformer (i.e. to the faulted point) passes through the transformer impedance. The current seen in fig. 4.12 is small because of the transformer impedance. This current in steady state condition after the current peak does not reach to the value which activates its operation.

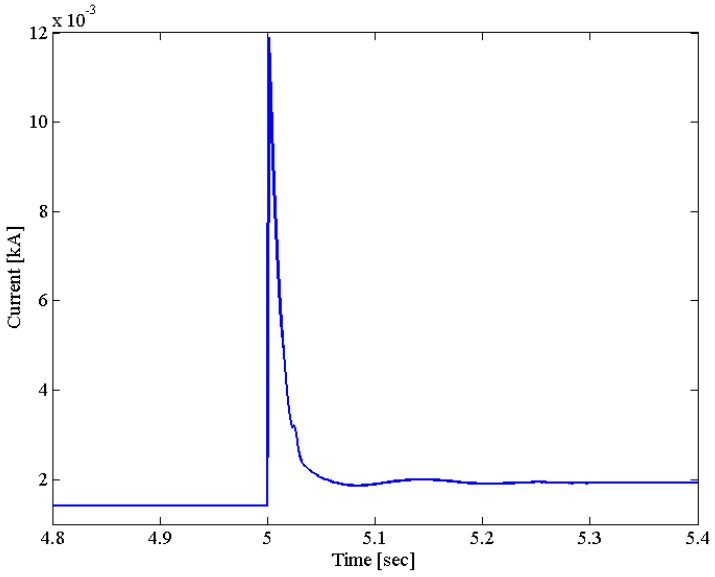

Fig. 4.12 The current seen by fuse F2 in case of a three phase fault with fault impedance of 0 Ω at MV bus.

A circuit breaker is used to clear this kind of the fault in the islanded portion of the network. The circuit breaker receives a trip signal from the under voltage relay R0. The circuit breaker named VD4 made by ABB is used in this regard. The minimum opening time of this circuit breaker lies between 33-60 ms [104]. The minimum opening time of circuit breaker used for this study is selected as 33 ms. The time of operation of fuse F1 and circuit breaker receiving trip signal by under voltage relay R0 is shown in fig. 4.13.

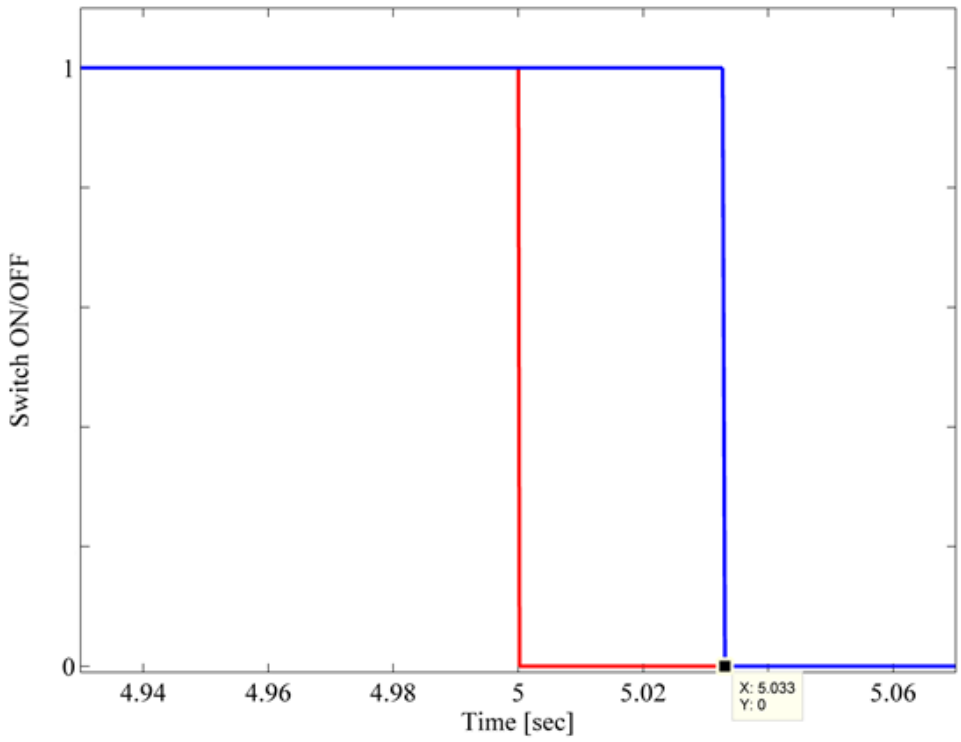

Fig. 4.13 The time of operation of fuse F1 and the circuit breaker

The 1 on the plot in fig. 4.13 depictsthe normal operation of fuse and tells that the contacts of the circuit breaker are in a close position whereas 0 displays that a fuse has been blown out and the breaker contacts are opened. It can be seen in fig.4.13 that fuse F1 clears the fault from the grid side faster than the circuit breaker used on the DGs side of the network. A fuse blows faster because of severe current flowing across its melting element.

The current flowing through the 400 kVA transformer in its LV and HV windings is shown in fig. 4.14. It can be seen that the current which passes through the DG side of the transformer (LV winding) is comparably more than the current in HV winding. Both the currentsbecome zero when the fault is cleared by the circuit breaker.

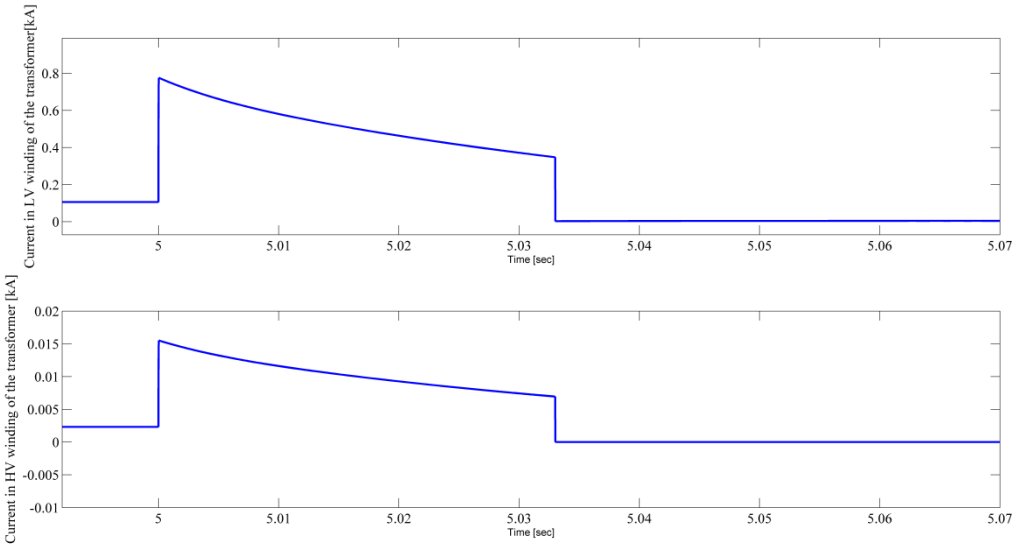

Fig. 4.14 The current flowing through LV and HV winding of the transformer in case of a three phase fault with fault impedance of 0 Ω at MV bus.

The clearance of the fault from both the sides of the network enters the LV CIGRE distribution network into island condition where all DG units (i.e. Two PV units, one WTG and two batteries together with the loads) form a Micro Grid (MG). The detailed study about the islanding operation of the distribution system is presented in chapter 5.

4.2.2 Protection of the network in case of 3-phase faults with fault impedance

To analyze the behavior of the protection devices, the study of the network is performed by applying three phase faults with some fault impedance.The short circuit current flowing through the faulted line in the case of fault with fault impedance is small compared to the fault without fault impedance. The inclusion of fault impedance delays the tripping of the over current protection devices. In order to observe the response of the protection schemes in the CIGRE distribution network,a three phase fault with a fault impedance of 0.1 ohms (Z_f =0.1) is applied on the terminals of WTG (i.e. bus R19) at the time equal to t=5 s. There is bidirectional flow of the current (i.e. one from the grid and other from a WTG) to the faulted point. As three single phase loads are connected on bus E which makes the voltage on this bus unbalanced, the current flowing through cable RE-R19 will also be unbalanced. The current flowing through the three phases of the cable RE-R19 in this case is shown in fig. 4.15. I can be seen in fig. 4.15 that the current flowing in the three phases of the cable increases at the instant of fault at t=5 s. The current in the three phases during the fault is little bit different because of the voltage unbalance.

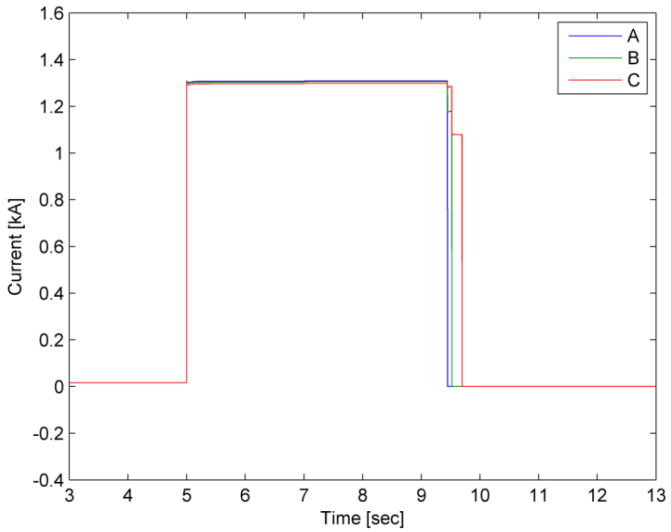

Fig. 4.15 Current flowing through cable RE-R19 in case of a three phase fault with fault impedance of 0.1 Ω at R19 bus.

The disconnection of the faulted section from the grid is ensured by using fuses F6 (backup) and F8. Both fuses have the same rated current; therefore the coordination of these two fuses in made in a way to ensure the disconnection of the portion nearest to the faulted point. Because of this reason the next higher rating of fuse F6 is used than that of fuse F8 as shown in table 4.1. By doing this the three single phase loads arenot disconnected becauseof this fault, since the disconnection is made at the point where fuse F8 is used. Fuses in the different phases blow at different times since the current is slightly different in all phases as shown in fig. 4.15 which ensures the isolation of the fault from the grid side. The voltage on bus RE and bus R19 in this case is shown in fig. 4.16.

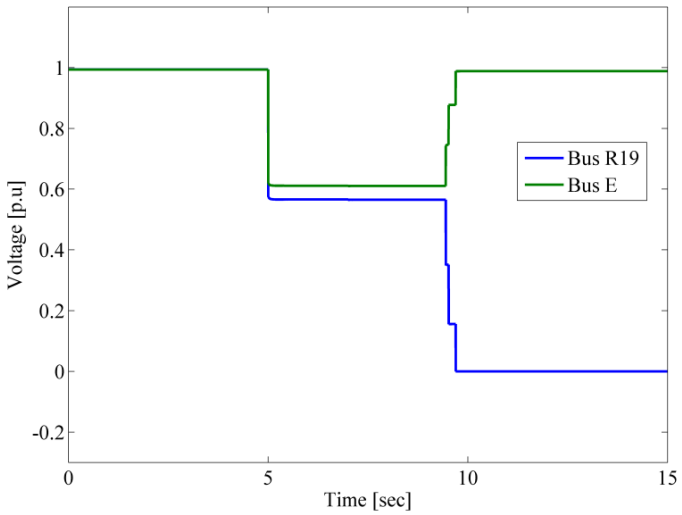

Fig. 4.16 Voltage on bus RE and bus R19 in case of a three phase fault with fault impedance of 0.1 Ω at R19 bus.

The voltage on both the buses is equal in normal operating conditions as shown in fig. 4.16. These voltages decrease at the instant of the fault. The voltage on bus RE returns to the nominal values and the voltage on bus R19 decreases to zero at the time when the fault is cleared from the grid side as shown in fig. 4.16. The switching in these voltages at the time of the fault clearing is due to the opening of the different phases at different times. Fig. 4.16 shows that the voltage at the terminal of the WTG is decreased to 0.56 p.u during the fault and it again decreases to zero when grid is isolated from the generator. Since the faulted section is only disconnected from the grid side and it should also be isolated from the generator side; the disconnection of the WTG can be made either by a current based protection device or a voltage based protection device.
The current delivered by the WTG in this case is shown in fig. 4.17 in order to investigate whether fuse or relay is the best choice for disconnection of the WTG from the grid. It can be seen in this figure that the WTG delivers a current surge at the instant of the short circuit fault. This current decreases to the value as shown in fig. 4.17. This reduction of the current during this period is because of the reduction in its terminal voltage. This current decreases to zero at the time when the grid is disconnected from the generator and is because of the loss of generator field excitation due to the disconnection of the grid. As there is only short time rise in the WTG current and it further decreases during the fault; fuse F9 does not detect this fault and hence the disconnection of the WTG is not possible by using fuse in this case.

Therefore, an under voltage relay is used for the disconnection of the WTG in this case. The current produced by the WTG in the case when an under voltage relay has isolated the machine from thefaulted point is shown in fig. 4.18. The time of the operation of the relay R1 is depending on the voltage left at its point of connection. Since the voltage on the terminals of the WTG is greater than 0.5 p.u. during the fault as shown in fig. 4.16; then according to ANSI CS84.1-1995 standards the relay R1 sends a trip signal to a circuit breaker which disconnects the WTG from the grid within 2 s.

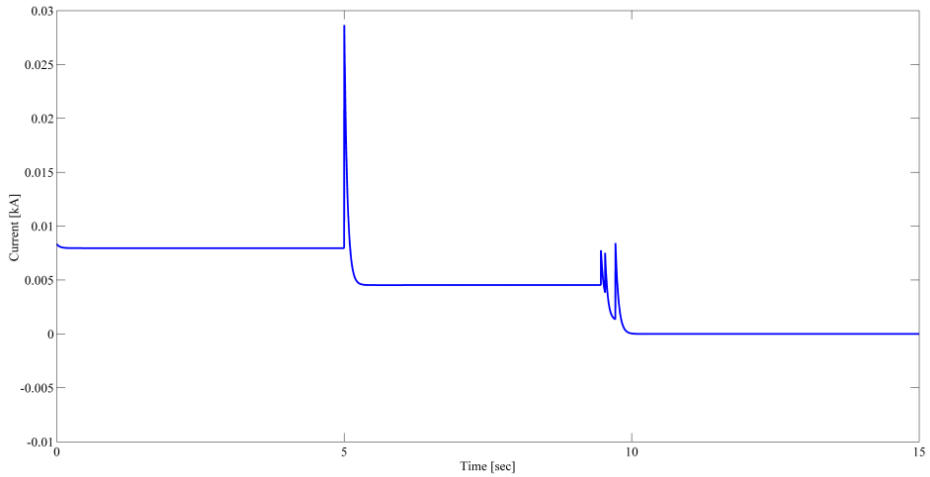

Fig. 4.17 The current delivered by the WTG in the case when fuse is used as protection device in case of a three phase fault with fault impedance of 0.1 Ω at R19 bus.

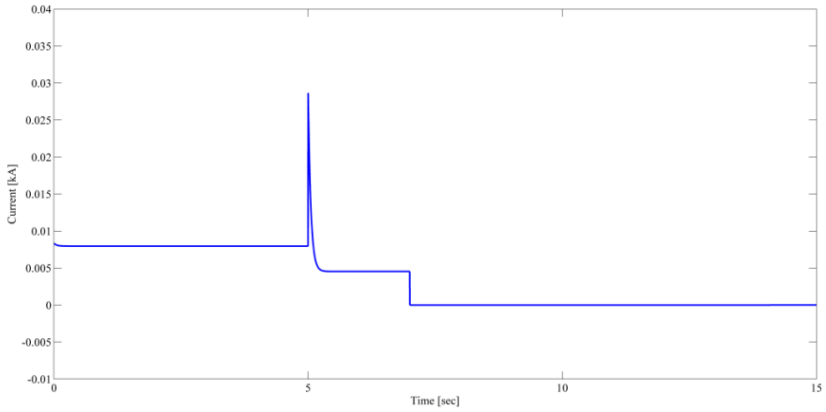

Fig. 4.18 The current delivered by the WTG in the case when relay is used as protection device in case of a three phase fault with fault impedance of 0.1 Ω at R19 bus.

It can be seen in fig. 4.18 that the WTG current decreases to zero at time equal to t=7 s (i.e. 2 s after the initiation of a fault). This decrease in current equal to zero at t=7 s is because of the opening of the circuit breaker at this time. Hence, the disconnection of the WTG is successfully made by using the under voltage relay R1 in this case. As the WTG has been disconnected from the grid therefore, the speed of the generator increases. The mechanical brake has been used to stop the generator in this regard. The speed of the generator in this case has been shown in fig. 4.19.

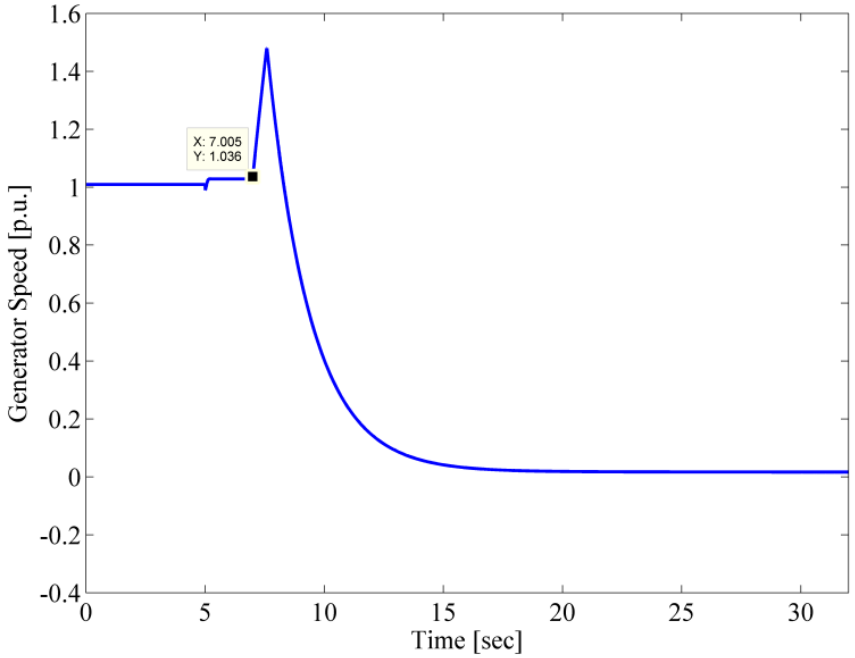

Fig. 4.19 The speed of Wind Turbine Generator in case of loss of grid

Different tests have been made in order to study the range of the protection devices. These tests have been performed by applying 3-phase fault at bus R19 using different values of the fault impedances. The summary about the range of the protection devices at different values of the fault impedances is presented in table 4.2.The voltage at bus RE and bus R19 and the current flowing through cable RE-R19 during the fault at different values of the fault impedances have been given in this Table. The time of the operation of fuse and an under voltage relay have also been shown and decision is made that up to which size of the fault impedance these protection devices (i.e. fuse and an under voltage relay) can operate. Theresults show that the protection devices can only operate in a certain range in the case of the fault impedance up to 0.6 ohms. This table also concludes that voltage based protection in general is faster than the current based protection in all the cases presented in this table.

Table4.2. The study about the range of protection devices with respect to the fault impedances in case of a three phase fault with fault impedance of 0.1 Ω at R19 bus.

in Z_f ohms	V_{RE} [KV]	V_{R19} [kV]	I_{RE-R19} [KA]	Fuse (F)	Time [sec]	Under voltage relay (UVR)	Time [sec]	Fast operation
0.3	0.82	0.80	0.630	Yes	125	Yes	2	UVR
05	0.89	0.87	0.410	yes	4900	Yes	2	UVR
0.6	0.91	0.89	0.339	No	-	Yes in bus R19 But No in RE	2	UVR
0.8	0.93	0.91	0.260	NO	-	No	-	-

Now in the case, if the fault impedance is high as for instance 2 ohms as for an arc, the protection devices shown in fig. 4.1 obviously will not work in this condition according to Table 4.2. The study about the protection against such kinds of the faults is described in [105], [106].

4.3Protection of the inverters used in the CIGRE network

To study the protection of the inverters used for the PV and battery applications in the CIGRE network; a fault is applied on one of the lines or the buses in the close vicinity of the inverters. A 3-phase short circuit fault with a fault impedance of zero ohm (Z_f =0) is applied on line R10-RC in this regard. This line is connected to bus RC where PV1 is connected. This is the line which is fed through the grid and a PV1 inverter; therefore, there is bidirectional flow of the current towards a short circuit point. There will be a surge of the current flowing from VSC3 towards the faulted line. The VSCs are very sensitive to over currents. The over currents in VSCs leads to thermal degradation of the IGBT valves and it may also cause a permanent damage to the IGBTs [72], [107], 108]. The IGBTs can withstand maximum currents of 2 p.u for 1 ms [109]. It is therefore, necessary to protect the IGBTs of the inverters by using ultra-fast protection devices. Fuse F25 is modeled as an ultra-fast (i.e. I-t characteristics are set in such a way that it blows very quickly) and acts instantly to protect VSC3 when the short circuit fault appears in line R10-RC. The current

of VSC3 is shown in fig. 4.20. It can be seen in fig. 4.20 that fuse F25 is blown when the current flowing through VSC3 increases abruptly during the short circuit. Line R10-RC is protected using fuse F23. The current flowing through this line is shown in fig. 4.21.

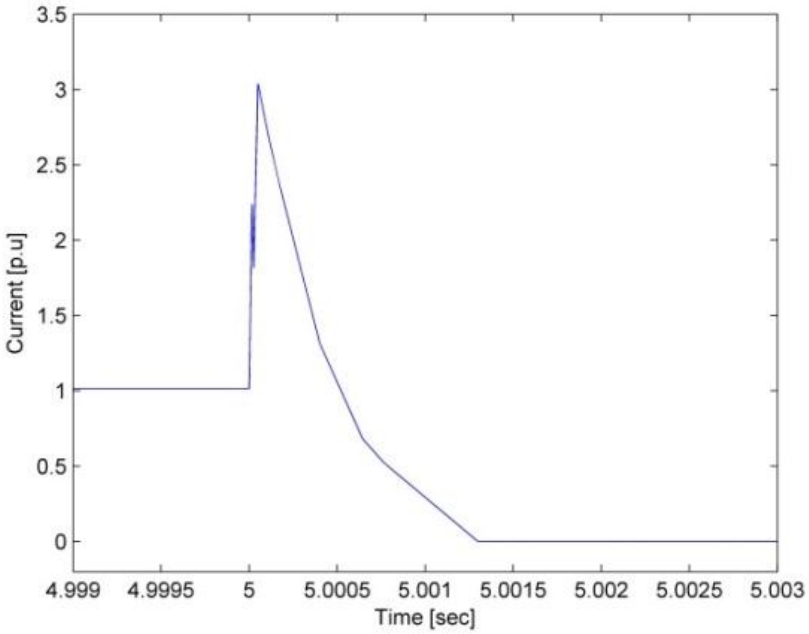

Fig. 4.20 The current of VSC3 in case of a three phase fault with fault impedance of 0 Ω on line R10-RC.

According to fig. 4.20 and fig. 4.21, fuse F25 which is used to protect VSC3 is faster acting than fuse F23. Fuse F23 disconnects line R10-RC from the healthy portion of the network within 68 ms whereas F25 isolates the PV inverter in a very short duration.

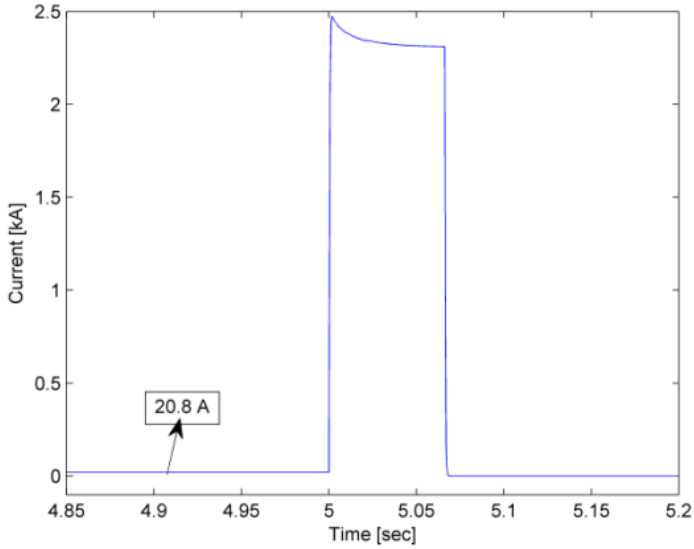

Fig. 4.21 The current flowing through R10-RC line in case of a three phase fault with fault impedance of 0 Ω on line R10-RC.

The solar structure of the PV power generating unit enters into islanding if such kinds of the fault are cleared from both the sides of line R10-RC. This might create problems with the insulation of the cell structure due to voltage rise at its DC connection. It is therefore, essential to protect the PV cell structure against such conditions.

PV inverters operate in a certain range of voltages. If voltage goes beyond nominal limits, it will stop its operation [110]. A three phase short circuit fault on the AC terminals of PV1 inverter causes the voltage to go down to zero and hence there is no transfer of power from PV1 towards the grid. The DC-link capacitor charges during this period and when it is fully charged there is no path for the current to flow and the PV operates at no load conditions. Due to this reason the DC-link voltage increases very fast. The PV generating units in real applications are normally disconnected from the DC bus in order to protect the insulation of PV cells against over voltages. In such a case, the PV panel presents open circuit voltage (i.e. it is the voltage across the terminals of a PV cell when the current flowing through the external circuit (I_{PV}) is zero) at its output with no power generation. The current flowing into the DC-link capacitor is shown in fig. 4.22.

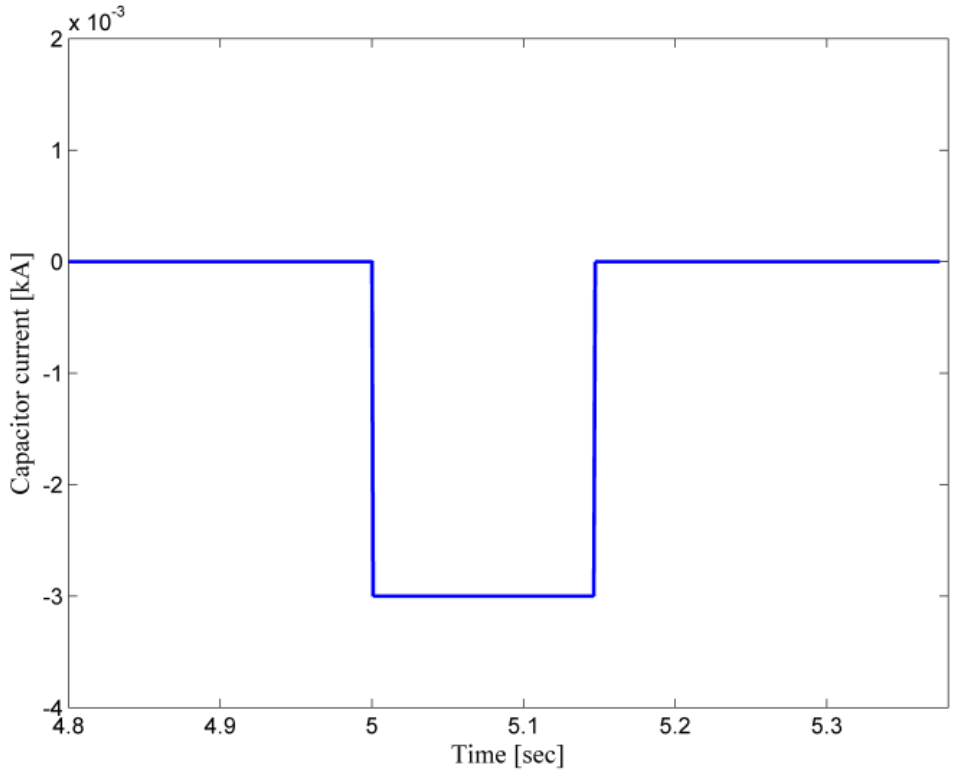

Fig. 4.22 The current of DC-link capacitor in case of a three phase fault with fault impedance of 0 Ω on line R10-RC.

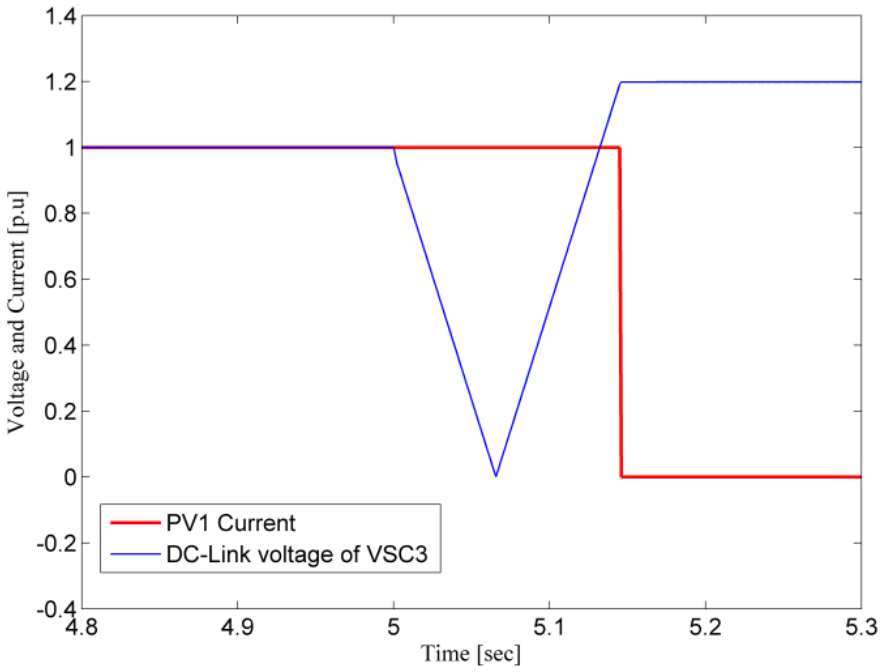

Fig. 4.23 PV1 current and DC bus voltage during normal and island operation in case of a three phase fault with fault impedance of 0 Ω on line R10-RC.

It can be seen in fig. 4.22 that there is no flow of current into the DC-link capacitor in the normal operating conditions, since all output power of the PV1 is transferred to the grid via VSC3. At the time of the grid isolation, the DC-link capacitor starts charging through current produced by PV1. Soon after 146 ms, this capacitor is fully charged as shown in fig. 4.22 and PV1 at this time operates at no load. The switch-disconnecting device (i.e. D1 as shown in fig. 4.1) isolates PV1 in such condition. The coordination between fuse F25 and switch disconnecting device D1 is made in such a way that, fuse F25 disconnects VSC3 from the grid due to the current surge produced at the time of the fault (i.e. t=5 s) according to its inverse time current characteristics. The disconnection of VSC3 from the grid causes the voltage rise at the DC bus where the PV1 cell is connected. Based on the voltage levels, D1 decides the disconnection of PV1 cell from the DC bus. The current produced by the PV1 and the voltage at the DC bus in the normal and at a time of its disconnection is shown in fig. 4.23. The protection of the other PV inverter (i.e. VSC4) in the grid connected mode is done in the same way by using fuse F13 and disconnection of the PV2 cell structure is made by D2.

When a fault appears on line R8-RA, fuses F16 and F17 are used to protect this line and VSC1 respectively. Fuse F17 is modeled as ultra-fast and is used to isolate battery1 from the healthy part of the network in case of the short circuit fault. The current seen by fuse F17 is shown in fig. 4.24. It can be seen in fig. 4.24 that fuse F17 is blown out when the current flowing through VSC1 increases abruptly during the short circuit. The current seen by fuse F16 is shown in fig. 4.25. It can be seen in this fig. that the current flowing through

line R8-RA in normal operating conditions is 43.9 A and increases up to 2.57 kA during the fault. Fuse F16 sees this excessive value of the current and is blown out within 50 ms. The power output of battery1 (i.e. Battery drawing current from the line R8-RA) in this case is shown in fig. 4.26.

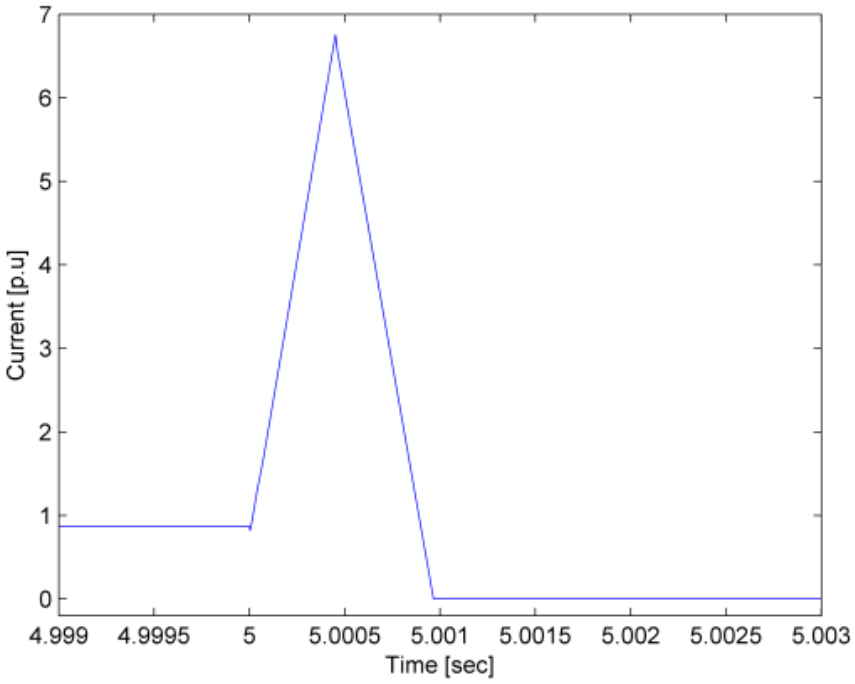

Fig. 4.24 The current of VSC1 in case of a three phase fault with fault impedance of 0 Ω on line R8-RA.

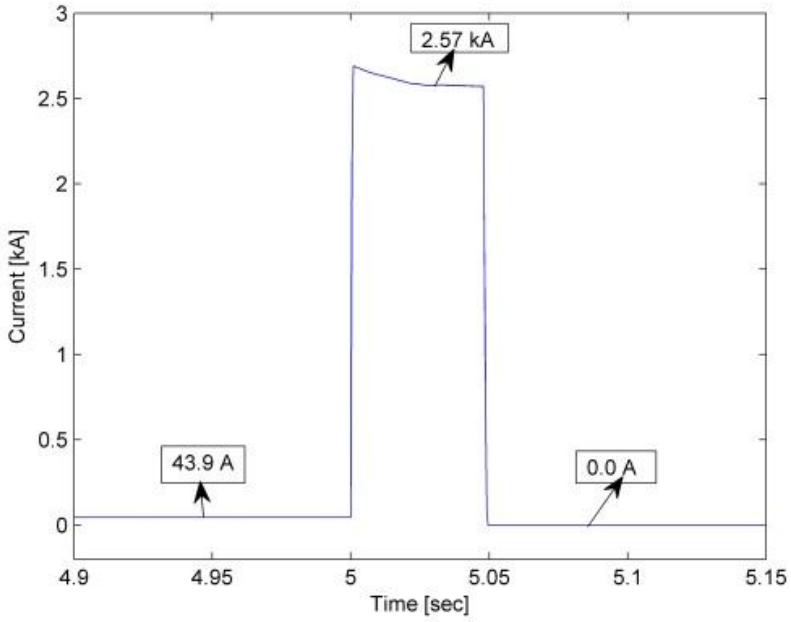

Fig. 4.25 The current flowing through R8-RA line in case of a three phase fault with fault impedance of 0 Ω on this line.

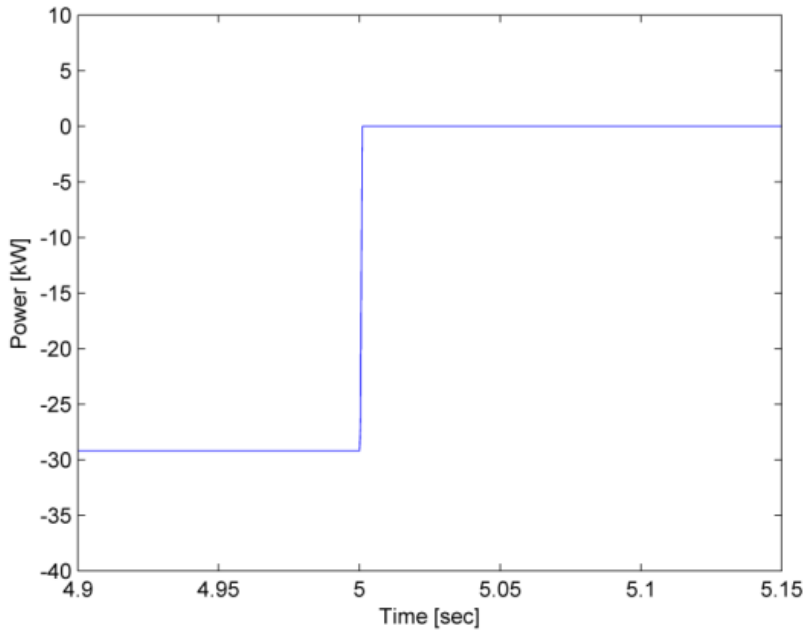

Fig. 4.26 The Power of battery1 in case of a three phase fault with fault impedance of 0 Ω on line R8-RA

It can be seen in fig. 4.26 that the battery is charging at full charging rate in the normal operating condition. When the battery is isolated from the network its power exchange becomes zero.

4.4Protection of the CIGRE network against single phase to ground faults

The study about the protection of the network in this case is carried out by applying a single phase to ground (L-G) fault at the different locations of the CIGRE network. Asymmetric fault involves all kinds of sequence quantities: Positive, negative and zero sequence and draws unbalanced currents from the network. The flow of the unbalanced current across the network makes the voltage in the different parts of the network unbalanced.The fuses and under voltage relays available at the different locations are used to clear this kind of fault.

To study the performance of the protection devices in the CIGRE network, aL-G fault with the fault on phase A having a fault impedance of zero ohms is applied at time equal to t=5 s on line R4-RE. There is bidirectional flow of the currents (i.e. one from the grid and other from the induction generator) towards the faulted line in the affected phase. It is therefore, essential to isolate the faulted sections at both ends in order to protect the healthy portions of the entire network and the power system components (i.e. cables, bus bars, WTG etc.) available in this portion of the network. In general, this kind of a short circuit should be cleared by opening the protection devices at bus R4 and RE but care must be taken if technical regulations for the grid connection/disconnection are to be followed. As there is a short circuit with afault impedance of zero ohms in phase A in line R4-RE, the voltage in phase A of the generator terminal becomes zero. Fuses F6, F8

and F9 as shown in fig. 4.1 are used to protect this portion of the network in this regard. Since the grid feeds the current to the faulted point and this current is first seen by fuse F6; therefore, if F6 is blown out then there will be no grid current which may flow to fuse F8. On the other side, the WTG delivers current which is seen by fuse F9 before F8. Therefore, if current produced by the WTG is enough to blow out fuse F9 then there will be no supply of the current to fuse F8. The short circuit clearing time of these fuses depends on their rated values and the magnitude of the current passing through their fusing elements. The current seen by fuse F6 and F9 in phase A is shown in fig. 4.27 and fig. 4.28respectively. It can be seen in fig. 4.27 and fig. 4.28 that current in phase A through line R4-RE and the WTG increases at the instant of the fault. It can be seen in these figures that fuse F9 opens faster than fuse F6 and this is because of its lower rating (i.e. 10A) as compared to fuse F6. The current in the healthy phases of line R4-RE is shown in fig. 4.29.

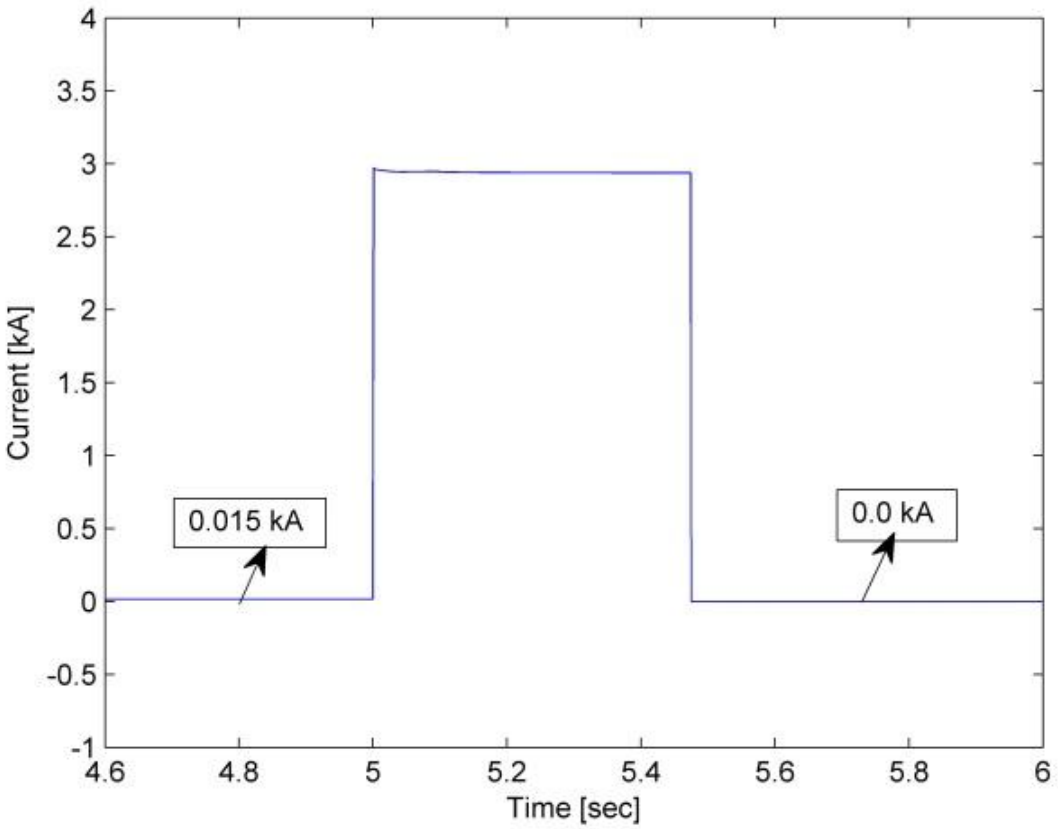

Fig. 4.27 The current in phase A of line R4-RE in case of single phase to ground fault with fault impedance 0 Ω on phase A of this line.

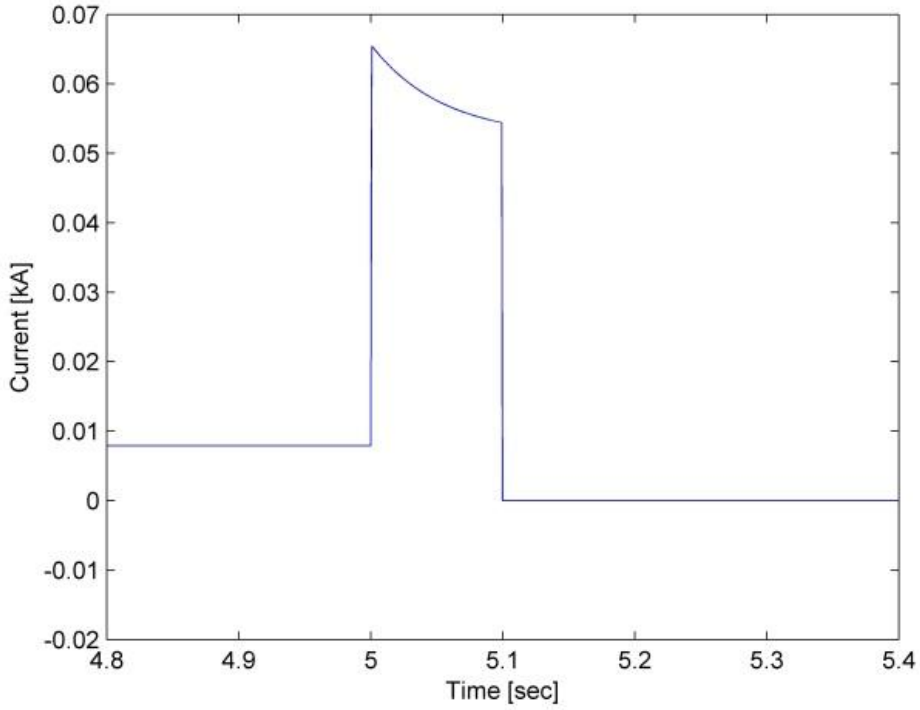

Fig. 4.28 The current in phase A of the WTG in case of single phase to ground fault with fault impedance 0 Ω on phase A of line R4-RE.

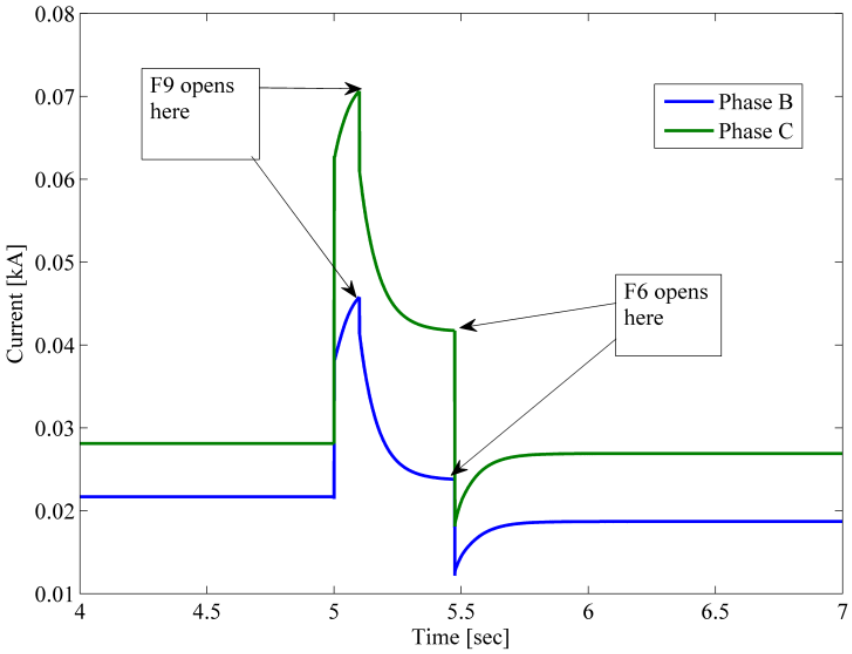

Fig. 4.29 The current in phase B and C of line R4-RE in case of single phase to ground fault with fault impedance 0 Ω on phase A of this line.

It can be seen in fig. 4.29 that the currents in the healthy phases (i.e. phase B & C) increase at the instant of thefault. When fuse F9 is blown out the currents in these phases' decrease, they further reduce when fuse F6 is opened as shown in fig. 4.29. This unbalance in the current creates the unbalance in the voltages in the network. The voltage in all three phases on bus RE in this case is shown in fig. 4.30.

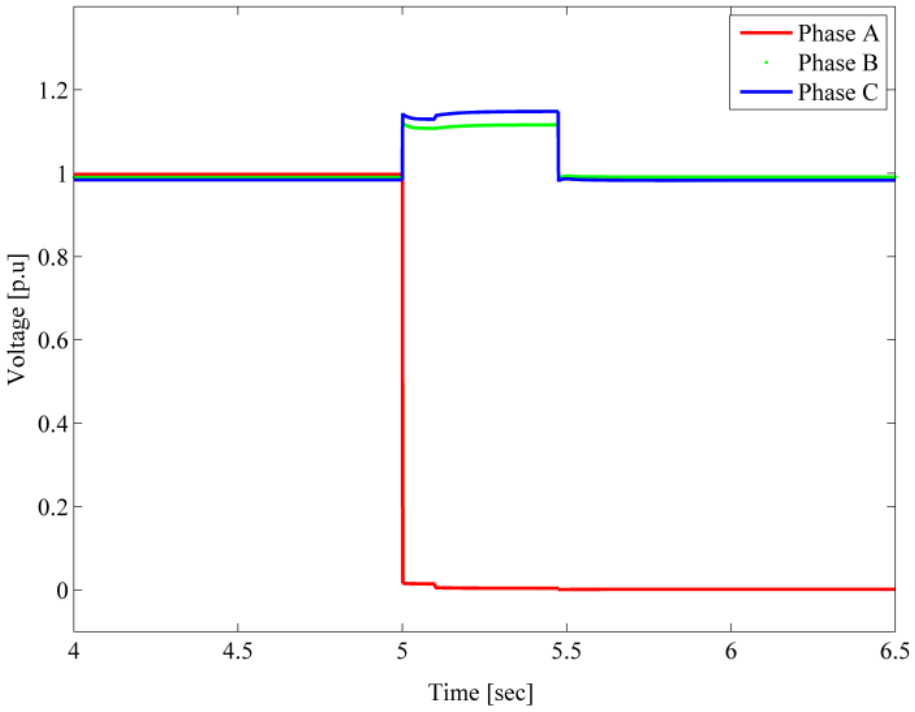

Fig. 4.30 The Voltage in three phases on bus RE in case of single phase to ground fault with fault impedance 0 Ω on phase A of line R4-RE.

It can be seen in fig. 4.20 that the voltage in the affected phase (i.e. phase A) becomes zero when the fault appears on time equal t=5 s. The voltages in the healthy phases increase during the fault and come back to the steady state value when the fault is cleared. The detailed explanation about the rise of the voltage in the healthy phases during the fault has been described in [111] and can also be calculated as shown in section 3.4.2.1.

The WTG delivers unbalanced stator currents if it is connected to unbalanced voltages. These unbalanced stator currents creates unequal heating in the stator winding which might degrade winding insulation and thereby reducing the life time of the stator winding [45], [46]. The currents produced by the WTG in its three phases in this case are shown in fig. 4.31.

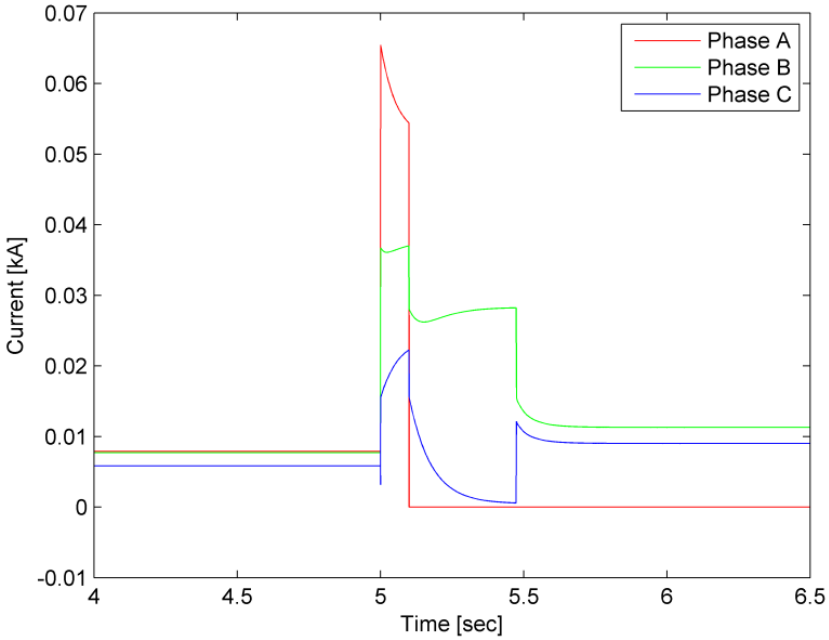

Fig. 4.31 Three phase current of the Wind Turbine Generator in case of single phase to ground fault with fault impedance 0 Ω on phase A of line R4-RE.

It can be seen in fig. 4.31 that there is a huge increase in the current in the phase A of the WTG as this is the faulty phase. The currents in the healthy phases during a fault also increase as shown in fig. 4.31 and this increase in the current is according to the magnetization current of the stator winding of the WTG. The active power produced by the WTG in each of the phases in this case is shown in fig. 4.32.

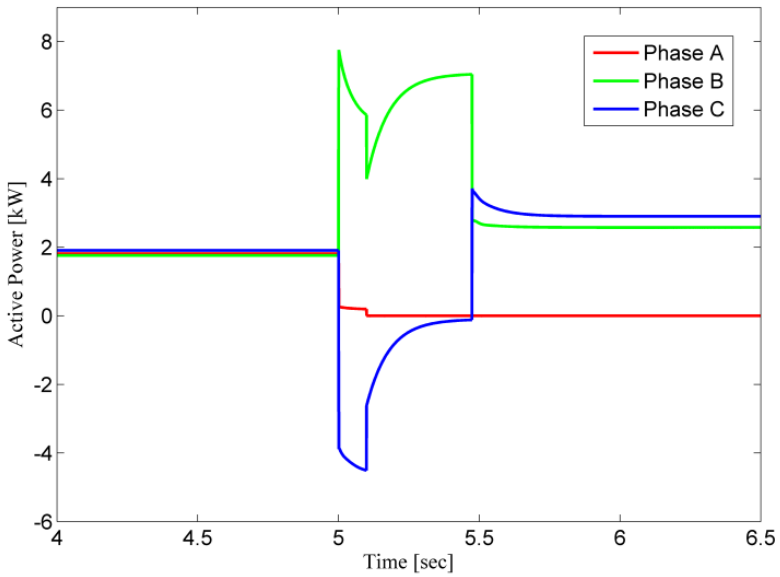

Fig. 4.32 The active power produced by the WTG in three phases in case of single phase to ground fault with fault impedance 0 Ω on phase A of line R4-RE.

The active power $(P=V*I*\cos\phi)$ produced by the WTG depends on three parameters ((i.e. voltage, current and the power factor). The power produced by the WTG in phase A becomes zero since the voltage in this phase due to the fault is zero. It can be seen in fig. 4.32 that phase C of the generator is absorbing active power. It is because of the leading power factor (i.e. power factor with minus sign) in this phase during a fault. The oscillations in the active power in each of the phases are due to the opening of the two fuses at different times. To see the power factor of the healthy phases, their angles between voltage and current are shown in fig. 4.33. It can be seen in fig. 4.33 that the power factor of phase C during fault is minus which is the reason for the absorption of the active power during the fault in phase C of the WTG.

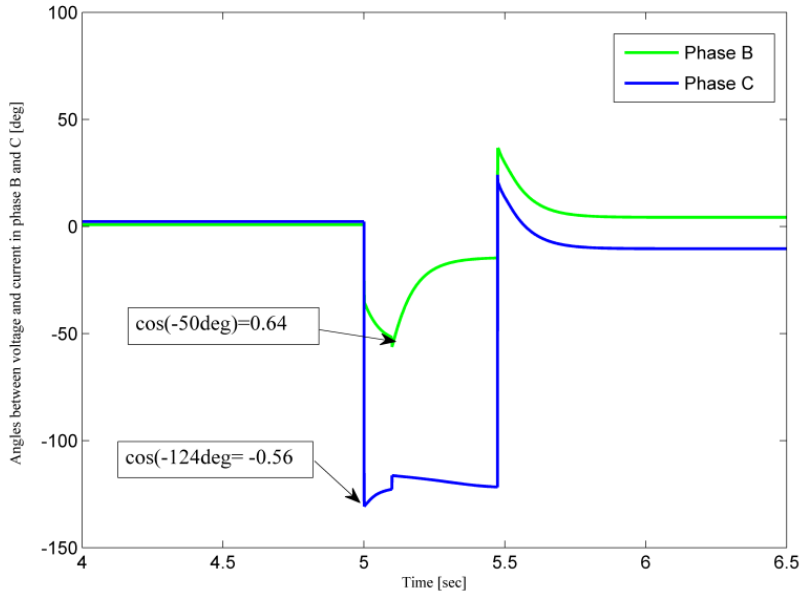

Fig. 4.33 The angles between voltage and current in phase B & C of the WTG in case of single phase to ground fault with fault impedance 0 Ω on phase A of line R4-RE.

These unbalances in the currents and thereby power output of the WTG might create serious problems in its winding structure etc. In order to protect the WTG unit, it should be disconnected from the grid in such cases.

The under voltage relay R1 is used to disconnect the WTG in this case. The setting of the relay is made in such a way that if the voltage in one of the phases decreases below 0.9 p.u. [112] it should disconnect all of its phases. The time of disconnection is according to ANSI CS84.1-1995. According to these standards when the voltage at the terminals of the generator is below 0.5 p.u, the relay R1 sends a trip signal to the circuit breaker which disconnects the WTG from grid within 160 ms. The electrical power delivered by the WTG in its three phases in this case when it is disconnected from the grid is shown in fig. 4.34. It can be seen in this figure that the power in all three phases decreases to zero when the relay has disconnected the WTG from the grid at 5.16 s.

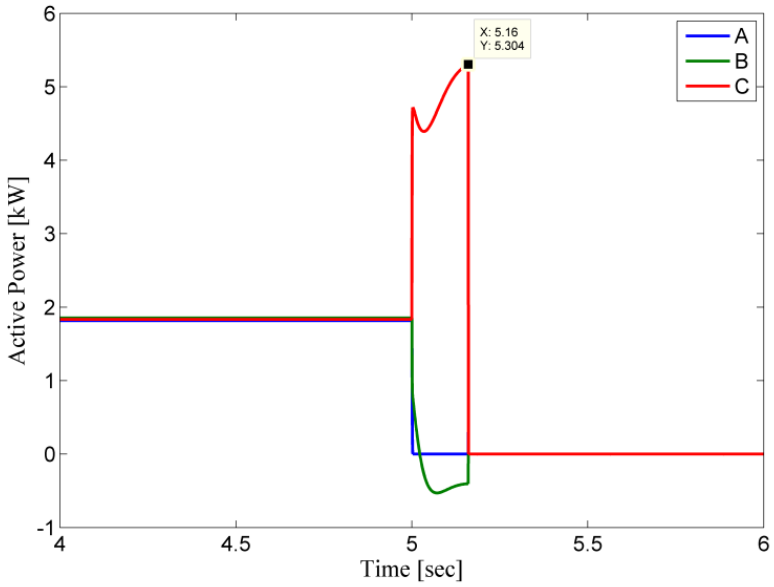

Fig. 4.34 The active power of the WTG in its three phases in case of single phase to ground fault with fault impedance 0 Ω on phase A of line R4-RE.

The speed of the generator increases in case of its disconnection from the grid; therefore, mechanical brakes can be applied in order to stop it as described previously.

4.5 Protection of the CIGRE network in its central parts

The protection of the CIGRE network grid in its central part (i.e. from node R1 to R10 of fig. 4.1) is designed in such a way that it ensures a proper overcurrent protective coordination in the network. The over current protection ensuring protection coordination in the central part of CIGRE network is made by using fuses F15, FA, F14, F10 and F5 as shown in table 4.1. Fuse F5 is the highest fuse among these fuses due to the reason of the protection coordination, if the fault occurs nearby the close vicinity of this fuse, it will take longer time to clear the fault. To overcome this problem, the protection in the central part is made by using the under voltage relay.

Again, the fault may occur in the central parts of the network with some fault impedance. The voltage based protection can be a better solution in this regard as well. To study the behavior of the protection devices in the central parts of the CIGRE, a 3-phase fault with a fault impedance of 0.1 ohms is applied on cable R7-R8 of the CIGRE network. The fault appears on this cable at time equal to t=2 s. The current flowing through this cable is shown in fig. 4.35. It can be seen in fig. 4.35 that 1.6 kA current is flowing through the cable during the fault. Fuse FA blows within 58 s according to its operating characteristics as shown in fig. B1 in appendixB. The fault persistin the network for the long time in this case; therefore, voltage based protection is introduced which clears fault faster.

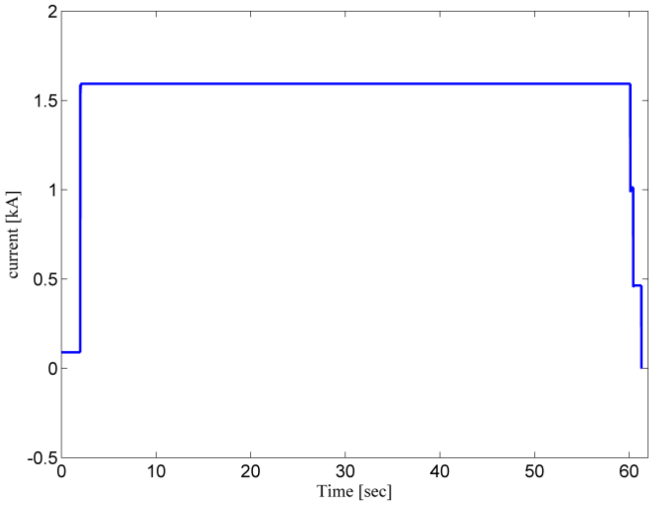

Fig. 4.35 The current flowing through the cable R7-R8when it is protected by fuse FA against 3-phase fault with a fault impedance of 0.1 ohms.

The under voltage relay is used at both ends of the cable instead of over current protection devices. These relays (i.e. RL1 and RL2) detect the fault if the voltage on the faulted point decreases below a threshold. The plot of the current flowing from both ends of the cable (i.e. from the grid side and from the DGs side) when under voltage relays are used at both ends of the cable is shown in fig. 4.36 and fig. 4.37 respectively. The under voltage relay used at the grid side end and the DG side of the cable measures the voltage and sends trip signal to the circuit breaker. It can be seen in fig. 4.36 and fig. 4.37 that the respective circuit breaker has disconnected the faulted section from the grid side and also from the DG side of the network within 100 ms. The over shoot in the current as shown in fig. 4.37 at the instant of fault is due the current surge produced by the inverter based DG units.

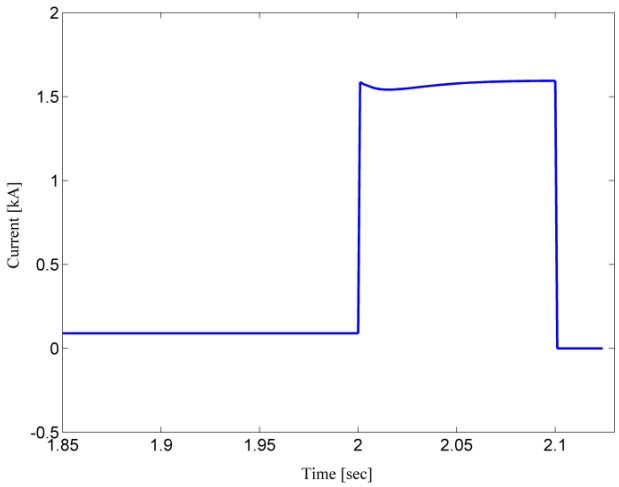

Fig. 4.36The current flowing through the cable R7-R8 from the grid sidewhen it is protected by a circuit breaker against 3-phase fault with a fault impedance of 0.1 ohms.

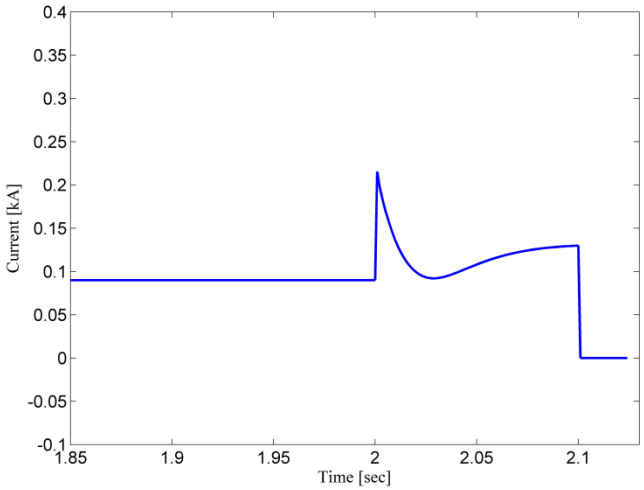

Fig. 4.37 The current flowing through the cable R7-R8 from the DGs side when it is protected by a circuit breaker against 3-phase fault with a fault impedance of 0.1 ohms.

4.6 Summary

The protection against 3-phase fault with and without fault impedance in different portions of the CIGRE network has been proposed in this chapter. Due to economic reasons, the protection of the CIGRE network is mainly proposed by using fuses. If fuses are unable to detect the fault as analyzed for the cases in different sections; the clearance of fault is done by using under voltage relays. The disconnection of the WTG in case of symmetrical and unsymmetrical faults is made by using current based and voltage based protection devices. For the case of loss of grid due to 3-phase and single phase to ground faults, the over speed protection of the WTG is applied by using mechanical brakes is also studied in this chapter. The over current protection of the inverters is made by using ultra-fast fuses and the disconnection of PV solar cell structure in the case of loss of grid is made by using switch disconnection devices. The protection of the CIGRE network in the case of the forward direction of the current (i.e. grid side) is made by using the fuses and the protection in the case of reverse direction of the current (i.e. DG side) due to islanding is made by using the under voltage relays.

Chapter 5

Island operation of distribution grid with Distributed Generation

5.1 Introduction

Islanding is a situation where the electrical system becomes electrically isolated from the rest of the power system and yet continues to be energized by DG units connected to it. This separation of the grid could be due to the operation of circuit breaker, fuse or any other protection device responding to the faults. Unintentional islanding in Low Voltage (LV) distribution networks in the presence of DGs is one of the major safety concerns for grid interconnection of generators. The main problems associated with unintentional islanding are [113]:

- Exceeding of the acceptable limits of voltage, frequency, unbalance etc. which can lead to malfunction or permanent damage of the network or customer equipment.
- Electric shock due to touching of live conductors which are supposed to be dead.
- Possible damage of the network equipments because of the protection problems due to the low short circuit power capacity of DG units

A low voltage network comprising large amounts of small sized generation units (i.e. Photovoltaic units, Wind Turbine Generator (WTG etc.) together with Battery Energy Storage Devices (BESS) in this study forms a local Micro Grid (MG) when it is islanded from the main grid. The current trend in power networks is to operate an islanded portion of the distribution system (i.e. MG) by controlling its voltage and frequency. The voltage and frequency in such conditions can be controlled by the available active and reactive powers in the local MG.

During islanding mode, if there is an imbalance between load and local generation, the MG frequency drifts from its nominal value. If the active power demand is higher than the active power production in the local island, the MG frequency decreases and vice versa. On the other if there is a deficit of the reactive power in the local island, the MG voltage decreases and vice versa. Therefore, the control system in the MG must be developed in such a way that it tackles issues related to the voltage and the frequency.

This chapter presents some of the problems related with islanding. These problems such as voltage and frequency are solved in this chapter. Section 5.2 describes the development of a suitable control system for the islanding operation of the network. The details about island detection technique are also presented in this section. The control of the voltage and the frequency of the islanded MG are described with the help of simulation results in section 5.3 and 5.4 respectively. The study about step load changes in the islanded MG is presented in section 5.5. The impact of the DG unit(s) loss in the islanded MG is studied in section 5.6. Finally summary of the chapter is presented in section 5.7.

5.2 The development of the control system for islanded operation of the LV CIGRE network

The CIGRE network comprising DG units enters into islanding if a 3-phase fault appears on bus R0 and is cleared as shown in fig. 4.13. The established MG now comprises two PV units of 3 kW and 4 kW, A WTG of 5.5 kW, two energy storage devices having energy capacity of 30 kWh and 21 kWh and some loads connected at bus RC, RD, RE, R11 and R17 as shown in fig. 2.1. The PV units are modeled in DIgSILENT power factory as constant current sources and Voltage Source Converters (VSCs) are used to transform DC power obtained from it into AC. The Battery Energy Storage Systems (BESS) are modeled as constant voltage sources in DIgSILENT power factory and VSCs here are also used to transform power into AC. The controllers for all these units in the grid connected mode are developed in PV/PQ mode and are detailed described in chapter 2.

The development of controllers for all the DG units in the islanded MG is different as compared to the grid connected mode. The controllers are developed in such a way that they ensure the constancy of the voltage and the frequency of the entire island MG. In case of several parallel inverters available in the network; one of the inverter controllers must be developed in VF mode and the others in either PV or PQ modes [114].

When the distribution network enters into islanding, it loses its slack reference as the external grid was chosen as the slack bus in the grid connected mode. The first and the most important thing is to establish a slack reference in the islanded MG. As most of the DG units in the MG are inverter based except the WTG which cannot be chosen as the slack reference because of its unpredictable generation.To establish slack reference in the islanded MG it is necessary to model one of the inverter based DG units as a slack reference in this regard. Therefore, one of the inverter for this study is modeled as slack reference (i.e. it operates in VF mode) and all others operate in PV mode. The operation of the MG with several PV inverters and a single VF inverter is similar to the operation of a MG with a synchronous machine as slack bus. The VF inverter establishes the voltage reference for the operation of all other PV inverters in the case of MG islanded from the main power grid. Acting as voltage source, the VF inverter is responsible for controlling the voltage and frequency of the islanded MG. It injects or absorbs active and reactive powers if frequency or the voltage in MG decreases or increases respectively. It requires a significant amount of energy available in the power source with very fast response. A VF control cannot be used for wind and solar power generations because they are unpredictable and depend on the weather conditions (i.e. wind speed and solar irradiance). This controller can be used for the inverters of the BESS system, especially the inverter of the bigger energy storage capability (i.e. VSC1 for this study).

The VF controller is modeled as a cascade controller and is shown in fig. 5.1 comprising the outer and the inner current controllers. The inputs to outer controller are the measured and reference frequency and voltage and its outputs are active and reactive reference currents as shown in fig. 5.1.

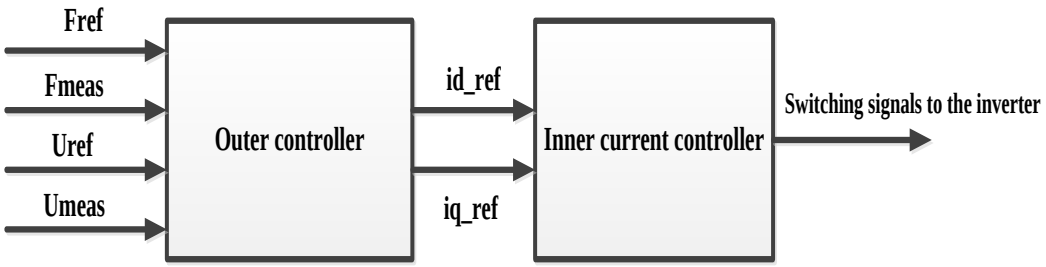

Fig. 5.1 The block diagram of VF controller

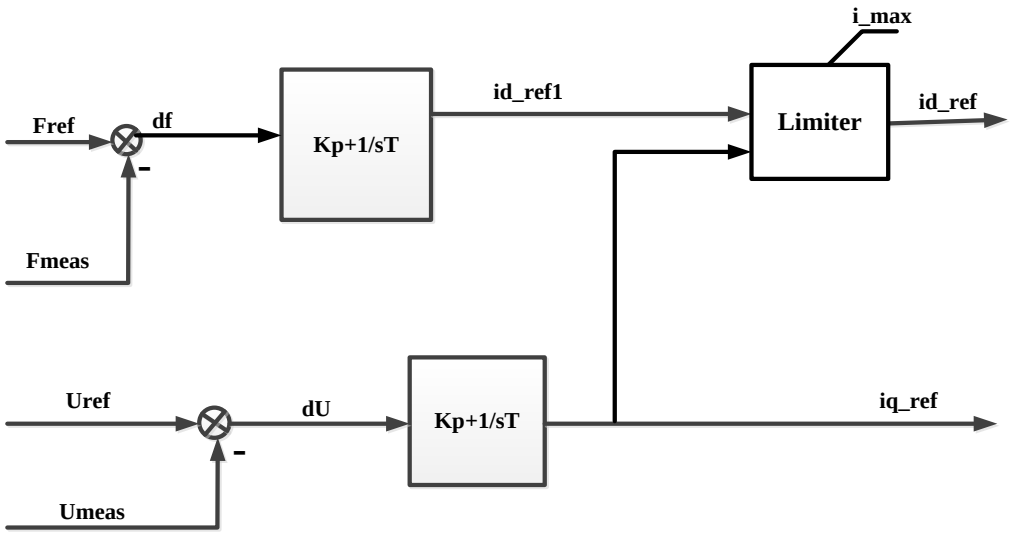

Fig. 5.2 The block diagram of the VF controller [115]

The purpose of the VF controller is to control the frequency of the MG by injecting or absorbing the desired amount of the active power. It is also used to control the voltage of MG by injecting or absorbing the desired amount of the reactive power. The block diagram of the VF controller which works as an outer controller is shown in fig. 5.2. This controller compares measured and reference frequency (i.e. Fref=50HZ) and sends the error signal 'df' to the PI controller which generates active current reference (id_ref1) as shown in fig. 5.2. It also compares measured and reference voltages at a certain bus and sends error signal 'dU' to the PI controller responsible for the voltage control. This PI controller generates the reactive current reference (iq_ref) and decides the injection or the absorption of the reactive power.

The frequency of the network depends on the availability of the active power. The active power according to the dq transformation is given by $p=u_d i_d+u_q i_q$. Since the q component of the voltage (i.e. u_q) is zero, the power $p=u_d i_d$. This relation implies that the active power p is directly proportional to the d component of

the current (i.e. i_d) if the voltage u_d is considered to be constant. This is the reason that the PI controller responsible for controlling the frequency produces the control signal (i.e. i_d_ref) at its output.

Similarly, the network voltage is dependant of the amount of the reactive power. The reactive power according to the dq transformation is given by $q=u_q i_d - u_d i_q$. As the q component of the voltage (i.e. u_q) is zero, the power $q=-u_d iq$. This relation implies that the reactive power q is directly proportional to the q component of the current (i.e. iq) if the voltage u_d is considered to be constant. This is the reason that the PI controller responsible for voltage control loop presents the control signal (i.e. i_q_ref) at its output.

The injection/absorption of the active and the reactive powers by the inverters is according to the values of these current references. These currents references are the inputs to the current controller which decides the duty cycle for the switches used in the converter. The block diagram and the other details of the current controller are already given in section 2.4.1. The share of the active and the reactive power from the VF inverter is according to the equation 5.1 and equation 5.2 and depends on if the control system has been given the voltage control or a frequency control priority.

$$id\_ref=\sqrt{i\_max^2 - iq\_ref^2} \quad \text{(Voltage control priority)} \quad (5.1)$$

$$iq\_ref=\sqrt{i\_max^2 - id\_ref^2} \quad \text{(Frequency control priority)} \quad (5.2)$$

Where i_max lies between +-1 p.u. The control system producing id_ref according to equation 5.1 is said to have the voltage control priority. If the inverter delivers 1 p.u of reactive power then according to equation 5.1, the inverter has no more active power to inject (i.e. id_ref=0). The controllers of the other inverters used in the CIGRE network have also been modeled to share the amount of the active and the reactive power according to equation 5.1.

The switching of the controller from the PV/PQ mode to VF is based upon the island detection. Several island detection techniques have been proposed in the literature [116-120].The island detection techniques can be generally divided into two categories: Active methods and passive methods. The main passive techniques used for islanding detection include under/over frequency, vector shift, Rate Of Change Of Frequency (ROCOF) [121], [122], Under/Over Voltage, rate of change of voltage and power factor [123] etc. The main active techniques include reactive power Error Export Detection (REED) [124], fault level monitoring [125], and system impedance monitoring [119].

Passive methods are familiar for detecting Loss of Grid (LOG) because of their simplicity and low cost. The ROCOF and vector shift methods are the most common methods used among the passive methods. These methods especially ROCOF method have some of the disadvantages that they do not properly discriminate between the island and transient conditions. Unnecessary tripping might occur in the case of sudden load changes, faults etc. by using ROCOF method.

The detection of LOG by using a new technique which is based on the voltage phase angle difference between the grid and the distribution system is described in this chapter. This method is described in [122] but further details are added in this section. This islanding technique is described with the help of the block diagram shown in fig. 5.3.

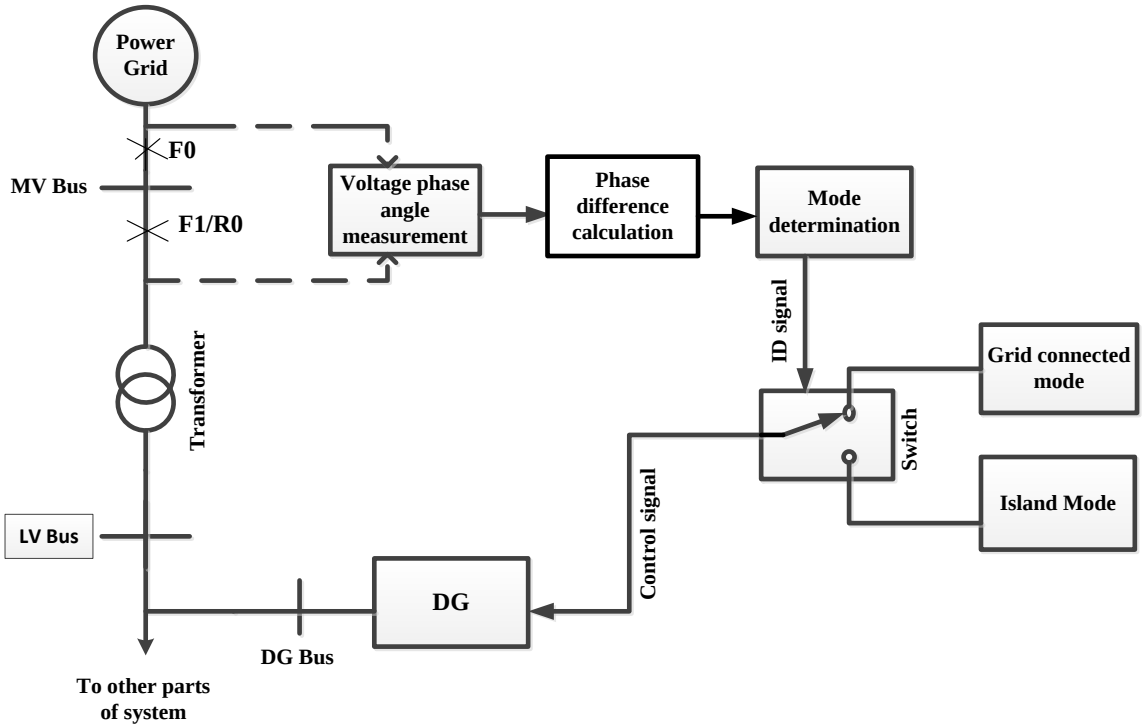

Fig. 5.3 The block diagram of the control mode determination

It can be seen in fig. 5.3 that the phase angles of the voltages at the grid side and DG side are measured and the difference of the phases is calculated. The network changes its mode of operation from the grid connected to islanding according to the difference of the voltage phase angles. The islanding is detected in the network if there is a phase angle difference between the two voltages as shown in fig. 5.4. The control diagram shown in fig. 5.3 is only used to determine the mode of the operation from the grid connected to the island mode. The same technique is not valid for reconnection detection. A more advanced technique will be described in the next chapter concerning the detection of reconnection in the network.

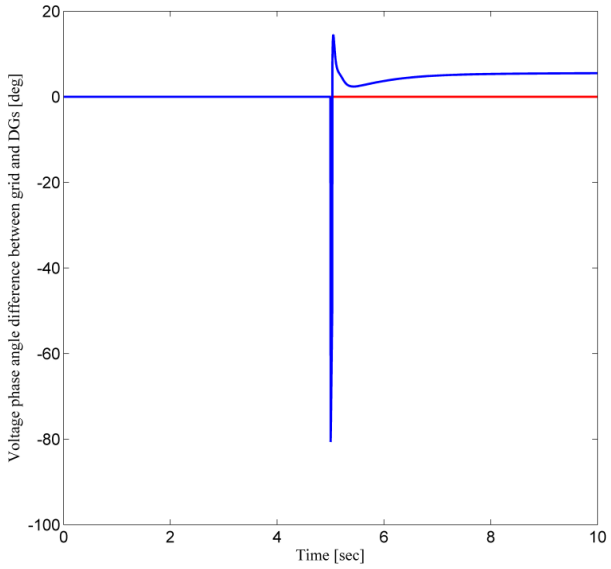

Fig. 5.4 Phase angle difference between the voltages in case of 3-phase fault on bus R0 with fault impedance of 0 Ω (Red: Transmission Grid, Blue: Distribution Grid)

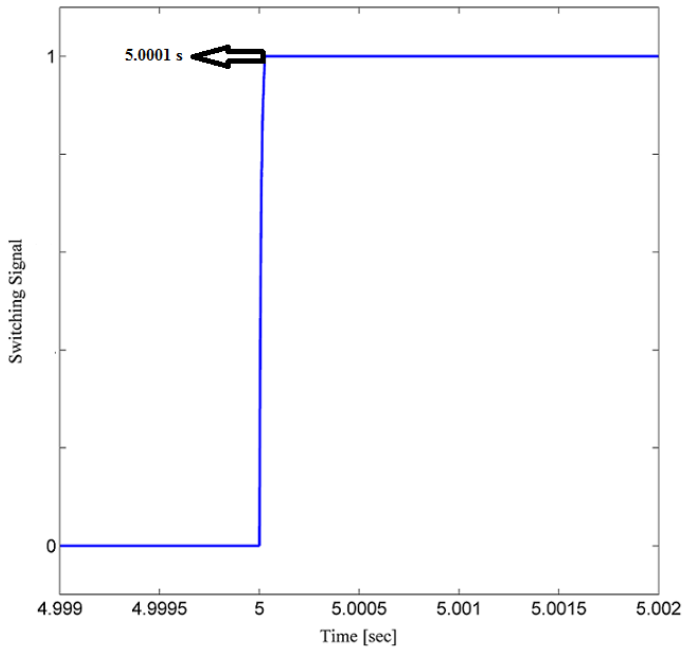

Fig. 5.5 Island Detection (ID) signal in case of islanding in case of 3-phase fault on bus R0 with fault impedance of 0 Ω

It can be seen in fig. 5.4 that the phase angle difference of the voltages at the mentioned points as shown in fig. 5.3 is zero in the normal operating conditions. This difference of the voltage phase angles changes when fuse F0 is blown out. The Island Detection (ID) signal is shown in fig. 5.5. This fig. describes that the system is connected to the grid when there is no difference between the voltage phase angles. The network switches

to the islanded mode when the difference in the voltage phase angles appears. Hence, LOG is detected at 5.0001 s in the CIGRE low voltage network.

This method of LOG detection performs well during sudden switching/variation of the loads and in the transient conditions. To see the effects of the transients and check whether this method may cause false detection in case of the faults somewhere in the other parts of the network, the study is performed by applying a 3-phase fault on bus R11 at the time equal to t=5 s. The voltage phase angles in this case can be read in fig. 5.6 and the ID signal is shown in fig. 5.7.

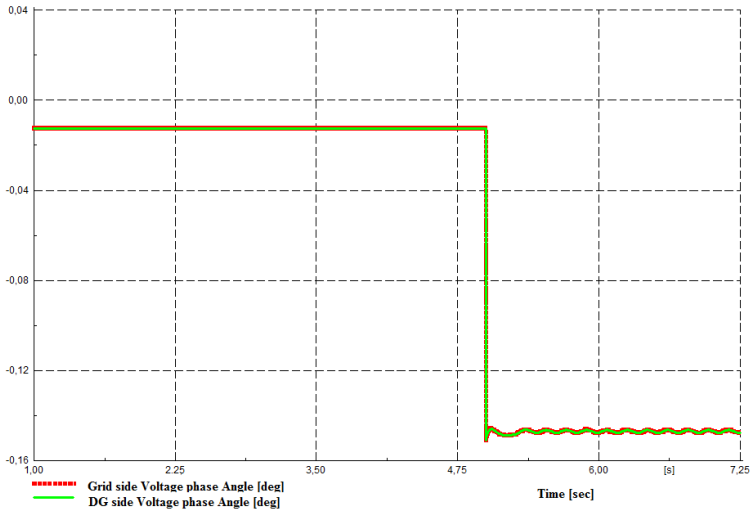

Fig. 5.6The Phase angle difference between the voltages in case of 3-phase fault on bus R11

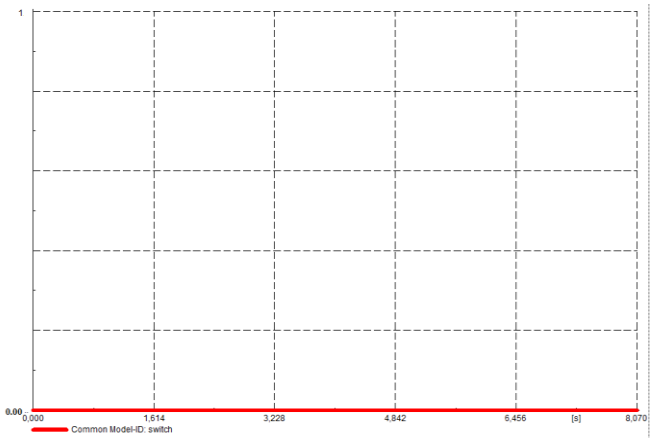

Fig. 5.7 The ID Signal in case of 3-phase fault on bus R11

It can be seen in fig. 5.6 that voltage phase angles at the time of short circuit fault i.e. t= 5 s changes but their difference is zero. Hence, the distribution system remains connected to the grid and there is no false detection by using this method as shown in fig. 5.7. This is the main advantage of this method over other methods of LOG detection.

The effectiveness of this method against the different power imbalances has been detailed described and verified in [122].

The inverter of battery1 (i.e. VSC1) operates in PQ mode in the grid connected mode. This controller (i.e. PQ controller) is used to control the active and the reactive power at the point of its connection. The control system of this inverter changes to the VF mode of operation when the distribution network is islanded from the grid. The switching of the control system from the PQ mode to VF mode is described with the help of the block diagram shown in fig. 5.8.

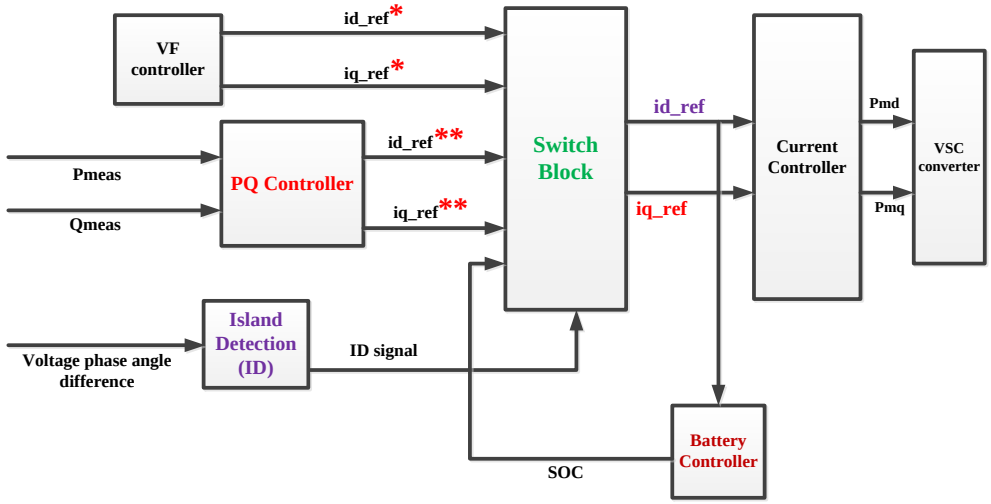

Fig. 5.8 The switching of control system from PQ to VF mode

It can be seen in fig. 5.8 that two different controllers (i.e. PQ and VF controllers) are used for the two different conditions (i.e. grid connected and island) of the network. The PQ controller described in section 2.5.1 generates signals (id_ref** and iq_ref**). The VF controller which is described with the help of fig. 5.2 produces the output signals (i.e. id_ref* and iq_ref*). The decision about the transition of the control system from the PQ mode to VF mode is made by the island detection (ID) block. The explanations and the description of the island detection are presented in the above text.

The switch block receiving the signals (id_ref** and iq_ref**) and (id_ref* and iq_ref*) from the PQ controller and VF controller respectively at its input, sends appropriate current references to the current controller according to the ID signal. If the ID signal is 0 (i.e. no islanding), the current controller receives the active and the reactive current references from the PQ controller and if ID signal is 1 (i.e. islanding detected), the current controller receives signals from the VF controller. The current controller receiving the signals from the PQ or VF controllers send the signals to the PWM block of the inverter and decide the duty cycle [56]. The details of the current controller are described with the help of fig. 2.8.

The battery controller block is also added in fig. 5.8. This block receives the active current reference (i.e. id_ref) from the current controller at its input and integrates it in order to get the State of Charge (SOC). The signal SOC is sent to switch block which in turn decides the amount of id_ref according to the value of SOC. The switch block makes the id_ref equal to zero if the SOC of the battery is either 20% or 95%. This is in order to avoid damage of the battery and to preserve battery life [32].

5.3 The behavior of DG units and voltage control in islanded Micro Grid

The voltage on the MV bus (i.e. bus R0) at the instant of a 3-phase short circuit fault at t=5 s decreases to zero as shown in fig. 5.9. The procedure of clearing such kinds of fault from both sides of the network as described above enters the distribution network into island condition. The voltage on the bus connected to the secondary of the transformer (i.e. bus R1) also decreases when the distribution network enters into island as shown in fig. 5.9.

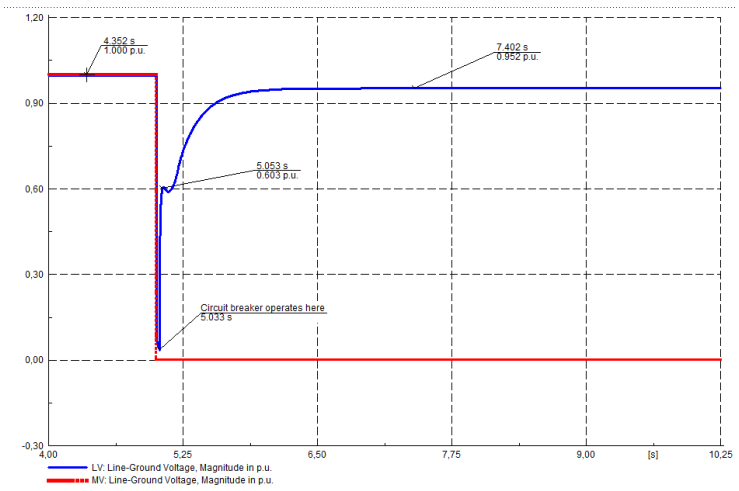

Fig. 5.9 The voltage on bus R0 and bus R1in case of grid connected and islanded mode

It can be seen in fig. 5.9 that when the circuit breaker operated by relay R0 has cleared the fault at t=5.033 s; the existing controllers (i.e. four STATCOM controllers) in the local MG quickly restores the voltage back to the acceptable limits (i.e. +-10% according to IEEE standard 1159-1995 and Danish standards [77]). The restoration of the voltage in the local MG is made by providing the desired amount of reactive power by the inverter based DG units. The disturbance in the voltage on bus R1 at t=5.053 s shown in fig. 5.9 is because of the current limiters which are responsible to limit the amount of the current.

The three STATCOM controllers of the inverter based DG units (PV1, PV2 and battery2) operate in PV mode. The control system of battery1 operates in PQ mode in the grid connected mode and switches to VF mode in island condition. All four inverters are modeled to counteract the voltage and the frequency

disturbances (i.e. VSC2, VSC3 and VSC4 with voltage control priority, VSC1 has frequency control priority). The control system of these inverters sends the control command to inject/absorb the reactive power in the buses where they are connected. If the voltage of the bus is greater than the voltage of an inverter connected on that bus, the reactive power is absorbed by the inverter and vice versa [78].

The contribution of the reactive power from the different converters (i.e. VSC1, VSC2, VSC3 and VSC4) is according to their rated power. The power and the voltage ratings of the inverters used in the network are shown in table. A2 in appendix A. The inverters mentioned in this table are used to provide the active and the reactive powers in order to control the voltage and the frequency at the same time. The share of the powers is according to equation 5.1 and equation 5.2.

The reactive powers injected by VSC1, VSC2, VSC3 and VSC4 are shown in fig. 5.10. It can be seen in fig. 5.10 that all four inverters do not inject/absorb reactive power in the normal operating condition. When the distribution system is islanded, VSC3 and VSC4 inject 16.108 kVAr and 21.477 kVAr of reactive power respectively in order to maintain the voltage within reasonable limits. VSC2 absorbs 22.374 kVAr in island condition as shown in fig. 5.10. The decision about the injection or absorption of the reactive power is made by the corresponding controllers and is according to the value of the voltage seen by the inverters at their points of the connection. VSC1injects only 0.501 kVAr in island mode because it has been assigned the priority to inject maximum amount of the active power in order to maintain the network frequency. The peaks observed in the reactive power of all the inverters at the instant of the fault are because of the reactive current flowing to the faulted point until it is cleared.

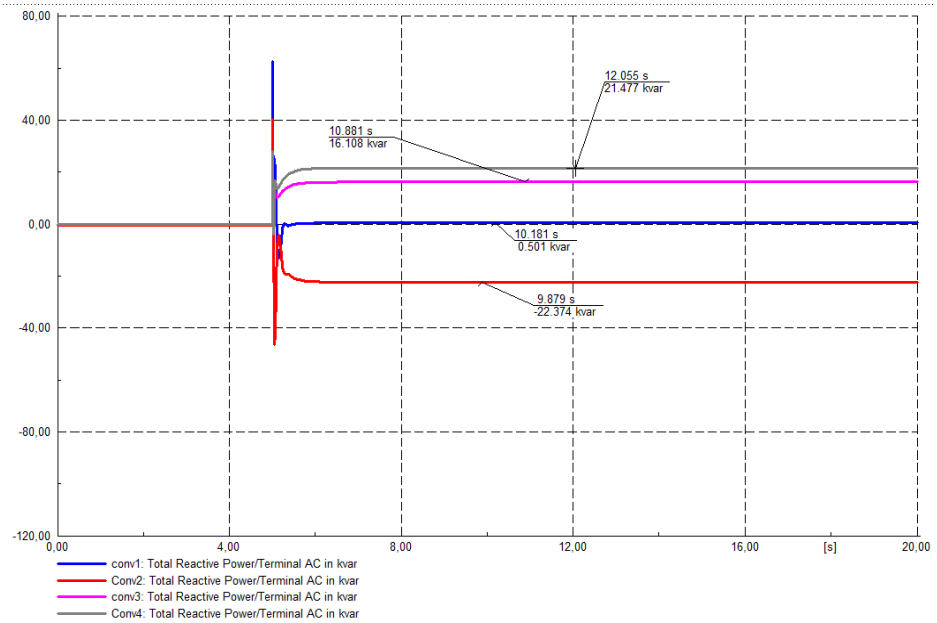

Fig. 5.10 The reactive power of VSC1, VSC2, VSC3 and VSC4in case of grid connected and islanded mode

The active and the reactive powers injected by VSC1 are shown in fig. 5.11. It can be seen in fig. 5.11 that VSC1 absorbs 28.747 kW in order to charge battery1at the maximum charging rate in the normal operating condition. Since this inverter operates in PQ control mode in the grid connected mode and the purpose of this controller is to inject/absorb maximum amount of active power by controlling the amount of the reactive power equal to zero. This is the reason that this inverter does not inject/absorb reactive power in the grid connected mode.

When the distribution system enters into islanding, the control system of VSC1 has been switched to VF control mode which injects 31.769 kW of active power in order to control the frequency of the network. The amount of reactive power injected by VSC1 depends on the control set up as shown in fig. 5.2 and is according to equation 5.2. The oscillations in the powers at the instant of the fault seen in fig. 5.11 are because of the occurrence of the fault, its clearance from the both sides etc. The study about the frequency of the network will be done in section 5.4.

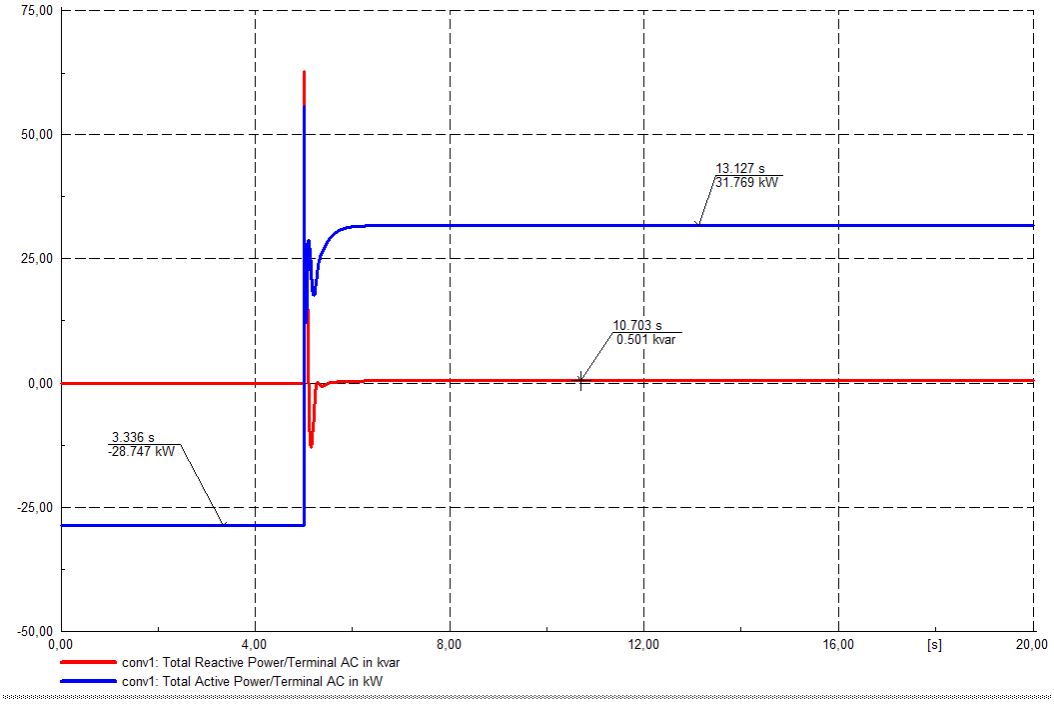

Fig. 5.11 The Active and the reactive power of VSC1in case of grid connected and islanded mode

The voltage in the different parts of the islanded MG is shown in fig. 5.12. The voltage on bus R19, A, B, C, D, E and bus R11 is shown in this figure. It can be seen in fig. 5.12 that the voltage in normal operating conditions on the different buses is different because of the different loads connected there. The voltage in all parts of the network decreases as shown in fig. 5.12 when the distribution system is islanded and is restored up to the acceptable limits by using the developed controllers.

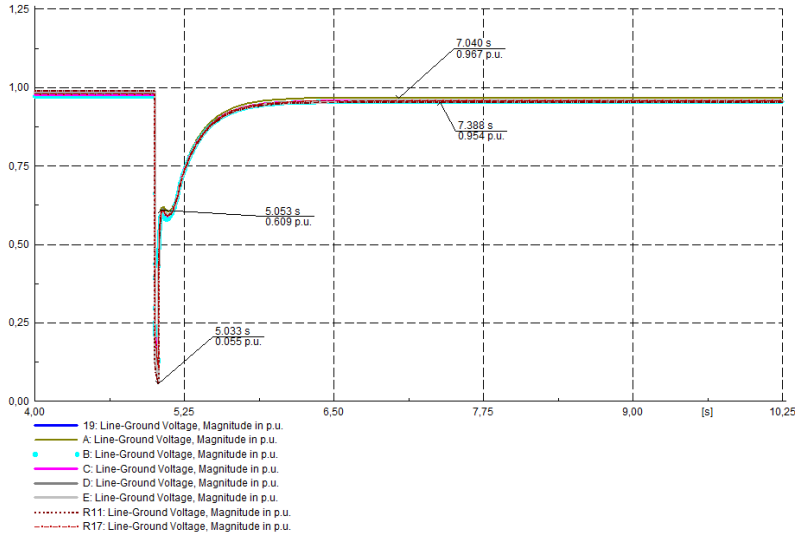

Fig. 5.12 Voltage on bus R19, A, B, C, D, E and bus R11in case of grid connected and islanded mode

To study about the behavior of the power production in the islanded MG; the power output of the 3 kW PV 1 and the 4 kW PV2 at the AC terminals of VSC3 and VSC4 are shown in fig. 5.13 and fig. 5.14 respectively. The power output of PV1 is described with the help of the DC-link voltage of its inverter (i.e. VSC3) as shown in fig. 5.15.

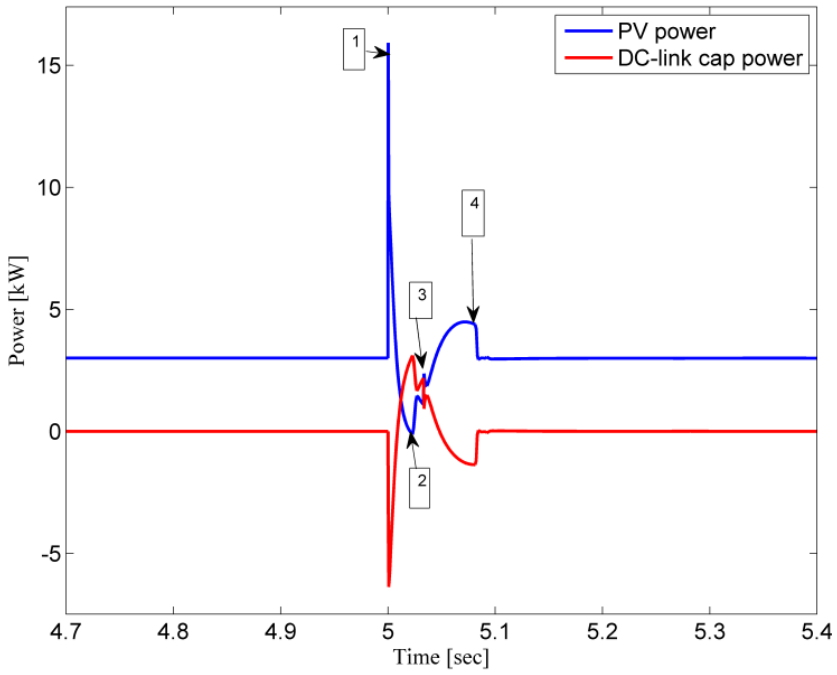

Fig. 5.13 The active power produced by PV1 and DC-link capacitorin case of grid connected and islanded mode

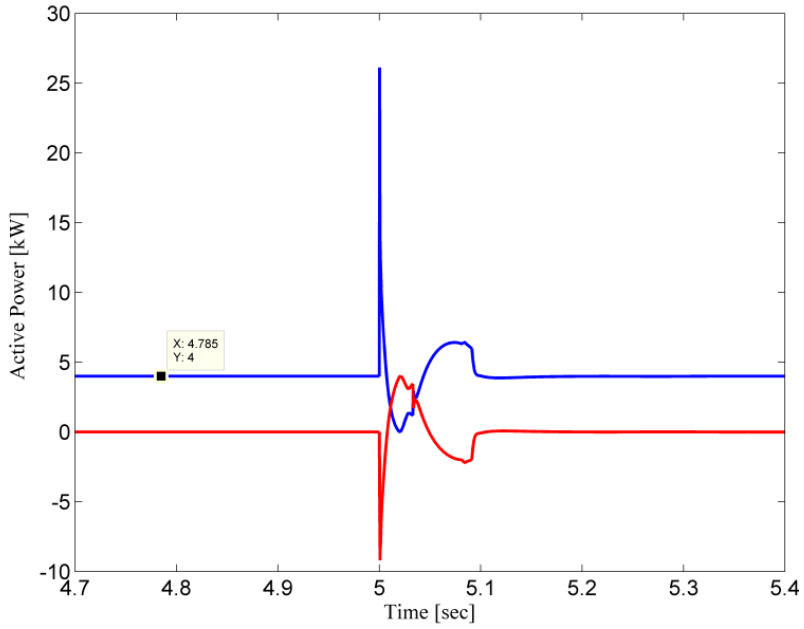

Fig. 5.14 The active power produced by PV2 and DC-link capacitorin case of grid connected and islanded mode

The different events in the power output of PV1 are described with the help of different points (i.e. points 1, 2, 3 and 4). It can be seen in fig. 5.13 that PV1 is producing 3 kW of power in the full sunny day in normal operating conditions. At the time of the fault there is short term increase in this power as shown in fig. 5.13. This peak in the active power of the PV1 at the instant of the fault is because of a current surge produced by the inverter at the time of the short circuit fault. The DC-link voltage as shown in fig. 5.15 decreases at this time.

The DC voltage controller is developed with responsibility to control the DC-link voltage and thereby by active power output of PV1. This controller is detailed described in section 2.4.1. This controller makes a decision for the DC-link capacitor to absorb active power when the power output of PV1 increases and vice versa. The injection and the absorption of the active power by the DC-link capacitor used for the PV1 inverter is shown in fig. 5.13.

At time equal to t=5 s the power output of PV1 increases because of the surge current and DC-link capacitor used at this bus absorbs this extra power in order to maintain the DC-link voltage of VSC3. At point 1 in fig. 5.13 fuse F0 blows and this power decreases as shown in this figure. The absorption of the power by the DC-link capacitor decreases during this time. At point 2 the power output of PV1 increases because of the DC-link voltage rise at VSC3 as shown in fig. 5.15. The DC-link capacitor exactly follows the magnitude and the

direction of the power produced by PV1. At point 3 the circuit breaker is opened at the MV bus and the magnitude of the power increases. The amount of power seen during this period is according to the value of voltage seen in fig. 5.15. It is clearly seen in fig. 5.13 that the DC voltage controller has maintained the power out of PV1 to its nominal values by controlling the DC-link voltage of VSC3.

Similarly, the power profile of a PV2 and the DC-link capacitor of PV2 inverter are shown in fig. 5.14. The behavior of the power and its controller is same as described for PV1. It can be seen in this fig. that the DC voltage controller for this unit has also restored the power to its nominal values.

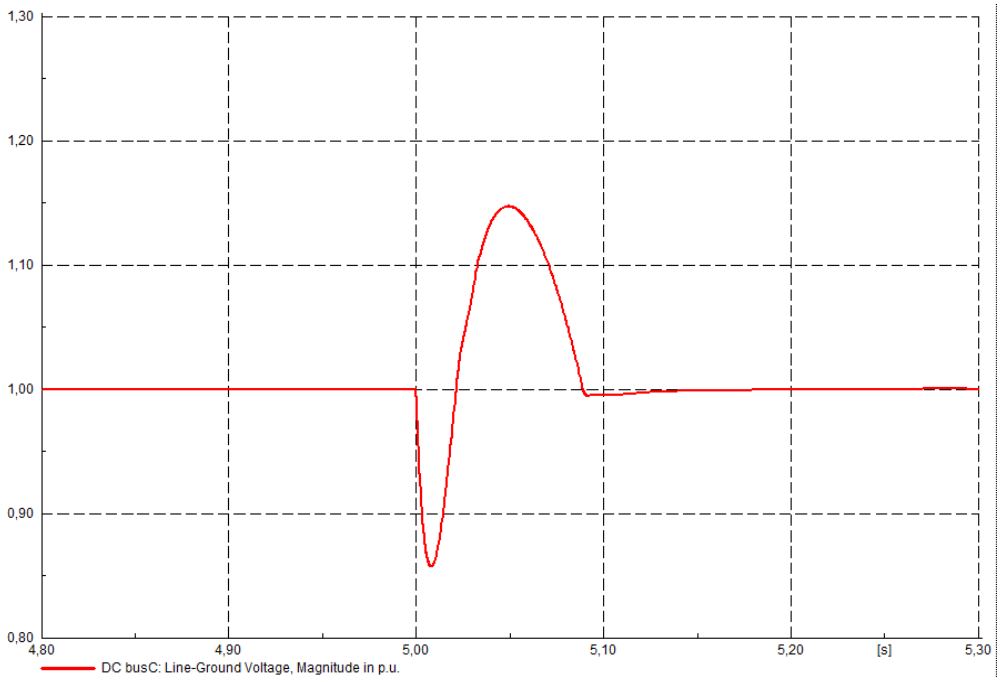

Fig. 5.15 The DC-link voltage of VSC3in case of grid connected and islanded mode

The power produced by the WTG is shown in fig. 5.16. In the normal operating conditions the WTG produces 5.5 kW of power at the nominal wind speed. When the distribution system is islanded the power output of the WTG decreases as shown in fig. 5.16. The switching in the power output of the WTG as shown in fig. 5.16 while it decreases is because of the fault clearance at the different time instances. The WTG absorbs active power at the time between 5.007 s-5.081 s and it is because of its leading power factor (P.f) in this period as shown in fig. 5.17. This power returns to the nominal values as shown in fig. 5.16.The oscillations in the angle between voltage and current at different time instants are because of some events such as occurrence of the fault, clearance of the fault from both sides etc. The angle between the voltage and the current of the machine in the normal operating conditions is -3^0 (i.e. P.f=0.9986) in the normal operating condition. This angle increases to 150^0 at the instant of a fault. Again it deceases to the value around -172^0 at

the time when fuse F0 is blown. The further oscillation in this angle at this time is because of the opening of the circuit breaker at the MV bus.

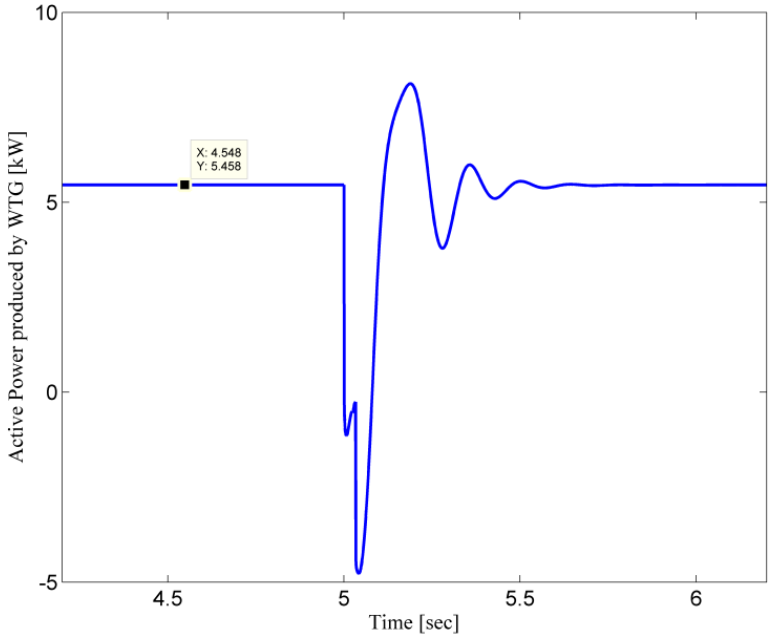

Fig. 5.16 Active power output of the WTGin case of grid connected and islanded mode

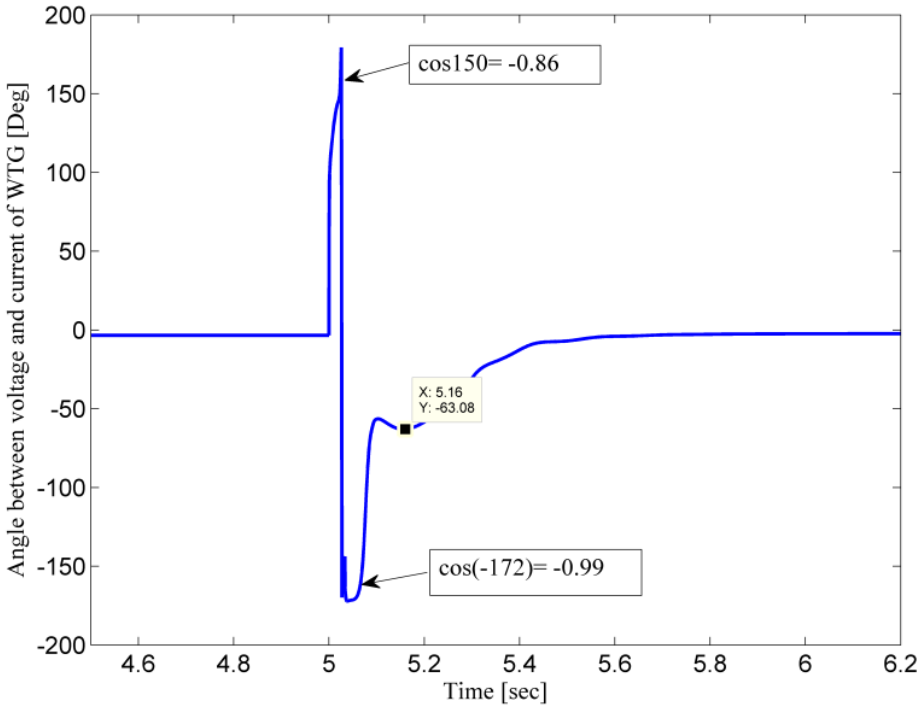

Fig. 5.17 The angle between voltage and current of a WTGin case of grid connected and islanded mode

5.4 Frequency Control in islanded Micro Grid

Any mismatch between the load demand and the active power generation causes deviations in the frequency of the network. If the active power demand is greater than the active power production in the local island, the MG frequency decreases and vice versa.

In the normal operating conditions (i.e. grid connected mode) some of the active power is supplied by the grid and the rest is provided by the DG units in order to meet the load demand. The active power produced by PV1, PV2 and WTG are shown in fig. 5.13, 5.14 and fig. 5.16 respectively. The active power delivered by the grid is shown in fig. 5.18. It can be seen in fig. 5.18 that the grid delivers 84.45 kW to the local grid in the normal operating condition in order to charge the batteries and to meet the load demand together with the DG units.

The different loads are connected at the different buses in the CIGRE network. Both the batteries charge in the normal operating conditions if they are not fully charged; hence, they act as loads in the grid connected modes. Table 5.1 shows the power produced by the power grid and DG units in the normal operating conditions. It also displays the active power consumed by the loads.

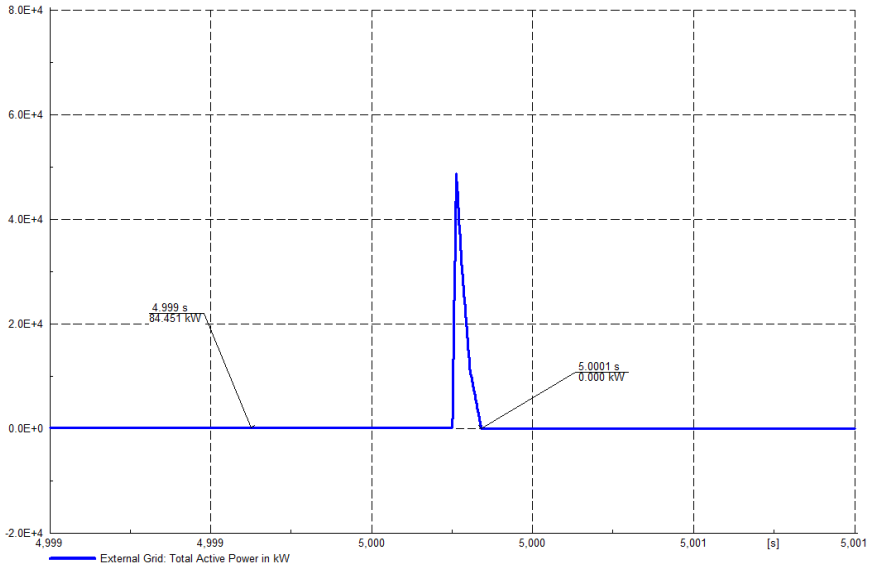

Fig. 5.18 The active power delivered by the grid in case of grid connected and islanded mode

Table 5.1.The powerproductionand the power consumption in case of grid connected and islanded mode

Active Power produced by Generating Units [kW]				**Active Power consumed by the loads [kW]**			**Power losses [kW]**
Grid	PV1	PV2	WTG	Battery1	Battery2	Other Loads	2.227
84.45	3	4	5.5	28.7479	20.511	45.464	
Total= 96.95				Total=94.7229			

When the distribution enters into island mode, it loses 84.45 kW of power as shown in fig. 5.18. The lost power must be delivered by the existing DG units in order to maintain the constancy of the frequency within the local MG. The active power delivered/absorbed by the inverter of battery1 and battery2 are shown in fig. 5.19 and fig. 5.20 respectively.

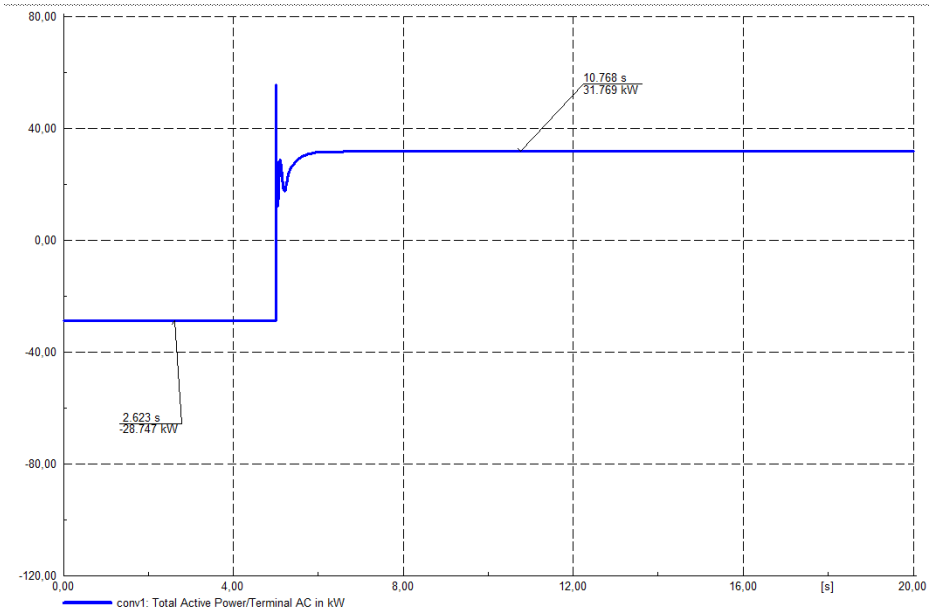

Fig. 5.19 The active power of battery1 inverter in case of grid connected and islanded mode

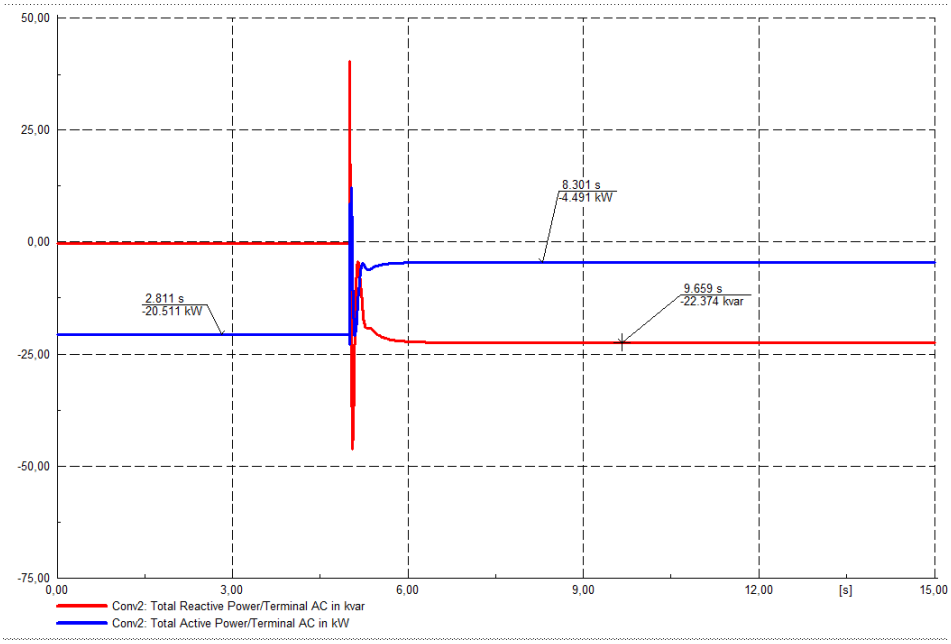

Fig. 5.20 The active and the reactive power of battery2 inverter in case of grid connected and islanded mode

It can be seen in fig. 5.19 that the inverter of battery1(i.e. VSC1) absorbs 28.7478 kW of active power in the normal operating conditions. When the distribution system enters into islanding it injects 31.769 kW of power. The transients in the power as shown in fig. 5.19 are because of the different events (i.e. occurrence of the fault, the clearance of the fault from the grid side and DGs sides at different instances) in the network. The peak in the active power at the instant of a fault is because of the inrush current produced by the inverter. This power decreases at the time when fuse F0 blows as shown in fig. 5.19. Another oscillation in the active power seen in this figure is because of the opening of the circuit breaker at 5.033 s.

Fig. 5.20 depicts that VSC2 absorbs 20.511 kW of active power in the grid connected mode. The control system of this inverter is developed with the voltage control priority; therefore, it absorbs 22.37 kVAr of reactive power in order to control the voltage at its point of the connection. It absorbs 4.491 kW of active power during this condition. The injection/absorption of the active power depends on the control structure described in section 5.2. This is decided according to equation 5.1.The peaks and the oscillations in the power of VSC2 are also because of the above mentioned events.

As described above, the voltage at the time of the short circuit decreases and it recovers up to the permissible operating conditions by the local existing controllers. The decrease in the voltage also reduces the active power of the loads. For simplicity the active power of the load on bus D in its three phases and the voltage in the three phases on bus D where this load is connected is shown in fig. 5.21 (a) (b) respectively.

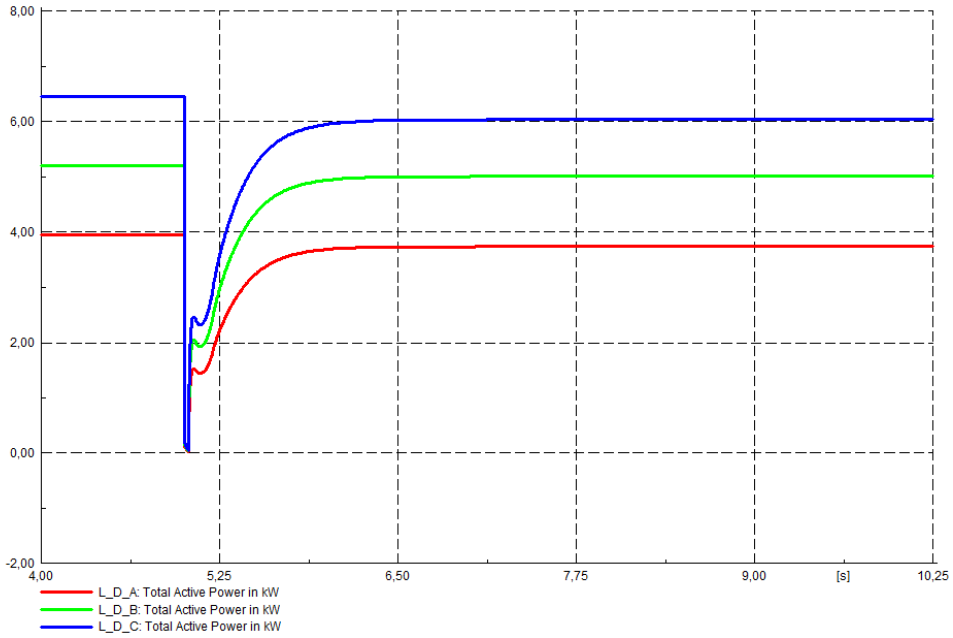

Fig. 5.21 (a) The active power of the load connected on bus D in its three phases in case of grid connected and islanded mode

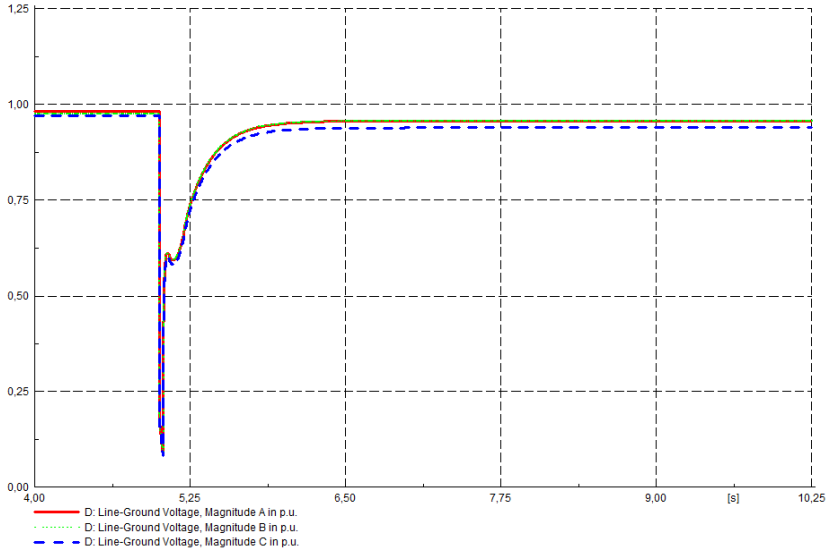

Fig. 5.21 (b) The voltage on bus D in its three phases in case of grid connected and islanded mode

It can be seen in fig. 5.21 that the magnitude of the active power of the load in the three phases on bus D in the island condition is reduced because the voltage of these phases on this bus is not fully restored to its pre-fault values. The restoration of the voltage in the local MG is according to the availability of the reactive power. The voltage on bus D as shown in fig. 5.21 (b) is not restored to its nominal values because the inverters do not have enough reactive power to have full compensation of the voltage.

Table 5.2 shows the power produced by the DG units and the active power consumed by the loads in the local MG during island conditions.

Table5.2.The power production and the power during island mode

Active Power produced by Generating Units [kW]				**Active Power consumed by the loads [kW]**		**Power losses [kW]**
PV1	PV2	WTG	Battery1	Battery2	Loads	3.74
3	4	5.45	31.769	4.491	35.99	
Total=44.219				Total=40.48		

It can be seen in this table that there is an availability of the active power to meet the active power load demand together with the line losses in the islanded MG. It can also be seen in table 5.1 and table 5.2 that the power losses in the island mode are more than the power losses in the grid connected mode. This is because of the excessive amount of the reactive power flowing in the system in island condition.

The balance between the generation of the active power and its consumption ensures the constancy of the frequency in the MG. The frequency of the MG in this case is shown in fig. 5.22. The first peak seen in fig. 5.22 is because of a short term power surge produced by the inverter based DG units. This surge in frequency falls as the power surge in the active power decreases because of the current limiters used in the controller of these inverters. At time equal to t=5.033 s, there is another peak in the frequency as shown in fig. 5.22. This peak is because of the opening of the circuit breaker at the MV bus. At time equal to t=5.085 s there is a minor change in the frequency as seen in fig. 5.22. This change in the frequency at this time is because of the small change in the active power of VSC2 at that time.

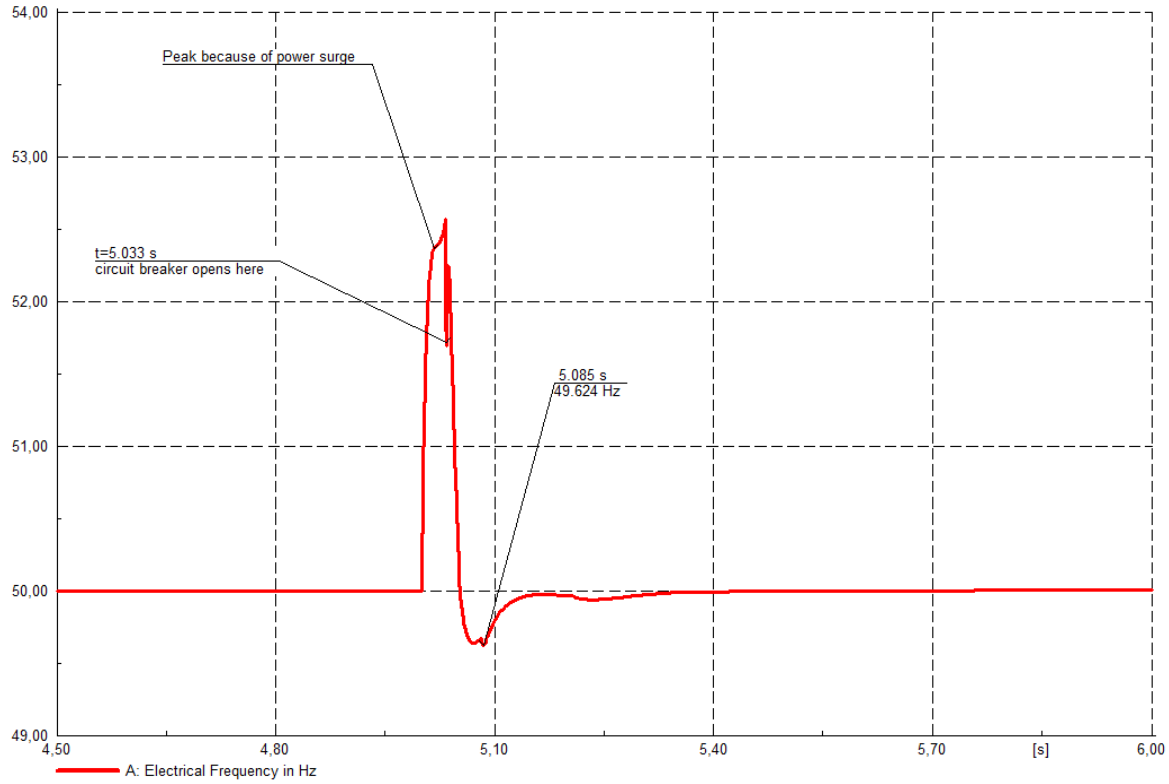

Fig. 5.22 Frequency of the distribution network in case of grid connected and islanded mode

It can be seen in fig. 5.22 that the frequency of the local MG had been restored to 50 HZ by using the local controllers.

To investigate how long time the local MG can survive in island mode, it is necessary to see the SOC of the batteries used in the network. Two cases will be shown one for the case when the initial SOC of batteries is considered to be at 50% and the other when the initial SOC is 95% (i.e. full charged battery) at the beginning of the simulations.

Case1. When SOC of batteries is considered to be 50%

The SOC of battery1 and battery2 for this case are shown in fig. 5.23. It can be seen in this figure that the initial SOC of both the batteries is at 50% at the beginning of the simulations. Fig. 5.23 shows that both the batteries are charging in the grid connected mode. During island condition, battery1 discharges at its maximum rate whereas battery2 charges with slow rate. The fast or slow rate of the batteries is according to the amount of active powers injected/absorbed by the batteries as shown in fig. 5.19 and fig. 5.20 respectively.

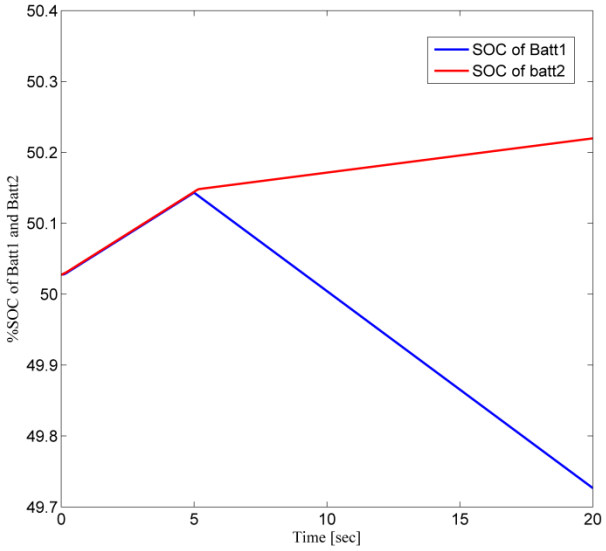

Fig. 5.23 The SOC of battery1 and battery2 in case of grid connected and islanded mode

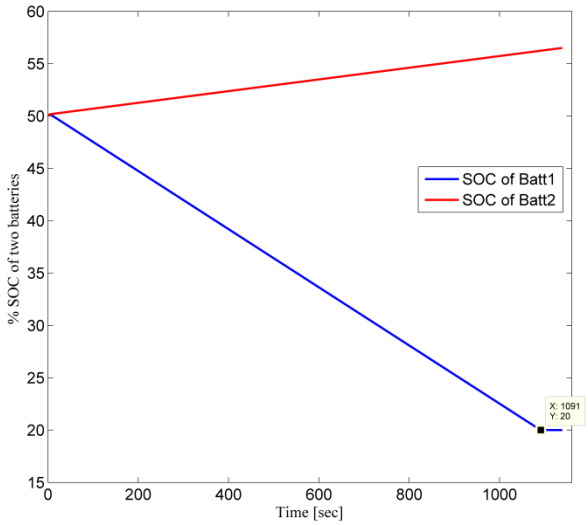

Fig. 5.24 The SOC of battery 1 when it hits the final discharging limit in case of grid connected and islanded mode

Fig. 5.24 shows the SOC of battery1 and battery2 when the SOC of battery1 reaches the final discharging limit (i.e.20%). At time equal to t=1091.167, battery1 discharges down to 20% as shown in fig. 5.24. The SOC of battery2 as shown in this figure keeps on increasing because the inverter of this battery absorbs active power during islanding as shown in fig. 5.20. The discharging of battery down to 20% is considered to be fully discharged due to economic reasons [32]. In fact battery2 should support the island MG by providing active power after the complete discharge of B1, but the control system of this battery (i.e. battery2) in this study is developed in such a way that it has been given voltage control priority. In the islanded MG, the controller of B2 finds a voltage rise at the point of its connection; therefore it absorbs reactive power as shown in fig. 5.20 in order to maintain the constancy of the voltage at that point. Due to this reason VSC2 has not enough active power to deliver according to the equation 5.1.

The active power produced by the inverter of battery1 at this time (i.e. t=1091.167 s) decreases to zero as shown in fig. 5.25. The oscillations obtained in the active power of VSC1 at this time are because of the sudden loss of battery1 from the system. The reactive power of VSC1 is also shown in fig. 5.25. It can be seen in this fig. that VSC1 absorbs 3.574 kVAr of reactive power after discharging of battery1. The voltage at the point of the connection of VSC1 (i.e. bus A) decreases due to this reason as shown in fig. 5.26. The reduction of the voltage on bus A further reduces the voltage in other parts of the network. The decrease in the voltage magnitude at the point of the connections of the inverters decreases their amount of the reactive power injection/absorption (i.e. $Q=VI\sin\phi$) as shown in fig. 5.27. This reduction of the reactive power in turn decreases the voltage in the different parts of the network as shown in fig. 5.28.

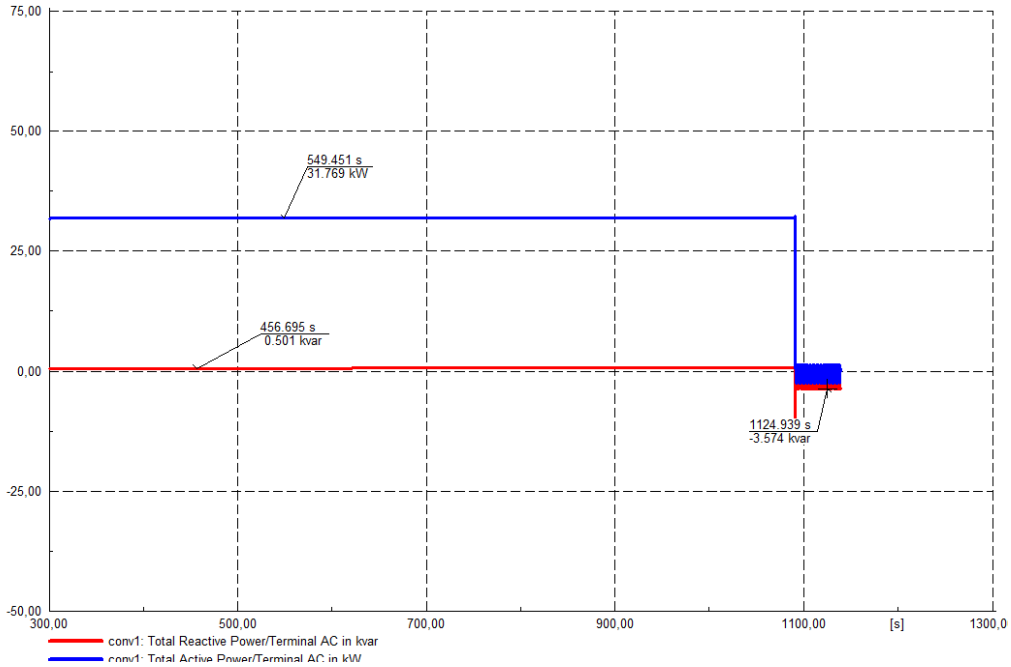

Fig. 5.25 The active and the reactive power of the inverter of Battery1 up to its final discharging limit

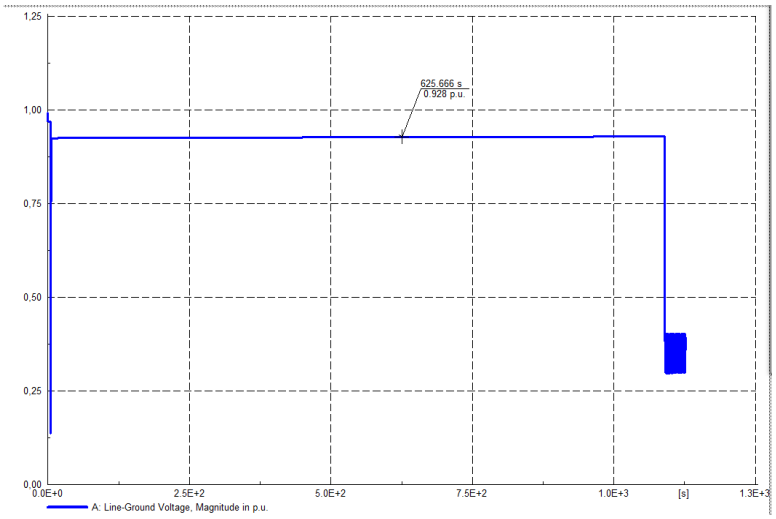

Fig. 5.26 The voltage on the bus A in case of loss of B1 in the islanded MG

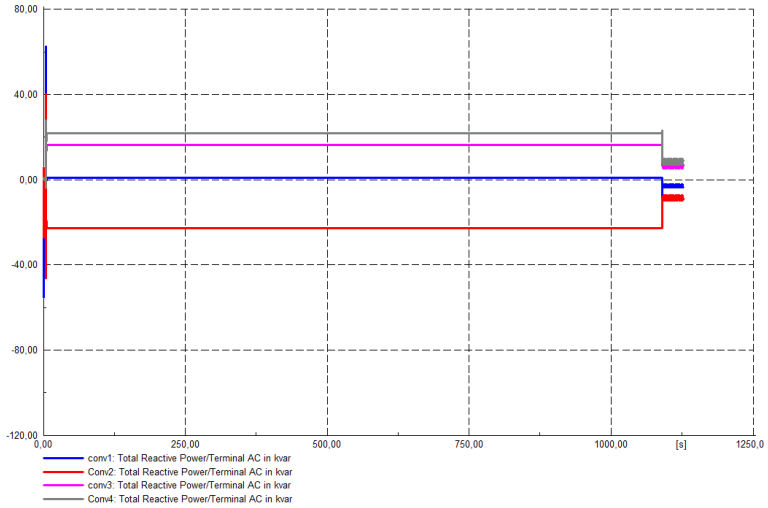

Fig. 5.27 The reactive power of all inverters used in the network in case of loss of B1 in the islanded MG

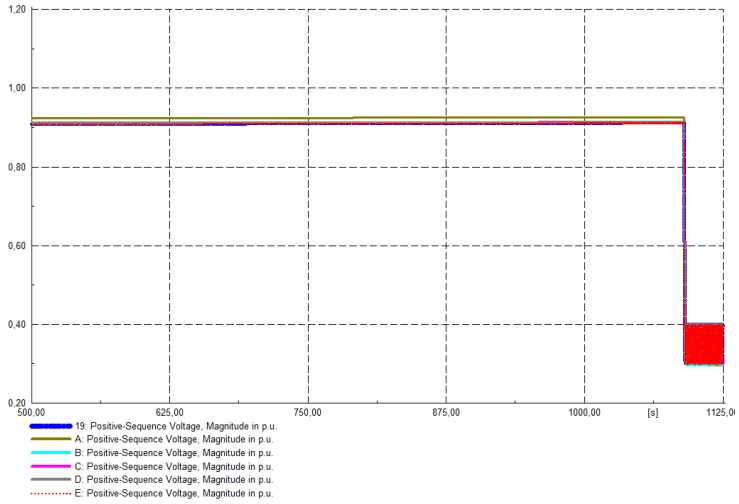

Fig. 5.28 The voltage in the different buses of the CIGRE network in case of loss of B1 in the islanded MG

The reduction in the voltage decreases the loads connected on the respective buses. The load connected on bus C in its three phases is shown in fig. 5.29 for the simplicity.

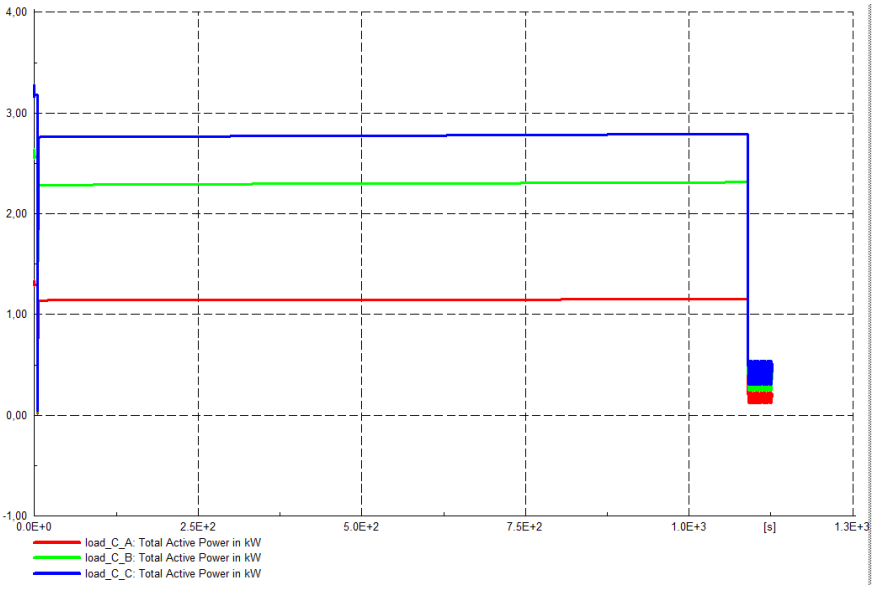

Fig. 5.29 The load on bus C in its three phases in case of loss of B1 in the islanded MG

The frequency of the network because of the loss of battery1 changes as shown in fig. 5.30. It can be seen in this figure that the frequency of the network in the islanded MG is maintained as long as battery1 has ability to deliver the active power. At time t=1091.167 s, it is fully discharged which causes the deviations in the frequency as shown in fig. 5.30. After the loss of battery1, the frequency oscillates between 49.832-48.916 HZ as seen in fig. 5.30. The frequency does not go to the worst conditions because there is not large mismatch between generation and the load demand. This is because of the reduction in the active power load demands due to the decrease in the voltage at their point of the connections.

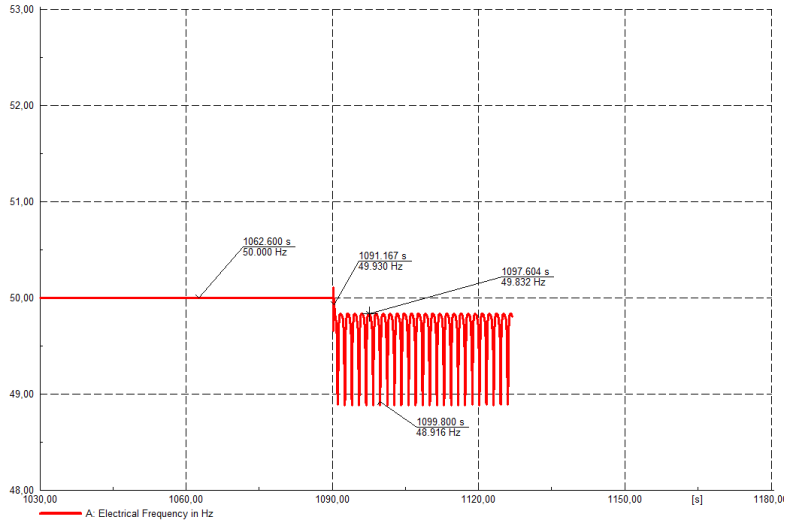

Fig. 5.30 The network frequency in case of the grid connected system and the islanded MG with the loss of B1

It can be seen in fig. 5.30 that network frequency is not stable as long as battery1 has been discharged. To be on the safe side the distribution network must be reconnected to the grid or DG units should be shut down in this regard. The process of the reconnection is described in chapter 6.

Case2. When SOC of batteries is considered to be at 95%

The SOC of both the batteries has been assumed 95% which means that both batteries are fully charged in the beginning of the simulation. The active and the reactive power delivered by the inverters of B1 and B2 in this case are shown in fig. 5.31 and fig. 5.32 respectively.

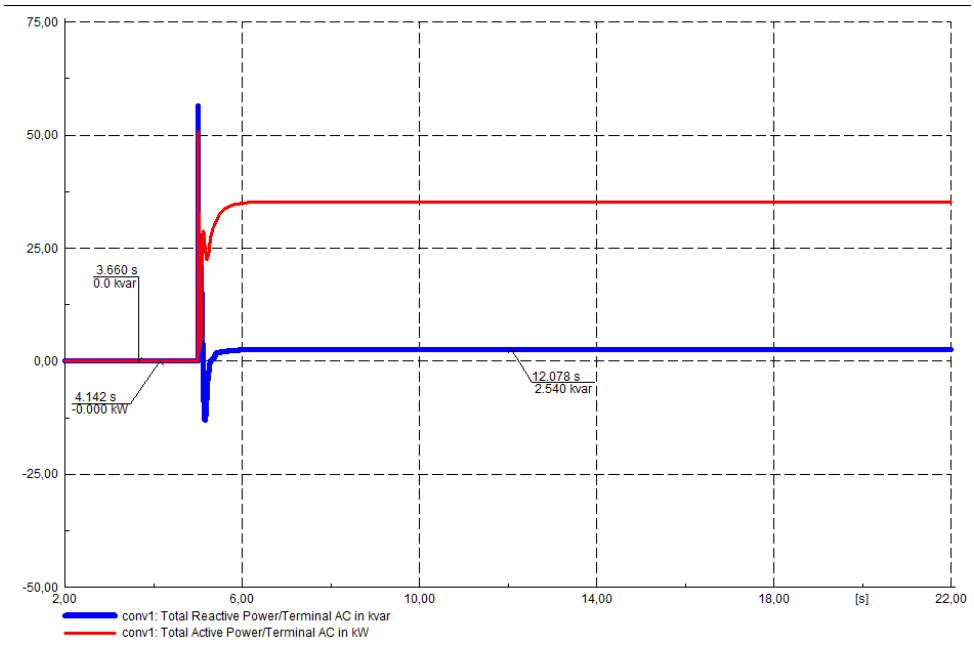

Fig. 5.31 The active and the reactive power of B1 inverter in case of grid connected and islanded mode

It can be seen in fig. 5.31 and fig. 5.32 that VSC1 and VSC2 do not inject active power in the normal operating condition since B1 and B2 are already charged at maximum level. As there is no flow of current in order to charge B1 and B2 in the normal operating conditions through lines R8-RA and R10-RB, therefore there is less voltage drop across the terminals of VSC1 and VSC2 as compared to the case when B1 and B2 are charged at full charging rates. Due to this reason the voltage in all parts of the network during the normal operating conditions is a little bit higher in magnitude than the previous case of the charging batteries at the full charging rate. For simplicity, the zoom of the voltages at bus B, C and bus D in the two cases (i.e. 1. when B1 and B2 are charging at full rate and 2. when B1 and B2 do not charge) are shown in fig. 5.33, 5.34 and fig. 5.35 respectively.

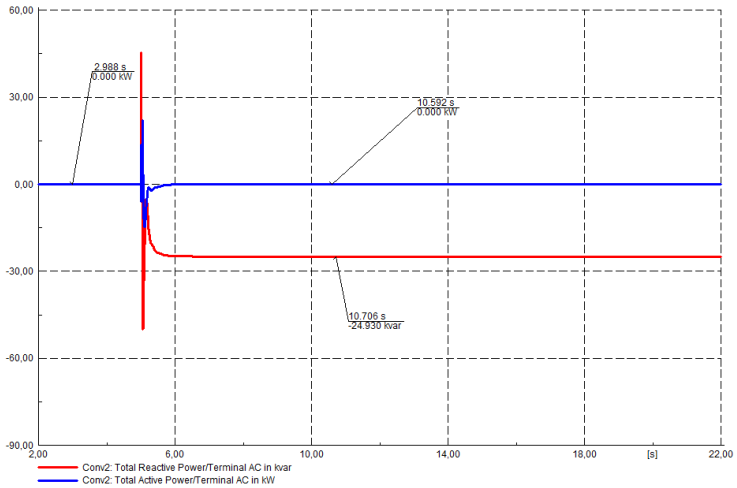

Fig. 5.32 The active and the reactive power of B2 inverter in case of grid connected and islanded mode

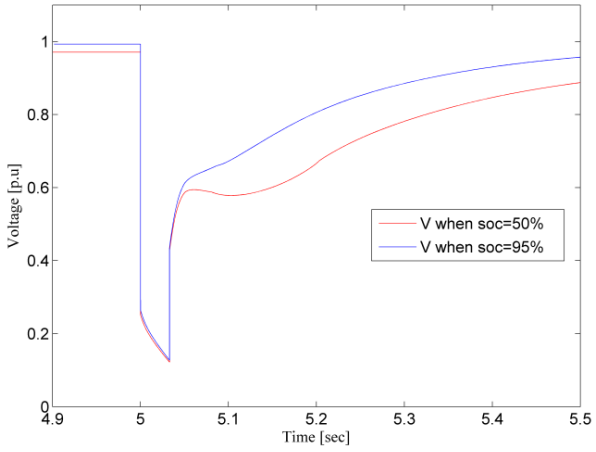

Fig. 5.33 The voltage on bus B for the two charging cases

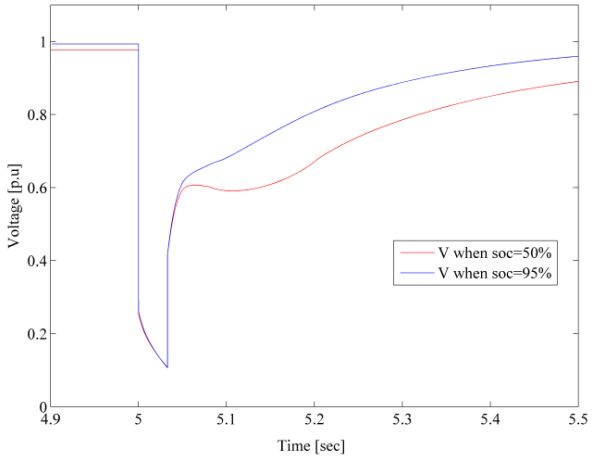

Fig. 5.34 The voltage on bus C for the two charging cases

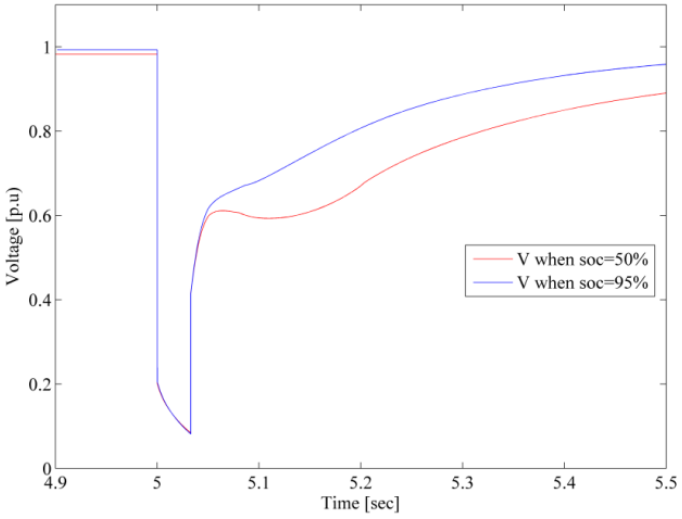

Fig. 5.35 The voltage on bus D for the two charging cases

The voltage shown in fig. 5.33, 5.34 and fig. 5.35 decreases at the instant of the fault on the MV bus. The voltage on the buses shown in these figures during this period is slightly higher (i.e. can be clearly seen if we zoon out the figures) than the one when SOC of batteries is considered to be 50%.

Since the injection of the reactive power depends on the magnitude of the voltage at the terminals of the inverters, the inverters inject more reactive power in the case when soc=95%. The inverters inject more reactive power compared to the case when soc=50% and is because of the voltages at their points of connections are bit improved in this case as shown in fig. 5.33, 5.34 and fig. 5.35. The injection of the reactive power by the inverters in the two different cases is shown in table 5.3. The existing controllers have improved the voltage in the different parts of the network in this case as shown in fig. 5.36.

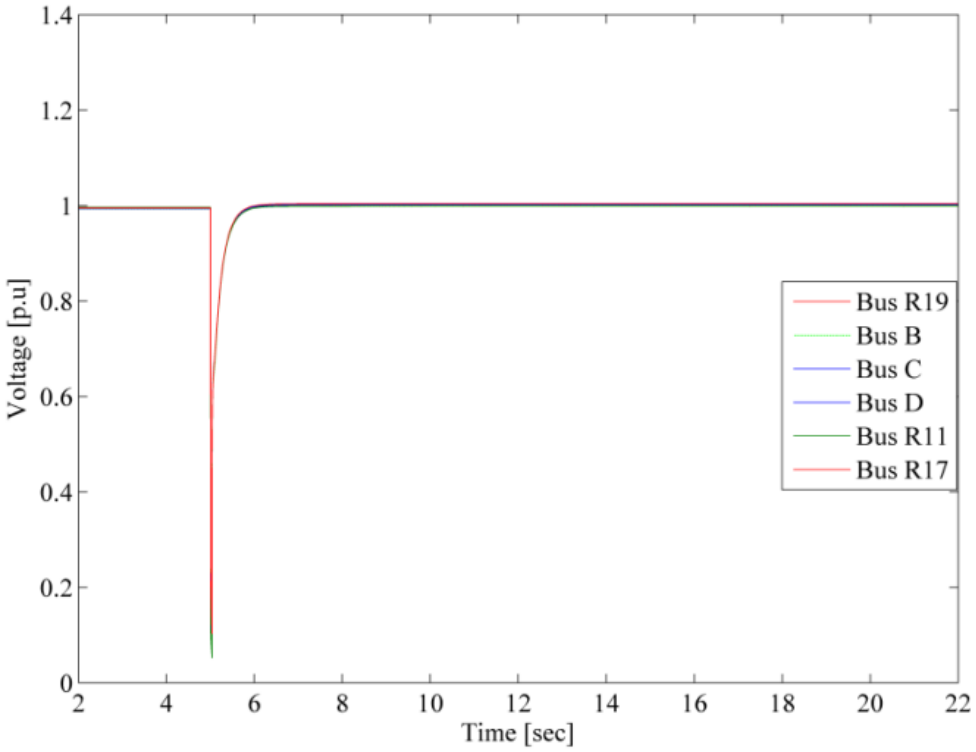

Fig. 5.36 The voltage in different parts of the network in grid connected and the islanded mode in the case when SOC=95%

It can be seen in fig. 5.36 that the voltage in the different parts of the network has been fully restored in the islanded MG in this condition. This restoration of voltages in the different parts of the network is because of the reactive injection by the inverters. The reactive power of the existing inverters in this case is shown in fig. 5.37.

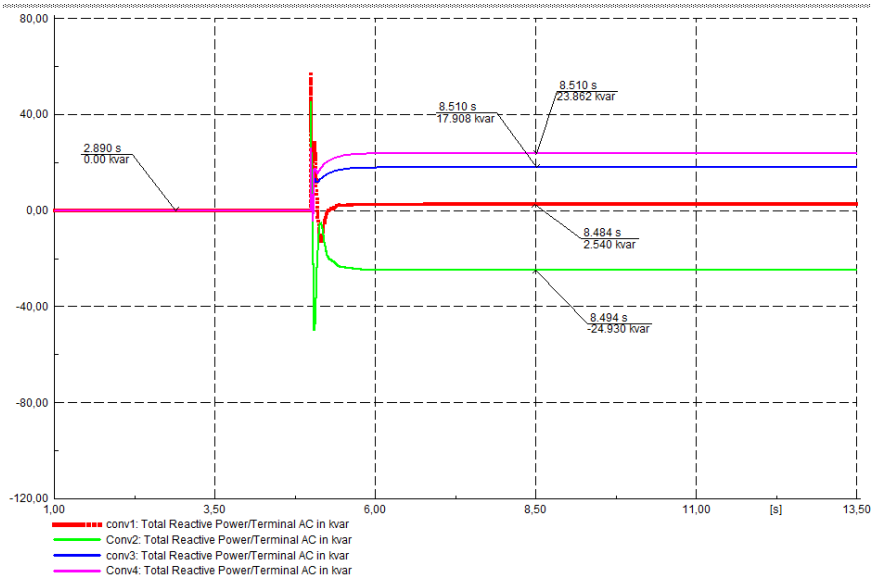

Fig. 5.37 The reactive power produced/absorbed by the inverters in grid connected and the islanded modes in the case when SOC=95%

Table53. The reactive power produced/absorbed by the inverters in two different cases

Inverters	Reactive Power (kvar) produced/absorbed by the inverters when SOC=50%	Reactive power (kvar) when SOC=95%
VSC1	0.502	2.54
VSC2	-22.374	-24.93
VSC3	16.108	17.908
VSC4	21.477	23.86

The SOC of the two batteries in this case is shown in fig. 5.38 in order to investigate how long the local MG can survive in island mode.

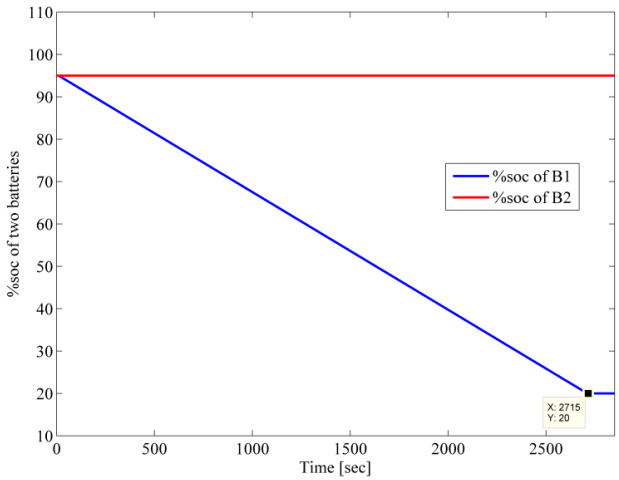

Fig. 5.38 The SOC of B1 and B2 when it hits the final discharging limit in the case when initial SOC=95%

It can be seen in fig. 5.38 that both the batteries are fully charged (i.e. SOC=95%) in the normal operating condition. B1 discharges at the time when the distribution network is islanded whereas B2 neither charges nor discharges (i.e. its SOC remains constant). The reason for such a behavior of B2 is because of voltage control priority given to its control system. It can be concluded from fig. 5.38 that the islanded MG can survive up to 2715 s (i.e. 45.25 minutes) ensuring the perfect control of the voltage and the frequency in the islanded MG.

5.5 Study of the network with load step change in islanded Micro Grid

To analyze the power system frequency response of the islanded MG, a step increase/decrease of the active power of a system load is simulated. The study is performed in the case when both the batteries are considered to be fully charged. The network frequency reduces if the demand increases. A step load increase of 30% is applied at time, t=8 s on the system load at bus E in its three phases. The load on this bus in its three phases with equal load step applied in all phases increases as shown in fig. 5.39.

At t=8 s, the active power of the load in the three phases on bus E increases because of the applied load step. The voltage on this bus as shown in fig. 5.40 decreases in this case. The decrease in the voltage on bus E is because of the more line voltage drop across line R4-RE as compared to the case with no load step (i.e. normal operating conditions). This reduction of the voltage on bus E reduces the active power of the load connected on this bus as shown in fig. 5.39. The pattern of the load reduction marked with a circle in fig. 5.39 is according to the decay of the voltage on bus E. The decrease in the voltage on bus E also reduces the voltage in the different parts of the network as shown in fig. 5.41.

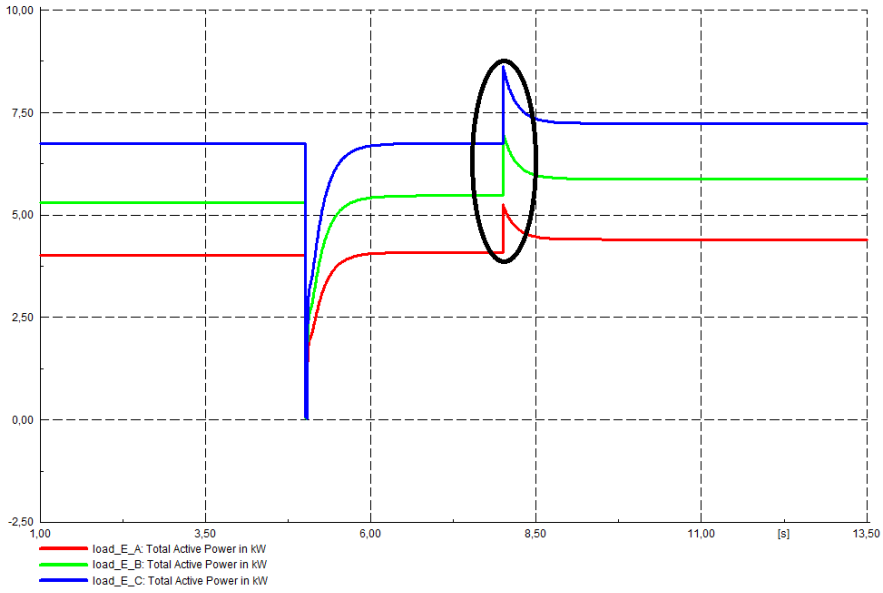

Fig. 5.39 The active power in three phases of the load on bus E in case of the islanded MG with a load step change

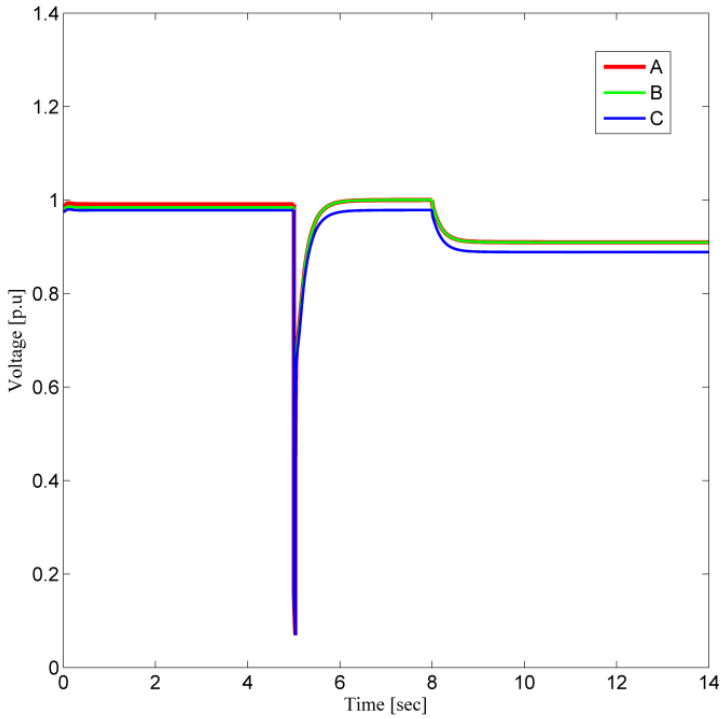

Fig. 5.40 The voltage in three phases of bus E in case of the islanded MG with a load step change

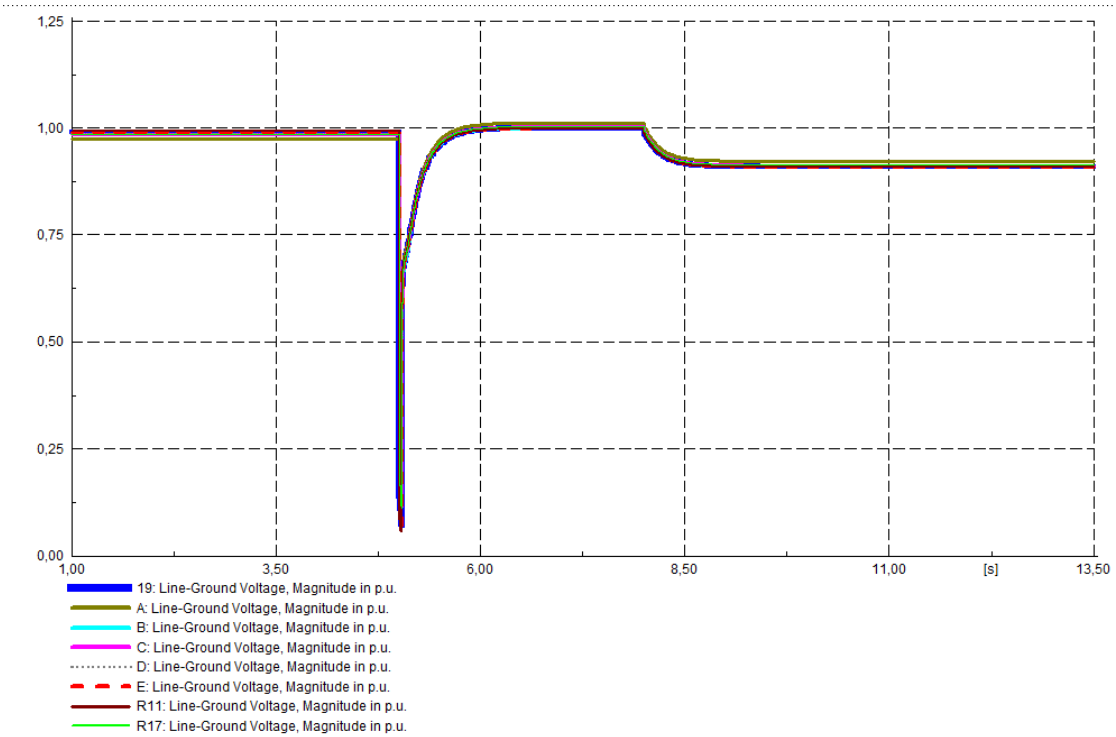

Fig. 5.41 The voltage on different buses of the network in case of the islanded MG with a load step change

The network voltage when it decreases at t=8 s might be improved if the existing inverters have enough reactive power. The reactive power of all of the inverters used in the network in this case is shown in fig. 5.42.

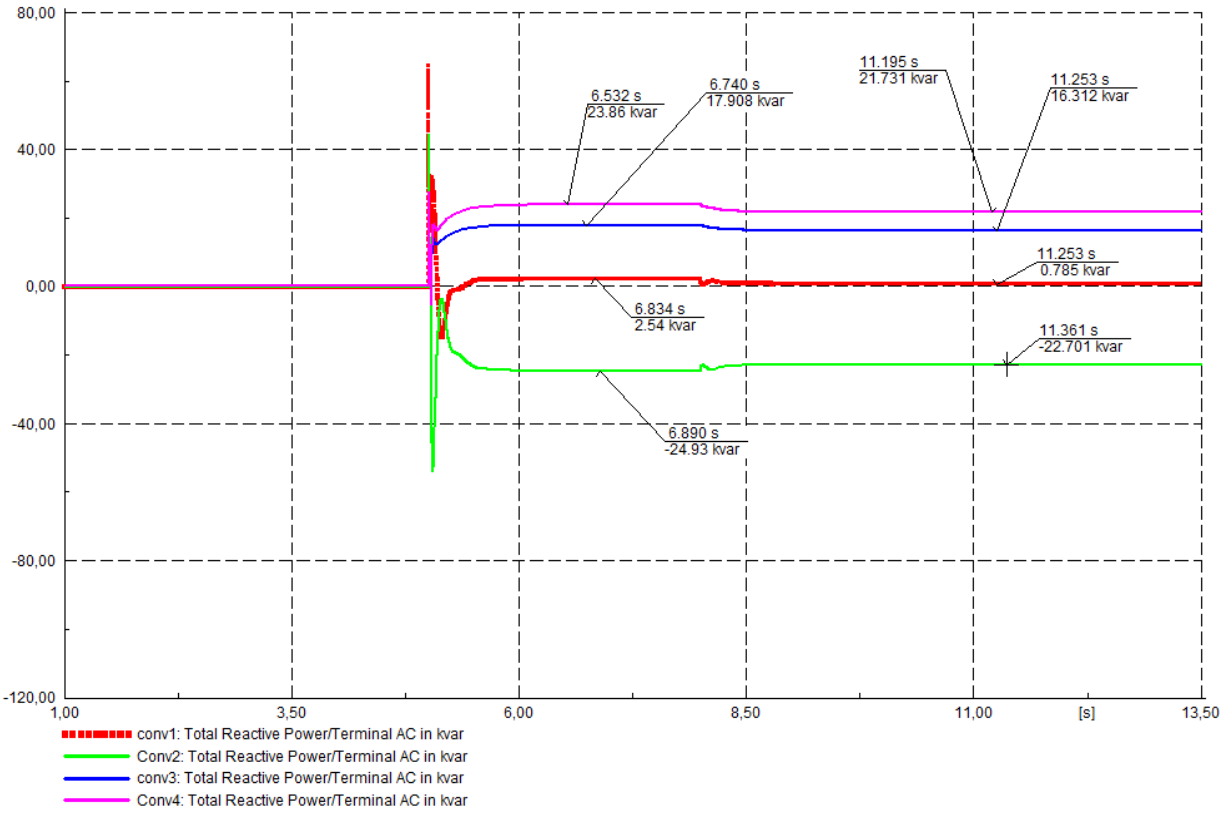

Fig. 5.42 The reactive power produced by VSC1, VSC2, VSC3 and VSC4 in case of the islanded MG with a load step change

The amount of reactive power injected/absorbed by the invertersis a function of the voltage. Once the voltage changes, the reactive power produced by them also changes, which further changes the voltage. It can be seen in fig. 5.42 that the reactive power produced by all inverters changes during the applied active power load step. At the time t=8 s, the voltage in different parts of the network decreases and the inverters do not have enough reactive power to compensate for it. Due to this reason the reactive power injected by these controllers at this time decreases further (i.e. $Q = VI \sin\phi$) as seen in Fig. 5.42.

The decrease in the voltage in all parts of the network at the time equal to t=8 scauses a reduction in the active power of the loads on the different buses. For the simplicity, the active power load on bus C in its three phases is shown in fig. 5.43. The decay of load power as shown in this figure marked with a circle is according to the voltage decay as shown in fig. 5.41.

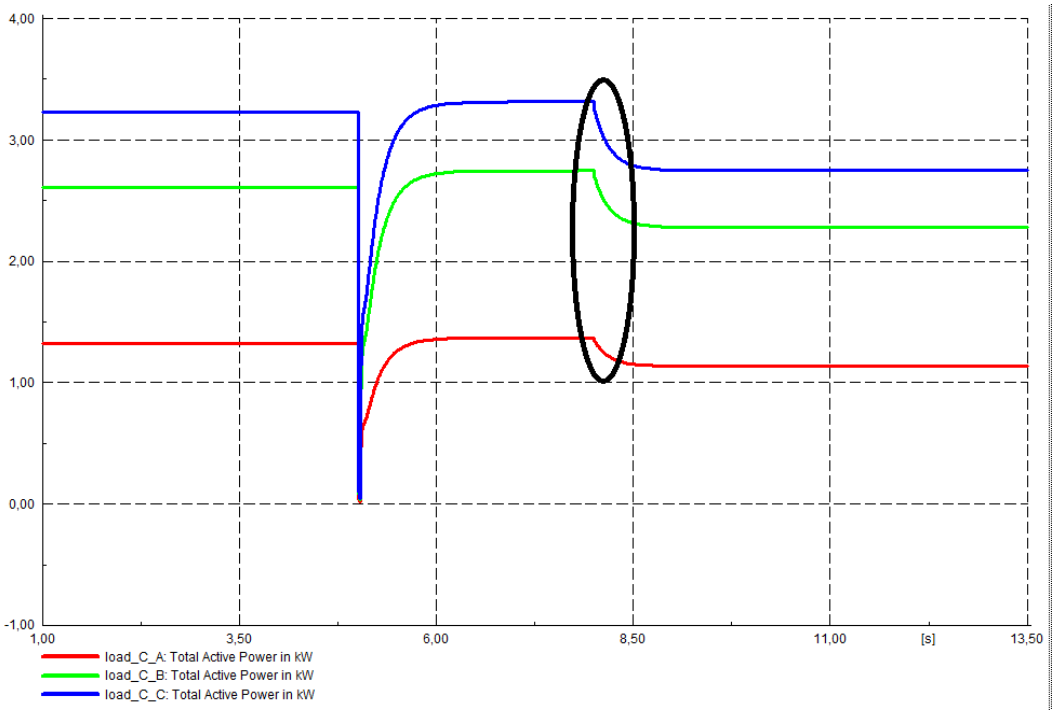

Fig. 5.43 The active of the load on the bus C in case of the islanded MG with a load step change

The frequency of the network is this new case is shown in fig. 5.44 (a) (b) and is controlled within the normal operating limits. Fig. 5.44 (b) shows a zoom of the frequency at the time when the step is applied in the load.

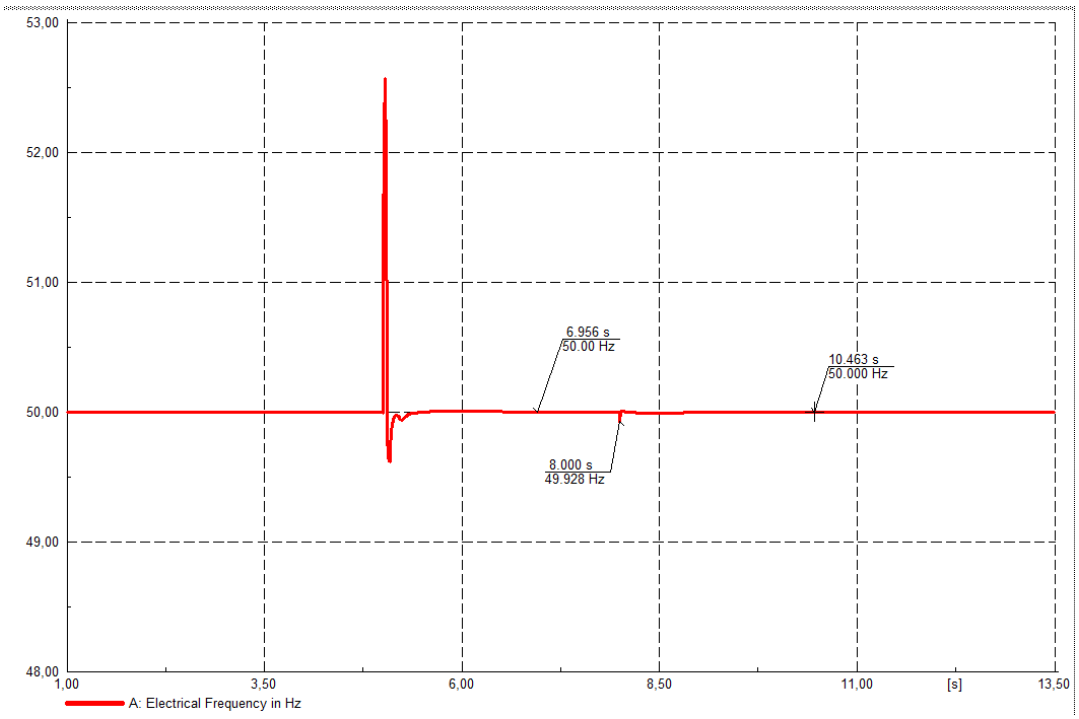

Fig. 5.44 (a) The frequency of the network in case of the islanded MG with a load step change

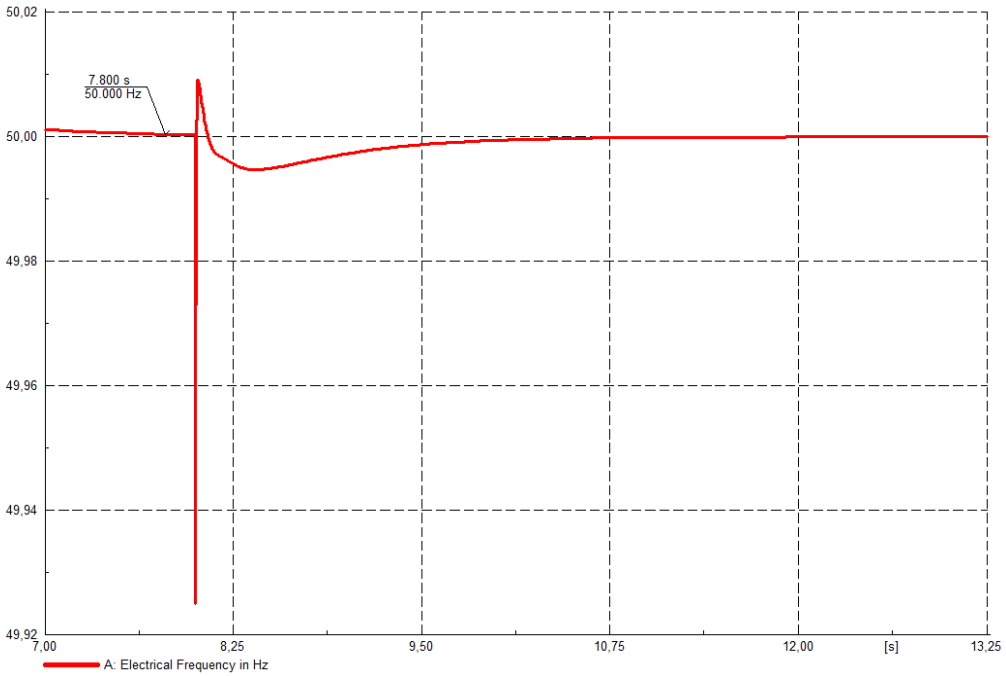

Fig. 5.44 (b) The zoom of the frequency at the time of the load step

It can be seen in fig. 5.44 (b) that the network frequency decreases at t=8 s at the time of the load step. It has been restored to the nominal values by the existing DG units.

5.6 The study of the network in case of the loss of generating unit(s) in islanded Micro Grid

The study about the behavior of the voltage and the frequency of the islanded MG in the case of loss of generating unit/units is carried out in this section. This is done by having the following case study:

At the time equal to t=8 s, the power out of both the PV units decreases to zero because of loss of solar irradiance. This loss of the solar irradiance could be because of darkness due to clouds or time instances when it is the night time. The power output of PV1 and PV2 in this case is shown in fig. 5.45. As the power output of these units decreases, AC and DC-link voltages at the terminals of both PV inverters decrease as shown in fig. 5.46.

It can be seen in fig. 5.46 that AC and DC-link voltages of the PV inverters (i.e. VSC3 and VSC4) decrease at t=8 s. The DC voltage controllers of the respective STATCOM controllers control the DC-link voltage up to the nominal values (i.e. 1 p.u). These controllers utilize the energy of the DC-link capacitors and provide the temporary support of the active power in order to control the DC-link voltages. The voltage on the AC sides of the inverters is not restored to the pre-fault fault value because of the reactive power deficiency in the network. The voltage reduction in the different parts of the network reduces the active power of the loads in different parts of the network. The frequency of the network in this case is shown in fig. 5.47. The

frequency of the network decreases at the time of the loss of PV units. This frequency is restored to the nominal values by using the BESS based STATCOM controllers.

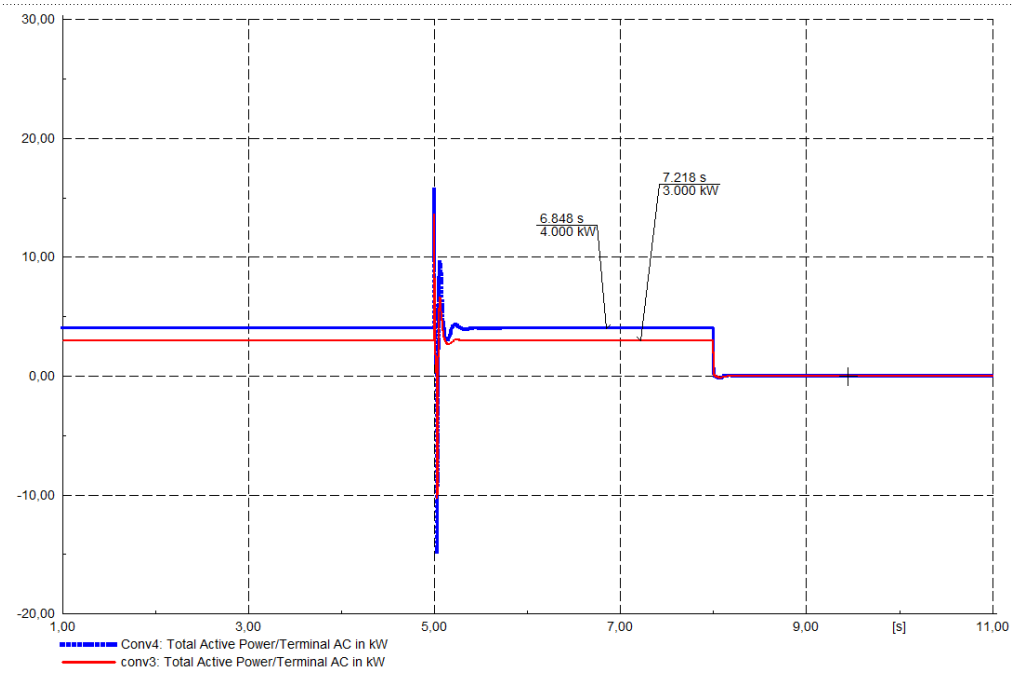

Fig. 5.45 The power output of the PV units in case of the islanded MG with the loss of solar irradiance

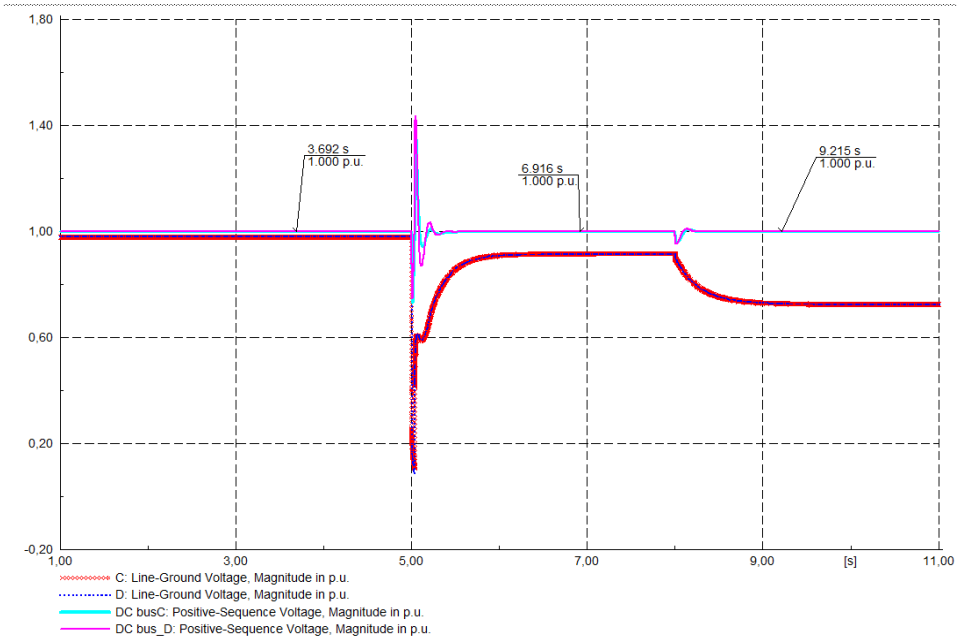

Fig. 5.46 The AC and DC-link voltages of PV inverters in case of the islanded MG with the loss of solar irradiance

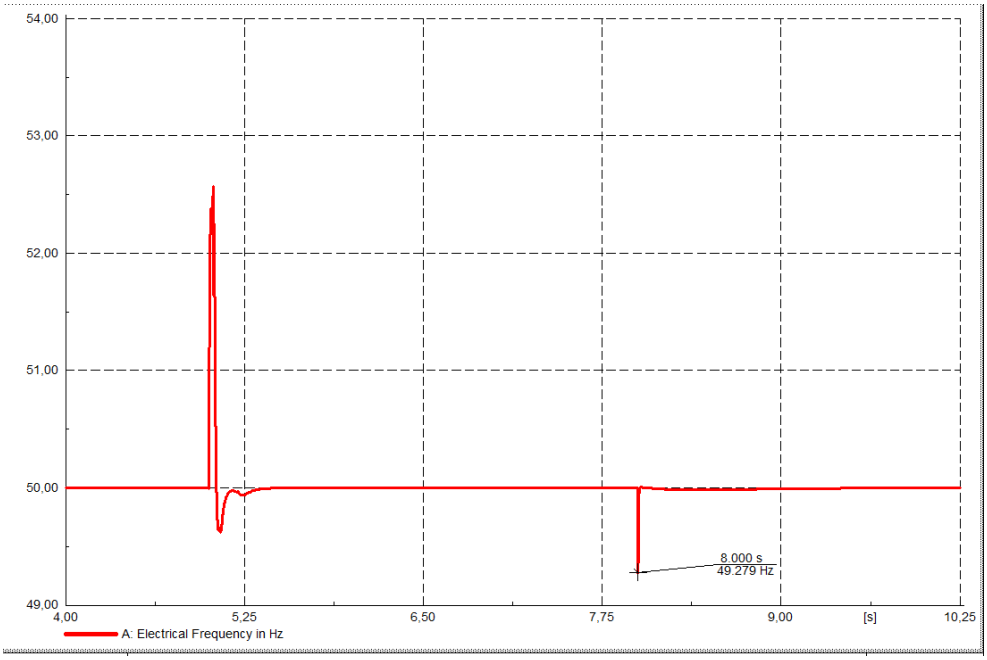

Fig. 5.47 The frequency of the network in case of islanded MG with the loss of solar irradiance

5.7 Summary

The study about an islanded portion of the CIGRE network has been carried out in this chapter. Some of the main issues related to the islanding such as the problems of the voltage and the frequency in the islanded MG have been described here. The issues of the voltage and the frequency in the islanded MG have been solved properly in this chapter. This is done by developing an appropriate control system which should be able to control voltage and the frequency of the local MG. The procedure about the development of the control system which should work in island mode has also been presented. It is suggested in this chapter that the control system of battery1 (i.e. bigger DG unit) should operate in VF control mode whereas the control system of the other DG units should either be in PQ or PV mode. The switching of the control system from grid connected mode to islanded mode is proposed by using an appropriate islanding detectiontechnique. The study about the island detection by using voltage phase angle difference between the DG side and the transmission grid is also carried in this chapter. This chapter concludes that the proposed island detection technique is performing well and the developed controllers have successfully controlled the voltage and the frequency of the islanded MG. The controllers have also ensured the constancy of the voltage and the frequency of the islanded MG in the different conditions such as load changes and the loss of the DG unit(s).

Chapter 6

Grid Reconnection

6.1 Introduction

In fact, the reliability of the power network is improved by allowing island operation; however the reliability of the small network operating in island condition is less compared to grid-connected operation [126]. Hence, it is essential to reconnect the distribution network back to the transmission system when the transmission system is operating in normal conditions. Reconnecting the distribution system to the transmission grid is similar to synchronizing a DG based distribution system to the transmission system. The magnitude and phase of the voltage and the frequency of the distribution system should be synchronized with the transmission grid. The difference of the voltage magnitude, voltage phase angles and the frequency of the distribution system and transmission system should be within a certain range before they can be reconnected. The frequency and the phase can be controlled by matching the generation and the load in the network. This is done by injecting/absorbing the desired amount of the active power. The voltage is controlled by providing the required amount of the reactive power in the network. The distribution system can be connected to the transmission grid if the following criteria are met and are based on [127].

i. The difference in the frequencies between the distribution system and the transmission grid is less than 0.1 Hz
ii. The difference in the voltages between the distribution system and the transmission grid is less than 5%, and
iii. The two systems are in phase.

This chapter presents an introduction about reconnection of the islanded portion of the network to the transmission grid. Section 6.2 presents adescription about the grid reconnection detection. The simulation results are presented in section 6.3. Finally summary of the chapter is given in section 6.4.

6.2 Grid Reconnection Detection

The status of the network changes from island to grid connected mode if system is reconnected back to the grid. The status is detected by the grid connection detection technique. Several reconnection techniques have been presented in the literature. Some of the techniques are detailed described in [128]. The grid reconnection in this study is detected by using a technique which measures the voltage magnitude, frequency and phase angles between the transmission grid and islanded distribution grid. Reconnection detection and the control mode determination from islanded to the grid connected mode are described with the help of the diagram as shown in fig. 6.1. This figure explains that the voltage, frequency and the phase angles at the points which are mentioned in the block diagram are measured and the difference is calculated. If all of the

above three requirements presented in section 6.1 are satisfied then the mode determination block sends a Reconnection Detection (RD) signal to the switch block. The switch determines the grid connected mode of the operation. Once the reconnection is detected; the control system of the VSC1 shifts from VF mode to PQ mode as it was operating in VF mode in islanded condition whereas the controllers of other inverters operate in the same mode (i.e. PV mode).

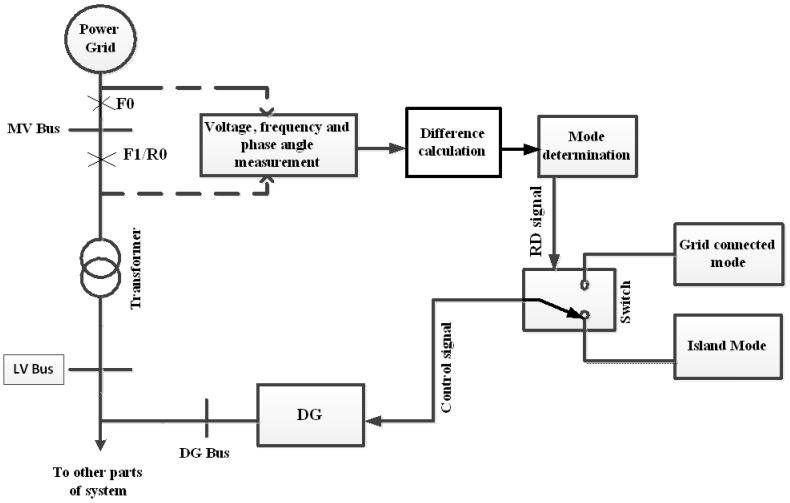

Fig. 6.1 The block diagram of the control mode determination and reconnection detection

The implementation of the control mode determination and reconnection detection in DIgSILENT is made according to block diagram shown in fig. 6.2.

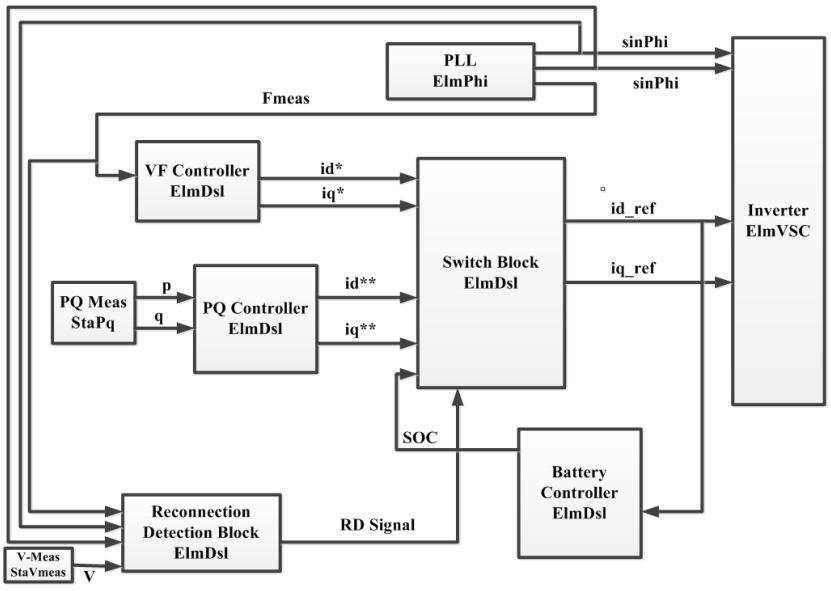

Fig. 6.2 The block diagram of the control mode determination and reconnection detection developed in DIgSILENT power factory software

It can be seen in fig. 6.2 that two different controllers (i.e. PQ and VF controllers) are used for the two different conditions (i.e. grid connected and island) of the network. The PQ controller described in section 2.5.1 generates signals (id_ref** and iq_ref**). The VF controller which is described with the help of fig. 5.2 produces the output signals (i.e. id_ref* and iq_ref*). The decision about the transition of the control system from the VF mode to PQ mode is made by the reconnection detection (RD) block. The explanations and the description of the reconnection detection are presented in the above text.

The switch block receiving the signals (id_ref** and iq_ref**) and (id_ref* and iq_ref*) from the PQ controller and VF controller respectively at its input, sends appropriate current references to the current controller which is built in the inverterblock of the DIgSILENT and is according to the RD signal. If the RD signal is 0 (i.e. no reconnection), the current controller receives the active and the reactive current references from the VF controller and if RD signal is 1 (i.e. reconnection detected), the current controller receives signals from the PQ controller. The current controller receiving the signals from the PQ or VF controllers send the signals to the PWM block of the inverter and decide the duty cycle [56]. The details of the current controller are described with the help of fig. 2.8.

The battery controller block is also added in fig. 6.2. This block receives the active current reference (i.e. id_ref) from the switch block at its input and integrates it in order to get the State of Charge (SOC). The signal SOC is sent to switch block which in turn decides the amount of id_ref according to the value of SOC. The switch block makes the id_ref equal to zero if the SOC of the battery is either 20% or 95%. This is in order to avoid damage of the battery and to preserve battery life [32].

6.3 Simulation Results

In order to see if the existing control systems have made it possible to satisfy the criteria of the reconnection of the distribution system to the transmission grid, some of the simulations results of the voltage magnitude together with the phase angles and the frequency of the network are presented here. The frequency of the distribution system and the transmission grid is shown in fig. 6.3.

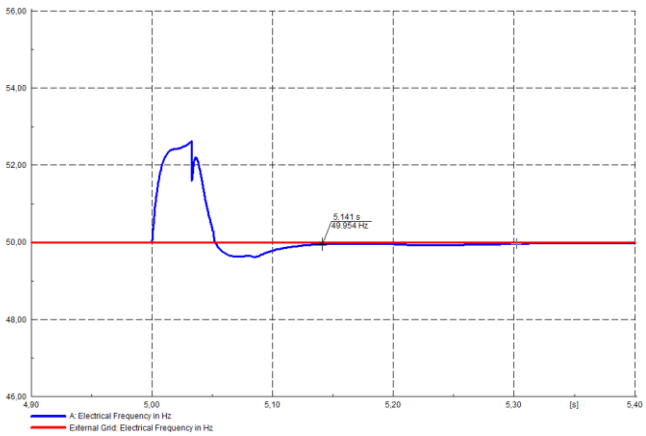

Fig. 6.3 The grid and the distribution system frequency in grid connected and islanded mode

It can be seen in fig. 6.3 that grid frequency and the distribution system frequency deviate from 50 Hz at the time when islanding appears. The existing controllers have restored the frequency of the islanded MG in very short time as shown in this figure.

The voltage phase angles in all three phases of the distribution system and the transmission grid are shown in fig. 6.4. Separate plots for the phases in each phase are shown and one of the plots shows all phases together in the same plot. It can be seen in this figure that the controllers have controlled the voltage phase angles within 500 ms (i.e. 5.5 s) after the instant of the fault

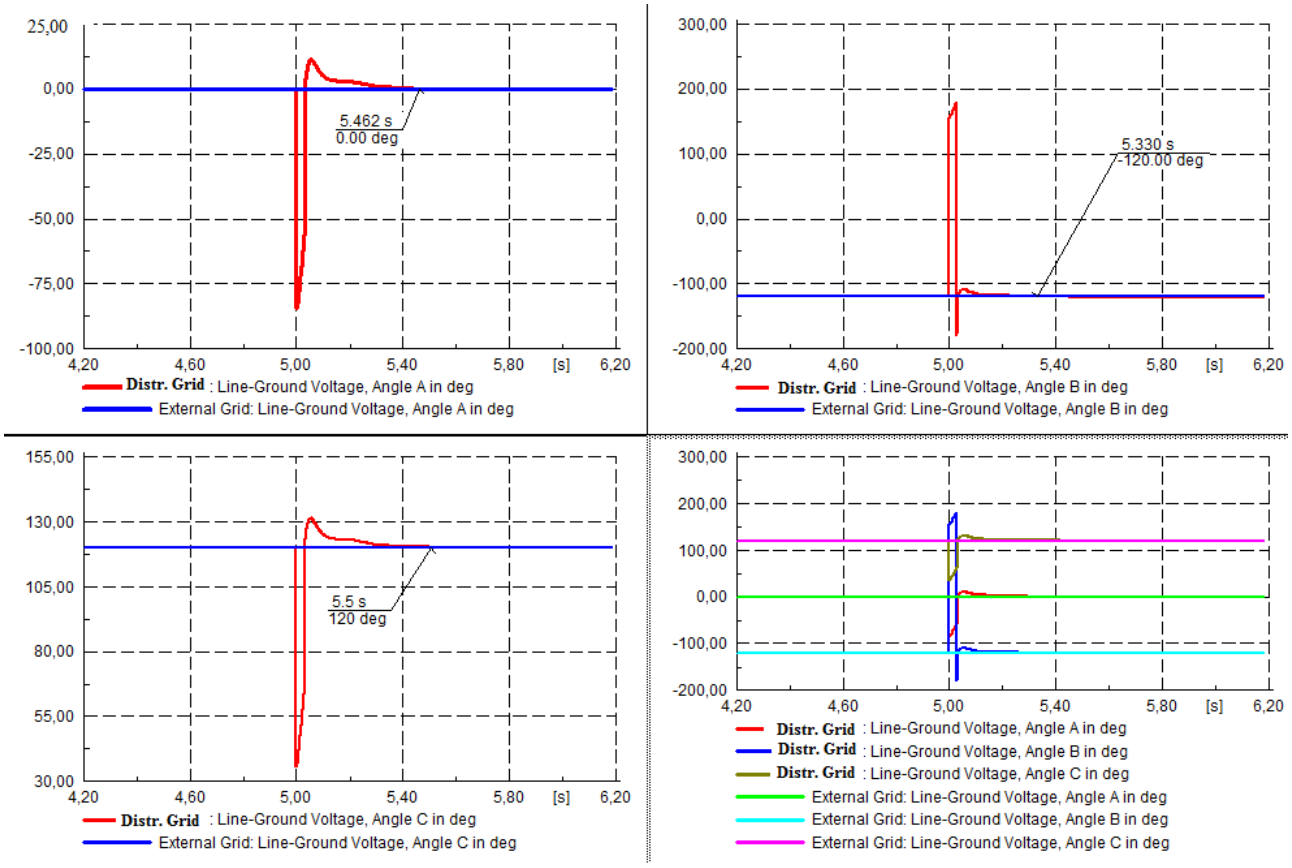

Fig. 6.4 The voltage phases angles of the distribution system and the transmission grid in grid connected and islanded mode

Fig. 6.5 shows the voltage of the distribution system and the transmission grid. It can be seen in fig. 6.5 that the controllers have controlled the voltage up to required limits where reconnection can be made.

It can be concluded from fig. 6.3, 6.4 and fig. 6.5 that the existing controllers have satisfied all the requirement of the grid reconnection. It can be seen in fig. 6.5 that the distribution system is connected to the grid at 6.1 s, which returns the voltage of the distribution network to the pre-fault values.

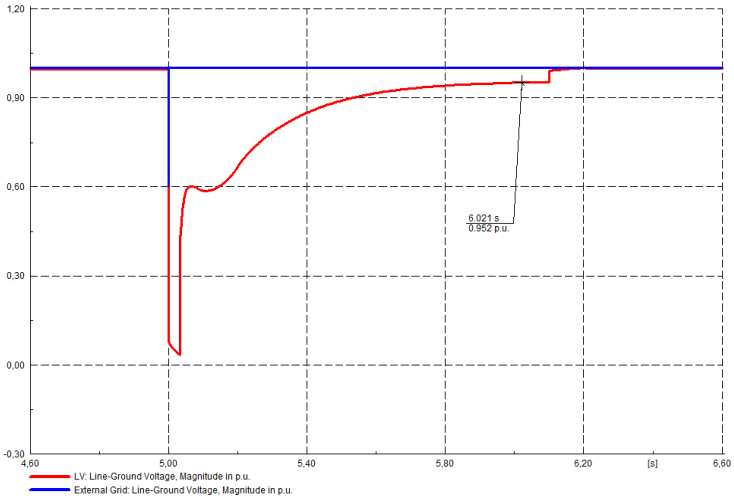

Fig. 6.5 The voltage of the distribution system and the transmission grid at islanding and reconnection

Grid reconnection is detected as shown in fig. 6.6. This fig. shows that grid is reconnected at 6.1 s and the control system changes its state from the islanded to the grid connected mode.

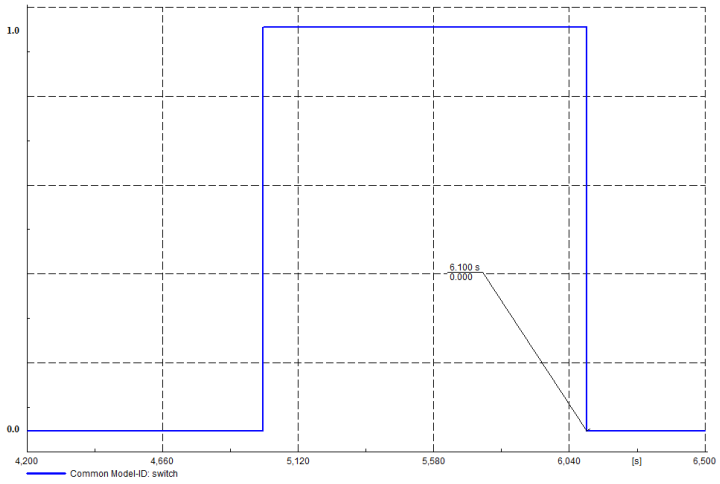

Fig. 6.6 Grid reconnection detection

The SOC of batterry1 in this case is shown in fig. 6.7. This figure describes three different modes of operation for battery1 and is explained with the help of the three different points (i.e. points 1, 2 and 3). Point 1 indicates the normal operating condition of the distribution system, and the battery is charging since it is not fully charged yet. The control system of B1 operates in PQ mode in this condition and thereby charges B1 at full charging rate during this time as shown in fig. 6.7. Point 2 presents the island operation of the network where the control system of B1 works in VF mode. During this time B1 discharges as shown in fig. 6.7. Point 3 presents the operation of the network after the grid reconnection process. The control system of B1 is switched from VF mode to PQ mode during this mode and B1 charges again as shown in fig. 6.7.

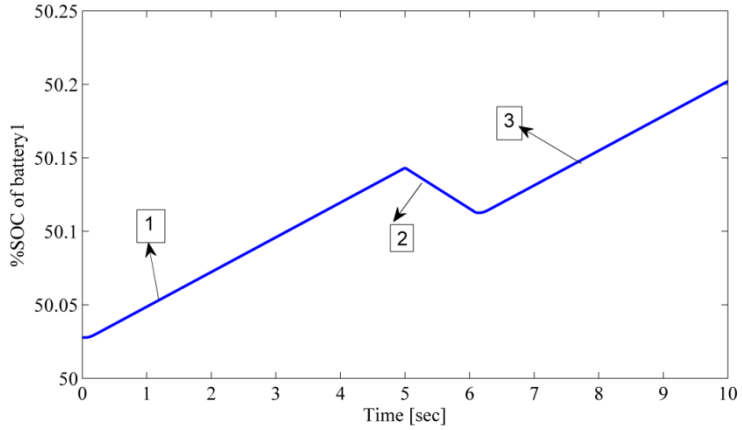

Fig. 6.7 Percentage SOC of battery1 for different control modes (Point 1: Grid connected mode, Point 2: islanded mode, Point 3: Reconnection mode).

If the distribution network is allowed to operate for longer time as shown in fig. 5.24 and fig. 5.38 in chapter 5, the island system loses its stability when B1 is fully discharged as shown in fig. 5.26 and fig. 5.30. The distribution system must be reconnected to the transmission grid in order to operate it in the controlled and the stable conditions in this regard. The reconnection detection signal in the case where SOC of the batteries was considered to be 50% is shown in fig. 6.8.

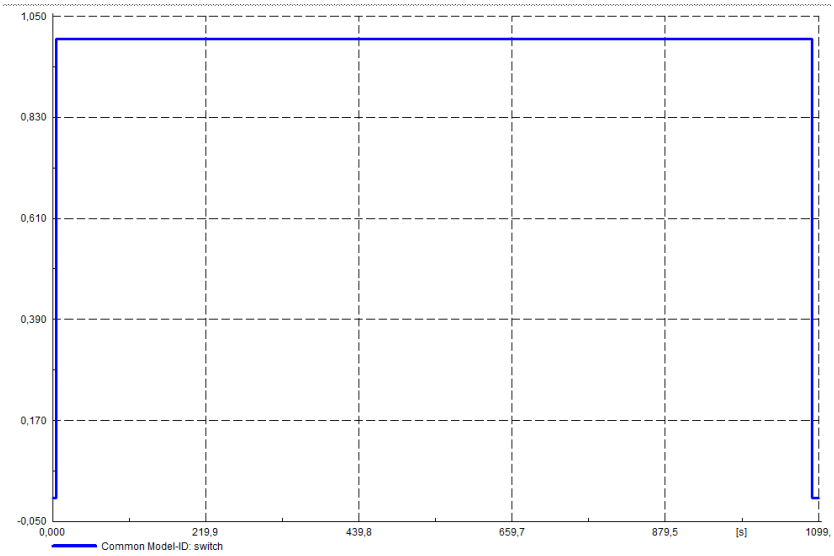

Fig. 6.8 Grid reconnection detection in this new case where reconnection is detected at 1090 s

Fig. 6.8 describes that grid reconnection has been detected at t=1090 s just before the time when B1 discharges completely (i.e. 1091 s). The SOC of the two batteries in this case of reconnection is shown in fig. 6.9. It can be seen in this figure that B1 changes its mode from islanding to the grid connection at t=1090

s. B1 charges in this mode. As the control system of B2 always operates in PV mode and does not switch from one mode to another so its SOC does not change during reconnection.

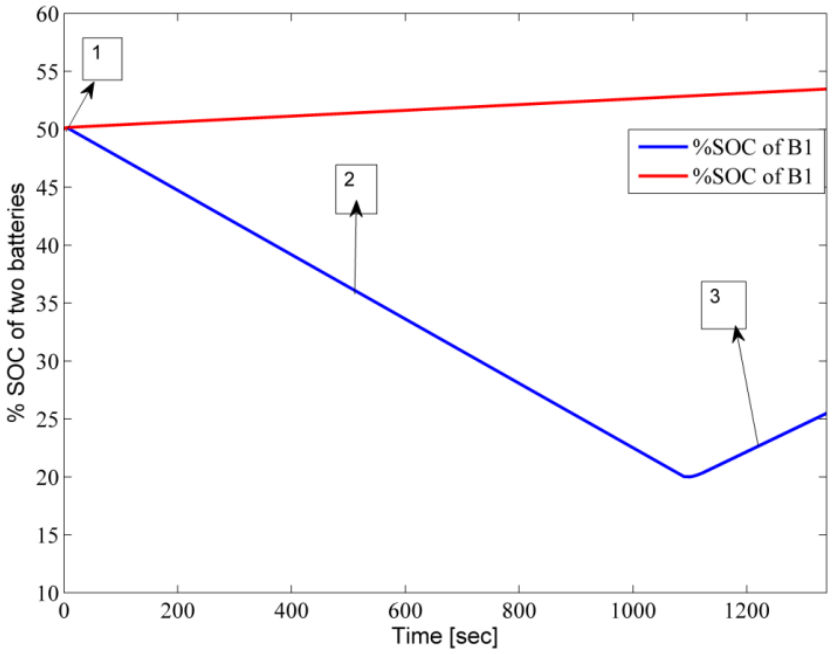

Fig. 6.9 Percentage SOC of battery1 and battery 2 for different control modes

6.5 Summary

The study about grid reconnection has been made in this chapter. The grid reconnection detection technique has been described with the help of the block diagram in section 6.2 of this chapter. Simulation results have been presented for the grid reconnection as long as the distribution system is synchronized with the transmission grid after islanding and also for the reconnection which is made after long time before the complete discharge of battery1

Chapter 7

Conclusions and Future work

7.1 Conclusions

Power quality is one the basic objectives of the modern power networks. The quality of the power system is disturbed if some of the electrical parameters such as voltage; frequency etc. deviates from the rated values.The intermittent and uncontrolled nature of renewable energy based DG units cause problems with the quality of the power. This quality related problems include disturbances in the voltage, oscillations in power flow through the lines etc. The disturbance in the voltage might cause disconnection of sensitive equipment and may lead to the huge economic losses due to damaged products.This dissertation has addressed various technical issues with the quality of the power in case of the large scale integration of renewable energy based Distributed Generation units into the transmission grid.

The intermittent and the uncontrolled nature of the power output produced by some of the DG units such as the WTGs and photovoltaics as in this dissertation causes problems with the network voltages and produces power oscillations in the entire network grid. The DGs can also have a transient effect on the voltage level such as in the case of sudden loss of the wind or solar irradiation which might cause occurrences of voltage sags in the network. The voltage sags are undesirable and might lead to the tripping of power generating units in the power networks.

Voltage unbalance is also one of PQ related problem. Voltage in power systems can be unbalanced due to the several reasons such as uneven distribution of the single phase loads, unbalanced faults etc. The network with the unbalanced voltages draw unbalance currents which create unequal heating in each of the phases and creates unbalance heating in cables and other parts of the network, which might reduce the life time of the cables and other components.

These PQ related problems have been introduced to the CIGRE LV distribution test system comprising WTG, PV units, energy storages, loads etc. and are compensated by using the different control strategies. This is done by developing appropriate controllers for the respective components of the CIGRE network. Initially different components of the CIGRE network have been modelled in DIgSILENT power factory software version 15.0. The STATCOM controllers for the PV applications have been developed. These controllers are responsible to control the AC and DC-link voltages and thereby control the power output of PV units. The control system of BESS-STATCOM has been developed for the battery application together with charge controlling capabilities. These controllers for BESS are also developed to charge the batteries at different charging rates (i.e. fast of slow charging of batteries). It has been concluded in this dissertation that these controllers are able to control the network voltages in case of variations in the wind speed and solar irradiation. The control system is also developed in order to control the reactive power of the CIGRE

network in order to improve the active power transfer capabilities through the transmission lines and improve the power factor of the DG units.The mitigation of voltage sags (i.e. balanced and unbalanced) and the compensation of the voltage unbalances have been verified in this dissertation. This is done by using the existing controllers in the CIGRE network.

A fault in the power system is an occurrence of an abnormal condition. Faults usually occur due to the lightning flash over, insulation failure, physical damage, short circuit to ground or short circuit in between live conductors. A short circuit fault is typically the most common fault in power systems. A short circuit fault carries huge amount of current compared to the normal operating current. The excessive amount of the current flowing through a circuit can generate a tremendous amount of heat which poses risks of fire, damage to the other equipment and potential electrical shocks to people. If a short circuit is not removed or a faulty portion is not quickly isolated from the healthy system, it will spread into healthy part of the network and may cause over loads and possibly damages to the transmission lines/cables, bus bars and other equipments. It is therefore, necessary to protect the power system against short circuits by using short circuit protection devices by ensuring proper coordination in order to avoid false tripping.

The significant penetration of DG units presents complexity in the protection of the power network due to bi-directional flow of the current and different short circuit power. The protection of the network with DGs in modern power network is a challenge for the protection engineers. Protection of the CIGRE network against symmetrical and unsymmetrical faults has been presented in this dissertation. This study is performed in such a way that it follows the economic criteria and ensures protection coordination. The protection of the network is mainly done by using fuses but under voltage relays are also used if fuses are not enough to protect in certain conditions.The magnitude of current during the fault depends on available sources. Transmission grids generally have higher short circuit power compared to small DG units. There is a significant difference in short circuit power when the distribution system is connected to the transmission grid and when it is islanded. If a protection system is designed to operate in grid connected mode, it will take longer time to clear the fault if the distribution system is islanded. This delay in the fault clearance is undesirable and causes problems not only with the loads but also with DG units. Designing protection system for islanded operation might cause unnecessary tripping of the protection devices in the normal operating conditions. In order to get rid of these problems, voltage based protection is used. One of the under voltage protection devices which is used in this thesis is an under voltage relay. An under voltage relay is used to sense the voltage in case of short circuit fault and sends trip signal to the corresponding circuit breaker which clear the fault within a specified time. The study about the over speed protection of the WTG in case of grid disconnection because of symmetric or unsymmetrical faults has been successfully carried out in this thesis. This is done by using mechanical brakes. The protection of the inverters for the PV and batteries applications has carried by using ultra-fast fuses. The protection of the solar PV structure in the case of islanding against over voltages has also been carried out here.

The CIGRE network enters into islanding if fault is cleared at the MV bus.The main problems associated with unintentional islanding are disturbances with the voltages and the frequency which can cause malfunction of the network equipment or create disturbances to the customers. In the past, utilities demanded to shut down the DG units once islanded was detected. The current trend in the power network is to operate an islanded portion of distribution network (i.e. MG) by controlling its voltage and frequency. The voltage and frequency in such conditions can be controlled by the availability of the active and the reactive powers in the local MG.

During islanding mode, if there is an imbalance between load and local generation, the MG frequency drifts from its nominal value. If the active power demand is higher than the active power production in the local island, the MG frequency decreases and vice versa. On the other if there is a deficit of the reactive power in the local island, the MG voltage decreases and vice versa. Therefore, the control system in the MG must be developed in such a way that it tackles issues related to the voltage and the frequency. Most of DG units of the CIGRE network except the WTG operate in PV/PQ mode in the grid connected mode whereas they operate in VF mode if the distribution system is islanded from the transmission grid. The switching of the control mode from the PV/PQ to VF mode is according to the islanding detection techniques. Many islanding detection techniques have been described in the literature but island is detected in this dissertation by using the voltage phase angle difference between the two systems (i.e. transmission and the distribution system). This technique has been validated in this thesis and it shows the correct detection of islanding in case of the transient conditions as well.

The technical issues in case of islanding such as the voltage and the frequency of the network have been controlled successfully in this thesis. The voltage and the frequency of the network in case of the sudden load changes and the sudden loss of the generating units have also been restored successfully here.

Although, the island operation of the distribution system increases the reliability of the power networks, however the reliability of the system in case of the grid connected system is more than in the islanded network. Hence, when the transmission grid is back to the normal operating condition, it is desirable to reconnect the distribution system back to the transmission grid. This is done by synchronizing voltage, frequency and phases of the two systems according to IEEE standard 1547 recommendations.The study about the grid reconnection has been carried out in this dissertation. It is concluded that the distribution system together with the DG units has been successfully reconnected once the two systems are synchronized with each other.

The main contributions of the thesis are listed below:

1. Modeling of the CIGRE low voltage network together with the control system for PV solar generating units based on the STATCOM principles. The purpose of the PV-STATCOM controller is to regulate AC and DC-link voltages in the distribution network.
2. A methodology to compensate the voltage and the power disturbances in the distribution network due to the uncontrolled and the intermittent nature of DGs.
3. A study about mitigation of symmetric voltage sags.
4. A study about mitigation of asymmetric voltage sags and voltage unbalances.
5. Development of protection system for the distribution network against symmetric and asymmetric faults.
6. A methodology to control the voltage of the CIGRE low voltage test network has been developed for islanded system.
7. A methodology to control the frequency of the CIGRE low voltage test network has been developed for the islanded system.
8. The methodology to control the voltage and the frequency of the islanded MG in case of load step changes and the sudden loss of the generating units.
9. A methodology to study about the reconnection detection
10. A study about the grid reconnection and synchronization of the two systems (i.e. Transmission and the distribution system)

10.2 Future work

Although many aspects of the distribution system with the large integration of the DG units have been covered by this dissertation, several other issues are interesting for future investigation. Some of the issues that are deemed interesting are listed as follows:

- The tuning of the controllers in this dissertation is done by the trial and error method. The pole-zero method or other stability analysis by using other techniques can be used to have accurate tuning of the controllers.
- The negative sequence current increases in the case of a single phase to ground fault. The study about the control of the negative sequence current in the CIGRE network in this dissertation is missing. The study about the control of the negative sequence current can be one of the future works.
- As the power output of all DG units exceptthe WTG in the CIGRE network is DC and needs to be transformed into AC. This is done by using VSCs. Since VSC is a power electronic device, it

drawsdistorted current throughout the network. This leads to the appearance of harmonics. The harmonics compensation in the CIGRE network needs to be studied in future.

- PV units in this dissertation are modelled by using DC current source model available in the DIgSILENT library. This is a simple model and does not account the detailsof the Maximum Power Point Tracking (MPPT) and temperature effects. The detailed model of PV units showing the MPPT and temperature effects can be modelled in the future.
- Protection in the islanded MG can be one of hot issue in the near future. The N-2 contingency (i.e. fault in the islanded MG) analysis needs to be investigated in the future. This study might include the protection in case of N-2, voltage and the frequency control in this case.
- The overall study presented in this thesis is only done on 0.4 kV distribution network but same investigations can be doneat the MV voltage networks.
- This study presented in this thesis is only simulation based;the results obtained by the simulations can be verified and validated by using Real Time Digital Simulator (RTDS) in future.
- The modeling and control set up of battery2 can be done in such a way that it can also support the Island MG when battery1 is fully discharged. This is one of the future work.

References

[1] Eurelectric (July 2003), "Efficiency in Electricity Generation", Available online at: http://www.google.dk/url?sa=t&rct=j&q=&esrc=s&source=web&cd=1&ved=0CCcQFjAA&url=http%3A2F%2Fwww.eurelectric.org%2FDownload%2FDownload.aspx%3FDocumentID%3D13549&ei=pvPoUu2cH-mGywOGxYDY.

[2] J. Casazza and F. Delea,"Understanding Electric Power Systems*:* An Overview of theTechnology and the Marketplace", New Jersey: IEEE Press, 2004.

[3] N. Jenkins, "Impact of dispersed generation on power systems", *Electra*, No. 199, pp. 6-13, Dec. 2001.

[4] A. Sannino, "Global power systems for sustainable development," in *IEEE General Meeting*, Denver, CO, Jun. 2004.

[5] P. Mahat, Z. Chen, B. Bak-Jensen, "Review of Islanding Detection methods for distributed generation", in proc. Int. Conf. on Electric Utility Deregulation and Restructuring and Power Technologies, Nanjing China, pp. 2743-2748, Apr. 2008.

[6] Hadjsaid, N; J. F. Carnard, F. Dumas, Dispersed Generation Impact on DistributionNetwork", IEEE Computer Applications in power 12, No.2, pp. 22-28, 1999.

[7] Renewable Energy Policy Network. (2010, Sept.).Renewables 2010 Global Status Report. [Online].Available:http://www.ren21.net/Portals/97/documents/GSR/REN21_GSR_2010_full_revised, 20th Sept2010, Pdf.

[8] International Energy Agency.(2010, July).Wind Energy 2009 Annual Report.[Online]. Available: http://www.ieawind.org/AnnualReports_PDF/2009/2009AR_92210.pdf.

[9] L. Willis and W. G. Scott. *Distributed Power Generation.* New York: Marcel Dekker, 2000.

[10] Eurostat, "Electricity generated from renewable sources," [Online]. Available: http://epp.eurostat.ec.europa.eu/tgm/table.do?tab=table&init=1&language=en&pcode=tsien050&plugin=1, May 2009 [9 June 2010].

[11] U.S. Energy Information Administration, "Total capacity of dispersed and distributed generators by technology type," [Online]. Available:http://www.eia.doe.gov/cneaf/electricity/epa/epat1p6c.html, Jan. 2010. [9 June 2010].

[12] The Institute of Energy and Technology, "Distributed generation," [Online]. Available:http://www.theiet.org/factfiles/energy/dist-gen.cfm, July 2008 [14 June 2010].

[13] P. Lund, "The Danish Cell Project - Part 1: Background and General Approach," in *Proc.* IEEEPES General Meeting, Tampa, USA, June 2007.

[14] Energinet.dk. (2009, Dec.).System Plan 2009.[Online]. Available: http://energinet.dk/EN/News/Documents/Systemplan2009summary.pdf.

[15] Energinet.dk. (Oct. 2007). System Plan 2007, [Online]. Available: http://energinet.dk/EN/News/Documents/Systemplan2007GB.pdf.

[16] Martin Clark, "Distributed generation markets in Europe expansion, investment and futureopportunities", Business Insights Ltd, March 2010.

[17] International Energy Association, "Distributed Generation in Liberalized Electricity Market," [Online]. Available: http://iea.org/textbase/nppdf/free/2000/distributed2002.pdf, 2002 [14 June 2010].

[18] Eto, J., Koomey, J., Lehman, B., en Martin, N., 2001. Scoping Study on Trends in the Economic Value of Electricity Reliability to the US Economy, LBLN-47911, Berkeley, p. 134.

[19] Mohit Singh, Surya Santoso, "Dynamic Models for Wind Turbines and Wind Power Plants", NREL (Oct. 2011), Austin, Texas.

[20] Bin Wu, Yungqiang Lang, NavidZargari, Samir Kauro, "Power conversion and control of wind energy systems", IEEE Press, Wiley, 2011, USA.

[21] Renewables (2013), "Global Status Report", available online at http://www.ren21.net/.

[22] F. Blaabjerg and Z. Chen, Power Electronics for Modern Wind Turbines, Morgan & Claypool Publishers, 2006.

[23] T. Ackermann, *Wind Power in Power System*, Wiley, Ltd, 2005.

[24] Selam T. Chernet, "Evaluation of Inverter Reconnection for Large Solar Parks", Master thesis, Chalmers University of Technology, Goteborg, Sweden, 2010.

[25] EPIA, "Global Market outlook of photovoltaics until 2014", May 2010. http://www.epia.org/fileadmin/EPIA_docs/public/Global_Market_outlook_for_photovoltaics_until_2014, pdf.

[26] Technical information about IGBT-Module FZ1800R17HP4_B29, material no. 32559, 2010.

[27] Standards Australia (2005), Installation of Photovoltaic (PV) Arrays, AS/NZS 5033.

[28] Transformer-less photovoltaic inverters online available:
http://azte.technologypublisher.com/technology/12310.

[29] Electricity Storage Association. (2010). [Online]. Available:
http://www.electricitystorage.org/ESA/technologies.

[30] K.C. Divya and Jacob Østergaard, "Battery energy storage technology for power systems—An overview," Electric Power Systems Research, vol. 79, no. 4, pp. 511-520, Apr. 2009.

[31] C.D. Parker, "Lead–acid battery energy-storage systems for electricity supply networks," Journal of Power Sources, vol.100, no. 1-2, pp. 18-28, Nov. 2001.

[32] Low Wen Yao, Aziz, J.A, "Modeling of Lithium Ion Battery with Nonlinear Transfer Resistance", IEEE applied power electronics Colloquium (IAPEC); 2011.

[33] Farivar M, Clarkey CR, Low SH, Chandy KM,"Inverter VAR control for distribution systems with renewables", Department ofElectrical Engineering, California Institute of Technology Southern California Edison, Rosemead, CA, USA, Department ofComputer Science, California Institute of Technology.

[34] Khadem SK, Basu M, Conlon MF,"Power quality in grid connected renewable energy systems: role of custom power devices", in *Proc.* of International conference on Renewable Energies and Custom Power Devices, ICREPQ'10, Spain: Granada; pp. 23-25, 2010.

[35] By Edward J. Coster, Johanna M. A. Myrzik, Bas Kruimer, W. L. Kling, "Integration Issues of Distributed Generation in Distribution Grids", Proceedings of the IEEE | Vol. 99, No.1, Jan. 2011.

[36] IEEE Recommended Practice for Monitoring Electric Power Quality, IEEE Standard 1159-1995, IEEE, 1995.

[37] A. von Jouanne and B. B. Banerjee, "Voltage unbalance: Power quality issues, related standards and mitigation techniques," Electric Power Research Institute, Palo Alto, CA, EPRI Final Rep, 2000.

[38] Aneel, "Contribution for the normalization of the quality of electric power-harmonic and unbalances in the electric networks," PhD Thesis, Federal University of Uberlandia, 2000.

[39] A. von Jouanne and B. Banerjee, "Assessment of voltage unbalance," IEEE Trans. Power Deliv., Vol. 16, No. 4, pp. 782-790, 2001.

[40] F. C. Pereira, J. C. de Oliveira, O. C. N. Souto, A. L.A. Vilaca and P. F. Ribeiro, "An analysis of costs related to the loss of power quality," in proc. on Harmonics and Power Quality, Vol. 2, pp. 14-16, Oct. 1998.

[41] J Manson, R Targosz, "European Power Quality Survey Report", pp. 3-15, 2008.

[42] G. Mustafa Bhutto, B. Bak-Jensen, CL-Bak, JR Pillai, "Protection of Low Voltage CIGRE distribution Network", Int. Jour. Of Smart Grids and Renewable Energy (SGRE), 2013.

[43] Tom Loix, Student Member, IEEE, Thomas Wijnhoven and Geert Deconinck, Senior Member, IEEE, "Protection of Microgrids with a High Penetration of Inverter-Coupled Energy Sources", IEEE PES/CIGRE SYMPOSIUM, CANADA, JUL. 2009

[44] Ahmed Razani Haron, Azah Mohammad, Hussain Sharif, "A review on protection schemes and coordination techniques in Microgrids system", Jour. of Applied Sciences, pp. 101-112, 2012.

[45] Dae-Geun Jin, Jong-Chan Choi, Dong-Jun Won,*, Hak-Ju Lee, Woo-KyuChae, Jung-Sung Park, **"**A Practical Protection Coordination Strategy Applied to Secondary and Facility Microgrids", Jour. on Energies, pp. 3248-3265, 2012**.**

[46] IEEE Standard for Interconnecting Distributed Resources into Electric Power Systems,IEEE Standard 1547TM, June 2003.

[47] Photovoltaic (PV) systems - Characteristics of the utility interface, IEC 61727 Standard,December 2004.

[48] Benchmark Systems for Network Integration of Renewable Energy Resources, version 7, Mar., 2011, CIGRE Task force C6.04.02.

[49] A. D. Hansen, F. Iov, P. Sørensen, N. Cutululis, C. Jauch, F. Blaabjerg. Dynamic wind turbine models in power system simulation tool DIgSILENT. Risø DTU, Denmark, Risø-R-1400(EN); 2007.

[50] S. M. Muyeen, M. Hasan Ali, R. Takahashi, T. Murata, J. Tamura, Y. Tomaki, A. Sakahara, E. Sasano,"Comparative study on transient stability analysis of wind turbine generator system using different drive train models. IET Renewable Power Generation", 2007; vol; 1; 2: 131-141.

[51] S. Santoso, H. T. Le. Fundamental time-domain wind turbine models for wind power studies. Renewable Energy; 2007: vol; 32; 14: 2436-2452.

[52] Jetstream III Series – Grid Connected Turbine – IEC Class 1 available at http://www.sabletech.ie/Downloads/wind%20turbines.pdf

[53] Leif Kristensen, Ole Rathmann, Sven ole Hnasen, "Extreme winds in Denmark",Risø National Laboratory, 2009.

[54] PV modelling by using DC current source, DIgSILENT Power Factory, Version 14.0 demo, DIgSILENT GmbH; Germany: Gomaringen.

[55] Technical reference for PWM inverter published by DIgSILENT GmbH,, Germany.

[56] Jan Svensson, "Grid-connected voltage source converter, control principle and wind energy applications", PhD dissertation, March1998, Chalmers University of Technology, Gothenburg, Sweden.

[57] Varma, R.k, Das, B.Axente, I. Vanderheide, T,"Optimal 24-hr utilization of a PV solar system as STATCOM (PV-STATCOM) in a distribution network", Power and Energy Society General Meeting; 2011: 1-8.

[58] Massimo Bongiorno,"Control of voltage source converters for voltage dip mitigations for shunt and series configurations",PhD dissertation, 2004, Chalmers University of Technology; Sweden: Gothenburg.

[59] Du, C, "The Control of VSC-HVDC and Its Use for Large Industrial Power System", PhD dissertation, Chalmers University of Technology; Sweden: Gothenburg, 2007.

[60] D. W. Dennis, V. S. Battaglia, and A. Belanger, "Electrochemical modelling of lithium polymer batteries", J. Power Sources, vol. 110, no. 2, pp. 310-320, 2002.

[61] P. M. Gomadam, J.W. Weidner, R. A. Dougal, and R. E. White, "Mathematical modeling of lithium-ion and nickel battery systems", Journal of Power Sources, vol. 110, no. 2, pp. 267-284, Aug. 2002.

[62] R. C. Kroeze and P. T. Krein, "Electrical battery model for use in dynamic electric vehicle simulations", Proc. of IEEE Power Electronics Specialists Conference, Rhodes, Greece, pp. 1336-1342, June 2008.

[63] Z. M. Salameh, M.A. Casacca, and W.A. Lynch, "A mathematical model for lead-acid batteries", IEEE Trans. on Energy Conversion, vol. 7, no. 1, pp. 93 - 98 Mar. 1992.

[64] K. Yoon-Ho and H. Hoi-Doo, "Design of interface circuits with electrical battery models", IEEE Trans. on Industrial Electronics,vol. 44, no.1, pp. 81 – 86, Feb. 1997.

[65] D. Linden, "Handbook of Batteries and Fuel Cells", McGraw-Hill, New York, 1984.

[66]M. Chen and G. A. Rincon-Mora, "Accurate electrical battery model capable of predicting runtime and I-V performance", IEEE Trans. Energy Conversion, vol. 21, no.2, pp. 504-511, June 2006.

[67] Tremblay, O. Dessaint, L.-A. Dekkiche, A.-I,"A Generic Battery Model for the Dynamic Simulation of Hybrid Electric Vehicles", Vehicle Power and Propulsion Conference, VPPC, pp. 284-289, 2007.

[68] Data sheet of Rechargeable Lithium-ion battery Li-Ion_Saft_VL_37570.pdf available on www.saftbatteries.com.

[69] Technical reference for DC voltage source in DIgSILENT.

[70] Technical reference for the general load model in DIgSILENT.

[71] Technical reference for the measurement file in DIgSILENT.

[72] Arindam Ghosh and GeradLedwich, "Power Quality Enhancement using Custom Power Devices", Kluwer's Power Electronics and Power Systems series, ISBN 978-1-4020-7180-5.

[73] Bousseau P, Gautier E, Garzulino I, Juston P, Belhomme R, "Grid impact of different technologies of wind turbine generator systems", in Proc. on EWEC03, June 2003

[74] Dittrich A, "Grid Voltage Fault Proof Doubly Fed Induction Generator System", EPE 03, Toulouse 2003

[75] Pierre Rousseau, Eric Gautier, Irina Garzulino, Philippe Juston, ReginеBelhormme. "Grid impact of different technologies of wind turbine generator systems," project: DISPOWER, ENK5-CT-2001-00522.

[76] George G. Karady, SaurabhSaksena, and Bauzhuang Shi, "Effects ofvoltage sags on house hold loads," IEEE Power Engineering Society GeneralMeeting, Vol. 3, pp. 2456–2461, 2005.

[77] Rekommandation 16, Spændingskvalitet I lavspændingsnet (voltage quality in low voltage networks), 4. Udgave, Aug. 2011.

[78] C. Hochgraf, R.H. Lasseter, "STATCOM control for operation with unbalanced voltages," IEEE Trans. on power deliv, Vol. 13, 1998, pp. 538-544.

[79] M. Mc Granaghan, D. R. Mueller, and M. Samotyj, "Voltage sag in industrial systems," IEEE Trans.Ind. Appl., vol. 29, 1993, pp. 397–403.

[80] V.J. Gosbell, S. Perera and V. Smith, "Voltage unbalance," Technical power quality center, university of wollongong, Technical note No.6, 2002.

[81] C.-Y. Lee, "Effects of unbalanced voltage on the operation performance of a three-phase induction motor," IEEE Trans. on En. Conv., vol. 14, no. 2, 1999, pp. 202–208.

[82] A. I. Maswood, G. Joos, P. D. Ziogas, and J. F. Lindsey, "Problems and solutions associated with the operation of phase-controlled rectifiers under unbalanced input voltage conditions," IEEE Trans. on Ind.Applications, vol. 27, 1991, pp. 765–772.

[83] M. T. Aung, and J. V. Milanovic, "The influence of Transformer winding connections on the propagation of voltage sags,"IEEE Trans. Power Deliv., Vol. 21, 2006.

[84] D. Das, "Electrical Power System," New Delhi, India, New age international (P) Publisher, ISBN (13): 978-81-224-2515-4, 2006.

[85] W. R. Mendes, M. I. Samesima, and F. A. Moura, "Influence of power transformer winding connections on the propagation of voltage sags through electricsystem," in Proc. IEEE EEM, 2008, pp. 1-6.

[86] Vector group of transformer, electrical notes & articles, online available at http://electricalnotes.wordpress.com/2012/05/23/vector-group-of-transformer.

[87] W. H. Kersting, "Distribution system modeling and analysis", New Mexico, Mexico, CRC press, ISBN 0-8493-0812-7, 2002.

[88] Remus Teodorescu, Marco Liserre, and Pedro Rodríguez, "Grid synchronization in three phase power converters," in Grid Converters for Photovoltaic and Wind Power Systems, 1st ed. West Sussex, United Kingdom: John Wily… Sons Ltd, 2011, pp. 169-181.

[89] Merlin Gerin, Square D and Telemecanique, "Selection of fuses for the protection of transformers," Schneider Electric, 2004

[90] Schneider Electric Industries SAS, "Safe and reliable Photovoltaic energy generation", EDCED112005EN, Rueil-Malmaison Cedex- France, 2012.

[91] Arthur Wright, P. Gordon Newbery Electric fuses 3rd edition, Institution of Electrical Engineers (IET), 2004, ISBN 0-86341-379-X, pp.2-10

[92] Les Hewitson, Mark Brown, Ben Ramesh and Steve Mackay, "Practical Power SystemsProtection**",** ISBN 0 7506 6397 9, Copyright © 2004.

[93] Juan M. Gers and Edward J. Holmes, "Protection of Electricity Networks", 3rd Edition, IET Power and Energy series 65.

[94] The technical regulations 3.2.1 for electricity generation facilities with a rated current of 16 A per phase or lower, Available online on http://www.energinet.dk.

[95] IEEE. IEEE 1547.2-2008 standards for Interconnecting Distributed Resources with Electric Power Systems, 2008.

[96] IEEE Std. 141-1993 Red Book – Electric Power Distribution for Industrial Plants.

[97] Kroposki, B., "Optimization of Distributed and Renewable Energy Penetration in Electric Power Distribution Systems", PhD dissertation, 2008, Golden, Colorado.

[98] Wind turbine safety, Danish Wind Industry Association, on available at http://ele.aut.ac.ir/~wind/en/tour/wtrb/safety.htm.

[99] Horizon Gitano-Briggs (2010). Small wind turbine power controllers, Wind Power, S M Muyeen (Ed.), ISBN: 978-953-7619-81-7, In Tech, Available from http://www.intechopen.com/books/wind-power/small-wind-turbinepower-controllers.

[100] Mitalkumar Kanabar and SrikrishnaKhaparde (2011). Rotor Speed Stability Analysis of a Constant Speed Wind Turbine Generator, Wind Turbines, Dr. Ibrahim Al-Bahadly (Ed.), ISBN: 978-953-307-221-0, InTech Available from http://www.intechopen.com/books/wind-turbines/rotor-speed-stability-analysis-of-a-constantspeed-wind-turbine-generator.

[101]K. Rajambal, B. Umamaheswari, C. Chellamuthu, “Electrical braking of large wind turbines”, Renewable Energy 30, 2005, pp: 2235–2245. Available online at www.sciencedirect.com.

[102] Niall McMahon, “On Electrodynamic Braking for Small Wind Turbines”, Centre for Renewable Energy at Dundalk Institute of Technology, Apr., 2013.

[103] Bussmann, “High speed fuses, Applications Guide”, Available online on http://www.bussmann.com.

[104] Medium voltage products, VD4 medium voltage vacuum circuit breakers (12-36 kV). Available online at: www.abb.com.

[105] Joe Mooney, P.E., Jackie Peer, “Application guidelines for ground fault protection”, Schweitzer Engineering Laboratories, Inc.

[106] John Tengdin, Ron Westfall, Kevin Stephan, “High Impedance Fault Detection Technology”, Report of PSRC Working Group D15.

[107] Mohan, N., T.M. Underland, and W.P. Robbins, eds. Power Electronics-converter, design and application.2nd edition, 1995, John Wiley.

[108] Pollanen, R., "Converter-flux-based current control of voltage source PWM rectifier analysis and implementation", PhD dissertation, Acta University, Lappeenrantaensis, Finland, Dec., 2003.

[109] Technical information about IGBT-Module FZ1800R17HP4_B29, material no. 32559, 2010

[110] VDE 0126:1999 Automatic disconnecting facility for photovoltaic installations with a rated output smaller than 4.6 kVA and a single-phase parallel feed by means of an inverter into the public low-voltage mains.

[111] G.M Bhutto, B. Bak-Jensen, P. Mahat, Carlo Cecati, “Mitigation of Unbalanced Voltage Sags and Voltage Unbalance in CIGRE Low Voltage Distribution Network”, Energy and Power Engineering,Vol.5, 2013, pp.551-559.

[112] Technical regulations 3.2.1 for electricity generation facilities with a rated current of 16 A per phase or lower.Online available at enrginet.dk.

[113] R. Bründlinger, Benoît Bletterie, “Unintentional islanding in distribution grids with a high penetration of inverter-based DG: Probability for islanding and protection methods”, DISPOWER technical report, 2001.

[114] Justin Au-Yeung, Greet M.A. Vanalme, Johanna M.A. Myrzik, PanagiotisKaraliolios, Martijn Bongaerts, Jan Bozelie, and Wil L. Kling, “Development of a Voltage and Frequency Control Strategy for an Autonomous LV Network with Distributed Generators,” Proc. Of Universities Power Engineering Conf. (UPEC), pp. 1-5, 2009.

[115] S. Conti, A.M. Greco, N. Messina, U. Vagliasindi, “Generators Control Systems in Intentionally Islanded MV Micro grids”, SPEEDAM 2008, International Symposium on Power Electronics, Electrical Drives, Automation and Motion.

[116] M. Ropp, K. Aaker, J. Haigh, and N. Sabhah, “Using Power Line Carrier Communications to Prevent Islanding”, in Proc. 28th IEEE Photovoltaic Specialist Conference, 2000, pp.1675-1678.

[117] W. Xu, G. Zhang, C. Li, W. Wang, G. Wang, and J. Kliber, "A power line signaling based technique for anti-islanding protection of distributed generators—part i: scheme and analysis," IEEE Tran. Power Del., vol. 22, no. 3, pp. 1758-1766, July 2007.

[118] G. Wang, J. Kliber, G. Zhang, W. Xu, B. Howell, and T. Palladino, "A power line signaling based technique for anti-islanding protection of distributed generators—part ii: field test results", IEEE Tran. Power Del., vol. 22, no. 3, pp. 1767-1772, July 2007.

[119] O' Kane, P. and Fox, B., "Loss of mains detection for embedded generation by system impedance monitoring", IEE 6th International conference on Developments in Power System Protection, pp. 95-98, March 1997.

[120] Usta, O., Redfern, M.A., Barrett, J.I., "Protection of dispersed storage and generation units against islanding", Proceedings. of 7th Mediterranean Electrotechnical Conference, April 1994 pp. 976 -979.

[121] C.M. Affonso, W. Freitas, W. Xu, L.C.P. da Silva, "Performance of ROCOF relays for embedded generation applications", IEE Proceedings - Generation Transmission and Distribution, 2005.

[122] X. Ding*, P. A. Crossley* and D. J. Morrow*, "Islanding Detection for Distributed Generation", Journal of Electrical Engineering & Technology, Vol. 2, No. 1, pp. 19-28, 2007.

[123] Salman, S.K., King, D.J., and Weller, G.: "New loss of mains detection algorithm for embedded generation using rate of change of voltage and changes in power factors", Seventh IEE Int. Conf. On Developments in Power System Protection, 2001, pp.82-85.

[124] Warin, J.W., "Loss of Mains Protections", ERA Conference on Circuit Protection for Industrial and Commercial Installations, London, 1990.

[125] COOPER, C.B., "Standby generation problems and prospective gains from parallel running", International power system protection conference, Singapore, 1989.

[126] M. Bollen, J. Zhong, O. Samuelsson, and J. Björnstedt, "Performance indicators for micro grids during grid-connected and island operation," in Proc. IEEE Bucharest Power Tech Conf., 2009.

[127] IEEE Standard for Interconnecting Distributed Resources into Electric Power Systems, IEEE Standard 1547TM, June 2003.

[128] Pukar Mahat, "The control and operation of islanded distribution network", PhD dissertation, 2010, department of Energy Technology, Aalborg University, Denmark.

[129] Inverse current characteristics of low voltage fuses according to VDE0636/IEC60269-2 standards.

List of Publications

Following is the list of the publications which are also attached in appendix C:

Paper 1: Ghullam Mustafa, Birgitte Bak-Jensen, Pukar Mahat, "Modeling of the CIGRE Low Voltage Test Distribution Network and the Development of Appropriate Controllers", International Journal of Smart Grids and Clean Energy (SGCE), Vol. 2 No. 2, pp. 184-192, 2013.

Paper 2: Ghullam Mustafa, Birgitte Bak-Jensen, Pukar Mahat, and Ribeiro P. F,"Mitigation of voltage sags in CIGRE Low Voltage Distribution Network" Proceedings of the 5th IEEE PES Asia-Pacific Power and Energy Engineering Conference, APPEEC 2013. IEEE Press, 2013.

Paper 3: Ghullam Mustafa, Birgitte Bak-Jensen, Pukar Mahat, Cecati Carlo, "Mitigation of Unbalanced Voltage Sags and Voltage Unbalance in CIGRE Low Voltage Distribution Network", Journal of Energy and Power Engineering (EPE), Vol. 5, pp. 551-559, 2013.

Paper 4: Ghullam Mustafa, Birgitte Bak-Jensen, Bak Claus Leth, Pillai, Jayakrishnan Radhakrishna, "Protection of Low Voltage CIGRE Distribution Network", Journal of Smart Grid and Renewable Energy, (SGRE)Vol. 4, No. 9, pp. 489-500,2013.

Appendix A

Table A1. Data about the different cables used CIGRE network

S: No	Node from	Node to	Type	Cross-section mm^2	R_{ph} /km Ω	X_{ph} /km Ω	R_o /km Ω	X_o /km Ω	L m	Installation
1	R1	R2	NA2XY	240	0.163	0.136	0.490	0.471	35	UG 3-ph
2	R2	R3	NA2XY	240	0.163	0.136	0.490	0.471	35	UG 3-ph
3	R3	R4	NA2XY	240	0.163	0.136	0.490	0.471	35	UG 3-ph
4	R4	R5	NA2XY	240	0.163	0.136	0.490	0.471	35	UG 3-ph
5	R5	R6	NA2XY	240	0.163	0.136	0.490	0.471	35	UG 3-ph
6	R6	R7	NA2XY	240	0.163	0.136	0.490	0.471	35	UG 3-ph
7	R7	R8	NA2XY	240	0.163	0.136	0.490	0.471	35	UG 3-ph
8	R8	R9	NA2XY	240	0.163	0.136	0.490	0.471	35	UG 3-ph
9	R9	R10	NA2XY	240	0.163	0.136	0.490	0.471	35	UG 3-ph
10	R3	R11	NA2XY	25	1.541	0.206	2.334	1.454	30	UG 3-ph
11	R4	RE	NA2XY	150	0.266	0.151	0.733	0.570	35	UG 3-ph
12	R6	RD	NA2XY	70	0.569	0.174	1.285	0.865	30	UG 3-ph
13	R10	RC	NA2XY	35	1.111	0.195	1.926	1.265	30	UG 3-ph
14	RE	R19	NA2XY	150	0.266	0.151	0.733	0.570	30	UG 3-ph
15	R8	RA	NA2XY	25	1.541	0.206	2.334	1.454	30	UG 3-ph
16	R9	R17	NA2XY	25	1.541	0.206	2.334	1.454	30	UG 3-ph
17	R10	RB	NA2XY	25	1.541	0.206	2.334	1.454	30	UG 3-ph

Table A2. Ratings of the inverters used in the network

Name of the inverter	Apparent power, S (kVA)	VDC (kV)	VAC (kV)
VSC1	35	0.714	0.4
VSC2	25	0.781	0.4
VSC3	18	1	0.4
VSC4	24	1	0.4

Table A3. Squirrel cage induction generator data

Parameter	Value
Type of Generator	Asynchronous
Rated Electrical Power [kW]	5.5
Rated Voltage [kV]	0.4
Power factor	0.91
Connection type	Dy
Efficiency at normal operation	94.815
Number of poles pairs	1
Stator resistance, [p.u.]	0.01
Stator reactance, [p.u.]	0.01
Rotor Resistance , [p.u.]	0.07
Rotor reactance, [p.u.]	0.11
Mag. Resistance, [p.u.]	0.074
Mag. Reactance, [p.u.]	0.122
Inertia Time constant [sec]	0.515

Table A4. Specifications of Li-ion battery for single cell [68]

Parameter	Value
Capacity	7 Ah
Nominal voltage	3.7 V
Maximum voltage	4.2 V
Minimum voltage	2.5 V

Table A5. Parameters of battery model

Parameter	Value
Initial Ampere-hour, Ci (Ah)	21
Battery Ampere-hour, Cb (Ah)	42
Series resistance, Rseries (ohms)	0.22
Transient resistance, Rtransient (ohms)	0.001
Transient Time constant, Ttransient (sec)	0.001
Battery SOC lower limit in percentage	20
Battery SOC upper limit in percentage	95

APPENDIX B

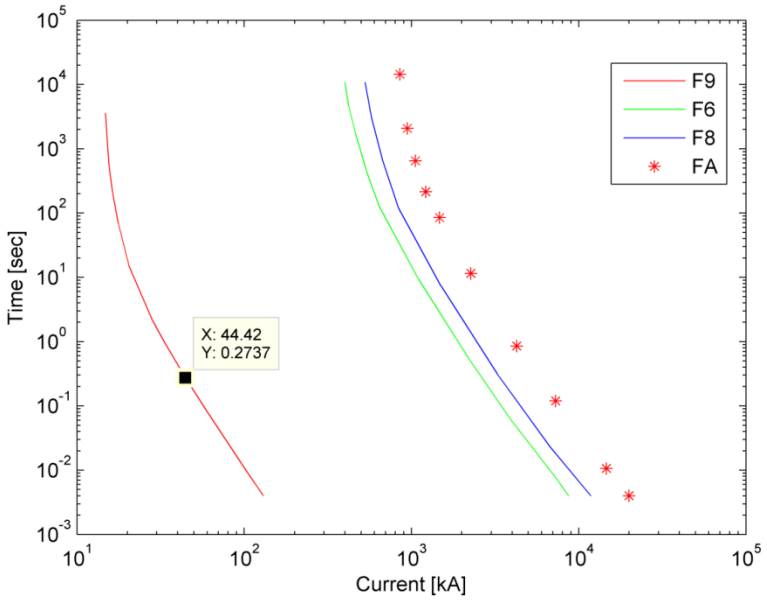

Fig. B1 Inverse current characteristics of some of the fuses used in CIGRE network [129]

Appendix C

International Journal of Smart Grid and Clean Energy

Modeling of the CIGRE Low Voltage Test Distribution Network and the Development of Appropriate Controllers

Ghullam Mustafa Bhutto[a,b]*, Birgitte Bak-Jensen[a], Pukar Mahat[a]

[a] *Department of Energy Technology, Aalborg University,* Pontoppidanstræde *101, Aalborg 9220, Denmark and*
[b] *Quaid-E Awam University of Engg. Sciences & Technology, Nawabshah 67450, Pakistan*

Abstract

The fluctuating nature of some of the Distributed Generation (DG) sources can cause power quality related problems like power frequency oscillations, voltage fluctuations etc. In future, the DG penetration is expected to increase and hence this requires some control actions to deal with the power quality issues. The main focus of this paper is on development of controllers for a distribution system with different DG's and especially development of a Photovoltaic (PV) controller using a Static Compensator (STATCOM) controller and on modeling of a Battery Storage System (BSS) also based on a STATCOM controller. The control system is tested in the distribution test network set up by CIGRE. The new approach of the PV controller is done in such a way that it can control AC and DC voltage of the PV converter during dynamic conditions. The battery controller is also developed in such a way that it can control its charge/discharge rate and also the reactive power flow through the lines in order to improve the power factor. Simulation results shows that the controllers are able achieve a good power quality in the test grid.

Keywords: Wind turbine generator, photovoltaic, voltage source converter, static compensator, battery energy storage system, energy storage equipped STATCOM, state of charge.

1. Introduction

DG technology and especially renewable energy sources have played a vital role in the modern power industry due to environmental and cost benefits. The important benefits of renewable based DGs are reduced CO_2 emission, reduced operational cost as almost no fuel is used for their operation and less transmission and distribution losses [1]- [3].

The intermittent and uncontrolled nature of the renewable energy sources cause problems with the quality of the power. This quality related problems include disturbances in the voltage, oscillations in power flow through the lines etc. The disturbance in the voltage can cause the disconnection of the sensitive equipment and may lead to huge economical loss due to the damaged products. Most of DGs such as Wind power, Photovoltaic etc. employ VSCs for their operation. The inverters are very sensitive to voltage disturbances. A disturbance in the voltage can cause disconnection of the inverters from the grid that leads to the loss of energy. Due to this reason the role of Custom Power Controllers (i.e. the power electronics based controllers used in distribution network) is increasing day by day. Some of the issues concerning DG have been proposed in [4]-[6].

The main focus of this paper is on development of a PV controller by using a STATCOM controller and on modeling of Battery Storage System (BSS) based on STATCOM controller. The introduction of the LV distribution network will be presented in the end of this section, the modeling of wind turbine generators (WTG) which are attached to the LV network will be given in section 2, and modeling of PV solar systems and battery storages including its control set up will be presented in sections 3 and 4,

* Manuscript received July 20, 2012; revised August 22, 2012.
Corresponding author. Tel.: +45-9940-9715; *E-mail address*: gmu@et.aau.dk, gmustafabhutto@yahoo.com

respectively. The simulation results and finally the conclusion of the paper will be presented in sections 5 and 6, respectively.

As mentioned, a test distribution network set up by CIGRE comprising of WTG and PV solar generation units, as well as energy storages and unbalanced loads has been chosen for the study. The single line diagram of this distribution system is shown in Fig. 1.

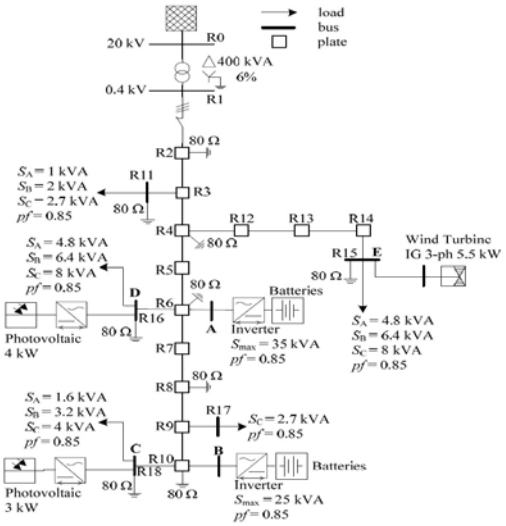

Fig.1. CIGRE distribution system test network [7]

In this network there are two PV solar generation units of 3kW and 4kW connected at bus C and D respectively. There is one fixed-pitch fixed speed wind turbine generator of 5.5 kW connected at bus E. The WTG is operated close to unity power factor with the use of a shunt capacitor. There are two batteries connected at bus A and at bus B. The unbalanced loads are aggregated at the 0.4 kV voltage levels and are connected at bus C, bus D, bus E, bus 11 and bus R17. The detailed data concerning bus bars, cables/lines and loads is given in [7].DIgSILENT Power factory 14.0 has been used to model the system. The standard built-in models available in the DIgSILENT library for different electrical components have been used and new models are developed for the controllers.

2. Modeling of Wind Turbine Generator

During implementation of the wind turbine model in DIgSILENT, different built-in models are used for the wind turbine components, e.g. generator and capacitor. The procedures of modeling the WTG are available in various literatures [8]-[10]. The WTG is modeled according to [11] as a fixed pitch and fixed speed wind turbine in this case.

A simplified block diagram of WT system comprising a measurement file 'ElmFile' for the stochastic wind speed is shown in Fig. 2 in DIgSILENT. The turbine model uses the stochastic wind speed as an input and produces the output signal 'Pwind' (i.e. Power available in the wind). It is the input of the shaft model which generates aerodynamic torque in the shaft and thereby producing P_{WT} (i.e. power from wind turbine to generator or the mechanical power)

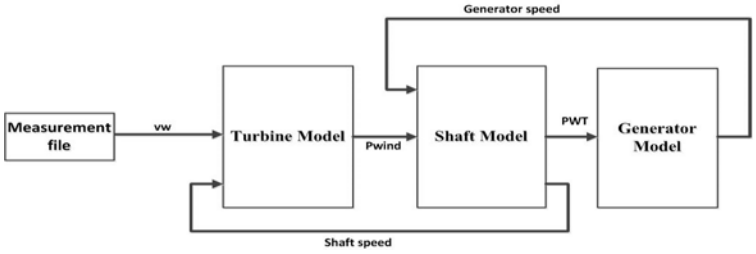

Fig.2. A simplified block of wind turbine system

3. Modeling of PV Generator System

The PV solar units used in this network are operated as STATCOMs and thereby named PV-STATCOM. The controller of the PV-STATCOM is used to regulate the voltage of the distribution network. This kind of controller is being developed in the university lab of Sarnia, Canada for a 10 kW PV system [12]. As the power output of the PV is current dependent, the solar cell can be modelled as a dc-current source [13].As the power output of the PV cell is DC, a VSC is used to convert DC power into AC power. The built-in model of a PWM AC/DC converter is used for the VSC.

A cascade controller is used for control of the VSC. It is comprised of an outer controller and an inner controller [14]. The selection of the outer controllers depends on the application. Here STATCOM controllers for the PV applications are used for the voltage regulation. They comprise of two outer controllers (i.e. AC and DC voltage controllers).The outer controllers are basically PI controllers that are used to eliminate errors [15]. They produce the reference d and q currents for the inner current controllers by comparing actual and reference signals. The inner controllers are the controllers which receives the current reference values from the outer controllers. In general, they should be very fast as compared to the outer controllers in order to achieve system stability. The procedure of modeling the control system for the PV-STATCOM in DIgSILENT is described with the help of a block diagram as shown in Fig. 3 [16].

The STATCOM controller is used to control the dc-link voltage as well as the voltage across the point of common coupling (i.e. AC bus of the corresponding VSC). The measured AC and DC voltages are sent to the voltage controllers (i.e. AC voltage controller and DC voltage controller) that are represented by the voltage controller block in Fig. 3. Both controllers are acting as outer controllers which produce d and q currents references for the inner current controllers.

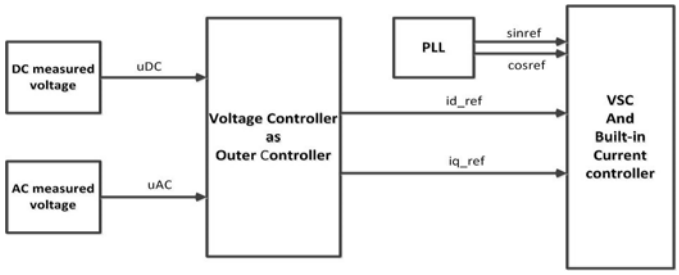

Fig.3. The block diagram of the STATCOM controller for PV solar system [16]

The current controllers (i.e. one for id_ref and other for iq_ref coming from the voltage controller) are built-in on the VSC. The three phase currents are measured from the grid and are transformed from 3-phase to $\alpha\beta$ and from $\alpha\beta$ to dq coordinates by using a Phase Lock Loop (PLL) transformation angle [11]. With chosen PLL [17], the d-component of current vector becomes active current component (d-current) and q-component becomes reactive current component (q-current). The actual currents i_{dq} and the reference currents i_{dq}^{*} are compared and the differences of the currents (error) are sent to the respective PI controllers of the built-in current controllers. The output of the PI controller is reference voltage $u^{*}(t)$. This reference is sent to the PWM block which sets the switching pattern for the transistors used in the converter and decides its duty cycle.

4. Modeling of Battery Storage System

The Battery Energy Storage System (BESS) is incorporated with STATCOM named as BESS-STATCOM or E-STATCOM, which has both active and reactive power controllability. The BESS-STATCOM is modeled using a Thevenin equivalent representation of the Lithium ion battery and is shown in Fig. 4 [18] and [19]. The specification of a single cell of lithium ion battery is taken from [20]. The built-in model of an infinite DC voltage source is used for modeling of the BESS in DIgSILENT power factory 14.0 [21].

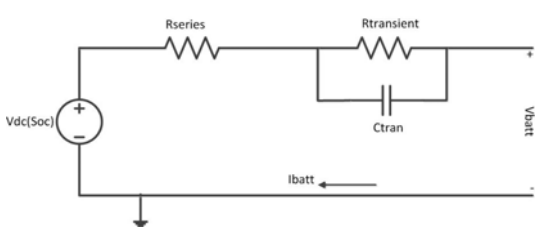

Fig.4. Electrical model of the Lithium ion battery [18] and [19]

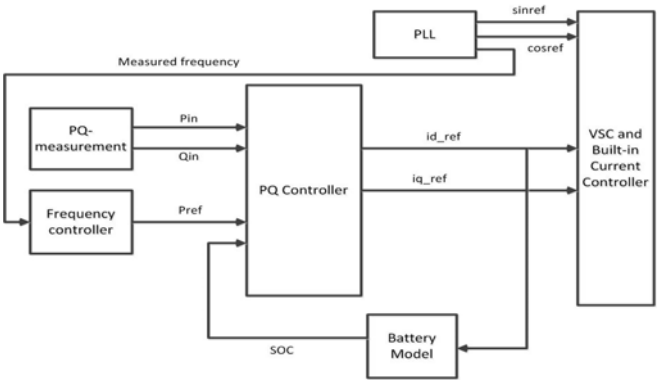

Fig.5. Block diagram of the battery storage controller

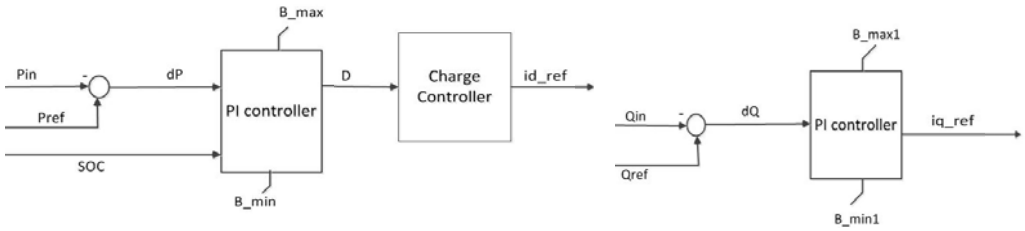

Fig. 6. PQ controller for BESS

As the power output of the battery is DC, an inverter is used to convert DC power into AC power. In order to control the charge/discharge rate of the battery, it is necessary to develop its controller. The block diagram of the control system of battery storage is shown in Fig. 5.

Two outer controllers (i.e. frequency controller and PQ-controllers) are used in this case. The frequency controller receives the reference frequency 'Fref' as its input which is supplied by a PLL. This controller compares measured and reference frequency and sends the error signals to a PI controller in order to generate P_{ref} .

The PQ controller is used to control charge/discharge rate of the battery and the flow of the reactive power through the lines. It also controls the flow of the reactive power through the lines. The PQ-controller in this case has measured active and reactive powers (i.e. P_{in} and Q_{in}), reactive power reference 'Qref', Active power reference 'Pref' supplied by the frequency controller and State of Charge 'SOC' supplied by the battery model as its inputs. The PQ controller is shown in Fig. 6. Comparison of measured and reference active and reactive powers are done and the differences are sent to the respective PI controllers which produce the active and reactive currents references. The PI controller receiving 'dP' and 'soc' as its inputs is designed in such a way that if there is mismatch between measured and reference active powers, the PI controller should generate the missing signal 'D' in order to make the error signal equal to zero and if the state of charge of battery is equal to 20% or 95%, the output signal 'D' of the controller should be zero. This is in order to avoid damage of the battery and to preserve battery life and thus, the SOC is limited within 20-95% [19]. The limits (i.e. B_max and B_min) have been set in this PI controller in order to model the battery for obtaining the desired amount of the power. The output 'D' of the PI controller is sent to the charge controller which controls the current in and out of the battery and decides it's charging and discharging rate.

The battery model is shown in Fig. 7. The current in or out of the PQ controller is integrated in order to give a relative charge 'Ch' which when added or subtracted (based on charging or discharging mode) to the initial charge 'Ch_i' in ampere-hours, gives the total charge 'ChT' of a battery as shown in equation1.

$$ChT = Ch_i + \int_{i_{\min}}^{i_{\max}} \left(I_{batt}\right).dt \tag{1}$$

This quantity is further normalized to the battery capacity so that the state of charge lies between 20 and 95%. A lookup table is used for finding battery state of charge from open circuit voltage. The resultant

battery voltage (V_{batt}) is obtained by combining series resistance voltage drop (V_{series}) and equivalent transient voltage response ($V_{transient}$) with the open circuit voltage (V_{oc}) as seen in equation 2.

$$V_{batt} = V_{oc} + V_{transient} + V_{series} \tag{2}$$

To get power output (Pbatt) of battery, the battery current (I_{batt}) and the battery resultant voltage (V_{batt}) is multiplied as seen in equation 3.

$$P_{batt} = V_{batt} I_{batt} \tag{3}$$

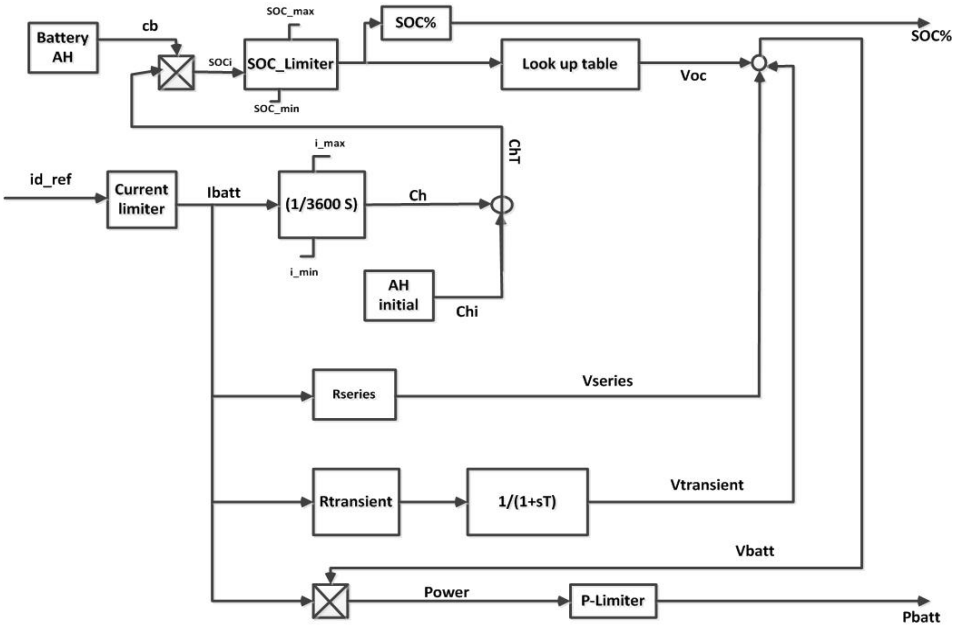

Fig. 7. The block diagram of battery model

5. Simulation Results

In order to verify the performance of the controllers used in the network, simulation results are presented in the case of some events applied on the network.

At 30 s, the output power of the PV system 2 is reduced in order to simulate the reduction in the solar radiation. The power output of PV2 is shown in Fig. 8. Initially, PV2 is producing full power (i.e. 4 kW). Due to clouds the power of the PV2 is reduced to 0.4 kW at 30 s. As the power output of PV2 decreases, AC and DC bus voltage also decreases. The STATCOM controller is controlling the voltage in very short duration. The voltage at DC bus and AC bus of PV2 converter is shown in Fig. 9.

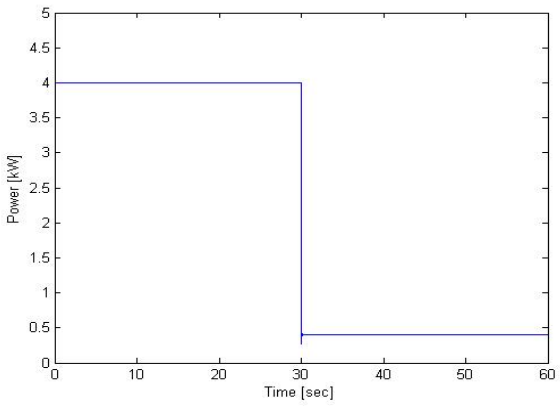

Fig. 8. Power delivered by PV2

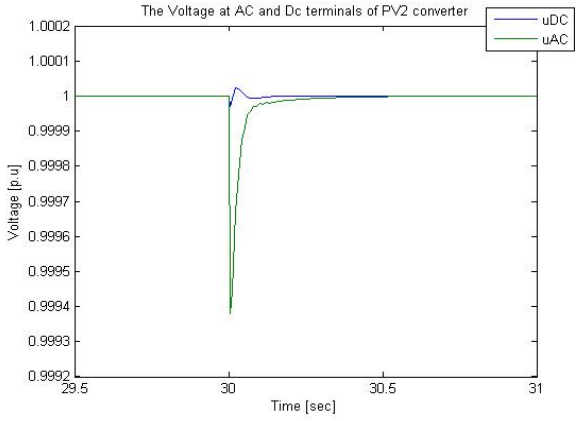

Fig. 9. Vltage at AC and DC terminals of PV2 converter

At the same time the grid is delivering power to charge the batteries. The PQ controller is charging the batteries at different C rates. The plots of currents flowing from the grid to charge the battery used at bus A at 1 C and ½ C rates are shown in Fig. 10. When battery is charged up to the specified limits, the flow of current from the grid as shown in Fig. 9 is decreasing to zero.

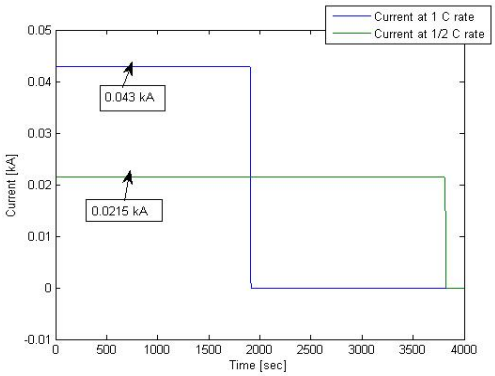

Fig.10. Currents to charge the battery at two different rates

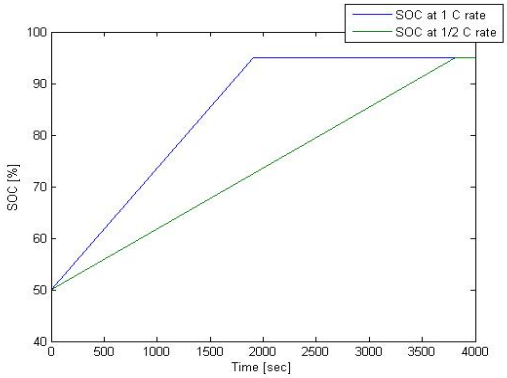

Fig.11. Sate of charge of the battery at two different rates

The plots for the battery SOC at two different rates (i.e. 1 C and ½ C rates) are shown in Fig. 11. The grid is delivering 43 A to charge the battery connected at bus A at 1 C rate. In this condition battery is charging faster. The battery is drawing half of the rated current at ½ C rate and is charging slower. It takes more time to charge up to the desired limit as shown in Fig. 11. The PQ controller is also used to control the reactive power through the lines and improve the power factor. The reactive flowing through line R8-A is shown in Fig. 12.

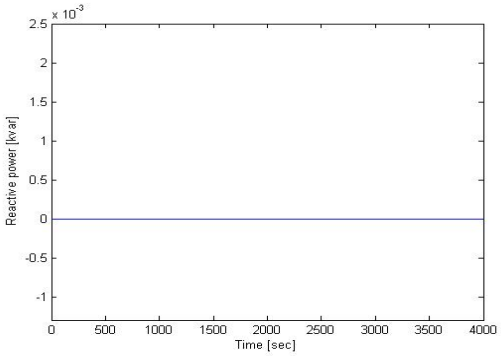

Fig.12. Reactive power through line R8-A

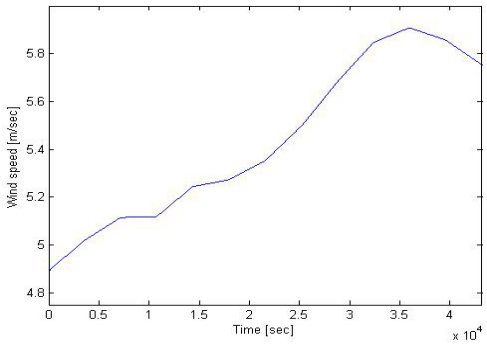

Fig.13. Wind variations of January 1, 2009 for East Denmark

Next the controllers are to be verified with e wind power fluctuations, fluctuations in the power output of a PV system and also load changes for the unbalanced load. The wind speed data of 1st January 2009 for East Denmark given by DTU wind energy is used, as shown in Fig. 13 and the power output of a PV system is assumed for the sunny day. The fluctuations in the power output of WTG and PV2 is shown in Fig. 14. The load variation for all three phases at bus D is shown in Fig. 15.

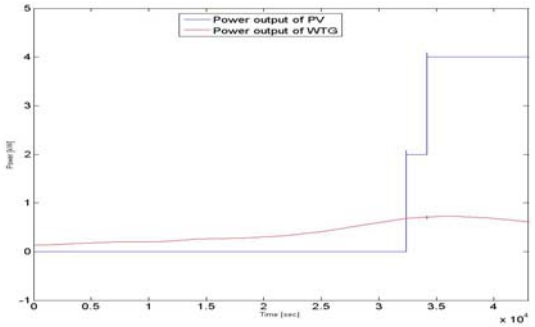

Fig. 14. The power output of PV2 and WTG

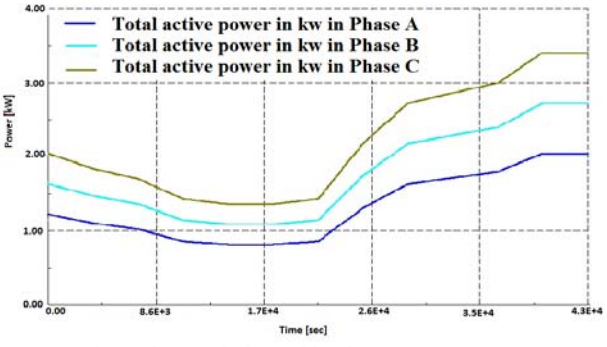

Fig. 15. Three phase unbalanced load at Bus D

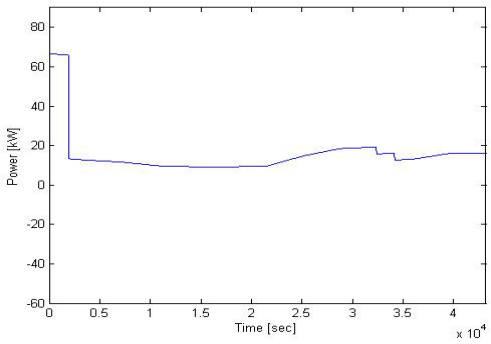

Fig.16. Power delivered by the grid

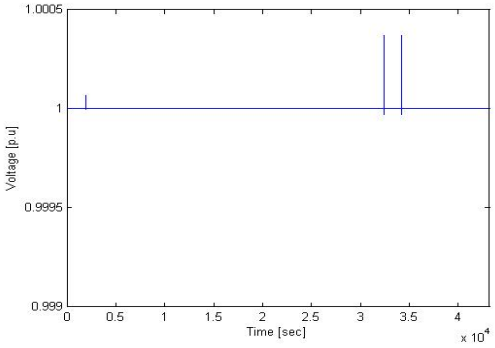

Fig.17. Voltage at bus D

The load demand is met by the WTG, PV system and the grid. The power delivered by the grid to meet the load demand and to charge the batteries is shown in Fig. 16. Initially the grid is delivering more power in order to charge the batteries and when both the batteries are fully charged it delivers less power as shown in Fig. 15.The fluctuations in the power delivered by the WTG, PV2 and the grid cause the problems with the network voltage. The fluctuations in the voltage are shown in Fig. 17. The first peak in the voltage is due to the power delivered by the grid to charge the batteries are minimized; the second and third peak is due the fluctuations in the power output of PV2. In all the cases control system is able to maintain the voltage in the desired range with very small and fast fluctuations.

6. Conclusions

The test network set up by the CIGRE comprising WTG, PVs, energy storages as well as unbalanced loads has been modeled in this paper. Because of small rating the WTG is modeled as a fixed pitch and fixed speed wind turbine. A new method of controlling PV solar system by using STATCOM controller has been proposed. It is shown in the simulation results that these controllers are successfully controlling the AC and the DC voltage during dynamic conditions. The BESS-STATCOM is also modeled and its controller is also developed. The battery controller is controlling the charge/discharge rate of the battery and has adequate control on the reactive power flow. In future these controllers will be tested in the transients and also in island conditions.

Acknowledgements

We are thankful to Kai Strunz for providing the CIGRE test network for LV distribution network. We are also thankful to DTU Wind Energy for providing wind speed data. I, Ghullam Mustafa am thankful to Quaid-E-Awam University of Engineering Sciences and Technology, Nawabshah, Sindh, Pakistan for their support and funding.

References

[1] Jenkins N. Impacts of dispersed generation on power systems. *Electra*, 2001; 199:6-13.

[2] Mahat P, Chen Z, Bak-Jensen B. *Review of Islanding Detection Methods for Distributed Generation*. China: Nanjing; 2008:6-9.

[3] International Energy Agency. (2010, July). Wind Energy 2009 Annual Report. [Online]. available: http://www.ieawind.org/AnnualReports_PDF/2009/2009AR_92210.pdf

[4] Farivar M, Clarkey CR, Low SH, Chandy KM. Inverter VAR control for distribution systems with renewables. Department of Electrical Engineering, California Institute of Technology Southern California Edison, Rosemead, CA, USA, Department of Computer Science, California Institute of Technology.

[5] Khadem SK, Basu M, Conlon MF. Power quality in grid connected renewable energy systems: role of custom power devices. In: *Proc. of International conference on Renewable Energies and Custom Power Devices, ICREPQ'10*, Spain: Granada; 2010: 23-25..

[6] Camacho EF, Samad T, Garcia-Sanz M, Hiskens I. Control for renewable energy and smart grids. In: Samad T, Annaswamy AM, editors. *The Impact of Control Technology*, 2011.
[7] Benchmark Systems for Network Integration of Renewable Energy Resources. Wersion 7. CIGRE Task force C6.04.02., 2011.
[8] Muyeen SM, Ali MH, Takahashi R, Murata T, Tamura J, Tomaki Y, Sakahara A, Sasano E. Comparative study on transient stability analysis of wind turbine generator system using different drive train models. *IET Renewable Power Generation*; 2007; 1(2):131-141.
[9] Santoso S, Le HT. Fundamental time-domain wind turbine models for wind power studies. *Renewable Energy*; 2007: 32(14): 2436-2452.
[10] Hansen AD, Iov F, Sørensen P, Cutululis N, Jauch C, Blaabjerg F. Dynamic wind turbine models in power system simulation tool DIgSILENT. *Risø DTU*, Denmark, Risø-R-1400(EN); 2007.
[11] Jetstream III Series–Grid Connected Turbine–IEC Class 1. [Online]. Available: http://www.sabletech.ie/Downloads/wind%20turbines.pdf
[12] Varma RK, Das B, Axente I, Vanderheide T. Optimal 24-hr utilization of a PV solar system as STATCOM (PV-STATCOM) in a distribution network. In: *Proc. of Power and Energy Society General Meeting*; 2011: 1-8.
[13] PV modelling by using DC current source, DIgSILENT Power Factory, Version 14.0 demo, DIgSILENT GmbH; Germany: Gomaringen.
[14] Bongiorno M. Control of voltage source converters for voltage dip mitigations for shunt and series configurations. PhD dissertation. Chalmers University of Technology; Sweden: Gothenburg; 2004.
[15] Du C. The Control of VSC-HVDC and Its Use for Large Industrial Power System. PhD dissertation. Chalmers University of Technology. Sweden, Gothenburg; 2007.
[16] Voltage control and stability of power systems in the presence of Distributed Generation. PhD dissertation. Division of Electric power Engineering, Department of Energy and Environment, Chalmers University of Technology. Sweden: Gothenburg; 2008.
[17] Harnefors L. Control of Variable-Speed Drives. V¨aster as, Sweden: Applied Signal Processing and Control. Dept. of Electronics, M¨alardalen University; 2002.
[18] Tremblay O, Dessaint LA, Dekkiche AI. A generic battery model for the dynamic simulation of hybrid electric vehicles. In: *Proc. of Vehicle Power and Propulsion Conference*, 2007:284-289
[19] Yao LW, Aziz JA. Modeling of lithium ion battery with nonlinear transfer resistance. In: *Proc. of IEEE Applied Power Electronics Colloquium (IAPEC)*, 2011.
[20] Data sheet of Rechargeable Lithium-ion battery LiIon_Saft_VL_37570.pdf. [Online]. Available: www.saftbatteries.com
[21] Technical reference for DC voltage source in DIgSILENT.

Mitigation of Voltage Sags in CIGRE Low Voltage Distribution Network

Ghullam Mustafa Bhutto[1,2], Birgitte Bak-Jensen[1], Pukar Mahat[1]
[1]Department of Energy Technology, Aalborg University, Denmark
[2]Department of Electrical Engineering Quaid-E-Awam University of Sciences & Technology, Nawabshah, Pakistan
gmu@et.aau.dk/gmustafabhutto@yahoo.com

P.f Ribeiro[3]
[3]Eindhoven University of Technology, Netherlands
pfribeiro@ieee.org

***Abstract*—Any problem in voltage in a power network is undesirable as it aggravates the quality of the power. Power electronic devices such as Voltage Source Converter (VSC) based Static Synchronous Compensator (STATCOM), Dynamic Voltage Restorer (DVR) etc. are commonly used for the mitigation of voltage problems in the distribution system. The voltage problems dealt with in this paper are to show how to mitigate voltage sags in the CIGRE Low Voltage (LV) test network and networks like this. The voltage sags, for the tested cases in the CIGRE LV test network are mainly due to three phase faults. The compensation of voltage sags in the different parts of CIGRE distribution network is done by using the four STATCOM compensators already existing in the test grid. The simulations are carried out in DIgSILENT power factory software version 15.0.**

***Index Terms*—Wind Turbine Generator (WTG), Photovoltaic (PV), Voltage Source Converter (VSC), Static Compensator (STATCOM), Battery Energy Storage System (BESS) and mitigation of voltage sags.**

I. INTRODUCTION

Power quality, reliability and stability are the prime requirement of modern power systems. It is the aim of the utilities to continuously deliver the power to the customers at constant voltage and constant frequency. The quality of the power might be lost due to the deviations in the voltage and frequency of the network. Deviations are due to faults, coupling transients, lightening etc. The modern power industry comprise of VSC based equipments which are very sensitive to voltage sags/swells. Sag or swells in the voltage may cause tripping of such sensitive equipments which can cause damage to the production of plants. This may lead to huge economical loss. An increase or decrease of the voltage in power network requires a desired amount of absorbed or injected reactive power to counteract the disturbance. The flow of reactive power through the lines/cables reduces the power transfer capability of the lines/cables as well as increases the current which leads to increased losses [1]. It is therefore, necessary to control the voltage and reactive power of the distribution network in order to ensure stable operation of the power system and operate the lines within their safe thermal loading limits.

Custom power devices can be used in this regard. Customs devices are the power electronics based devices such as (DVR), Distribution Static Compensator (D-STATCOM) etc. which are used to improve the quality of the power in electrical distribution network [2]. The VSC is a main component in these kinds of devices. Benefits of using VSCs are sinusoidal currents, controllable reactive power to regulate power factor or bus-voltage level and independent control of active and reactive power [3].

A test distribution network set up by CIGRE comprising WTG, PV solar generation units, two batteries and STATCOMs comprising VSCs at different locations has been chosen for the study. The single line diagram of this distribution system is shown in "Fig." 1. The introduction of different components of this network is described and the detailed data concerning the bus bars, cables/lines and the loads are given in [4].

The CIGRE network is modeled in DIgSILENT power factory software version 15.0. STATCOM controllers for both the PV systems have been developed in order to control oscillations in the AC and DC link voltage by injecting or absorbing the desired amount of the reactive power. The controllers for the Battery Energy Storage Systems (BESS) are developed and are able to charge/discharge the batteries at different charging rates and deliver reactive power when voltage in the network decreases. The BESS controllers are developed in such a way that they counteract voltage and frequency disturbances by receiving/delivering active and reactive powers at same time. The detailed methods of modeling these controllers together with mathematical representations are already described by the author in [5].

The project is financially supported by Aalborg University of Technology, Denmark and Quaid-E-Awam University of Engineering Sciences & Technology, Nawabshah, Pakistan

978-1-4799-2522-3/13/$31.00 ©2013 IEEE

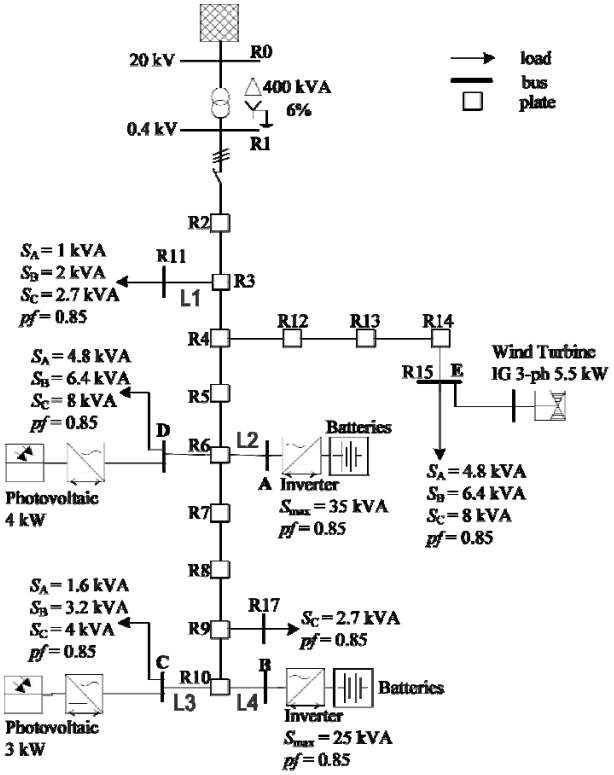

Figure 1. The single line diagram of LV CIGRE distribution system

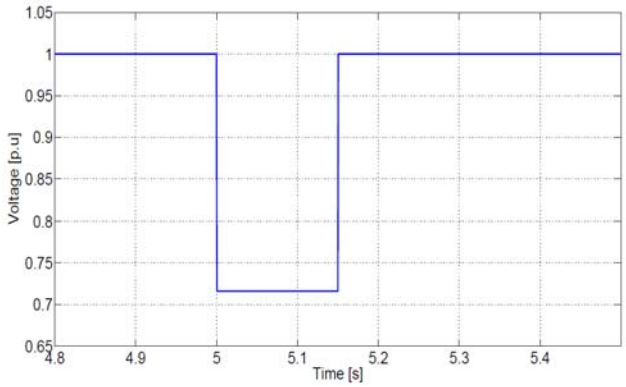

Figure 2 Voltage on MV bus

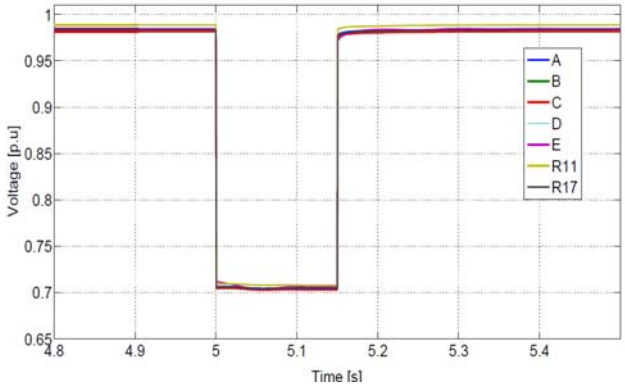

Figure 3. Voltage sag on different parts of network due to fault on MV bus

The four controllers (i.e. two D-STATCOM controllers for PV units and two BESS STATCOM based controllers for the batteries) are used for the mitigation of voltage sags in different parts of the network in this paper.

The paper is organized as follows: Section II presents the simulation results without using controllers. Mitigation of the voltage sags in different parts of the network for the two cases (i.e. when voltage sag of 28% and 12% is proposed by using appropriate controllers in section III. Finally, the conclusion about the paper is presented in section IV.

II. SIMULATION RESULTS WITHOUT USING CONTROLLERS

A three phase fault with a fault impedance of 1 Ω (Z_f =1 Ω) is applied at time t=5 s on the Medium Voltage (MV) bus and is cleared after 150 m s. Since a three phase fault is a symmetric fault, and this kind of fault affects the voltage in all three phases equally. In this kind of fault only positive sequence component of the voltage is considered. The positive sequence component of the voltage on MV bus decreases to a value of 0.72 p.u (i.e. it is voltage sag of 28%) as shown in "Fig." 2.

This kind of fault also causes voltage sag in different parts of the CIGRE network. Voltage sag is IEEE term which refers to percent decrease in voltage [6]. The voltage on bus A, bus B, bus C, bus D, bus E, R11 and bus R17 without compensation is shown in fig.3.

The depth of the voltage sag on different buses depends on the amount of current delivered by the grid and DG units and the network impedances between the fault and the current sources. The voltage sags are undesirable and cause adverse affects on different equipments used in power system. The behaviour of different components of CIGRE network during voltage sag is different.

The behavior of the wind turbine generator in the case of voltage sag depends on its technology. The 5.5 kW squirrel cage induction generator is used for the fixed pitch and fixed speed WTG for this study and is connected at bus E where voltage sag has been appeared. In the case of squirrel cage induction generator, there is a decrease in active power supplied to the grid due to the voltage sag. Similarly, the reactive power consumed by the machine is reduced due to the demagnetization of the generator. The severity of demagnetization depends of the depth of sag. When the fault is cleared the induction generator absorbs reactive power from the grid for its magnetization [7], [8]. Further, the mechanical torque of the machine is considered to be constant at constant wind speed and the voltage sag causes a reduction in the electrical torque which increases the speed of the generator [8]. If the over speed protection of the wind turbine limit is reached, the WTG has to be disconnected from the grid and stopped. This situation leads to an interruption of the production.

The detailed study about the effects of the voltage sags (i.e. symmetric or asymmetric) on WTG and its over speed

978-1-4799-2522-3/13/$31.00 ©2013 IEEE

protection in case of islanding is under the further consideration of the author.

The unbalanced loads are also connected at bus C, D, R11 and bus R17 of CIGRE network shown in "Fig." 1. Any deviation in the voltage adversely affects them. A sag in the voltage reduces the illuminating intensity of lighting loads. The effects of voltage sag are different for the different loads. The adverse effects of the voltage sag on sensitive house hold loads have been described in [9].

Similarly, voltage sag on the AC terminals of PV inverters causes the reduction in its DC-link voltage which in turn decreases the power output of PV units.

It is therefore, necessary to protect distribution system against voltage sags by using appropriate compensation devices.

III. MITIGATION OF VOLTAGE SAGS BY USING STACOM COMPENSATORS

When STATCOM is used in distribution systems it is called D-STATCOM. It utilizes a design consisting of an IGBT based VSC connected to the power system and exhibits high speed control of reactive power to provide voltage stabilization in distribution networks. It can protect distribution networks against voltage sags by injecting the required amount of reactive power. According to EN 50160 standards the voltage tolerance limit in low voltage Danish distribution network is +-10% [10].

Four D-STATCOMs, with proper controllers are employed at bus A, B, C and bus D. Two of them are used for PV applications and are only injecting/absorbing reactive power and the other two are equipped with batteries in order to inject/absorb both the active and reactive powers. These controllers are responsible for the voltage stabilization of the whole CIGRE network together with the external grid. Each D-STATCOM controller comprises two outer and two inner PI controllers and are detailed described in [5]. The two PV outer controllers are responsible for maintaining the AC and DC-link voltages. The inverters of the two BESS-STATCOMs are named VSC1 and VSC2 and are connected at bus A and B respectively. The inverters of the two PV STATCOMs are named VSC3 and VSC4 and are connected at bus C and D, respectively.

The voltage in the network is restored back to the permissible limits by the injection of reactive power by the controllers during a fault. All four controllers participate in the compensation of the voltage sag by delivering reactive power. The voltages on the AC and DC sides of bus C and bus D are shown in "Fig." 4. It can be seen in "Fig." 4 that the DC-link voltages of VSC3 and VSC4 decrease due to the voltage sag at a time equal to 5 s. A decrease in these voltages cause the power outputs of PV1 and PV2 delivered to the DC terminals of the respective inverters to decrease as shown in "Fig." 5.

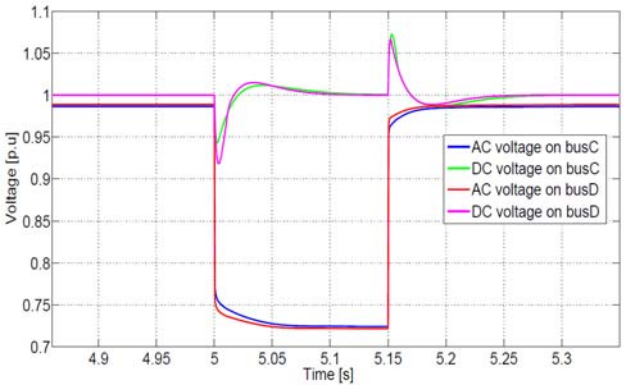

Figure 4 The DC-link voltage of VSC3 and VSC4 and voltage on AC side of bus C and bus D

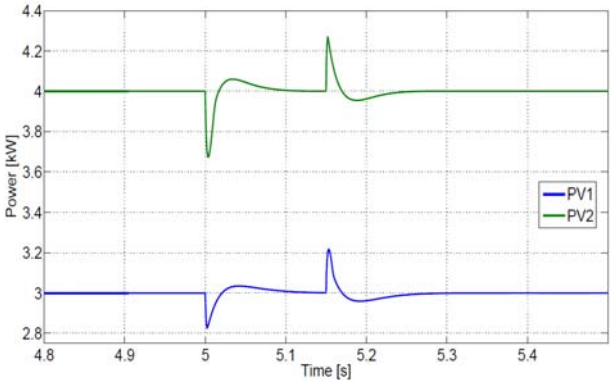

Figure 5 Power output of PV1 and PV2 on DC side of the VSC3 and VSC4

It can be seen in "Fig." 5 that PV1 and PV2 are producing rated powers (i.e. 3 kW and 4 kW) respectively in normal operating conditions (i.e. full sunny day) and decrease when voltage sag appears at t= 5 s.

The DC-link capacitors connected at the DC sides of VSC3 and VSC4 are used to provide temporary injection or absorption of active power in order to control the DC-link voltages and thereby active power outputs of PV1 and PV2.

The DC voltage controller of the D-STATCOM controllers compares the actual and the reference value (i.e. 1 p.u) of the DC-link voltage and sends the error signal to the PI controller. The PI controller makes the error signal equal to zero and decides the amount of active power injection or absorption by the DC-link capacitor.

At t=5 s the DC-link voltages (shown in "Fig." 4) and power outputs of PV1 and PV2 (shown in "Fig." 5) decrease and the respective controllers send signals to the capacitors to discharge and deliver the active powers. It is shown in "Fig." 4 and "Fig." 5 that the DC voltage controllers have controlled the DC-link voltages and maintained the power outputs of PV1 and PV2 at its pre-fault value in a short duration.

When a fault is cleared after 150 m s, the DC-link voltages shown in "Fig." 4 increase because of the short time availability of active power injection by the capacitors until they return to charging mode. This peak in DC-link voltage causes the active power output of these units to increase as shown in "Fig." 5. When the DC-link voltages are brought

978-1-4799-2522-3/13/$31.00 ©2013 IEEE

back to nominal values, the productions of these units come to the nominal value again.

The voltage on the AC side of the buses in the network is improved by delivering the proper amount of reactive power. The AC voltage controllers of the D-STATCOMs are developed to meet these requirements. The controllers are developed in such a way that they are responsible to bring the AC voltage back to 1 p.u after any disturbance depending on the availability of reactive power.

The reactive powers injected by VSC1 and VSC2 when their respective controllers charge the batteries at full charging rates and the reactive power delivered by VSC3 and VSC4 are shown in "Fig." 6 and "Fig." 7 respectively. The contribution of reactive power from the different converters (i.e. VSC1, VSC2, VSC3 and VSC4) is according to their rated power. The ratings of inverters used in the network are shown in Table. 1.

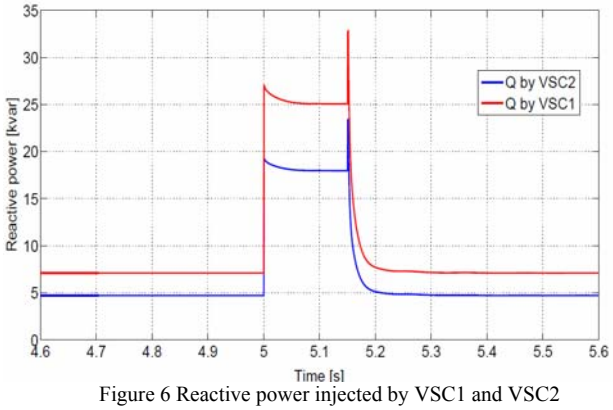

Figure 6 Reactive power injected by VSC1 and VSC2

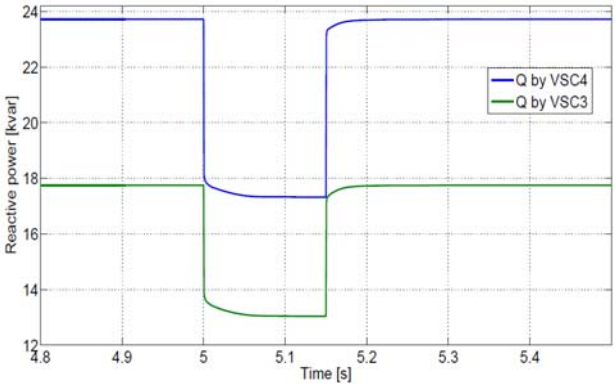

Figure 7 Reactive power injected by VSC3 and VSC4

TABLE 1
THE RATINGS OF THE INVERTERS USED IN THE NETWORK

Name of an inverter	Apparent power, S (kVA)
VSC1	35
VSC2	25
VSC3	18
VSC4	24

The inverters mentioned in Table 1 can deliver reactive power up to their rated value if they do not inject or absorb active power. As shown in "Fig." 6, VSC1 and VSC2 deliver small amounts of reactive power during steady state condition but inject maximum amount of reactive power during voltage sag. It can be seen in "Fig." 7 that VSC3 and VSC4 are injecting nearly full amount of reactive power in steady state operation in order to meet the line voltage drops and other load unbalances in the network. The reactive power delivered by these controllers is not enough to restore the voltage on these buses to 1 p.u during steady state operation, therefore when the voltage sag appears at t=5 s, the controllers do not have enough reactive power to compensate for it and hence the distribution system operates in under voltage condition. Due to this reason the reactive power injected by these controllers decrease further (i.e. $Q = VI\sin\varphi$) as seen in "Fig." 7.

The voltage on bus A, B, C, D, bus E, R11 and bus R17 in this case is shown in "Fig." 8. It can be seen in "Fig." 8 that all the controllers in the CIGRE test network are not able to compensate the voltage sag up to desirable operating limits.

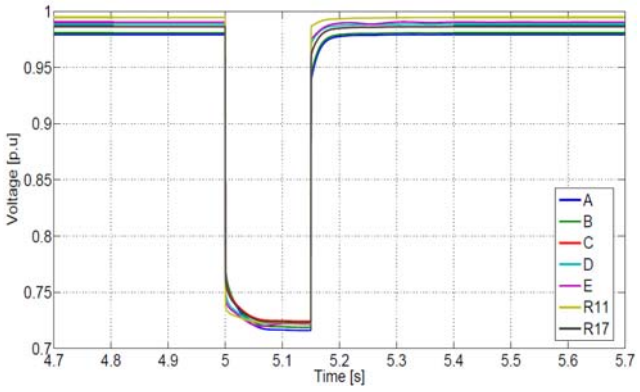

Figure 8 Voltage on different parts of network with compensation

On the other hand, the voltage sags in the distribution network can be mitigated to acceptable limits if batteries are charged at low rates instead of at full rates. The plots of the current drawn by both the batteries from the grid for two different charging rates (i.e. 1 C rate and 1/10 C rate) flowing through line L2 and line L4 is shown in "Fig." 9 and "Fig." 10 respectively.

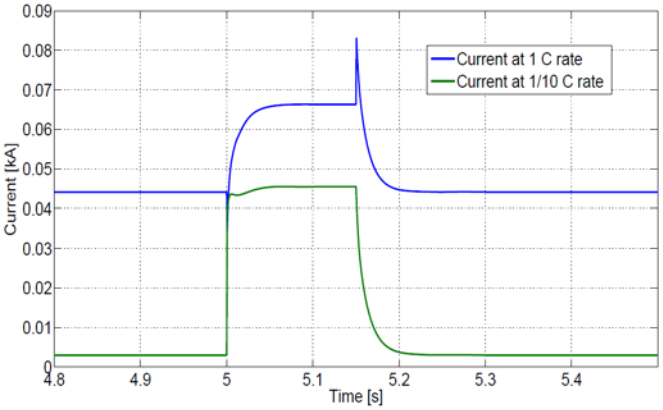

Figure 9 current through line L2 for the two different charging rates

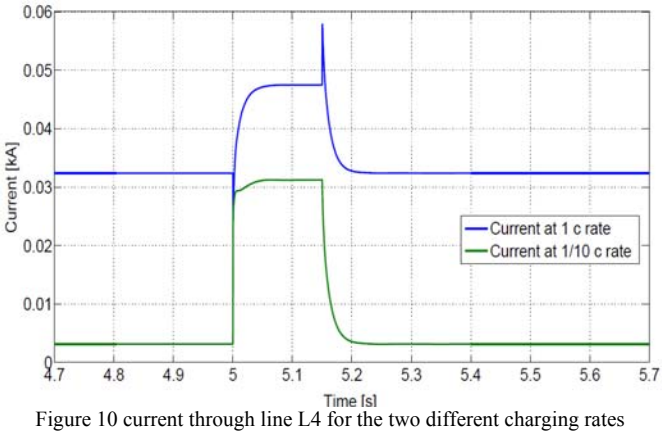

Figure 10 current through line L4 for the two different charging rates

It can be seen in "Fig." 9 and "Fig." 10 that both batteries carry different currents at different charging rates during steady state operation. The batteries are charged slowly when current flows according to $1/10^{th}$ rate. The current flowing through these lines increases when the short circuit fault occurs at t=5 s in the network. The increase in the current through these lines during a fault at a slower charging rate is less as compared to a faster one and gives less voltage drop across the lines.

The voltage on bus A, bus B, bus C, bus D, bus E, R11 and bus R17 in this case is shown in "Fig." 11. The voltage seen on bus C during voltage sag is oscillating and these oscillations are due to the behavior of the reactive power absorbed/injected by WTG. It can be seen in "Fig." 11 that the voltage in the low voltage CIGRE network has been improved a little but the existing controllers are still unable to compensate the voltage sags of this depth up to the desired level.

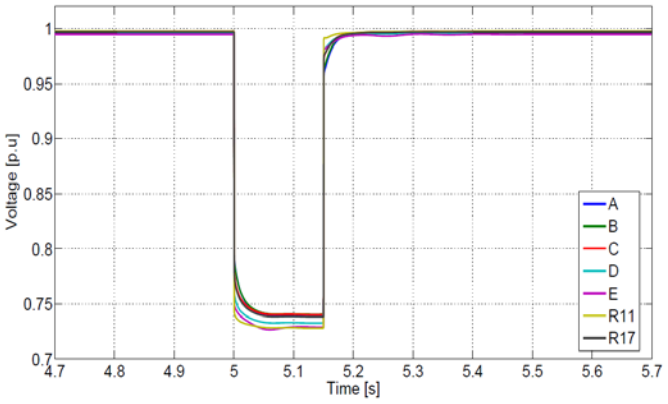

Figure 11 Voltage on different parts of the network with compensation when batteries are charged at 1/10th charging rate

Alternately, a three phase fault with a fault impedance of 2 Ω (Z_f =2 Ω) is applied at time t=5 s on the MV bus instead. This is done in order to test the effectiveness of the controllers for less deep voltage sags as compared to previous case. The voltage on the MV bus and the voltage sag in the other parts of network without using controllers are shown on "Fig." 12 and "Fig." 13 respectively.

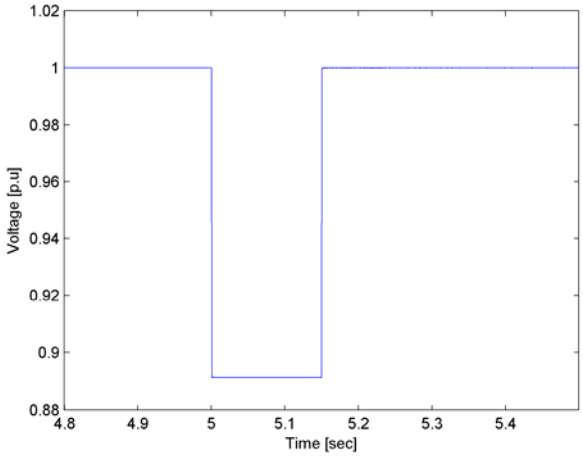

Figure 12 Voltage on MV bus when fault appears with 2Ω fault impedance

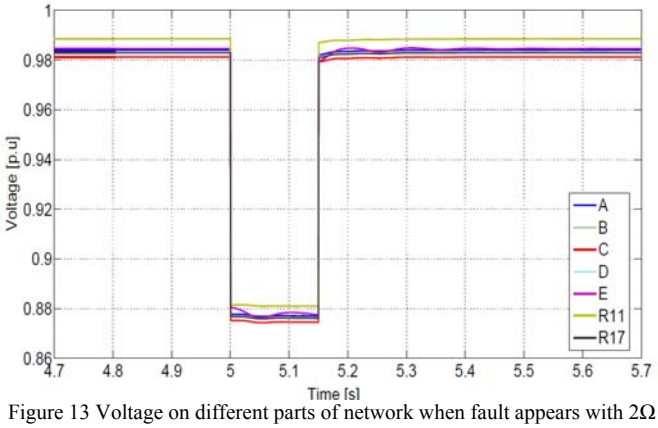

Figure 13 Voltage on different parts of network when fault appears with 2Ω fault impedance

The positive sequence component of voltage on MV decreases to a value of 0.88 p.u (i.e. voltage sag of 12%) in this case as shown in "Fig." 12. The sag depth is shallow because of bigger fault impedance as compared to the previous case. In can be seen in "Fig." 13 that the voltage sag on bus R11 is slightly less than on the other buses because there is less current flow in that direction as the three single phase loads on that bus are small as compared to the other existing loads in the network.

The compensation in this case is made when all four controllers are injecting reactive power in order to maintain the quality of power in the network. The voltage on different buses of the network when batteries are charged at full charging rates is shown in "Fig." 14. It can be seen in this fig. that the voltage in the network is improved but it is still less than the power quality limits for Danish low voltage grids [10].

By implementing the method of slow charging of the batteries, the voltage in the network has been restored to the permissible limits according to Danish standards as shown in "Fig." 15.

978-1-4799-2522-3/13/$31.00 ©2013 IEEE

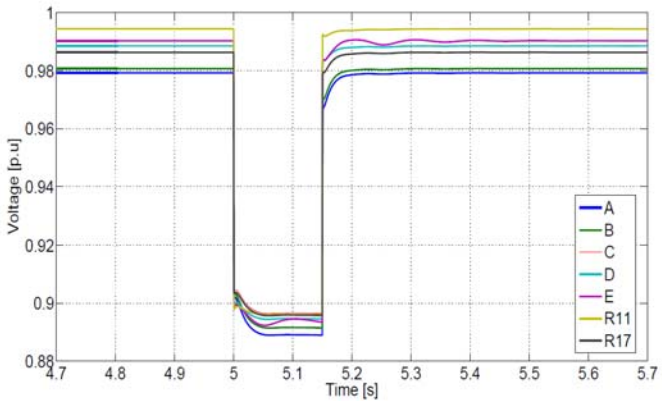

Figure 14 Voltage on different parts of network when batteries charge at full charging rate

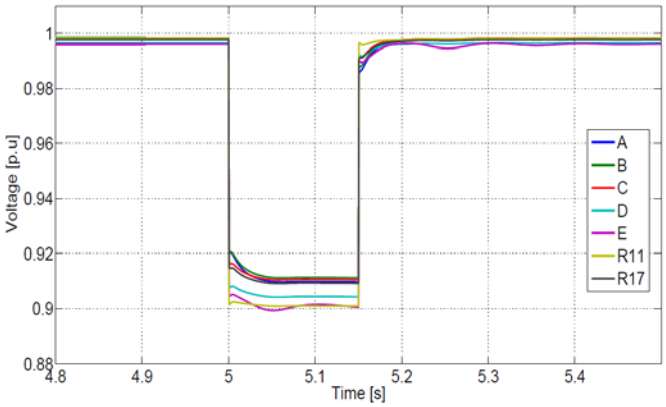

Figure 15 Voltage on different parts of network when batteries charge at slow rate

The D-STATCOM controller of battery2 and STATCOM controller of PV1 are delivering reactive power which is summed up at the same connection point (i.e. R10 in "Fig." 1). This is the reason why the voltage on the buses of these controllers (i.e. bus B and Bus C) is improved more than the other buses as shown in "Fig." 15. The voltage on Bus B during voltage sag is improved slightly better than the voltage on bus C because of a higher rating of an inverter (i.e. VSC2) used on bus B which delivers more reactive power as compared to the inverter on bus C (i.e. VSC3).

The sum of the reactive power of the above mentioned controllers passing through point R10 flows to other parts of the network in order to compensate the voltage sags there. The remaining amount of reactive power after the compensation of voltage sag on bus R17 flows towards the other parts of network again where it adds with the reactive power delivered by the STATCOM controller of battery 2 and the STATCOM controller of PV2 and corrects the voltage on the other buses.

IV. CONCLUSION

A brief introduction about the effects on voltage sags on WTG, the loads and on the output power of PV units have been presented in this paper. The mitigation of voltage sag has been performed by using two D-STATCOM and two BESS based STATCOM controllers. The compensation for the two different cases (i.e. voltage dip of 72% and 88%) has been performed. It has been shown that when batteries are charged at full charging rates, controllers have not enough reactive power to compensate the voltage sag to a satisfactory limit. It is concluded that the mitigation of voltage sags in this network by using existing services is only possible if batteries are charged at slow rate. The batteries have been charged at slow rates for the two cases in order to mitigate the voltage sag in the network to the permissible limits. It has been observed that the existing controllers can mitigate the voltage dip of up to 88% depth. If the depth of the voltage dip is more than that the controllers cannot restore the voltage up to the operating limits. This has been verified in simulation results. In future work the controllers will be tested in island conditions as well. The effects of different types of voltage sags on the WTG and its protection against over speeding of the generator in island operation will be studied in future.

ACKNOWLEDGMENT

The authors are thankful to Kai Strunz for providing the CIGRE test network for LV distribution network. I, Ghullam Mustafa am thankful to Quaid-E-Awam University of Engineering Sciences and Technology, Nawabshah, Sindh, Pakistan for the support and funding.

REFERENCES

[1] Joe H, Chow, Felix F. Wu and James Momoh, "Applied Mathematics for restructured electric power sysyetms, optimisation, control, and computational intelligentce," Power electronics and power systems 2005: pp 11-24.

[2] T. Devaraju, Dr. V.C. Veera Reddy and Dr. M. Vijaya Kumar, "Role of custom power devices in Power quality enhancement: A review," trans. on Engineering Sciences and Technology, Vol. 28, pp. 3628-3634, 2010.

[3] Massimo Bongiorno, "Control of voltage source converters for voltage dip mitigations for shunt and series configurations," PhD dissertation; Department of Energy system, Chalmers University of Technology; Sweden: Gothenburg, 2007.

[4] Benchmark Systems for Network Integration of Renewable Energy Resources, version 7, March2011, CIGRE Task force C6.04.02.

[5] Ghullam Mustafa, Birgitte Bak-Jensen and Pukar Mahat, "Modeling of the CIGRE low voltage test distribution network and the development of appropriate controllers," in trans. of Smart Grid and Clean Energy, vol. 2, no. 2, pp. 184–191, May 2013.

[6] Terry Chandler. "The effects of voltage sags," IEEE Hong Kong Section, May 31, 2002

[7] Bousseau P, Gautier E, Garzulino I, Juston P, Belhomme R, "Grid impact of different technologies of wind turbine generator systems," in Proc. On EWEC03, June 2003

[8] Dittrich A, "Grid Voltage Fault Proof Doubly Fed Induction Generator System," EPE 03, Toulouse 2003

[9] George G. Karady, Saurabh Saksena, and Bauzhuang Shi, "Effects of voltage sags on house hold loads," IEEE Power Engineering Society General Meeting, Vol. 3, pp. 2456–2461, 2005.

[10] Rekommandation 16, Spændingskvalitet I lavspændingsnet (voltage quality in low voltage networks), 4. Udgave, Aug. 2011.

Energy and Power Engineering, 2013, 5, 551-559
Published Online November 2013 (http://www.scirp.org/journal/epe)
http://dx.doi.org/10.4236/epe.2013.59060

Scientific Research

Mitigation of Unbalanced Voltage Sags and Voltage Unbalance in CIGRE Low Voltage Distribution Network*

Ghullam Mustafa Bhutto[1,2#], Birgitte Bak-Jensen[1], Pukar Mahat[1], Carlo Cecati[3]
[1]Department of Energy Technology, Aalborg University, Aalborg, Denmark
[2]Department of Electrical Power, Quaid-E-Awam University of Sciences & Technology, Nawabshah, Pakistan
[3]Department of Information Engineering, Computer Sciences and Mathematics, Via G. Gronchi, L'Aquila, Italy
Email: gmu@et.aau.dk, #gmustafabhutto@yahoo.com, bbj@et.aau.dk, pma@et.aau.dk, carlo.cecati@univaq.it

Received September 28, 2013; revised October 28, 2013; accepted November 5, 2013

ABSTRACT

Any problem with voltage in a power network is undesirable as it aggravates the quality of the power. Power electronic devices such as Voltage Source Converter (VSC) based Static Synchronous Compensator (STATCOM) etc. can be used to mitigate the voltage problems in the distribution system. The voltage problems dealt with in this paper are to show how to mitigate unbalanced voltage sags and voltage unbalance in the CIGRE Low Voltage (LV) test network and networks like this. The voltage unbalances, for the tested cases in the CIGRE LV test network are mainly due to single phase loads and due to unbalanced faults. The compensation of unbalanced voltage sags and voltage unbalance in the CIGRE distribution network is done by using the four STATCOM compensators already existing in the test grid. The simulations are carried out in DIgSILENT power factory software version 15.0.

Keywords: Power Quality; Unbalanced Voltage Sags; Mitigation of Voltage Unbalance; Voltage Unbalance Factor (VUF); Distributed Static Compensator (STATCOM)

1. Introduction

Power quality (PQ) is one of the primary objectives of the modern power system. Among the various phenomena responsible of performance degradation, Voltage Sags (VS) defined by IEEE standards 1159-1995 as the reduction in the value of RMS voltage between 0.1 to 0.9 p.u at the power frequency with the duration from 0.5 cycles to 1 min represent one of the most important causes of poor power quality [1]. The main causes of voltage sags are short circuit faults occurring in transmission or distribution systems, transformer energizing, switching of the capacitor banks and starting of large induction motors [2]. Their effects are multiple and change with different loads. The case of sensitive house hold loads has been deeply described in [3].

Voltage sags can be symmetric or asymmetric depending on the type of short circuit faults. The majority of faults in power system are single-phase-to-ground faults [4], and consequently result in unbalanced sags. A symmetric fault involves all kinds of sequence quantities: positive, negative and zero sequence, whereas voltage sags due to symmetric fault contain only positive sequence quantities. Depending on both the type of faults and the transformer connections between medium voltage and the low voltage, different types of voltage sags can be distinguished. A detailed discussion about the influence of the transformer winding connection on the propagation of voltage sags is presented in [5,6]. The transformer winding (delta/wye) connection used in this network blocks the flow of zero sequence components from the voltage [5]. An extended analysis of voltage sag and their classification has been carried out in [7-9].

Voltage in power system can be unbalanced due to the several reasons. One of the major reasons of voltage unbalance is an uneven distribution of single phase loads that draw unbalanced currents from the system [10,11]. These unbalance currents will create unequal heating in each of the phases which creates unbalance heating in cables and other parts of the network, which might reduce the life time of the cables and other components [12,13]. Another reason for voltage unbalance is due to unbalanced faults. The unbalance in the voltage due to this rea-

*1) Subject Classification: Smart Grids; 2) All authors are mutually agreed; 3) It's the original work of all the authors; 4) We did not submit this manuscript before.
#Corresponding author

son is severe.

According to European standards, the percent Voltage Unbalance Factor (VUF) is defined by the ratio of the negative sequence voltage to the positive sequence voltage [14-16].

$$\%VUF = V_2/V_1 * 100 \quad (1)$$

where V_1 and V_2 are the positive and negative sequence components of the voltage respectively. According to IEEE Std. 1547.2 - 2008 the voltage unbalance factor should be below "2% to 3%".

The aim of this paper is to investigate how to mitigate unbalanced voltage sags and also voltage unbalance in a CIGRE low voltage distribution network. This is done by using custom power devices: two D-STATCOMs and two BESS-STATCOMs used at different locations of the network.

The paper is organized as follows: Section 2 gives the description of CIGRE LV distribution network, Section 3 presents the description about the control structure; Section 4 presents the simulation results without using controllers. Mitigation of the voltage sag and the voltage unbalance for the two cases (*i.e.* when voltage sag of 42.3% and 43.4% on phase A and phase B of bus R1 and when voltage sag of 13% on phase B of the same bus) is proposed by using appropriate controllers in Section 5. Finally, the conclusion about the paper is presented in Section 6.

2. Description of CIGRE Network

In order to achieve the described goal, a test distribution network set up by CIGRE comprising Wind Turbine Generator (WTG), Photovoltaic (PV) solar generation units, two batteries and STATCOMs comprising Voltage Source Converters (VSCs) at different locations has been chosen for the study [17]. Unbalanced loads are aggregated at the 0.4 kV voltage levels and are connected at bus RC, RD, R11, R15 and bus R17. The detailed data concerning bus bars, cables/lines and loads is given in [17]. The Distributed Generation (DG) units are integrated into the grid using a delta-wye with neutral (D-YN) transformer used at the beginning of the radial as shown in **Figure 1**. The neutral of the transformer is grounded with low impedance, $Z = (0.0032 + j0.0128)\Omega$. The single line diagram of this distribution system is shown in **Figure 1**. The considered network is details are described in [17].

In case of a WTG connected to an unbalanced voltage, the stator currents will be unbalanced. These unbalanced stator currents creates unequal heating in stator winding which might degrade winding insulation and thereby reducing the life time of the stator winding. The impacts of voltage unbalance on WTG's have been studied in [18]. The impacts of voltage unbalance on PV inverters are studied in [19,20]. The CIGRE network is modeled in

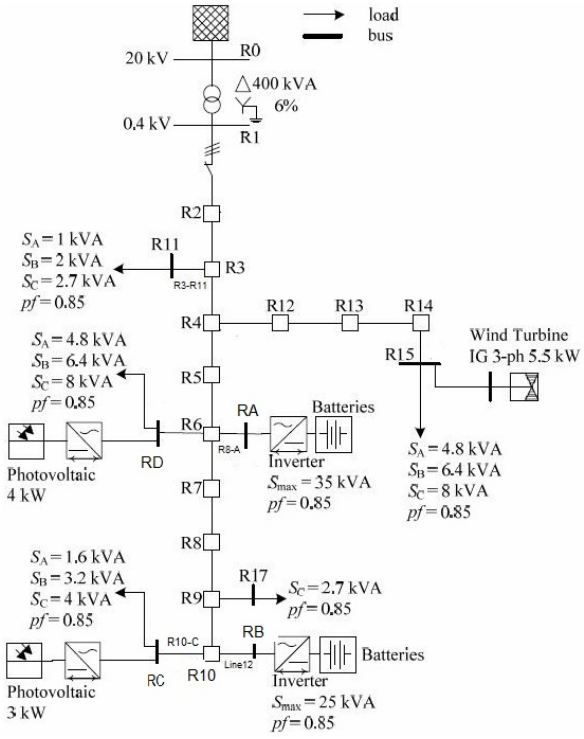

Figure 1. Single line diagram of CIGRE LV distribution system.

DIgSILENT power factory software version 15.0.

3. Description of Control System

The control system developed by the author used for this study is detailed described [21]. A brief introduction of the control system is presented in this paper only. The D-STATCOM controllers for both PV systems have been developed in order to control dc-link and AC voltages by injecting/absorbing active and reactive powers respecttively [21]. The controllers for the Battery Energy Storage Systems (BESS) are developed and are able to charge/discharge the batteries at different charging rates. The BESS controllers are developed in such a way that they counteract voltage and frequency disturbances by receiving/delivering active and reactive powers [21]. The inverters of the PV units and battery units are modeled in such a way that they can deliver unbalance currents in order to mitigate unbalanced voltage sags and prevent the problems of the voltage unbalance in the network [21]. The focus in this paper is only on the control of the AC side of the voltage. The problems of the dc-link voltages on the PV inverters are discussed in [19,21] and charging/ discharging of the batteries are described in [21].

4. Study of the System without Using Controllers

To have a base study case, all the controllers have been

disabled in order to study the impacts of unbalanced loads and unbalanced faults on the voltage in different parts of the low voltage CIGRE network. The voltage unbalance exists from the beginning as unbalanced loads are connected to the network. Next, a single line to ground fault on phase A with a 0 Ω fault impedance is applied at time equal to t = 2 s on the 20 kV Medium Voltage (*i.e.* R0) bus in order to simulate a case of severe unbalance. The fault is cleared at 2.15 s. The magnitude and phase angle of voltage in the three phases at the bus R0 is shown in **Figures 2(a)** and **(b)**.

It can be seen that voltage in all three phases of the bus R0 are nearly the same during normal operating conditions as there is only minor load unbalance. At time equal to t = 2 s, the voltage in the effected phase becomes zero and the voltage in the other two phases remain nearly the same as shown in **Figure 2(a)**. The results shown in **Figure 2(a)** are matching with the reference [5,22].

The voltage angles in its three phases on bus R0 are shown in **Figure 2(b)**. It can be seen in **Figure 2(b)** that the angle of the voltage is changed in the affected phase only, whereas the voltage angles of the healthy phases remains unchanged.

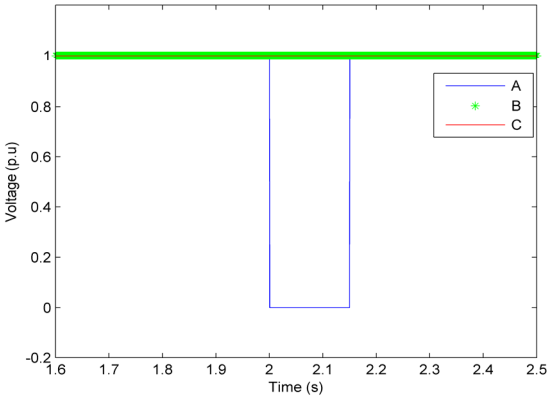

(a)

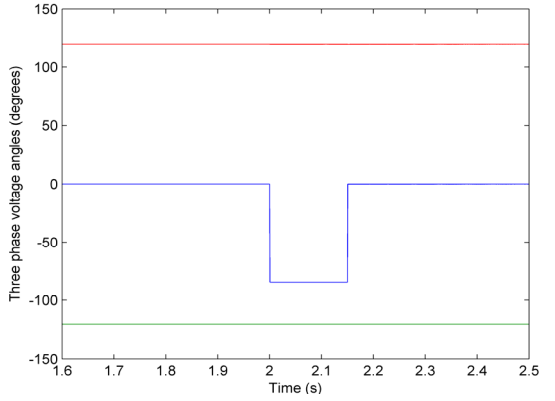

(b)

Figure 2. (a) Voltage in the three phases of the R0 bus for single phase to ground fault on phase A with $Z_f = 0$ Ω. (b) Angles of three phase voltages on bus R0 in case L-G fault on phase A with $Z_f = 0$ Ω (blue line: phase A, green line: phase B, red line: phase C).

The transformation of voltages from primary (*i.e.* delta) of the transformer to its secondary (*i.e.* star) is described with the help of **Figure 3** [23].

In delta wye configuration of the transformer, the value of phase to neutral voltage on secondary (*i.e.* shown with colored lines R, Y and B) is equal to that of the line voltage at the primary divided by $\sqrt{3}$ [24]. The line to line primary voltages are given in "Equation (2)".

$$\begin{aligned} V_{ba} &= V_b - V_a \\ V_{cb} &= V_c - V_b \\ V_{ac} &= V_a - V_c \end{aligned} \tag{2}$$

Putting the values of phase voltages with respect to their phase angles obtained from **Figure 2** in "2," line to line voltages on the primary of the transformer can be calculated.

$$V_{ba} = 1 < -120^0 - 0 < -84^0$$

$$V_{ba} = 1 < -120^0$$

The voltage V_{ba} on the primary corresponds to the voltage in phase B on the secondary of the transformer as shown in **Figure 3** and is given by $V_{bN} = v_{ba}/\sqrt{3}$ which is equal to $0.578 < -120^0$ p.u.

$$V_{cb} = 0.999 < 120^0 - 1 < -120^0$$

$$V_{cb} = 1.723 < 90^0$$

The voltage V_{cb} on the primary corresponds to the voltage in phase C on secondary of the transformer as shown in **Figure 3** and is given by $V_{cN} = v_{cb}/\sqrt{3}$ which is equal to $0.999 < 90^0$ p.u.

$$V_{ac} = 0 - 0.999 < 120^0 \quad V_{ac} = 0.999 < -60^0$$

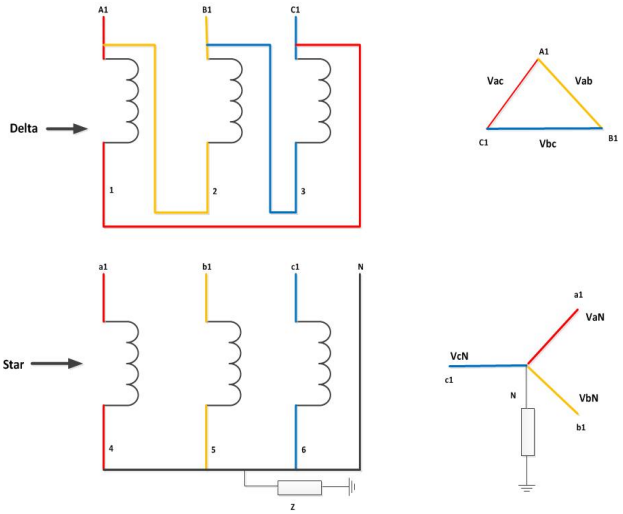

Figure 3. The transformation of voltages from primary of DYN1 transformer to secondary.

The voltage V_{ac} on the primary corresponds to the voltage in phase A on the secondary of the transformer as shown in **Figure 3** and is given by $V_{aN} = v_{ac}/\sqrt{3}$ which is equal to $0.578 < -60^{0}$ p.u.

The voltage in the three phases at the bus R1 is shown in **Figure 4**. At t = 2 s, the voltage profile on this bus changes as shown in **Figure 4**.

It can be seen in **Figure 4** that there is voltage sag of 42.3% in phase A and 42.4% in phase B on the bus R1. Phase C on this bus is unaffected. A slight difference in voltage sag on phase A and B is due to the slight difference in their loadings. The load on phase B is slight more than the load on phase A, so voltage sag on phase B is slightly deeper than on phase A. When the fault is cleared after 150 m s, the voltage in all the phases return to prefault values. The results shown in **Figure 4** also match with [5,6,9].

The voltage at different phases on bus RA, RB, RC and Bus RD is shown in **Figures 5(a)-(d)** respectively. Similar to **Figure 4**, there is mild unbalance in voltage in normal operating conditions due to unbalanced loads and severe unbalance due to the unbalanced fault.

Table 1 shows the unbalance factor in different parts of CIGRE distribution network under mild and severe unbalance.

It can be seen in **Table 1** that there is a mild unbalance due to the unbalanced loads connected on different buses

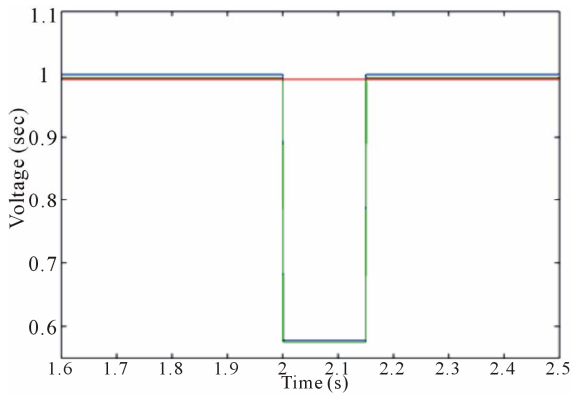

Figure 4. Voltage on R1 bus (blue line: phase A, green line: phase B, red line: phase C).

Table 1. Unbalance Factors in different parts of network for the two conditions.

Bus No	%(VUF) in normal operating conditions	%(VUF) during fault
RA	0.45	49.64
RB	0.48	49.6
RC	0.5	49.59
RD	0.43	49.638
R11	0.31	49.66
R15	0.395	49.74
R17	0.55	49.55

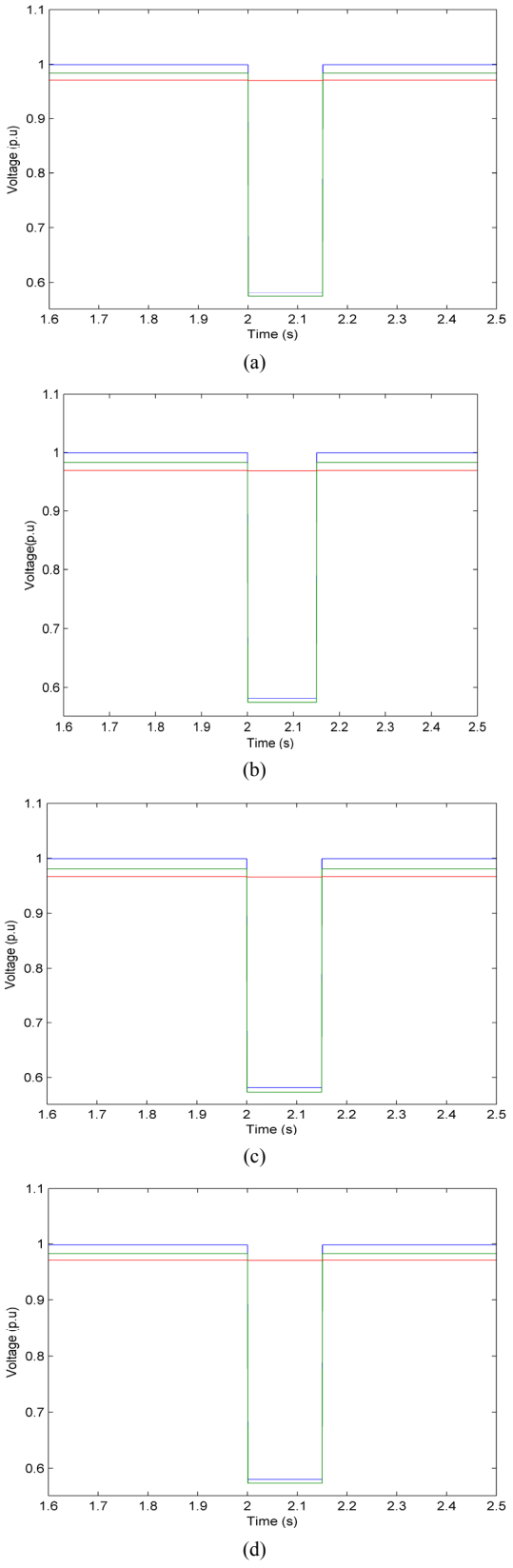

Figure 5. (a) Voltage on bus RA. (b) Voltage on bus RB. (c) Voltage on bus RC. (d) Voltage on bus RD. (blue line: phase A, green line: phase B, red line: phase C).

in normal operating condition and severe unbalance in the network grid due to a fault. The difference in the unbalance factor during normal operating conditions is due to different loadings on the buses in the network grid.

5. The Mitigation of Unbalance Voltage Sag and Voltage Unbalance

Four STATCOM controllers are used in order to inject/absorb the desired amount of reactive power in each of the phases in order to restore the voltage of different phases to permissible limits and mitigate the problems of voltage unbalance. The reactive power injected/absorbed by all of the four VSCs in the three phases of bus RA, RB, RC and bus RD are shown in **Figures 6(a)-(d)** respectively.

Since all four inverters are modeled for voltage regulation, they inject or absorb reactive power in different phases of the buses where they are connected. If the voltage of the bus in any of the phase is greater than the voltage of an inverter connected on that bus, the reactive power in that phase is absorbed by the inverter and vice versa [25]. Two of the inverters (*i.e.* VSC1 and VSC2) are used for battery applications and the other two (VSC3 and VSC4) for the PV units.

The contribution of reactive power from the different converters (*i.e.* VSC1, VSC2, VSC3 and VSC4) is according to their rated power. The power and voltage ratings of the inverters used in the network are shown in **Table. 2**. The inverters mentioned in **Table 2** can deliver reactive power up to their rated value if they do not inject or absorb active power. The batteries are charged at very slower rates (*i.e.* 1/100 rate) so that battery inverters can provide maximum amount of reactive power in order to mitigate voltage sags. The PV inverters are also set to deliver maximum amount of reactive power.

It can be seen in **Figure 6** that reactive power is injected in different phases of the bus RA, RB, RC and bus RD in the normal operating conditions in order to reduce the unbalance factor. As shown in **Figures 6(a)** and **(b)**, VSC1 and VSC2 deliver small amounts of reactive power during steady state condition but inject/absorb maximum amount of reactive power during unbalanced voltage sag. Since the two phases (*i.e.* phase A and phase B) have seen voltage sag in the network buses therefore all of the inverters are injecting reactive power in these two phases at t = 2 s as shown in **Figure 6**.

Table 2. The ratings of the inverters used in the network.

Name of an inverter	Apparent power, S (kVA)	$V_{DC\ (kV)}$	$V_{AC\ (kV)}$
VSC1	35	0.714	0.4
VSC2	25	0.781	0.4
VSC3	18	1	0.4
VSC4	24	1	0.4

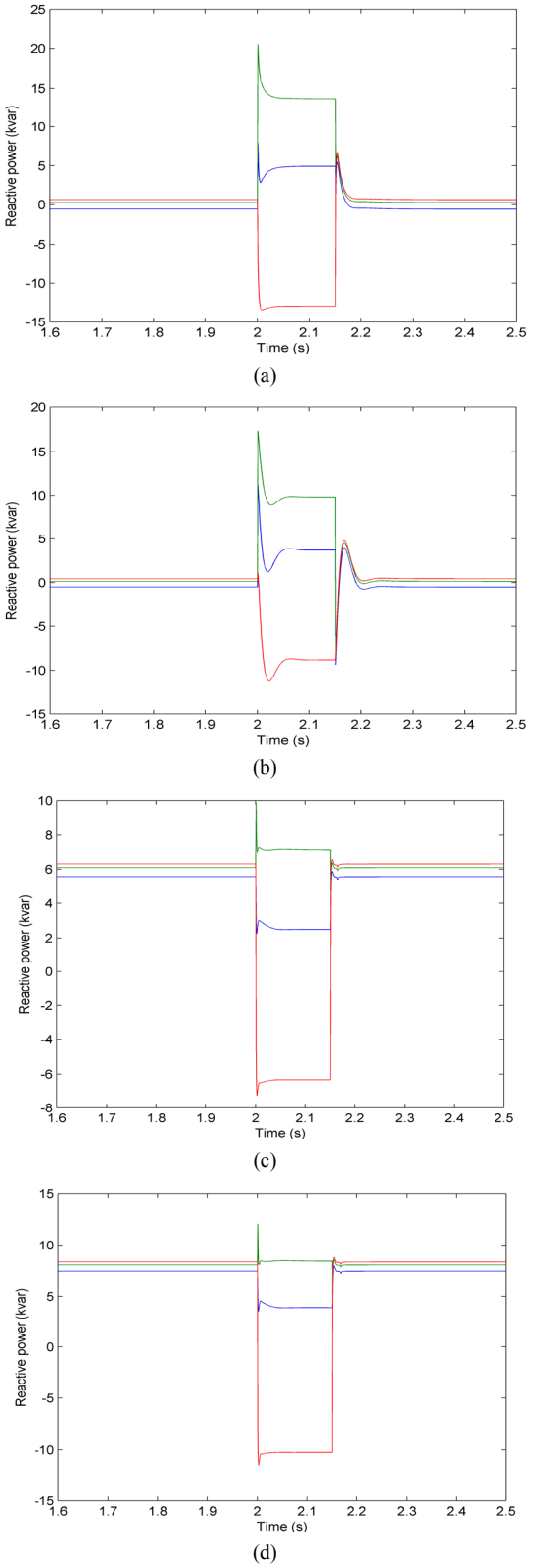

Figure 6. (a) Reactive power of VSC1 in three phases. (b) Reactive power of VSC2 in three phases. (c) Reactive power of VSC3 in three phases. (d) Reactive power of VSC4 in three phases. (blue line: phase A, green line: phase B, red line: phase C).

The reactive power injected by all of the inverters in phase B is little bit higher than phase A because voltage sag in phase B is little deeper than phase A in all branches. The phase C in all branches has not seen volt age sag so in general there should be no injection of reactive power by the inverters in this phase. But the purpose of the controllers developed for this study is not only to mitigate voltage sag but also to compensate against voltage unbalance in the network. Due to this reason the reactive power is absorbed in phase C in order to reduce unbalance factor.

When fault appears in some part of the network, there is an increase in the flow of the currents delivered by the inverters used in the network. The rise of the current in the inverters is controlled by using current limiters so the IGBTs may not damage against over currents. The peaks in the reactive powers of VSC1 and VSC2 in each of the phase as shown in **Figures 6(a)** and **(b)** are due to this phenomenon.

It can be seen in **Figures 6(c)** and **(d)** that VSC3 and VSC4 are injecting nearly full amount of reactive power in steady state operation in order to meet the line voltage drops and other load unbalances in the network. When the unbalanced voltage sag appears at t = 2 s, the controllers do not have enough reactive power to compensate for it and hence the distribution system operates in under voltage conditions across these points. Due to this reason the reactive power injected by these controllers in some of the phases decrease further (*i.e.* $Q = VI \sin\phi$) as seen in **Figures 6(c)** and **(d)**.

The peaks in **Figures 6(c)** and **(d)** at the beginning and at the end of voltage sag are due to the charging and discharging of DC-link capacitors in order to maintain DC-link voltage of PV1 and PV2.

The new value of voltage in each of the phases in per unit in different parts on network after using compensation and the voltage unbalance factors in normal and fault periods are shown in **Table 3**.

Table 3 shows that the controllers to some extent have mitigated the voltage sags in the different phases and have improved the unbalance factors. The unbalance factors in fault conditions are still not within an acceptable range and also the voltages in phase A and phase B are not improved up to the acceptable limits [26] because the converters do not have enough reactive power capacity to mitigate voltage sag and voltage unbalances of such big depth.

To figure out the limit of the converters in relation to the voltage sag depth after voltage sag compensation, a single phase to ground fault on phase A at the R0 bus with a fault impedance of 3 Ω is applied on time equal to t = 2 s. The fault is cleared at 2.15 s. The voltages in the three phases of the R0 bus in this case are shown in **Figure 7**. It can be seen in **Figure 7** that voltage in the effected phase during the fault is reduced but not equal to zero as in the last case.

The fault on R0 bus creates unbalanced voltage sags in different parts of the network gird. The transformation of voltage sag from the delta side of the transformer to its wye side is according to **Figure 3**. The voltages in three phases of bus R1 obtained by using above transformation method in this new case is shown in **Figure 8**. The values of the voltage during fault in each of the phases have been verified by using (2) and the results are matching with the results shown in **Figure 8**.

For simplicity the voltage on one of the buses (*i.e.* bus RA) with and without controllers in this new case is shown in **Figures 9(a)** and **(b)**. It can be seen in **Figure 9(a)** that without using controllers phase B of bus RA of the network is less than 90% which is not within a tolerable limit according to IEEE standard 1159-1995 and Danish standards [26]. By using controllers the voltages in all of the phases are restored within the permissible limits of ±10% according to Danish standards.

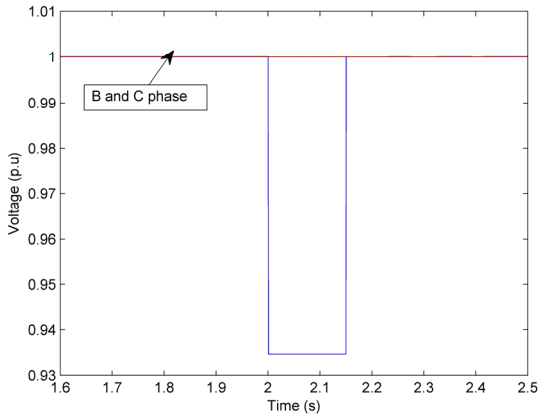

Figure 7. The voltage in three phases of R0 bus when single phase to ground fault on phase A with $Z_f = 3$ Ω. (blue line: phase A, green line: phase B, red line: phase C).

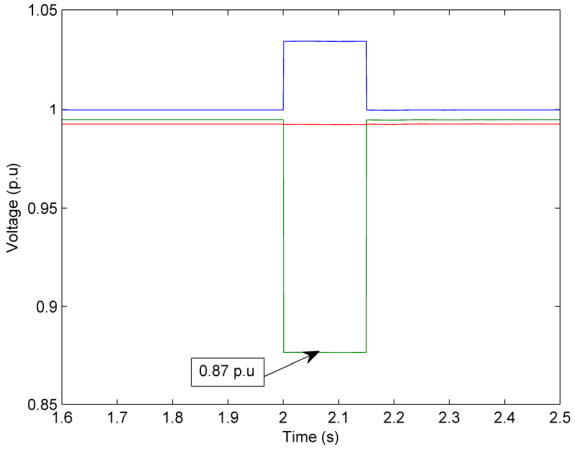

Figure 8. Voltage on the R1 bus. (blue line: phase A, green line: phase B, red line: phase C).

Table 3. Voltage in different phases in different parts of the network and unbalance factors.

Bus number	VOLTAGE IN NORMAL CONDITIONS			%UF IN NORMAL OPERATION	VOLTAGE DURING FAULTS			%UF DURING FAULT
	A	B	C		A	B	C	
RA	1.007	0.9986	0.9949	0.299	0.69	0.54	0.912	33.2
RB	1.0066	0.9991	0.9956	0.32	0.691	0.545	0.9087	32.4
RC	1.0078	0.9982	0.994	0.34	0.68	0.55	0.91	32.55
RD	1.0061	0.9977	0.9936	0.299	0.654	0.56	0.926	35.5
R11	1.0045	0.9976	0.9945	0.22	0.61	0.579	0.95	40.2
R15	1.0052	0.996	0.9904	0.295	0.626	0.57	0.939	38.3
R17	1.0077	0.9992	0.992	0.39	0.67	0.56	0.914	33.33

Table 4. Voltages in different phases in different parts of the network with and without controllers and unbalance.

Bus number	VOLTAGE IN NORMAL CONDITIONS			%UF IN NORMAL OPERATION	VOLTAGE DURING FAULTS			%UF DURING FAULT
	A	B	C		A	B	C	
RA	1.034	0.867	0.97	9.22	1.0366	0.919	0.97	6.46
RB	1.034	0.866	0.969	9.2	1.0367	0.92	0.97	6.3
RC	1.034	0.864	0.966	9.26	1.037	0.918	0.97	6.38
RD	1.033	0.866	0.97	9.4	1.0356	0.91	0.979	6.9
R11	1.034	0.87	0.98	9.27	1.033	0.90	0.988	7.69
R15	1.0336	0.879	0.974	9.45	1.034	0.90	0.98	7.38
R17	1.035	0.867	0.967	9.24	1.036	0.916	0.975	6.5

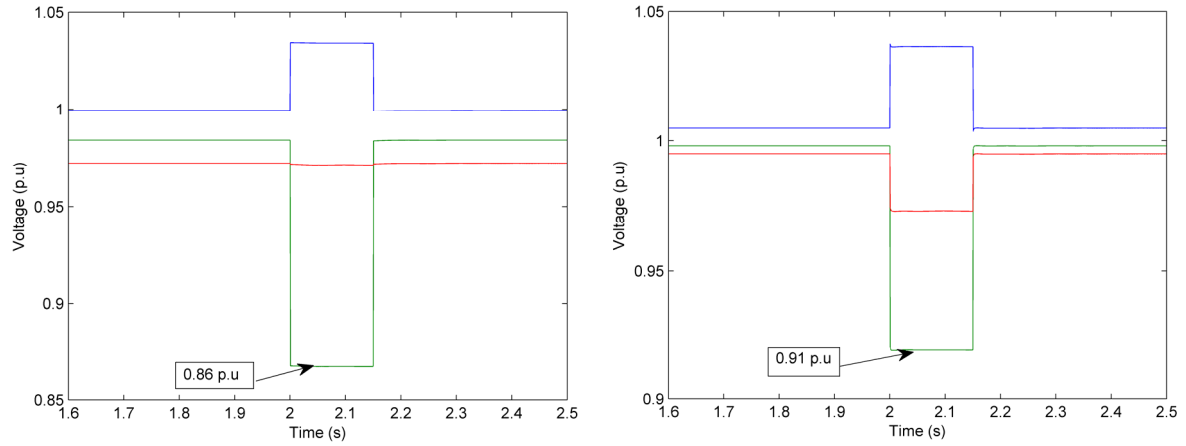

Figure 9. (a) Voltage on bus RA without controllers. (b) Voltage on bus RA with controllers. (blue line: phase A, green line: phase B, red line: phase C).

It can be seen in **Table 4** that voltage in all parts of network in each of the phases are restored within permissible limits and the voltage unbalance during fault are also reduced to a smaller value by using the developed controllers. The controllers have successfully mitigated the unbalanced voltage sags in all parts of the network grid but they are unable to maintain unbalance factor according to IEEE standards 1547.2-2008 during a fault. The only way to restore the unbalance factor according to the standards is to use bigger size of the battery units rather than the existing ones.

6. Conclusion

The mitigation of the voltage unbalance during normal and faulted conditions and the mitigation of unbalanced voltage sag have been performed by using two D-STATCOM and two BESS based STATCOM controllers. The compensation for two different cases (*i.e.* voltage sag of 42.3% and 43.4% on phase A and phase B respectively and when voltage sag of 13% on only phase B) has been performed. It has been observed that the existing controllers can mitigate the voltage sag of up to 13% depth

in any of the phases. If the depth of the voltage sag in any phase is more than that, the controllers cannot restore the voltage up to the operating limits. By using the existing controllers, the unbalance in voltage has been reduced to a small value for the case when the voltage sag in one of phases is not more than 13%, but this voltage unbalance is still not in the acceptable limits. This has been verified in simulation results. The compensation of voltage unbalance in the network grid is proposed by using bigger energy storage units rather than existing one. In future work, the controllers will be tested in island conditions as well.

7. Acknowledgements

We are thankful to Kai Strunz for providing the CIGRE test network for LV distribution network. I, Ghullam Mustafa am thankful to Quaid-E-Awam University of Engineering Sciences and Technology, Nawabshah, Sindh, Pakistan for the support and funding.

REFERENCES

[1] IEEE Standard 1159-1995, "IEEE Recommended Practice for Monitoring Electric Power Quality," IEEE, 1995.

[2] H. J. B. Math, I. Y. H. Gu, P. G. V. Axelberg and E.Styvaktakis, "Classification of Underlying Causes of Power Quality Disturbances: Deterministic versus Statistical Methods," *EURASIP Journal on Applied Signal Processing*, Vol. 1, 2007, pp. 172-172.

[3] G. G. Karady, S. Saksena and B. Z. Shi, "Effects of Voltage Sags on House Hold Loads," *IEEE Power Engineering Society General Meeting*, Vol. 3, 2005, pp. 2456-2461.

[4] M. Mc Granaghan, D. R. Mueller and M. Samotyj, "Voltage Sag in Industrial Systems," *IEEE Transactions on Industry Applications*, Vol. 29, 1993, pp. 397-403. http://dx.doi.org/10.1109/28.216550

[5] M. T. Aung and J. V. Milanovic, "The Influence of Transformer Winding Connections on the Propagation of Voltage Sags," *IEEE Transactions on Power Delivery*, Vol. 21, 2006.

[6] W. R. Mendes, M. I. Samesima and F. A. Moura, "Influence of Power Transformer Winding Connections on the Propagation of Voltage Sags through Electric System," *Proceedings of the IEEE*, 2008, pp. 1-6.

[7] L. D. Zhang and M. H. J. Bollen, "A Method for Characterizing Unbalanced Voltage Dips (Sags) with Symmetrical Components," *IEEE Power Engineering Review*, Vol. 18, No. 7, 1998, pp. 50-52. http://dx.doi.org/10.1109/MPER.1998.686958

[8] C. Di Perna, P. Verde, A. Sannino, M. H. J. Bollen, "Static Series Compensator for Voltage Dip Mitigation with Zero-Sequence Injection Capability," 2003 IEEE Bologna Power Tech Conference Proceedings, Bologna, 23-26 June 2003.

[9] R.Teodorescu, M. Liserre and P. Rodríguez, "Grid Synchronization in Three Phase Power Converters," In: *Grid Converters for Photovoltaic and Wind Power Systems*, John Wily & Sons Ltd., Chichester, 2011, pp. 169-181.

[10] A. von Jouanne and B. B. Banerjee, "Voltage Unbalance: Power Quality Issues, Related Standards and Mitigation Techniques," Electric Power Research Institute, Palo Alto, EPRI Final Rep, 2000.

[11] Aneel, "Contribution for the Normalization of the Quality of Electric Power-Harmonic and Unbalances in the Electric Networks," Ph.D. Thesis, Federal University of Uberlandia, 2000.

[12] A. von Jouanne and B. Banerjee, "Assessment of Voltage Unbalance," *IEEE Transactions on Power Delivery*, Vol. 16, No. 4, 2001, pp. 782-790.

[13] F. C. Pereira, J. C. de Oliveira, O. C. N. Souto, A. L.A. Vilaca and P. F. Ribeiro, "An Analysis of Costs Related to the Loss of Power Quality," *Proceedings on Harmonics and Power Quality*, Vol. 2, 1998, pp. 14-16.

[14] V. J. Gosbell, S. Perera and V. Smith, "Voltage Unbalance," Technical Power Quality Center, University of Wollongong, Technical Note No. 6, 2002.

[15] C.-Y. Lee, "Effects of Unbalanced Voltage on the Operation Performance of a Three-Phase Induction Motor," *IEEE Transactions on Energy Conversion*, Vol. 14, No. 2, 1999, pp. 202-208. http://dx.doi.org/10.1109/61.956770

[16] A. I. Maswood, G. Joos, P. D. Ziogas and J. F. Lindsey, "Problems and Solutions Associated with the Operation of Phase-Controlled Rectifiers under Unbalanced Input Voltage Conditions," *IEEE Transactions on Industry Applications*, Vol. 27, 1991, pp. 765-772. http://dx.doi.org/10.1109/28.85494

[17] Benchmark Systems for Network Integration of Renewable Energy Resources, Version 7, CIGRE Task Force C6.04.02, 2011.

[18] E. Muljadi, C. P. Butterfield, T. Batan and D. Yildirim, "Understanding the Unbalanced Voltage Problems in Wind Turbine Generation," National Renewable Energy Laboratory (NREL), 1999.

[19] J. Alonso-Martínez, J. Eloy-García and S. Arnaltes, "Control of a Three-Phase Grid Connected Inverter for Photovoltaic Applications with a Fuzzy MPPT under Unbalanced Conditions," *Proceedings on Power Electronics and Applications*, 2009, pp. 1-7.

[20] L. Fan, Z. Miao, and A. Domijan, "Impact of unbalanced grid conditions on PV systems," IEEE power and energy society general meeting, 2010, pp. 1-6.

[21] G. M. Bhutto, B. Bak-Jensen and P. Mahat, "Modeling of the CIGRE Low Voltage Test Distribution Network and the Development of Appropriate Controllers," *Transactions on Smart Grid and Clean Energy*, Vol. 2, 2013, pp. 184-191.

[22] D. Das, "Electrical Power System," New Age International (P) Publisher, New Delhi, 2006.

[23] Vector Group of Transformer, Electrical Notes & Articles. http://electricalnotes.wordpress.com/2012/05/23/vector-group-of-transformer.

[24] W. H. Kersting, "Distribution System Modeling and Analysis," CRC Press, New Mexico, 2002.

[25] C. Hochgraf, R. H. Lasseter, "STATCOM Control for Operation with Unbalanced Voltages," *IEEE Transactions on Power Delivery*, Vol. 13, 1998, pp. 538-544. http://dx.doi.org/10.1109/61.660926

[26] Rekommandation 16, Spændingskvalitet I lavspændingsnet (voltage quality in low voltage Networks), 4. Udgave, 2011.

Smart Grid and Renewable Energy, **2013, 4, 489-500**
Published Online December 2013 (http://www.scirp.org/journal/sgre)
http://dx.doi.org/10.4236/sgre.2013.49056

Protection of Low Voltage CIGRE Distribution Network

Ghullam Mustafa Bhutto[1,2*], Birgitte Bak-Jensen[1], Claus Leth Bak[1], Jayakrishnan R. Pillai[1]

[1]Department of Energy Technology, Aalborg University, Aalborg, Denmark; [2]Department of Electrical power, Quaid-E-Awam University of Sciences & Technology, Nawabshah, Pakistan.
Email: *gmu@et.aau.dk, *gmustafabhutto@yahoo.com, bbj@et.aau.dk, clb@et.aau.dk, jrp@et.aau.dk

Received November 9th, 2013; revised December 9th, 2013; accepted December 17th, 2013

ABSTRACT

High quality electricity services are the prime objectives in the modern power systems around the world. One of the main players to achieve this is the protection of the system which needs to be fast, reliable and cost effective. The study about the protection of the Low Voltage (LV) CIGRE distribution grid and networks like this has been proposed in this paper. The main objective of this paper is to develop protection against short circuit faults which might appear anywhere in the network. The protection of the power networks that comprises of renewable energy generation units is complicated because of the bidirectional flow of the current and is a challenge for the protection engineers. The selection of the protection devices in this paper is made to protect the network against faults in grid connected and island mode of operation. Ultra-fast fuses are proposed in order to protect the inverters used for Photovoltaic (PV) and battery applications. The disconnection of the PV solar panels when in island mode is made by proposing switch disconnecting devices. ABB is currently using these kinds of disconnection devices for the purpose of protecting solar panels against over voltages in the case of islanding. The over speed protection of the existing Wind Turbine Generator (WTG) in the CIGRE network in case of grid loss is also proposed in this paper.

Keywords: Current Based Protection; Voltage Based Protection; Over Speed Protection; Fuse; Under Voltage Relay; Circuit Breaker; Switch Disconnector

1. Introduction

The purpose of the electrical power system is to deliver good quality, safe and reliable power to the consumers, load centers, industrial plants, etc. The quality and security of power system are disturbed due to the system faults and failures occurring. Faults usually occur due to the lightening flash over, insulation failure, physical damage, short circuit to ground or short circuit in live conductors [1]. A short circuit fault is the most common fault in power systems. A short circuit fault carries huge amount of the current other than the normal operating current. The excessive amount of the current flowing through a circuit can generate tremendous heat which poses risks of fire, damage to the other equipments and potential electrical shocks to the people. If a short circuit is not removed or a faulty portion is not quickly isolated from the healthy system, it will spread into healthy part of the network and may cause over loads and possibly the damage to the transmission lines/cables, bus bars and other equipments. It is therefore, necessary to protect the power system against the short circuits by using short circuit protection devices and ensuring their proper coordination in order to avoid false tripping.

A test distribution network set up by CIGRE comprising WTG, PV solar generation units and sensitive equipment such as VSCs at different locations has been chosen for the study. The single line diagram of this distribution system modeled in DIgSILENT power factory software 15.0 together with appropriate protection devices is shown in **Figure 1**.

In this network, there are two PV solar generation units of 3 kW and 4 kW connected at bus RC and RD respectively. There is one fixed-pitch fixed speed wind

*Corresponding author.
1) Subject Classification: Smart Grids.
2) All authors are mutually agreed.
3) It's the original work of all the authors.
4) We did not submit this manuscript before.

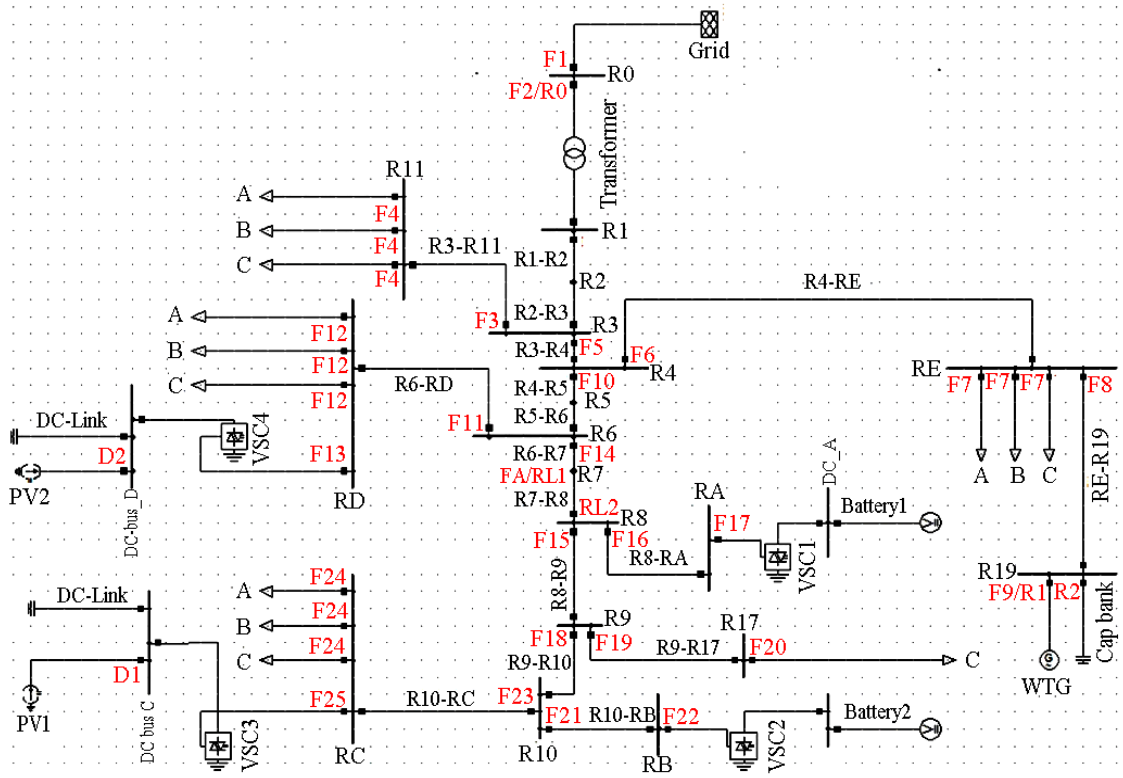

Figure 1. The single line diagram of CIGRE network modeled in DIgSILENT power factory [2].

turbine generator of 5.5 kW connected at bus R19. The WTG is operated close to unity power factor by using a shunt capacitor. There are two batteries connected at bus RA and at bus RB. These Distributed Generating (DG) units are integrated into the grid by using 0.4 MVA, 20 kV/0.4 kV DyN transformer. The neutral of the transformer is grounded with low impedance, (*i.e.* $Z = (0.0032 + j0.0128)\Omega$. Unbalanced loads are aggregated at the 0.4 kV voltage levels and are connected at bus RC, RD, RE, R11 and bus R17. The detailed data concerning different cables/lines used in the network are given in **Table 1** in the appendix.

STATCOM controllers for both the PV systems have been developed in order to control oscillations in the DC link and AC voltages by injecting or absorbing the desired amount of the active and reactive powers [3]. The controllers for the Battery Energy Storage Systems (BESS) are developed and are able to control the flow of active and reactive powers through the lines [3]. These controllers also charge/discharge the batteries at different charging rates [3].

The different components of the CIGRE network (*i.e.* transformer, WTG, lines, bus bars, battery inverters and PV inverters) can be protected either by circuit breakers or by fuses. Typically, transformers below 1000 kVA are protected by using fuses [4]. According to Schneider electric [5] and Danfoss, Low voltage inverters for PV applications and battery storage are protected against short circuit currents by using fuses. Therefore, this study about the protection of LV CIGRE distribution network against short circuit current is mainly performed by using fuses as protection devices. The under voltage relays are used to clear a fault if fuses are unable to clear faults in some conditions. These relays are also used in the case when fuses take longer time to clear fault, such as fault with some fault impedance. The disconnection of the PV solar panels is made by using switch disconnection devices in this study.

The ratings of fuses selected to protect different components of CIGRE network are labeled in **Figure 1** and are presented in **Table 2** in the appendix. Fuses are selected to allow passage of normal current plus a marginal percentage (*i.e.* 25%) to allow excessive current only for short duration [5-7].

Some of fuses selected in **Table 2** of the appendix are even little less than 125% of the rated current because the next available fuse is of bigger rating. For example, fuse selected for the load-RE is 40 A, whereas 125% of the rated current in the phase C of this load is 43.4 A which is higher than the fuse rating. A 40 A fuse is selected because next available fuse is 50 A, therefore, if 50 A fuse is selected for this load, then it might cause delay in the protection. The selected rating of fuses denoted by '*' shown in the **Table 2** is different because of coordination

purposes.

The paper is organized as follows: Section 2 presents the simulation results when protection is made against 3-phase faults with and without fault impedance. The over speed protection of the WTG in the case of grid loss due to 3-phase fault is also described in this section. The protection of the CIGRE inverters is presented in section 3. The disconnection of the solar PV cell structure in the case when in island is also described in this section. Section 4 presents the results about the protection against single-phase to ground fault and the disconnection of the WTG in that case. The protection of the CIGRE network in its central part is presented in section 5. Finally, the conclusion about the paper is presented in section 6.

2. The Protection of the Network against 3-Phase Faults

The study about the protection of the network in this case is carried out by introducing a 3-phase fault with and without fault impedance at the different locations of the CIGRE network. The fuses and under voltage relays available at the different locations are used to clear this kind of fault.

2.1. Protection of the Network in Case of 3-Phase Fault without Fault Impedance

For the first case a three phase fault with fault impedance of zero ohm ($Z_f = 0$) is applied at time equal to t = 5 s at the terminals of the WTG (*i.e*. bus R19). This kind of fault must be isolated from the grid side and from the WTG side in order to ensure reliability and security in the other parts of the network. The procedure of clearing the fault from both the sides of the applied fault is described below:

The voltage at the WTG bus (*i.e*. bus R19) due to this kind of fault becomes zero and hence, the active power output of generator becomes zero. According to the technical regulations 3.2.1 for electricity generation facilities with a rated current of 16 A per phase or lower, a WTG must be disconnected if its terminal voltage falls below 0.9 p.u.

When a short circuit appears at the terminals of an induction machine which is operating as WTG in this network, the current produced by WTG starts to increase to a very high value before decaying completely to zero as shown in **Figure 2**. The rise in this current at t = 5 s is because of inrush current flowing to the faulted point. The induction machines deliver about six times rated current during this time [8-10]. This fault characteristic is due to the inertia in the presence of field flux produced by the induction from the stator. This flux decays on the loss of voltage because of the fault at the terminals of the machine. This current decays to zero as shown in **Figure 2** and is because of the loss of field excitation (*i.e*. loss of stator flux).

The current shown in **Figure 2** decays to zero before reaching to the activation time of fuse F9 (*i.e*. 273 ms at this value of current as seen in **Figure A** in appendix). The observed current is not within the range of the selected fuse operating characteristics; therefore, the isolation of the WTG from the faulted point is not possible by using the fuse in this case.

An under voltage relay is then used. The voltage is sensed by relay R1 shown in **Figure 1** and sends trip signals to the circuit breaker which disconnects the WTG from the faulted point. The time of operation of this relay depends on how low the voltage is at the terminal of the WTG. According to ANSI CS84.1-1995 if the voltage is below 0.5 p.u then the time to clear a fault should be below 0.16 s and if the voltage is in between 0.5 p.u and 0.88 p.u the time to clear fault should be less than 2 s. Since the voltage on the terminals of the WTG due to the fault is zero (*i.e*. voltage is below 0.5 p.u); therefore, the fault should be cleared within 0.16 s. The operation of the circuit breaker receiving the trip signal by relay R1 is shown in **Figure 3**. The Breaker status is closed when it shows 1 on the plot and is opened when it displays 0 on the plot as shown in **Figure 3**.

It can also be seen in **Figure 1** that a capacitor bank is used at bus R19 in order to improve the power factor of the WTG; this capacitor also needs protection against the fault at bus R19. The voltage of this capacitor decreases to zero due to the short circuit fault appeared on its point of the connection as shown in **Figure 4**. The production of the reactive current by the capacitor bank which is required to magnetize the stator winding of the WTG decreases to zero because of its zero voltage at this time t = 5 s. This current is shown in **Figure 5**.

It can be seen in **Figure 5** that the capacitor bank delivers some amount of the reactive current (Minus sign

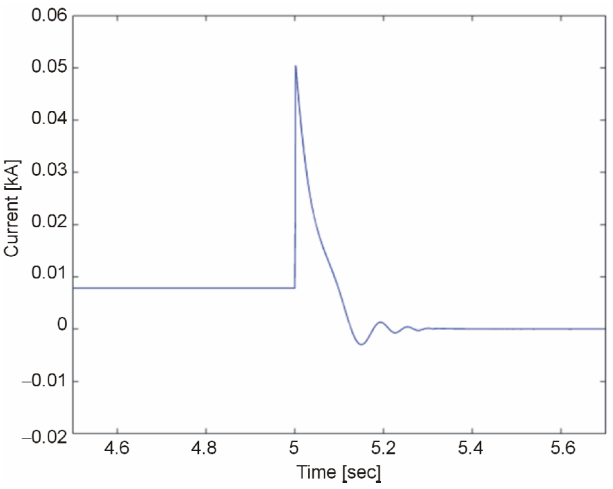

Figure 2. Current of the WTG when fault on its terminals.

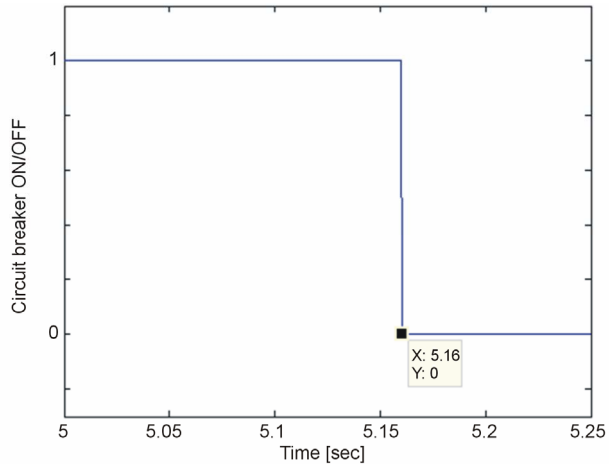

Figure 3. The circuit breaker operation.

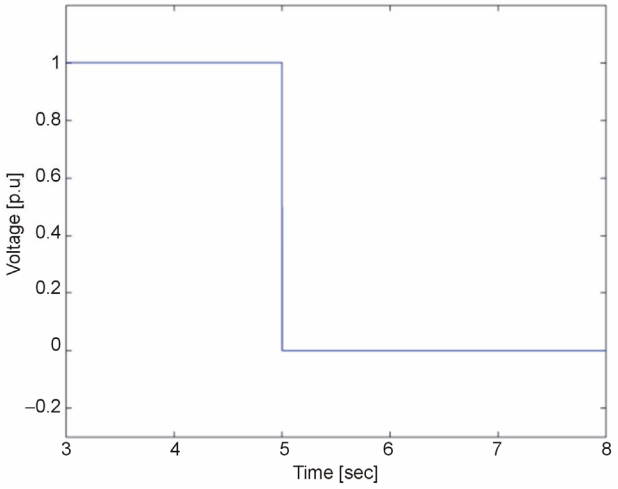

Figure 4. The voltage of the capacitor bank.

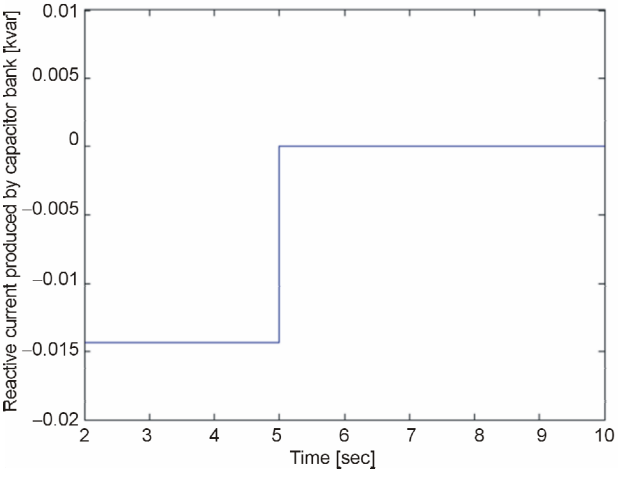

Figure 5. Reactive current delivered by the capacitor bank connected at bus R19.

shows current is injected) in order to excite the stator of the WTG in the normal operating conditions. When the voltage at its terminals becomes zero as shown in **Figure 4**, its current injection also becomes zero as shown in **Figure 5**; therefore, the current based protection is not valid in order to protect this capacitor. The under voltage relay R2 shown in **Figure 1** is used in this regard. The operation of the circuit breaker used to disconnect the capacitor bank is same as shown in **Figure 3** because both the relays are sensing the same voltage and are connected at the same bus.

As three single phase loads are connected on the bus E which makes the voltage on this bus unbalanced, the short circuit current flowing through the upstream cable RE-R19, which is connected on bus R19 (*i.e.* faulted bus) will also be unbalanced. The current flowing through the three phases of the cable RE-R19 is shown in **Figure 6**. In normal operating condition, a current with magnitude of 16.5 A is flowing in the three phases of the cable RE-R19. This current increases to 2.56 kA at the instant of fault at t = 5 s as shown in **Figure 6**. The short circuit currents in the three phases during the fault are a little bit different because of the voltage unbalance.

Fuse F8 is used to disconnect this faulty section of the network from the grid side blows in 313 ms according to the inverse time current characteristics of this fuse as shown in **Figure A** in the appendix. It can be seen in **Figure 6** that the disconnection in the different phases is made at different times since the current is bit different in all the phases. Hence, the fault has been isolated from both the sides of network (*i.e.* grid side and WTG side).

A WT receiving a constant wind speed, and with no transfer of electrical power, rapidly increases the speed of the generator. Therefore, it is essential that the wind turbines stop automatically if the generator is disconnected from the electrical grid [11]. The Danish wind turbines are required to be protected either by aerodynamic brakes or mechanical brakes [11]. Aerodynamic braking uses pitch angle mechanism and it is used for

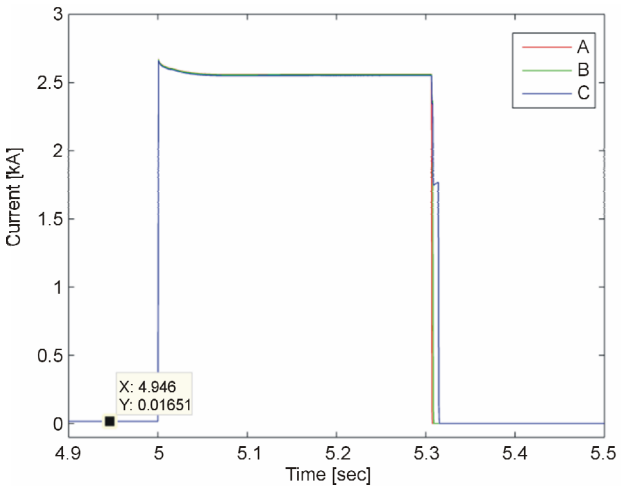

Figure 6. The current flowing through cable RE-R19.

pitch controlled wind turbines or active stall controlled turbines and is expensive for small wind turbines like the ones considered under this study. Mechanical braking is the most common method used for the small wind turbines [12,13] and this mechanism is used to stop the 5.5 kW wind turbine used in the CIGRE network in the case of the loss of the grid supply in this paper.

The block diagram of the mechanical brake model developed in DIgSILENT power factory version 15.0 is shown in **Figure 7**.

The brake model comprises a switch together with a first order time lag function which is represented by the transfer function 1/1+sT, where T is the time constant that ensures the actuation time of the brake. During normal operating conditions, the generator operates at the speed of 1 p.u and the position of switch remains at 1. However, if the speed of the rotor increases beyond 1.2 p.u [13], the switch changes its position from 1 to 0 and makes the shaft reference speed equal to zero which in turn reduces the mechanical torque of the machine in order to stop the generator. The actuation time (*i.e.* 10 s) of the brake [14,15] is ensured by setting the time constant (T) of time lag function

The braking mechanism is activated at t = 5.6 s as the generator speed observed is more than 1.2 p.u and the brakes are applied on the turbine shaft. The speed of the WTG with braking mechanism is shown in **Figure 8**. It can be seen in **Figure 8** that the WTG has been stopped in the case of grid loss due to 3-phase fault within the actuation time of t = 10 s.

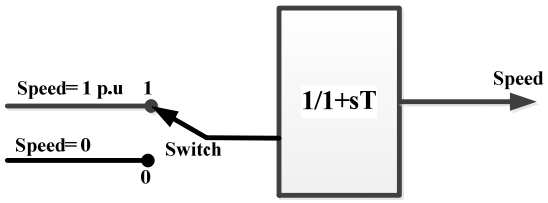

Figure 7. The model of mechanical brake.

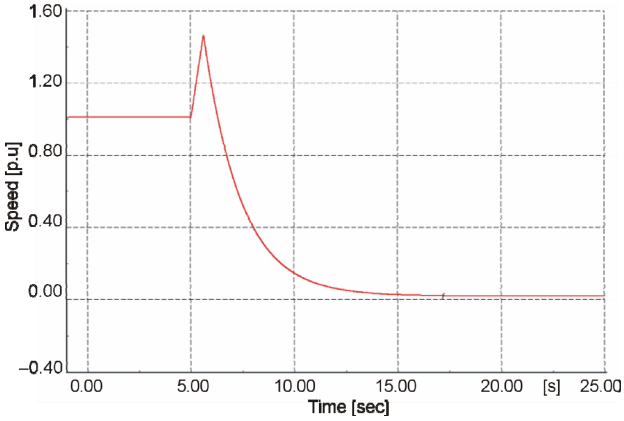

Figure 8. The speed of the WTG with braking mechanism.

2.2. Protection of the Network in Case of 3-Phase Fault with Fault Impedance

A three phase fault with a fault impedance of 0.1 ohms (Z_f = 0.1) is applied on the terminals of WTG (*i.e.* bus R19) at the time equal to t = 5 s. The short circuit current flowing through the faulted line in the case of fault with fault impedance is small compared to the fault without fault impedance. The inclusion of fault impedance delays the tripping of the over current protection devices. The current flowing through the three phases of the cable RE-R19 in this case is shown in **Figure 9**.

It can be seen in **Figure 9** that the current flowing in the three phases of the cable increases at the instant of the fault at t = 5 s. The currents in the three phases during the fault are a bit different because of the voltage unbalance.

Fuses F6 (backup) and F8 are used to disconnect this faulty section of the network from the grid side. Both fuses have the same rated current; therefore the coordination of these two fuses in made in a way to ensure the disconnection of the portion nearest to the faulted point. The rating of fuse F6 is therefore selected higher than that of fuse F8 as shown in **Table 2**. By doing this the three single phase loads are not disconnected due to this fault, since the disconnection is made at the point where fuse F8 is used.

It can be seen in **Figure 9** that the fuses in the different phases blow at different times since current are slightly different in all phases and hence the faulty section from the grid side is isolated. The voltage on the bus RE and bus R19 is shown in **Figure 10** respectively.

It can be seen in **Figure 10** that the voltage on both the buses is equal in normal operating conditions and it decreases at the instant of the fault. When the fault is cleared from the grid side; the voltage on bus RE returns

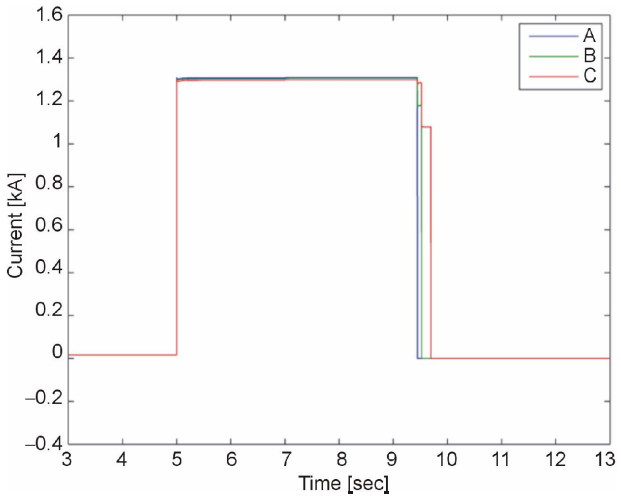

Figure 9. Current flowing through cable RE-R19.

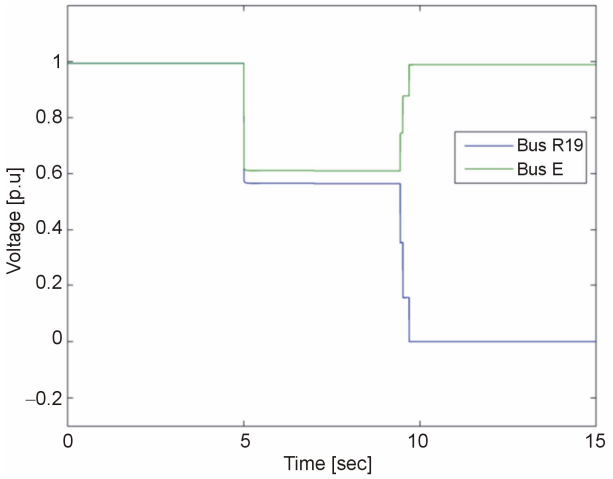

Figure 10. Voltage on bus RE and bus R19.

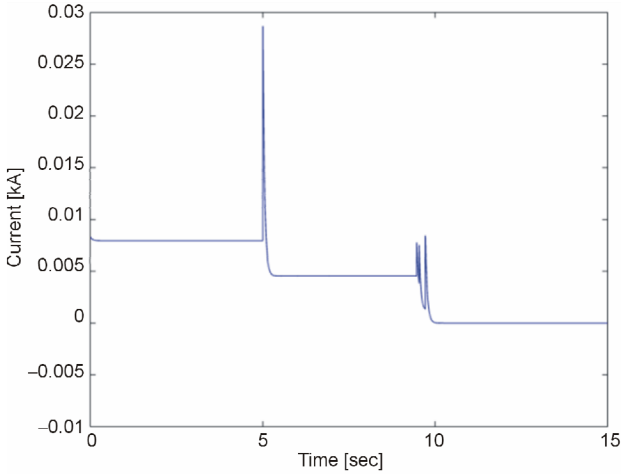

Figure 11. Current delivered by WTG in the case when fuse is used as protection device.

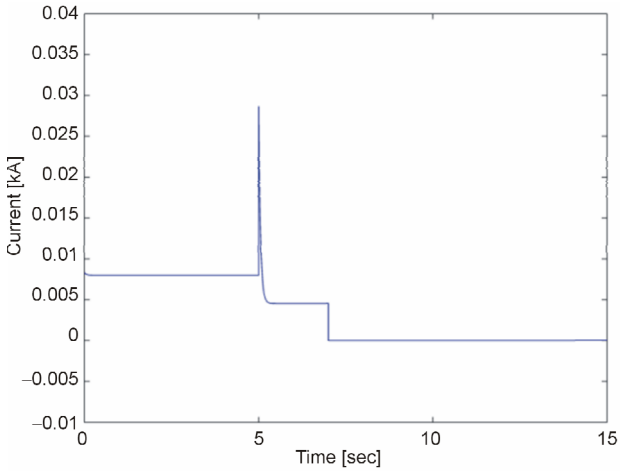

Figure 12. Current delivered by WTG in the case when relay is used as protection device.

to the nominal values and the voltage on bus R19 decreases to zero. The switching in these voltages at the time of the fault clearing is due to the opening of the different phases at different times. It can also be seen in **Figure 10** that the voltage at the terminal of the WTG is decreased to 0.56 p.u during the fault and it again decreases to zero when grid is isolated from the generator.

Since a fault is only cleared from the grid side and it should also be cleared from the generator side; the disconnection of the WTG can be made either by a current based protection device or a voltage based protection device.

The current delivered by the WTG is shown in **Figure 11**. It can be seen in this figure. that there is a surge of the current produced by the WTG at the instant of the fault. This current decreases to the value as shown in **Figure 11**. The reduction in the current shown in **Figure 11** is because of the reduction at its terminal voltage. At the time when the grid is disconnected, this current decrease to zero since the WTG has lost grid excitation current. As there is only short time rise in the WTG current and it further decreases during the fault; fuse F9 does not detect this fault and hence the disconnection of the WTG is not possible by using a fuse in this case.

Therefore, an under voltage relay is used in order to disconnect the WTG in this case. The current of the WTG in the case when an under voltage relay has isolated the WTG from the faulted point is shown in **Figure 12**. Since the voltage on the terminals of the WTG is greater than 0.5 p.u during this fault; then according to ANSI CS84.1-1995 standards the relay R1 sends a trip signal to a circuit breaker which disconnects the WTG from the grid within 2 s.

The speed of the WTG in case of the loss of grid increases beyond the acceptable limits. The mechanical brakes are applied in order to stop the generator as is done in the previous case.

To study about the size of the fault impedance where the prescribed protection devices do not detect the fault, various tests have made by applying 3-phase fault at bus R19 using the different values of the fault impedances. The summary about the range of the protection devices at the different values of fault impedances is presented in **Table 3** in the appendix.

The voltage at bus RE and bus R19 and the current flowing through cable RE-R19 during the fault at different values of the fault impedances have been presented in this table. The time of the operation of fuse and an under voltage relay have also been shown and decision is made that up to which size of the fault impedance these protection devices (*i.e.* fuse and an under voltage relay) can operate. This table describes that the protection devices can only operate in a certain range in the case of the fault impedance up to 0.6 ohms. This table also shows that voltage based protection in general is faster than current

based protection in all the cases presented in this table.

Now in the case, if the fault impedance is high as for instance 2 ohms as for an arc, the protection devices shown in **Figure 1** obviously will not work in this condition according to **Table 3**. The procedure about the clearing of such kind of faults is described in [16,17].

3. The Protection of the Inverters Used in the CIGRE Network

To study about the protection of the inverters used for the PV and battery applications in the network; a fault should be applied on one of the lines or the buses in the close vicinity of the inverters. A 3-phase short circuit fault with fault impedance of zero ohm ($Z_f = 0$) is applied on line R10-RC which is connected to the bus RC where PV1 is connected in this regard. This is the line which is fed through the grid and a PV1 inverter; therefore, there is bidirectional flow of the current towards a short circuit point. There will be a surge of the current flowing from the VSC3 towards a faulted line. The VSCs are very sensitive to over currents. The over currents in VSCs lead to the thermal degradation of the IGBT valves and it may also cause a permanent damage [18-20]. The IGBTs can withstand maximum currents of 2 p.u for 1 ms [21]. It is therefore, necessary to protect the IGBTs of the inverters by using ultra-fast protection devices. The fuse F25 is modeled as an ultra-fast (*i.e.* I-t characteristics are set in such a way that it blows very quickly) and acts instantly to protect VSC3 when the short circuit fault appears in line R10-RC.

The current of the VSC3 is shown in **Figure 13**. It can be seen in **Figure 13** that fuse F25 is blown when the current flowing through VSC3 increases abruptly during the short circuit. The line R10-RC is protected by using fuse F23. The current flowing through this line is shown in **Figure 14**.

It can be seen in **Figure 13** that fuse F25 quickly isolates the inverter from the grid and fuse F23 disconnects line R10-RC from the healthy portion of the network within 68 m s as shown in **Figure 14**.

PV inverters operate in a certain range of voltages. If voltage goes beyond limits, it will stop its operation [21]. A three phase short circuit fault on the AC terminals of PV1 inverter causes the voltage to go down to zero and hence there is no transfer of the power from a PV1 towards the grid. The dc-link capacitor charges during this period and when it is fully charged there is no path for the current to flow and the PV operates at no load conditions. Due to this reason the dc-link voltage increases very fast. PV generating units in real applications are normally disconnected from the DC bus in order to protect the insulation of PV cells against over voltages. In such a case, the PV panel presents open circuit voltage

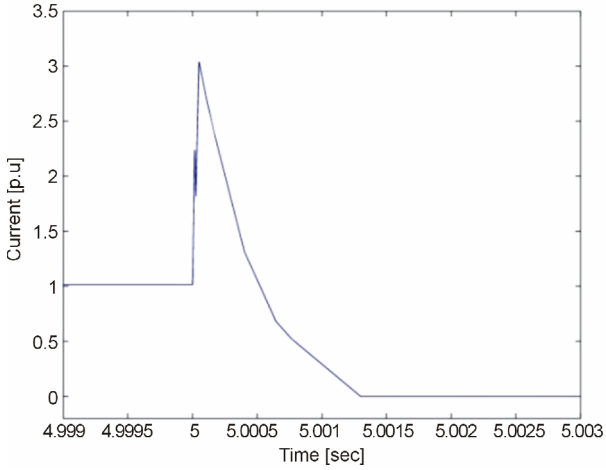

Figure 13. Current of VSC3.

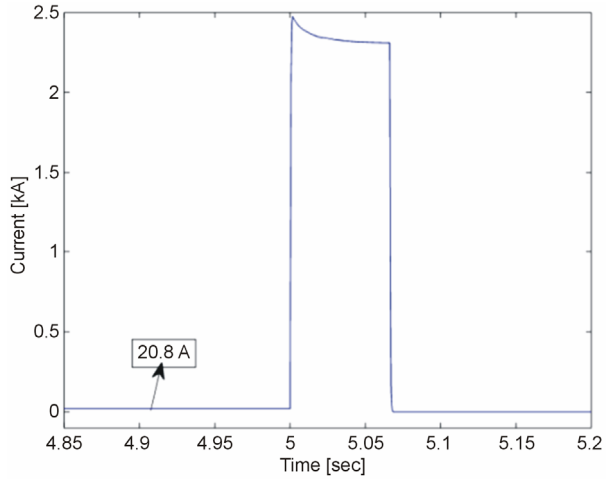

Figure 14. Current flowing through R10-RC line.

(*i.e.* it is the voltage across the terminals of a PV cell when the current flowing through the external circuit (I_{pv}) is zero) at its output with no power generation. The current flowing into the dc-link capacitor is shown in **Figure 15**.

It can be seen in **Figure 15** that there is no flow of the current into dc-link capacitor in the normal operating conditions, since all output power of PV1 is integrated into the grid via VSC3. At the time of grid isolation, dc-link capacitor starts charging through current produced by PV1. Soon after 146 ms, this capacitor is fully charged as shown in **Figure 15** and a PV 1 at this time operates at no load and switch-disconnecting device (*i.e.* D1 as shown in **Figure 1**) isolates PV1 in this condition. The coordination between fuse F25 and switch disconnecting device D1 is made in such a way that, fuse F25 disconnects VSC3 from the grid due to current surge produced at the time of fault (*i.e.* t = 5 s) according to its inverse time current characteristics. The disconnection of VSC3 from the grid causes the voltage rise at the DC bus

where PV1 cell is connected. Based on the voltage levels, D1 decides the disconnection of PV1 cell from the DC bus. The current produced by PV1 and the voltage at DC bus in normal and at a time of its disconnection is shown in **Figure 16**.

The protection of other the PV inverter in the grid is also done in the same way by using fuse F13 and disconnection of the PV cell structure is made by D2. The protection of the battery inverters is made by using ultra-fast fuses F17 and F22.

4. Protection of the CIGRE Network against Single Phase to Ground Faults

The majority of faults in the power system are single phase to ground faults [22], and consequently it draws unbalanced currents resulting in unbalanced voltage sags in the network. A single line to ground fault with a fault on phase A having fault impedance of zero ohms is applied at time t = 5 s on line R4-RE in order to observe the performance of the fuses used in the network. The Fuse F6 opens the faulty phase 'phase A' from the grid side and fuse F9 opens the same phase from the WTG side. The voltage on bus E due to this kind of the fault is shown in **Figure 17**.

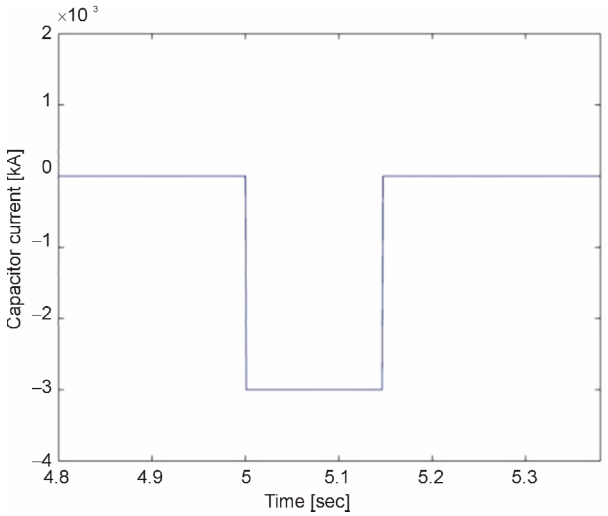

Figure 15. Current of dc-link capacitor.

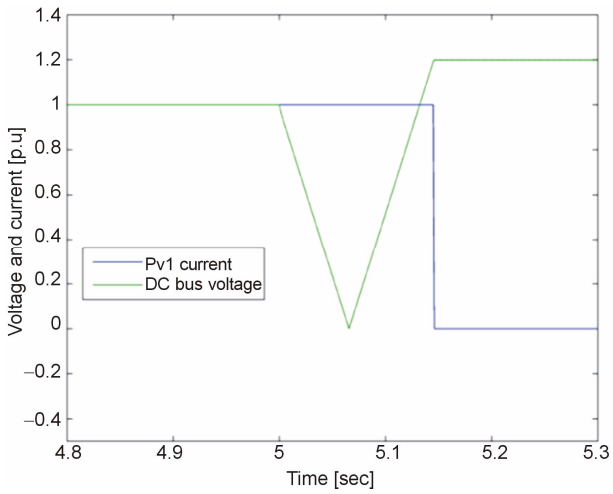

Figure 16. PV1 current and DC bus voltage during normal and island operation.

It can be seen in **Figure 17** that the voltage of the affected phase (*i.e.* phase A) becomes zero when the fault appears on time equal t = 5 s. The voltages in the healthy phases increase during the fault and come back to the steady state value when the fault is cleared. The detailed explanation about the rise of the voltage in the healthy phases during the fault has been presented by the authors in [23].

In case of a WTG connected to unbalanced voltages, the stator currents will be unbalanced. These unbalanced stator currents creates unequal heating in the stator winding which might degrade winding insulation and thereby reducing the life time of the stator winding [24] [25]. The current produced by WTG in its three phases is shown in **Figure 18**. It can be seen in **Figure 18** that there is a huge increase in the current in the phase A of the WTG as this is the faulty phase. The currents in the healthy phases during a fault also increase as shown in **Figure 16** and this increase in the current is according to the magnetization current of the stator winding of the WTG.

In order to be on safe side, the WTG should be disconnected in this condition. This disconnection is made by using the under voltage relay R1. As one of the phase is at zero voltage, therefore the relay sends trip signal to a circuit breaker which clears the fault within 160 ms in this case of a fault.

The speed of the generator increases in the case of the disconnection; therefore, mechanical brakes can be applied in order to stop it as mentioned previously.

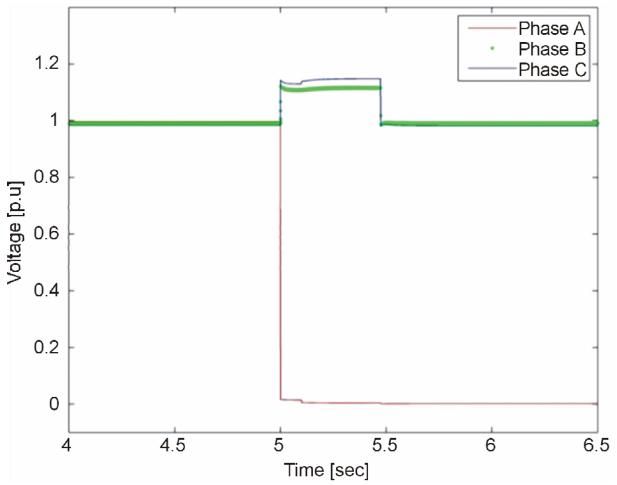

Figure 17. Voltage in three phases on bus RE.

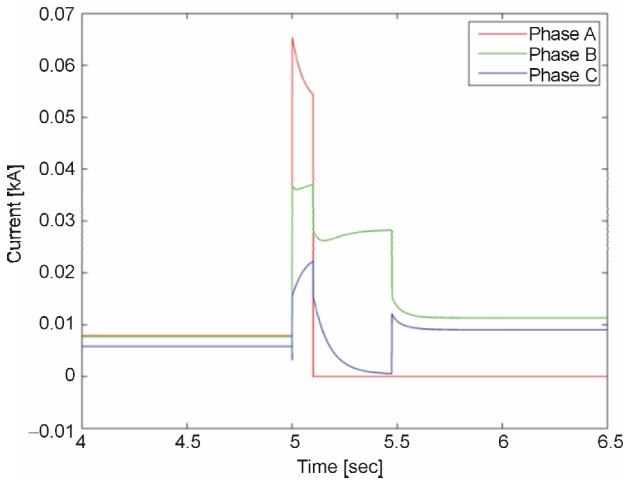

Figure 18. Three phase current of Wind Turbine Generator.

5. Protection of the CIGRE Network in Its Central Parts

The protection of CIGRE in its central part (*i.e.* from node R1 to R10 in **Figure 1**) is designed in such a way that it ensures a proper over current protective coordination in a network. The over current protection coordination in the central part of CIGRE network is made by using fuses F15, FA, F14, F10 and F5 as shown in **Table 2**. Fuse F5 is highest fuse among these fuses due to coordination so if fault occurs nearby the close vicinity of this fuse, it will take longer time to clear the fault. To overcome this problem, the protection in the central part is made by using the under voltage relay.

Again, the fault may occur in the central parts of the network with some fault impedance. The voltage based protection can be a better solution in this regard as well. A 3-phase fault with a fault impedance of 0.1 ohms is applied on the cable R7-R8 of the CIGRE network. The fault appears on the cable at time equal to t = 2 s. The current flowing through this cable is shown in **Figure 19**. It can be seen in **Figure 19** that 1.6 kA current is flowing through the cable during a fault and fuse FA blows within 58 s according to its operating characteristics shown in **Figure A** in appendix. The fault persist in the network for the long time in this case; therefore, voltage based protection is introduced which clears fault very fast.

The under voltage relay is used at both ends of the cable instead of over current protection devices. These relays (*i.e.* RL1 and RL2) detect the fault if the voltage on the faulted point decreases below a threshold. The plot of the current flowing from the both ends of the cable (*i.e.* from the grid side and from the DGs side) when under voltage relays are used at the both ends of the cable is shown in **Figures 20** and **21** respectively.

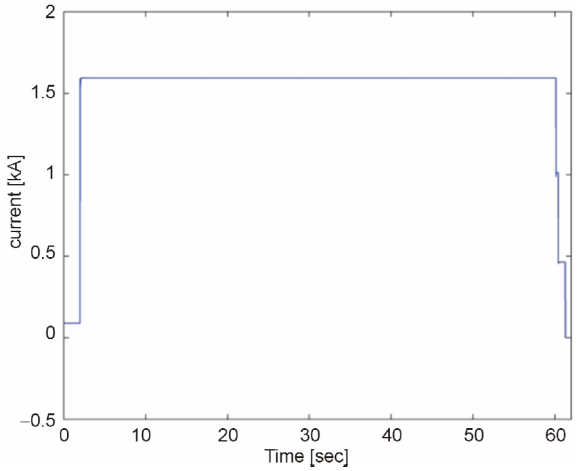

Figure 19. Current flowing through cable R7-R8.

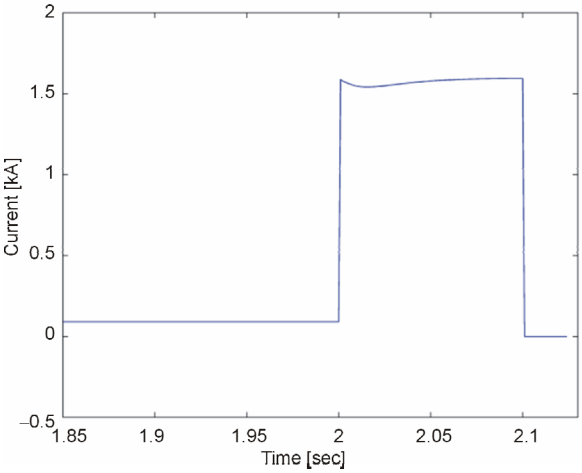

Figure 20. Current flowing through cable R7-R8 from the grid side.

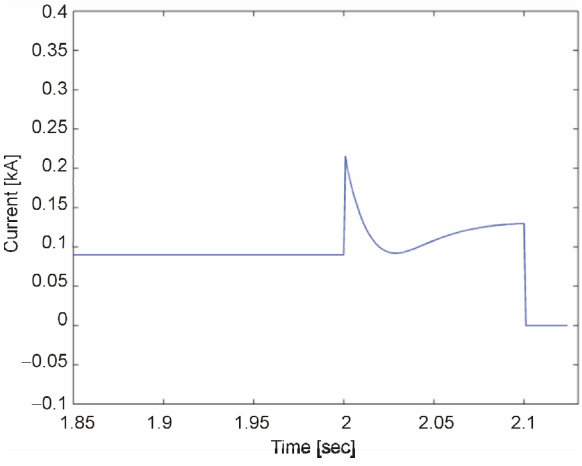

Figure 21. Current flowing through cable R7-R8 from the DGs side.

The under voltage relay used at the grid side end of the cable measures the voltage and sends trip signal to the

circuit breaker. It can be seen in **Figure 20** that the circuit breaker has disconnected a faulted section from the grid side within 100 ms. Similarly, the under voltage relay used on the DGs side of the cable sends the trip signal to its circuit breaker which clears fault within 100 ms as shown in **Figure 21**. The over shoot in the current as shown in **Figure 21** at the instant of fault is due the current surge produced by the inverter based DG units.

6. Conclusion

The protection against 3-phase fault with and without fault impedance in different portions of the CIGRE network has been proposed. The clearance of the fault in CIGRE network is mainly proposed by using fuses because of economic reasons and if fuses are unable to detect the fault as analyzed for the cases in previous section, the clearance of fault is done by using the under voltage relays. The disconnection of the WTG in case of the symmetrical and unsymmetrical faults is made by using current-based and voltage-based protection devices. The over speed protection in the case of grid loss due to 3-phase and single phase to ground fault by using mechanical brakes is also studied in this paper. The over current protection of the inverters is made by using ultra-fast fuses and the disconnection of PV solar cell structure in the case of loss of grid is made by using switch disconnection devices. The protection of the CIGRE network in case of the forward direction of the current (*i.e*. grid side) is made by using the fuses and the protection in the case of reverse direction of the current (*i.e*. DG side) due to islanding is made by using the under voltage relays.

7. Acknowledgements

We are thankful to Kai Strunz for providing the CIGRE test network for LV distribution network. I, Ghullam Mustafa am thankful to Quaid-E-Awam University of Engineering Sciences and Technology, Nawabshah, Sindh, Pakistan for the support and funding.

REFERENCES

[1] J. R. Lucas, "Power System Analysis: Faults," EE 423, 2005.

[2] Benchmark Systems for Network Integration of Renewable Energy Resources, Version 7, CIGRE Task Force C6.04.02, 2011.

[3] G. M. Bhutto, B. Bak-Jensen and P. Mahat, "Modeling of the CIGRE Low Voltage Test Distribution Network and the Development of Appropriate Controllers," *Transactions on Smart Grid and Clean Energy*, Vol. 2, 2013, pp. 184-191.

[4] Merlin Gerin, Square D and Telemecanique, "Selection of Fuses for the Protection of Transformers," Schneider Electric, 2004.

[5] Schneider Electric Industries SAS, "Safe and Reliable Photovoltaic Energy Generation," EDCED112005EN, Rueil-Malmaison Cedex-France, 2012.

[6] A. Wright and P. G. Newbery, "Electric Fuses," 3rd Edition, Institution of Electrical Engineers (IET), 2004, pp. 2-10.

[7] L. Hewitson, M. Brown, B. Ramesh and S. Mackay, "Practical Power Systems Protection," Elsevier, Amsterdam, 2004.

[8] IEEE, "Standard for Interconnecting Distributed Resources with Electric Power Systems," IEEE 1547.2-2008.

[9] Electric Power Distribution for Industrial Plants, IEEE Std 141-1993 Red Book.

[10] B. Kroposki, "Optimization of Distributed and Renewable Energy Penetration in Electric Power Distribution Systems," Submitted Thesis to CSM for Partial Degree of Doctor of Philosophy (Engineering Systems), Golden, Colorado, 2008

[11] Wind Turbine Safety, Danish Wind Industry Association. http://ele.aut.ac.ir/~wind/en/tour/wtrb/safety.htm

[12] H. Gitano-Briggs, "Small Wind Turbine Power Controllers, Wind Power," 2010. http://www.intechopen.com/download/get/type/pdfs/id/9563

[13] M. Kanabar and S. Khaparde, "Rotor Speed Stability Analysis of a Constant Speed Wind Turbine Generator," 2011. http://www.intechopen.com/download/get/type/pdfs/id/14817

[14] K. Rajambal, B. Umamaheswari and C. Chellamuthu, "Electrical Braking of Large Wind Turbines," *Renewable Energy*, Vol. 30, No. 15, 2005, pp. 2235-2245. http://dx.doi.org/10.1016/j.renene.2004.11.002

[15] N. McMahon, "On Electrodynamic Braking for Small Wind Turbines," Centre for Renewable Energy at Dundalk Institute of Technology, 2013.

[16] P. E. Joe Mooney and J. Peer, "Application Guidelines for Ground Fault Protection," Schweitzer Engineering Laboratories, Inc., Pullman.

[17] J. Tengdin, R. Westfall and K. Stephan, "High Impedance Fault Detection Technology," Report of PSRC Working Group D15.

[18] C. Du, "The Control of VSC-HVDC and Its Use for Large Industrial Power System," Licentiate Thesis, Chalmers University of Technology, Göteborg, 2003.

[19] N. Mohan, T. M. Underland and W. P. Robbins, Eds., "Power Electronics-Converter, Design and Application," 2nd Edition, John Wiley, New York, 1995.

[20] R. Pollanen, "Converter-Flux-Based Current Control of Voltage Source PWM Rectifier Analysis and Implementation," Ph.D. Dissertation, Acta University, Lappeenrantaensis, 2003.

[21] Technical Information about IGBT-Module, FZ1800R17 HP4_B29, Material No. 32559, 2010.

[22] M. Mc Granaghan, D. R. Mueller and M. Samotyj,

"Voltage Sag in Industrial Systems," *IEEE Transactions on Industry Applications*, Vol. 29, No. 2, 1993, pp. 397-403. http://dx.doi.org/10.1109/28.216550

[23] G. M. Bhutto, B. Bak-Jensen, P. Mahat and C. Cecati, "Mitigation of Unbalanced Voltage Sags and Voltage Unbalance in CIGRE Low Voltage Distribution Network," *Energy and Power Engineering*, Vol. 5, 2013, pp. 551-559. http://dx.doi.org/10.4236/epe.2013.59060

[24] A. von Jouanne and B. Banerjee, "Assessment of Voltage Unbalance," *IEEE Transactions on Power Delivery*, Vol. 16, No. 4, 2001, pp. 782-790. http://dx.doi.org/10.1109/61.956770

[25] F. C. Pereira, J. C. de Oliveira, O. C. N. Souto, A. L. A. Vilaca and P. F. Ribeiro, "An Analysis of Costs Related To The Loss of Power Quality," 8*th International Conference on Harmonics and Power Quality*, Athens, 14-16 October 1998, pp. 777-812.

Appendix

Table 1. The data about the different cables used CIGRE network.

S:No	Node from	Node to	Type	Cross section	R_{ph}	X_{ph}	R_o	X_o	L	Installation
				mm^2	Ω/km	Ω/km	Ω/km	Ω/km	m	
1	R1	R2	NA2XY	240	0.163	0.136	0.490	0.471	35	UG 3-ph
2	R2	R3	NA2XY	240	0.163	0.136	0.490	0.471	35	UG 3-ph
3	R3	R4	NA2XY	240	0.163	0.136	0.490	0.471	35	UG 3-ph
4	R4	R5	NA2XY	240	0.163	0.136	0.490	0.471	35	UG 3-ph
5	R5	R6	NA2XY	240	0.163	0.136	0.490	0.471	35	UG 3-ph
6	R6	R7	NA2XY	240	0.163	0.136	0.490	0.471	35	UG 3-ph
7	R7	R8	NA2XY	240	0.163	0.136	0.490	0.471	35	UG 3-ph
8	R8	R9	NA2XY	240	0.163	0.136	0.490	0.471	35	UG 3-ph
9	R9	R10	NA2XY	240	0.163	0.136	0.490	0.471	35	UG 3-ph
10	R3	R11	NA2XY	25	1.541	0.206	2.334	1.454	30	UG 3-ph
11	R4	RE	NA2XY	150	0.266	0.151	0.733	0.570	35	UG 3-ph
12	R6	RD	NA2XY	70	0.569	0.174	1.285	0.865	30	UG 3-ph
13	R10	RC	NA2XY	35	1.111	0.195	1.926	1.265	30	UG 3-ph
14	RE	R19	NA2XY	150	0.266	0.151	0.733	0.570	30	UG 3-ph
15	R8	RA	NA2XY	25	1.541	0.206	2.334	1.454	30	UG 3-ph
16	R9	R17	NA2XY	25	1.541	0.206	2.334	1.454	30	UG 3-ph
17	R10	RB	NA2XY	25	1.541	0.206	2.334	1.454	30	UG 3-ph

Table 2. The ratings of the different fuses used at different location of the CIGRE network.

Lines/DGS/VSCS/Loads	Current in normal operation [A]	Fuse current [A] *i.e.* 125% of Inom	Fuse selected	Name of the fuse in network
Grid	11.5	14.45	20	F1
T/f. Prim	11.55	14.45	16	F2
R3-R11	162	202.5	200	F3
R3-R4	401	501.25	500 1000*	F5
R4-RE	304	380	400 500*	F6
RE-R19	304	380	400	F8
R4-R5	401	501.25	500 800*	F10
R6-RD	199	248.75	250	F11
VSC4	34.68	43.35	40	F13
R6-R7	401	501.25	500 630*	F14
R7-R8	401	501.25	500 630*	FA
R8-R9	401	501.25	500 630*	F15

Continued

R8-A		162	202.5	200	F16
VSC1		50.58	63.32	63	F17
R9-R10		401	501.25	500	F18
R9-R17		162	202.5	200	F19
R10-RB		162	202.5	200	F21
VSC2		36.13	45.16	50	F22
R10-C		162	202.5	200	*F23*
VSC3		26	32.5	32	*F25*
WTG		8.69	10.86	10	*F9*
	Phase A	6.9	8.7		
Load_RC	Phase B	13.9	17.4	20	F24
	Phase C	17.4	21.7		
	Phase A	20.86	26		
Load_RD	Phase B	27.8	34.8	40	F12
	Phase C	34.8	43.4		
	Phase A	20.86	26		
Load_RE	Phase B	27.8	34.8	40	F7
	Phase C	34.8	43.4		
	Phase A	4.35	5.44		
Load_R11	Phase B	8.7	10.87	16	F4
	Phase C	11.74	14.67		
Load_R17	Phase C	11.74	14.67	16	F20

Table 3. The study about the range of the detection of the protection devices with respect to fault impedance.

Z in ohms	V_{RE} [KV]	V_{R19} [kV]	$I_{RE} - R_{19}$ [KA]	Fuse (F)	Time [sec]	Under voltage relay (UVR)	Time [sec]	Fast operation
0.3	0.82	0.80	0.630	Yes	125	Yes	2	UVR
05	0.89	0.87	0.410	yes	4900	Yes	2	UVR
0.6	0.91	0.89	0.339	No	-	Yes in bus R19 But No in RE	2	UVR
0.8	0.93	0.91	0.260	NO	-	No	-	-

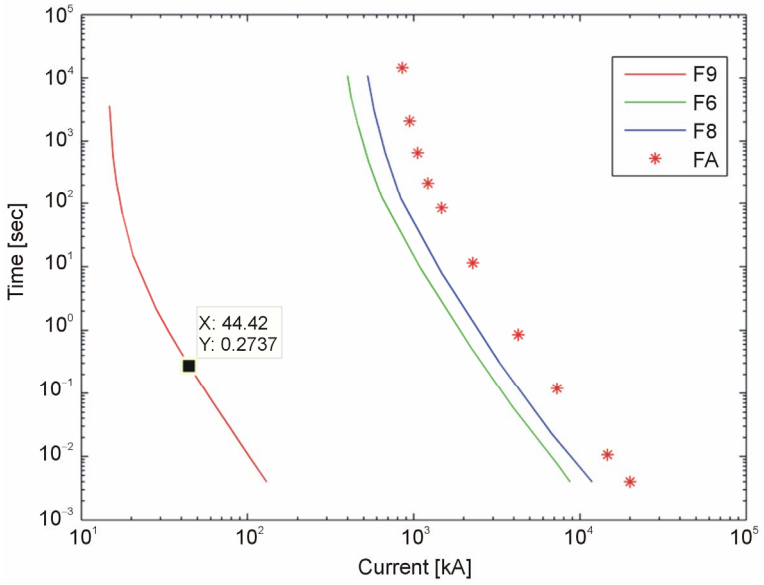

Figure A. Inverse current characteristics of some of the fuses used in CIGRE network.